INVESTIGATIONS ON AUTOMATED AND NON-LINEAR CONTROL SYSTEMS

A Thesis Submitted

In Fulfilment of the Requirements

for the Degree of

DOCTOR OF PHILOSOPHY

In

Electrical Engineering

By

BASANT TOMAR

(Enrollment No.: 2K20/PHDEE/04)

Under the Supervision of

PROF. NARENDRA KUMAR II

Professor in Dept. of Electrical Engineering, DTU

PROF. MINI SREEJETH

Professor in Dept. of Electrical Engineering, DTU

Department of Electrical Engineering

DELHI TECHNOLOGICAL UNIVERSITY

(Formerly Delhi College of Engineering)

Shahbad Daulatpur, Main Bawana Road, Delhi-110042, INDIA

SEPTEMBER 2024

ACKNOWLEDGEMENTS

First and Foremost, I gracefully thank the Almighty God for giving me strength, knowledge, ability, inspiration and opportunity to undertake this research work and to persevere and complete it satisfactorily. I owe a deep sense of gratitude to his comprehensive soul whose divine light has enlightened my path throughout the journey of my research. The PhD journey has been challenging and full of learning opportunities and experiences that have helped me up my research acumen. It is by God's grace I have come thus far.

I take the opportunity to humbly submit my sincere and heartfelt thanks to my research supervisors **Prof. Narendra Kumar II** & **Prof. Mini Sreejeth** from the Department of Electrical Engineering, Delhi Technological University, Delhi for their valuable guidance, enthusiastic encouragement and persistent support. I am truly grateful from the core of my heart for their meticulous approach, wonderful assistance of their perspective and fruitful discussions on the research topic. Their immense contribution and rare dedication in providing the much-needed guidance is worth of much honors. Their careful supervision and personal attention have given me a lot of confidence and enthusiasm, during the different stages of my doctoral investigations. They are academic giants under whose watch am molded into a seasoned research scholar. I invariably fall short of words to express my sincere gratitude for their patience and motivation.

I am extremely thankful to **Prof. Rachana Garg**, **Head of the Department of Electrical Engineering,** Delhi Technological University, Delhi & other faculty members of the Dept. of Electrical Engineering, Delhi Technological University, Delhi, for the endless support and cooperation throughout this dissertation.

I also thank the management of Delhi Technological University, India for countenancing me to pursue a Ph.D. at Dept. of Electrical Engineering, Delhi Technological University. I am thankful to all staff members of the Department of Electrical Engineering for their kind help and support during the entire period of my research. My appreciation also goes to my colleagues in the Dept. of Electrical Engineering, Delhi Technological University, Delhi, for their constant guidance and assistance throughout this dissertation.

I dedicate this thesis to my family for their endless love, support, encouragement and blessings throughout my academics. I would like to offer my most humble gratitude to my

grandfather, **Late Shri Brijwasi Ji** who always wanted me to be a doctor, for his unsurpassed love, care, support and warm wishes for my life. My father, **Shri Rameshwar** and my mother **Smt. Anita Devi** has been a source of motivation and strength during moments of despair and discouragement throughout this research period. I am greatly indebted to my dear friend **Dr. Ishu Tomar**, without whom I could not imagine being enrolled in PhD, for her unwavering encouragement, undeterred faith in me and being the biggest pillar of strength who supported me all the way till the end. Indeed, a plethora of words would not suffice to say what I owe to them. I feel very lucky to have a great family who have supported me throughout the journey of my research work.

Last but not the least, I acknowledge each one of those who directly or indirectly have helped me during the whole period, thus making it a well-rounded experience of learning. Many thanks to all of you, this thesis would have no sense without any person I named!

Basant Tomar

DELHI TECHNOLOGICAL UNIVERSITY

(Formerly Delhi College of Engineering)

Shahbad Daulatpur, Main Bawana Road, Delhi–110042

CANDIDATE'S DECLARATION

I **Basant Tomar** (Roll No.: 2K20/PHDEE/04) hereby certify that the work which is being presented in the thesis entitled "**Investigations on Automated and Non-Linear Control Systems**" in fulfillment of the requirements for the award of the Degree of Doctor of Philosophy, submitted in the Department of **Electrical Engineering**, Delhi Technological University is an authentic record of my own work carried out during the period from August 2020 to June 2024 under the supervision of **Prof. Narendra Kumar II** and **Prof. Mini Sreejeth**.

The matter presented in this thesis has not been submitted by me for the award of any other degree in this or any other Institute.

Candidate's Signature

This is to certify that the student has incorporated all the corrections suggested by the examiners in the thesis and the statement made by the candidate is correct to the best of our knowledge.

Signature of Supervisor(s)   **Signature of External Examiner**

CERTIFICATE BY THE SUPERVISOR(s)

Certified that **Basant Tomar** (Roll No.: 2K20/PHDEE/04) has carried out the research work presented in this thesis entitled "**Investigations on Automated and Non-Linear Control Systems**" for the award of **Doctor of Philosophy** from the Department of Electrical Engineering, Delhi Technological University, Delhi, under our supervision. The thesis embodies results of original work, and studies are carried out by the student himself and the contents of the thesis do not form the basis for the award of any other degree to the candidate or anybody else from this or any other University/Institution.

Prof. Narendra Kumar II
Supervisor
Department of Electrical Engineering
Delhi Technological University,
Delhi –110042, India

Prof. Mini Sreejeth
Co-Supervisor
Department of Electrical Engineering
Delhi Technological University,
Delhi –110042, India

Date: 12/09/2024

This thesis is dedicated to my grandfather

For his endless love, support and encouragement

ABSTRACT

A control system can range from a single home heating controller to large industrial control systems for controlling different processes or devices. Control theory evolution leads to the development of analytical controller design techniques and an automatic decision-making process that improves the performance of control benchmark problems in real time. Lately, automation has been gaining traction globally owing to its huge social, economic and environmental benefits. However, most of the industrial plants have hard non-linearities, which makes it difficult to design and analyse closed-loop control systems as compared to linear ones. However, a significant portion of the literature exists for traditional control through distributed control systems (DCS) and field-bus technologies to monitor and control all the processes of industrial automation control systems. But none of them have resulted in an intelligent and highly productive real-time control of the plant. Also, the current systems used for industrial monitoring and control have various drawbacks related to expensive hardware and difficulty of integration with other network protocols. Very little research is focused on Programmable Logic Controller (PLC) and Supervisory Control and Data Acquisition (SCADA) based real-time automation systems to accelerate industrial processes and perform industrial operations remotely.

Additionally, nonlinearity plays an important role in the controlled process or controllers in nonlinear control systems. Nonlinear control systems are used in numerous engineering systems like aerospace control, industrial process control, autonomous robots, position control, trajectory tracking, path planning, etc. A nonlinear controller through robustness or adaptability can handle the consequences due to hard nonlinearities, and model uncertainties. Non-linear systems behave differently at different operating points and hence it is not preferred for industrial applications due to its complexity, non-flexibility in tuning and poor reconfigurability.

Thus, there is a need for an adaptive method to resolve the issues of non-linearities in the traditional control of industrial automation systems and improve the performance and stability of non-linear control systems like inverted pendulum and ball balancer systems. The objective of this thesis is to investigate automated and non-linear control systems and propose robust, reliable, and efficient methods for various automated and non-linear control systems. In this research, a variety of techniques are applied to automated and non-linear control

systems. Some newly introduced applications of automation and ratio control strategy in the Industry 4.0 concept are also studied. Various methods have been designed and applied to improve the performance and stability of non-linear control systems along with the implementation of various optimization techniques to these non-linear control systems. The contributions presented in this thesis are outlined below:

- A PLC and SCADA-based control framework is proposed to automate the process industry plant and monitor all the processes using a single screen Human Machine Interface (HMI). The proposed method addresses a dynamic real-world problem for the mixing of raw materials, filling of final product composition, capping, labelling and sorting of containers on the basis of both size and type using a single assembly line by applying the developed model in a real-life case study of an assembly line from a chemical process industry supplier in north India to verify the design for effectively balancing a real-world assembly line in a process industry.

- A PLC-based control framework is developed to automate the processes in the heat exchanger plant and monitor all the processes using SCADA. A PLC and SCADA-based control framework is designed to control the temperature of a heat exchanger system through Proportional Integral Derivative (PID) and Fractional Order PID ($PI^{\lambda}D^{\mu}$) controllers and the performance of the controllers is optimized using Genetic algorithm (GA), Ant Colony Optimization (ACO) and Particle Swarm Optimization (PSO) techniques.

- Intelligent controllers are introduced for the real-time balancing and position-tracking control of a 2-DOF ball balancer using
    i. PID with Integral ANTI-WINDUP controller with different velocity setpoints values
    ii. Neuro Integrated Fuzzy PID controllers with different V_{sw} values

- A continuous Linear Quadratic Gaussian (LQG) controller is proposed for optimal control of a rotary inverted pendulum to swing up the rotary inverted pendulum upward from its stationary downward position and maintain an equilibrium in the vertical upward position.

- A PID and Fractional Order PID ($PI^{\lambda}D^{\mu}$) controller with Integral ANTI-WINDUP technique is designed for swing-up and stabilization control of rotary inverted pendulum system by using metaheuristic optimization techniques. Simulation and real-

time experimentation analysis of the pendulum angle, rotary arm angle, controlled input voltage, transient response and steady-state response have been done for the proposed controllers. The proposed method is efficient in

    i.   keeping the pendulum balanced and preserving some degree of tolerance for a vertical upright position.

    ii.   bringing the pendulum out of its state of passive equilibrium to achieve balance.

    iii.   both reference tracking and rejection of external disturbances in comparison to the existing literature

Simulation and real-time experimental analysis have been done extensively to prove the efficacy of the developed solutions.

LIST OF PUBLICATIONS

Journal Papers

1. **Basant Tomar,** Narendra Kumar, Mini Sreejeth, "Augmentation in Performance of Real-Time Balancing and Position Tracking Control for 2-DOF Ball Balancer System Using Intelligent Controllers," *Wireless Personal Communications*, vol. 138, pp. 2227–2257, 2024, **SCIE**, (**IF: 1.9**), DOI: 10.1007/s11277-024-11591-5. (**Published**)

2. **Basant Tomar,** Narendra Kumar, Mini Sreejeth, "PLC and SCADA based Temperature Control of Heat Exchanger System through Fractional Order PID Controller using Metaheuristic Optimization Techniques," *Heat and Mass Transfer*, vol. 60, pp. 1585–1602, 2024, **SCIE**, (**IF: 1.7**), DOI: 10.1007/s00231-024-03509-5. (**Published**)

3. **Basant Tomar,** Narendra Kumar, Mini Sreejeth, "Robust control of Rotary Inverted Pendulum using Metaheuristic Optimization Techniques Based PID and Fractional Order $PI^\lambda D^\mu$ Controller," *Journal of Vibration Engineering & Technologies*, 2024, **SCIE**, (**IF: 2.1**), DOI: 10.1007/s42417-024-01399-9. (**Published**)

4. **Basant Tomar,** Narendra Kumar, Mini Sreejeth, "Real-Time Balancing and Position Tracking Control of 2-DOF Ball Balancer using PID with Integral ANTI-WINDUP Controller," *Journal of Vibration Engineering & Technologies*, vol. 12, pp. 5055-5071, 2023, **SCIE**, (**IF: 2.1**), DOI: 10.1007/s42417-023-01179-x. (**Published**)

5. **Basant Tomar,** Narendra Kumar, Mini Sreejeth, "Real Time Automation and Ratio Control Using PLC & SCADA in Industry 4.0," *Computer Systems Science & Engineering,* vol. 45, no. 2, pp. 1495-1516, 2022, **SCIE**, (**IF: 4.397**), DOI: 10.32604/csse.2023.030635. (**Published**)

6. **Basant Tomar,** Narendra Kumar, Mini Sreejeth, "A Smart PLC and SCADA based Control Framework for Automated Assembly Line in Process Industry with Effluent Ratio Control Strategy," *IEEE Transactions on Automation Science and Engineering,* 2024, **SCIE**, (**IF: 5.4**), (**Under Review**).

Conference Papers

1. **Basant Tomar,** Narendra Kumar, Mini Sreejeth, "Optimal Control of Rotary Inverted Pendulum Using Continuous Linear Quadratic Gaussian (LQG) Controller," In Proceedings of *14th International Conference on Computing Communication and Networking Technologies (ICCCNT)*, pp. 1-6, 2023. **(SCOPUS),** DOI: 10.1109/ICCCNT56998.2023.10306449. (**Published**)

2. **Basant Tomar,** Narendra Kumar, "Fuzzy Logic Based Braking System for Metro Train," In Proceedings of *IEEE International Conference on Intelligent Technologies (CONIT)*, pp. 1-4, 2021. **(SCOPUS),** DOI: 10.1109/CONIT51480.2021.9498360. (**Published**)

3. **Basant Tomar,** Narendra Kumar, "Method and System for Developing an Automated Assembly Line in a Chemical Process Plant," *International Conference on Innovations and Ideas Towards Patents (ICIIP 2021)*, **Official Journal of the Indian Patent Office**, Journal No. 35/21, (**Published**), Application No. 202111035331 A.

4. **Basant Tomar,** Narendra Kumar, "PLC and SCADA based System for Automating Industrial Operations," *International Conference on Innovations and Ideas Towards Patents (ICIIP 2021)*, **Official Journal of the Indian Patent Office**, Journal No. 37/21, (**Published**), Application No. 202111040407 A.

Patents

1. **Basant Tomar,** Narendra Kumar, "Method and System for Developing an Automated Assembly Line in a Chemical Process Plant," **Official Journal of the Indian Patent Office**, Journal No. 35/21, (**Published & Reply to FER Filed**), Application No. 202111035331.

2. **Basant Tomar,** Narendra Kumar, "PLC and SCADA based System for Automating Industrial Operations," **Official Journal of the Indian Patent Office**, Journal No. 37/21, (**Published and Under examination for Grant**), Application No. 202111040407.

TABLE OF CONTENTS

6. OPTIMAL CONTROL OF ROTARY INVERTED PENDULUM USING CONTINUOUS LINEAR QUADRATIC GAUSSIAN CONTROLLER   94-104

LIST OF TABLES

LIST OF FIGURES

function

LIST OF ABBREVIATIONS

DCS	Distributed Control Systems
PLC	Programmable Logic Controller
SCADA	Supervisory Control and Data Acquisition
B&P	Ball and Plate
PID	Proportional Integral Derivative
GA	Genetic Algorithm
ACO	Ant Colony Optimization
PSO	Particle Swarm Optimization
LQG	Linear Quadratic Gaussian
MATLAB	Matrix laboratory
VRC	Vapor Recompression
DWC	Dividing Wall Column
IP	Inverted Pendulum
RotIP	Rotary Inverted Pendulum
FLC	Fuzzy Logic Controller
SMC	Sliding Mode Control
FPID	Fractional Order Proportional Integral Derivative
MRAC	Model Reference Adaptive Controller
FOPD	Fractional Order Proportional Derivative
ITSE	Integral time square error
LQR	Linear Quadratic Regulator
HMI	Human Machine Interface
SOA	Service Oriented Architecture
SMPS	Switched Mode Power Supply
ICS	Industrial Control Systems
EtherCAT	Ethernet Control Automation Technology
CPR	Capacitive Proximity Sensors
IPR	Inductive Proximity Sensors

VFD	Variable Frequency Drive
LED	Light-emitting diode
BM	Blender DC Motor
MDRs	Motor Driven Rollers
STHEX	Shell and Tube Heat Exchanger
RTDs	Resistance temperature detectors
FOPTD	First Order Plus Time Delay
SOPTD	Second Order Plus Time Delay
O.H. Tank	Overhead Tank
PI	Proportional Integral
ISE	Integral Square Error
IAE	Integral Absolute Error
ITAE	Integral Time Absolute Error
DOF	Degrees of Freedom
PD	Proportional-Derivative
BB	Ball Balancer
SRV02	Servo Input Voltage
DAQ	Data Acquisition
1DBB	1D Ball Balancer
EOM	Equation of Motion
FBD	Free Body Diagram
PV	Proportional-Velocity
Ni-F	Neuro-Fuzzy Controller
ADRC	Active Disturbance Rejection Control
NiF-PID	Neuro-Integrated Fuzzy with PID
ANFIS	Adaptive Neuro-Fuzzy Inference System
RLQR	Reduced Linear Quadratic Regulator
VSAF	Variable Structure Adaptive Fuzzy
LQE	Linear Quadratic Estimator
SDA	Spiral Dynamic Algorithm

SIMO	Single Input Multiple Output
FMINCON	Find minimum of constrained nonlinear multivariable function
FOMCON	Fractional-Order Modelling and Control

Chapter 1

Introduction

1.1 BACKGROUND

A control system uses control loops to manage, command, and regulate the behaviour of various devices or systems. It can range from a single home heating controller to large industrial control systems for controlling various processes or devices. The control theory evolution emphasises on the methods of analytical controller design techniques, technological advancements, and the implementation of these techniques in real time [1]. The control system is an area that correlates with diverse disciplines and approaches, which leads to the development of an automatic decision-making process that improves the performance of control benchmark problems [2].

1.1.1 Automated Control Systems

In a technical context, automation is simply the management of any operation or the development and application of many technologies to generate final goods with very little human involvement [3]. As a result, all industries throughout the world are moving towards the automation concept of Industry 4.0 to examine the importance of digital manufacturing revolution principles [4]. Earlier, the industries relied heavily on human labour, which was costly in terms of both time and money and somewhat inefficient. However, automation has now eliminated all the drawbacks and decreased the likelihood of errors which eventually led to resource conservation [5,6]. Industry 4.0 can be viewed as a comprehensive method of integrating numerous machines, software, smart sensors & actuators and contemporary controllers in a structured way to organize, analyze, forecast and use the controller's information for complex industrial processes [7]. In the last ten years, the field of industrial automation has undergone a digital transformation to increase equipment efficiency, product/process

quality, flexibility, autonomy, interoperability, and overall productivity to achieve intelligent management of the manufacturing process in Industry 4.0 [8].

Automated control systems are used for temperature control of heat exchanger systems [9,10], automating real-time operations like assembly line balancing and ratio control in Industry 4.0. The improvement in production flexibility has a significant impact on the productivity of manufacturing systems with assembly lines. Assembly lines are unique flow-line manufacturing systems in industries producing a large quantity of standardized commodities [11]. The configuration planning of an assembly line is extremely important because of the high capital requirements, especially in the process control industry. A common limitation in assembly lines is the setup time between different operations. The most crucial procedure in process industries like beverage, chemical, pharmaceutical and paint industries is the ratio control where the mixing of raw ingredients and filling of final product composition takes place. There are many theoretical frameworks which use impedance spectroscopy, and robotic arm conveyors to fill the containers to a desired level. However, these methods face various difficulties in the process measurement, non-linearity compensation for sensors and multi-input multi-output.

The heat transfer processes account for more than 80% of global energy use today [12,13]. Heat exchangers are used for controlling the outlet fluid temperature of an industrial process such as chemical production [14], gas turbines, oil refineries [15], air conditioning, power generation etc. with respect to the variations in the operating conditions [16]. Temperature control systems are required to stabilize the temperature of many industrial processes to achieve an ideal value and enhance heat transmission efficiency.

1.1.2 Non-Linear Control Systems

Non-linearity plays a significant role in a nonlinear controlled process or in the controller itself. Nonlinear control systems are primarily used for the improvement of linear control systems. These are used for analysing the hard non-linearities, uncertainties and simple designs. A nonlinear controller can easily handle the implications of model uncertainties through robustness or adaptability. They can easily control a system that is not linearly controllable or observable. Nonlinear control systems are used in a variety of engineering applications such as automotive control, aerospace control, mechanical systems, industrial process control etc. A significant area of control has been the management of autonomous robots performing difficult tasks in dynamic environments like vehicle balancing [17,18] and position control [19], trajectory tracking and path planning [20-22] etc. In the past, numerous attempts have been made to control autonomous robots. There are a lot of control benchmark issues that are concerned with engineering systems like the inverted pendulum [23], the Furuta Pendulum [24,25], the beam and ball system [26], the hovercraft [27], and the ball and plate (B&P) system [28,29].

The Inverted Pendulum and ball balancer system are highly unstable underactuated mechanical systems having fewer inputs than the number of degrees of freedom. An inverted Pendulum is used as a benchmark in non-linear dynamics for testing various control techniques that require a pendulum to be controlled against its natural equilibrium position. The position tracking and balance control in robotic ball balancer systems is a widely researched problem because of its nonlinearity and instability. Generally, these systems find their application as benchmark systems for testing control laws and developing control strategies for problems related to the movement of robotic manipulators.

1.2   ASSOCIATED CHALLENGES

Industrial automation control systems integrate various devices, machines, and equipment inside a manufacturing plant. For a long time, field-bus technologies have been used in industrial automation because of their predictable characteristics. Rapid advancement in modern industries facilitates the gathering and transfer of factory data to the corporate world through an industrial control network for providing intelligent and highly productive real-time control of the plant.

However, most of the industrial plants have hard non-linearities, which makes it difficult to design and analyse closed-loop control systems in comparison to linear ones. However, a significant portion of the literature exists for conventional control through distributed control systems (DCS) to monitor and control all the system processes. Very little research is focused on Programmable Logic Controller (PLC) and Supervisory Control and Data Acquisition (SCADA) based real-time automation systems. A key challenge is relatively expensive hardware and the difficulty of integration with other network protocols.

Non-linear systems behave differently at different operating points and hence linear controllers designed for one operating point do not give a satisfactory performance at the other points. Additionally, it is not preferred for industrial applications due to its complexity, non-flexibility in tuning and poor reconfigurability. Many control techniques have been proposed in the past for stabilizing and swinging up the pendulum angle. Even though these control strategies are successfully used to regulate the inverted pendulum system's angular position with greater accuracy and oscillation dampening, but they have problems such as nonlinearities, time delays, chattering, discontinuity and higher order. The approaches in literature not only use a lot of energy but also do not eliminate fluctuations in control input and output signals. Additionally, there are large variations in control input signals that cause the system to become unstable. Some approaches have additional fluctuations and steady-state errors. Therefore, there is a need to design and develop a more stable, reliable, robust and high-performance controller to control the dynamics of rotary inverted pendulum.

Due to its intrinsic complexity, the ball balancer system has two key issues i.e. controlling point stabilisation and balancing the ball on a plate. Apart from linearization-based techniques, control of

underactuated mechanical systems has been mainly along the cascade nonlinear systems and using energy-based methods combined with supervisory-based switching control. Optimization techniques sometimes may get trapped in local minima due to their random and probabilistic nature. As a result, there will be glitches in results while optimizing real-time systems, which again provides a chance of improvement. Therefore, there is a need to find effective control design methods for a broad range of highly underactuated systems used in robotics and aerospace applications.

1.3 MOTIVATION

There is continual research geared towards studying and management of automated and non-linear control systems in tasks like assembly line balancing and ratio control in process industries, temperature of a heat exchanger and underactuated mechanical systems like inverted pendulum and ball balancer systems. However, there are several challenges in the course of their study and management. The main objective of this thesis is to develop effective control design methods for automated and non-linear control systems. The specific problems addressed in this thesis are as follows:

a) Currently, industries are using different production lines for producing different sizes & types of containers in the batch process which increases the assembly line setup cost and workforce cost. Therefore, centralized monitoring of critical production parameters is required to maintain a continuous flow of materials and avoid time delays between production regions.

b) There are only theoretical frameworks in the state-of-art for the ratio control of material flows, mixing of raw ingredients and filling of final product composition. An acceptable raw material ratio must be chosen quantitatively, accurately, and efficiently during the mixing of raw ingredients with adequate technology and without manual involvement.

c) It is difficult to control the temperature of a heat exchanger system because of its complex and nonlinear nature due to unknown fluid characteristics, non-causalities, time-varying qualities and ambiguous mechanics. Therefore, there is a need to design an effective control strategy and hardware design which regulates the outlet fluid temperature of a heat exchanger to a certain reference value and enhances the heat transmission efficiency irrespective of the external disturbances, non-linearity and delay characteristics.

d) A majority of methods for balancing and position-tracking control of ball balancers have complicated controller designs, and unwanted chattering and do not guarantee the convergence of balancing and tracking errors. Therefore, there is a need to introduce hybrid controllers for real-time balancing and position-tracking control of the 2-DOF ball balancer system that is used in robotic systems analysis.

e) The current state-of-art controllers for stabilisation control and swing-up control of rotary inverted pendulum are not totally independent of the optimum parameter setting and are not entirely insensitive to model uncertainties and disruptions. These controllers have inherent limitations like dependency on controller gains, latency in angular position sensing and the need of continuous tuning. Therefore, an energy-efficient controller with less computational complexity is needed to stabilize the pendulum when it swings up closer to the upright equilibrium position.

1.4   SCOPE AND OBJECTIVES OF THE THESIS

Automation is required in diverse fields of scientific and technological applications specifically in real-time control and management of various applications and industries. Automation assures improved monitoring and control to enhance the quality of work performed by control systems. Whereas, non-linear systems are primarily used for the improvement of linear control systems, analysing hard nonlinearities and uncertainties in various control benchmark systems like the inverted pendulum, and the ball balancer systems. This motivated the development of new control design methods for different classes of both automated and nonlinear control systems. As a result, the main body of this thesis involves the following topics:

- **Industrial automation and control.** Automated control systems are used for temperature control of heat exchanger systems, automating real-time operations like assembly line balancing and ratio control in Industry 4.0. Heat exchangers are used to control the outlet fluid temperature of an industrial process with respect to variations in operating conditions. Temperature control systems are required to stabilize the temperature of many industrial processes to achieve an ideal value and enhance heat transmission efficiency.

- **Control the dynamics of underactuated systems.** There are a lot of control benchmark issues associated with highly unstable underactuated mechanical systems like the Inverted Pendulum and ball balancer systems. The inverted pendulum is used as a benchmark in non-linear dynamics to control a pendulum against its natural equilibrium position. Ball balancer systems are used as benchmark systems for testing control laws, position tracking and balance control of robotic manipulators because of their nonlinearity and instability. These controllers for these underactuated systems have inherent limitations like dependency on controller gains, latency in angular position sensing and the need for continuous tuning.

Effective control design methods are required for automated and non-linear control systems for various reasons and challenges associated with getting the information in real-time which have been discussed in section 1.1.

The following are the objectives of the thesis:

❖ The improvement in production flexibility has a significant impact on the productivity of manufacturing systems with assembly lines. In order to increase the throughput of the process industry plant, the idle time between the batch processes must be eliminated by improving the existing design with proper modifications so that the task duration of each workstation can be reduced to match the cycle time for maximizing profits. Thus, a smooth flow of work is required for balancing and optimization of assembly lines along with an effluent ratio control strategy with minimal bottlenecks.

❖ Temperature control has a common time delay issue that negatively impacts the performance and stability of controlled systems. Temperature control of heat exchanger systems is challenging due to difficulties like strong non-linearity, disturbance, uncertainties, large response and delay time of the controlled objects which further results in uncontrollable feedback for precise control. In the presence of external interference, the current conventional control approaches exhibit high-temperature fluctuation and longer stability correction times. Therefore, an effective control strategy and hardware design is required to maintain a smaller temperature fluctuation amplitude around the desired temperature value for a fluid and heat transfer system.

❖ Non-linear systems behave differently at different operating points. Some of the major challenges associated with the dynamics of underactuated systems are the latency in angular position sensing, chattering, discontinuity, the need for continuous tuning and dependency on controller gains. The approaches in the literature not only use a lot of energy but also have large variations in the control input signals that cause the system to become unstable. Therefore, there is a need to develop robust and optimal techniques for the balancing and position-tracking control of the ball balancer, and swing-up and stabilization control of the rotary inverted pendulum.

1.5   CONTRIBUTIONS IN THE THESIS

The problems mentioned in section 1.2 provides the motivation to come up with their solutions which are presented in detail in this thesis. In this thesis, effective solutions have been put forward to address the challenges of assembly line balancing and ratio control in process industries, temperature control of heat exchanger systems, real-time balancing and position tracking control of 2-DOF ball balancer systems, stabilisation and swing-up control of rotary inverted pendulum. The main contributions of the work done in this thesis are as follows:

i. A PLC and SCADA-based control framework is proposed to address a dynamic real-time problem of an automated assembly line in the process industry with an effluent ratio control strategy for the mixing of raw materials, filling of final product composition, capping, labelling and sorting of containers on the basis of both size and type using a single assembly line. The developed model is applied to a real-life case study of an assembly line from a chemical processing industry in north India to verify the design for effectively balancing a real-world assembly line in a process industry.

ii. Real-time monitoring and control strategies have been developed to automate the processes in the heat exchanger plant. In these techniques, a simulated prototype of PLC and SCADA-based control framework is designed to control the temperature of a heat exchanger system through Proportional Integral Derivative (PID) and Fractional Order PID ($PI^\lambda D^\mu$) controllers and the performance of the controllers is optimized using Genetic algorithm (GA), Ant Colony Optimization (ACO) and Particle Swarm Optimization (PSO) techniques.

iii. For the real-time balancing and position tracking control of a 2-DOF ball balancer, different compensators like PID with Integral ANTI-WINDUP and neuro-integrated fuzzy PID controllers with different V_{sw} values along with different inputs are implemented over the ball balancer system. The ball position, input voltage and plate angle comparisons were executed with different compensators for both simulation and real-time experimentation purposes.

iv. A continuous Linear Quadratic Gaussian (LQG) controller is proposed for optimal control of the rotary inverted pendulum to swing up the rotary inverted pendulum upward from its stationary downward position and maintain an equilibrium in the vertical upward position.

v. A PID and Fractional Order PID ($PI^\lambda D^\mu$) controller with the Integral ANTI-WINDUP technique is designed for the robust swing-up and stabilization control of a rotary inverted pendulum system using metaheuristic optimization techniques. Simulation and real-time experimentation analysis of the pendulum angle, rotary arm angle, controlled input voltage, transient response and steady-state response have been done for the proposed controllers. The proposed method is efficient in keeping the pendulum balanced while maintaining both reference tracking and rejection of external disturbances in comparison to the existing literature.

1.6   OUTLINES OF THE THESIS

The thesis layout is as follows:

1. **Chapter 1: Introduction**

   Chapter 1 discusses the nature and significance of automated control systems and non-linear control systems along with the challenges associated with them. Contributions and thesis layout are also discussed.

2. **Chapter 2: Literature Review**

   Chapter 2 discusses a detailed study of the various automated control systems and non-linear control systems. This chapter covers the existing state-of-the-art techniques for automating real-time operations in Industry 4.0, balancing and tracking of 2-DOF ball balancer system, control of inverted pendulum and temperature control system for heat exchangers.

3. **Chapter 3: PLC and SCADA-based control framework for automating real-time operations in Industry 4.0**

   This chapter discusses a PLC and SCADA-based control framework to address a dynamic real-world problem of balancing an assembly line in a process industry plant, a ratio control framework for adjusting the ratio and mixing of raw materials, filling of final product composition, capping, labelling and sorting of containers on the basis of both size and type using a single assembly line and monitoring all the processes using a single screen HMI.

4. **Chapter 4: Temperature control of a heat exchanger system**

   This chapter presents a PLC and SCADA-based control framework to automate and supervise the temperature control processes in the heat exchanger plant. The temperature of the heat exchanger system is controlled through PID and Fractional Order PID controllers with Integral ANTI-WINDUP technique and the performance of the controllers is optimized using GA, PSO and ACO optimization techniques.

5. **Chapter 5: Real-time control of 2-DOF ball balancer system using intelligent controllers**

   This chapter presents a technique for real-time balancing and position tracking control of a 2-DOF ball balancer using a neural-fuzzy PID controller and PID with Integral ANTI-WINDUP controller with different velocity setpoints values.

6. **Chapter 6: Optimal control of rotary inverted pendulum using continuous Linear Quadratic Gaussian controller**

   This chapter presents a continuous Linear Quadratic Gaussian (LQG) controller based on the optimal control strategy for swinging up the rotary inverted pendulum and maintaining an equilibrium in the vertical upward position. Gradient descent and algebraic descent are the numerical methods used for obtaining optimal control functions.

7. **Chapter 7: Robust control of rotary inverted pendulum using metaheuristic optimization techniques based PID and Fractional Order PID controller**

   This chapter presents an approach for the modelling and optimal design of a PID and Fractional Order PID controller with an Integral ANTI-WINDUP technique along with variable velocity setpoints for the stabilization and swing-up control of a rotary inverted pendulum system by using metaheuristic optimization techniques.

8. **Chapter 8: Conclusions, Future Scope and Social Impact**

   In this chapter, a brief summary of all the ideas, observations and contributions of each objective is presented. Also, future scope and social impact are outlined.

Chapter 2

Literature Review

2.1 INTRODUCTION

As discussed in the previous chapter, our contributions to the thesis are in the areas of automated and non-linear control systems. Therefore, this chapter discusses the state-of-art in the areas of automated control systems which include (a) assembly line balancing and ratio control techniques in Industry 4.0 (b) techniques for temperature control of heat exchangers; and non-linear control systems which include (a) methods for balancing and position tracking control of ball balancer system (b) techniques for balancing and swing-up control of inverted pendulum.

2.2 ASSEMBLY LINE BALANCING AND RATIO CONTROL TECHNIQUES IN INDUSTRY 4.0

Assembly lines are unique flow-line manufacturing systems in industries producing a large quantity of standardized commodities. The improvement in configuration planning and production flexibility also has an impact on the productivity of manufacturing systems with assembly lines because of the high capital requirements. Ratio Control is the most crucial procedure in the process industries for the mixing of raw ingredients and filling the final product composition. An adequate raw material ratio must be chosen quantitatively and efficiently during the mixing process without any manual involvement. Pardi et al. [4] reviewed the evolution of automotive manufacturing technologies and organizations and analyzed the impact of "4th industrial revolution" concepts on their current transformations for employment and work, to assess the potential of the digital manufacturing revolution (Industry 4.0) in the automation sector.

In the past, various researchers have worked to overcome the difficulties in balancing the assembly lines [30,31]. Christler et al. [6] introduced the importance of semi-automated process analytics to reduce the operator-specific influence on test results of typical analytical methods using liquid handling stations for different biochemical tests like binding affinity and endotoxins. Huo et al. [32] proposed a type-1 fuzzy control system to monitor, control and re-balance a real-time assembly line and a type-2 fuzzy control system for adjusting the production rates to decrease the workload of workstations. The machine's health condition is monitored using a three-state Markov Chain. Geurtsen et al. [33] suggested a deep Q-reinforcement learning technique to address the complex problem of assembly line maintenance and planning using a Markov decision process. Didden et al. [34] proposed a genetic algorithm-based approach to overcome the difficulties in balancing of assembly lines in the automotive sector, which can be used as a decision support system for mixed-model production.

Ghita et al. [35] proposed a theoretical framework for the ratio control of material flows in the pharmaceutical sector using impedance spectroscopy which continuously monitors and detects changes in different fluids and porous material properties. Sreejeth et al. [36] developed a PLC-based experimental design prototype of a liquid mixing and bottle-filling system which mixes two different liquids in predetermined quantities. However, these methods face various difficulties in process measurement, non-linearity compensation for sensors and issues in multi-input multi-output.

Communication protocols play an important role in the automation industry. By merging variable sampling and predictive control techniques, Rahmani et al. [37] presented a scheme for internet-based control of linear automation systems. When actuators receive a new control input signal from the controller, sensors are activated to sample the plant outputs (based on data-driven events). This method offered an easier way of analyzing closed-loop stability in comparison to other methodologies. Zegzhda et al. [38] reviewed the classic DA/HDA/A&E protocols based on Microsoft DCOM and RPC technologies and discussed the vulnerabilities of industrial automation protocols of the OPC series. The methods of Ethernet-compatible real-time protocols such as PROFINET, EtherNet/IP, Powerlink, EtherCAT, Foundation Fieldbus HSE and Modbus TCP were studied by Aristova et al. [39] along with the characteristics and application domains of Wireless Ethernet networks.

2.3 TECHNIQUES FOR TEMPERATURE CONTROL OF HEAT EXCHANGER

The primary goal of designing control techniques for Heat exchangers in industrial processes is to increase energy efficiency. Heat exchanger systems are mostly used in industrial process applications including chemical production processes, boilers and turbines, power generation, refrigeration [40],

and petroleum industries [41] etc. for transferring thermal energy between hot and cold fluids through a solid wall to control the temperature levels of unit operations for the smooth production process and energy-efficient operations [42]. Heat exchangers can withstand tremendous pressure by maintaining a specific temperature condition for controlling the outlet fluid temperature with respect to the variations in the operating conditions. Therefore, some adequate control schemes must be designed for controlling the temperature of a heat exchanger system.

Temperature control algorithms have been widely studied in the process industries [43,44]. Proportional Integral Derivative (PID) controllers are most commonly utilized for temperature control in many industrial applications due to their simplicity and applicability [45,46]. However, it is very difficult to identify the optimal PID parameters in the controller design to obtain the optimal system performance [47,48]. The evident overshoot in the control cannot be eliminated by the conventional PID controllers.

Advanced control methods such as model predictive control [49], Fractional order PID [50], disturbance-observer-based control [51], fuzzy control [52] and neural network control [53] are used in case of difficulties like large inertia, time delay, and multiple disturbances in the temperature control process. Al-Dhaifallah et al. [54] proposed a fractional-order fuzzy PID controller for the temperature control of a tubular heat exchanger under load variation within the reference environment. The parameters of fractional-order controllers are changed via a rule-based fuzzy logic control method in order to have improved control performance, resilience and flexibility than conventional PID control schemes. Lu et al. [55] proposed composition-temperature cascade control strategies for controlling the vapour recompression (VRC) assisted dividing wall column (DWC) with side condenser and reboiler process configurations. These control structures provide high energy efficiency and effective controllability for the industrialization of side heat exchanger processes.

Bobič et al. [56] proposed a 1D discretized lumped-parameter system based on the finite volume method to understand the dynamic properties such as inlet and outlet temperature disturbances and various fluid flow configurations of a counterflow plate heat exchanger. The predicted transient responses due to temperature disturbances are experimentally verified by using infrared thermography technology tests. Damasceno et al. [57] presented the modelling and simulation of a PI controller for a shell and tube heat exchanger where the controller parameters are tuned and optimized using different techniques like bat algorithms, particle swarm optimization (PSO), flower pollination algorithm and cuckoo search algorithm to get the best transient response.

Xu et al. [58] proposed an Adam optimization-based recurrent neural network controller with an integral-PD controller for the temperature control of a single-phase hotplate system. The RNN controller was driven by a reference model and feed-forward controller to provide better learning reference. Hussein et al. [59] introduced an adaptive PID control technique for the temperature control of electric furnaces in industrial applications which used the balloon effect and whale optimization

algorithm for tuning the parameters of the controller. Zeng et al. [60] proposed a control design for analyzing the outlet temperature and performance of the temperature control unit over the frequency domain to achieve optimal attenuation, high precision and environmental adaptability.

2.4 REVIEW OF CONTROL TECHNIQUES FOR 2-DOF BALL BALANCER SYSTEM

Underactuated systems are those MECHATRONIC systems that have fewer degrees of actuation such as pendubot [61], flexible joint robot [62,63], inverted pendulum [64], acrobot [65], translational oscillator with rotational actuator [66], etc (see Fig. 2.1).

(a)   **(b)**
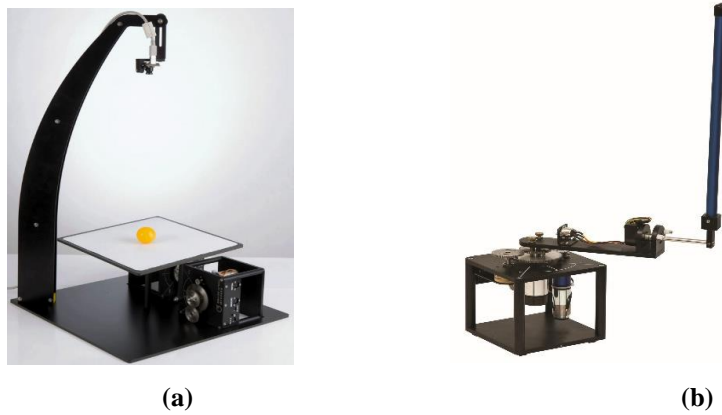
Figure 2.1. Examples of underactuated systems **(a)** Ball Balancer System **(b)** Inverted pendulum

Ball Balancer System is used for position tracking and balancing control in robotic systems. It is used for testing and developing control strategies for benchmark systems like vehicle balancing [67] and position control [68], trajectory tracking [69], vertical take-off aircraft, path planning [70], vertical thrust control in rockets [71], etc. In order to adhere to all real-time requirements for position tracking and balance control, various studies have been conducted by researchers in the past. Various controller architectures like fuzzy [72], sliding mode [73], Linear Quadratic control [74-76], PID controller [77] and metaheuristic techniques [78] have been used in the past for trajectory tracking, stabilization and control of ball balancer system.

Conventionally, classical controllers made their way to be implemented with these systems. The proportional-derivative and PID controllers were applied with the B&P system for the closed-loop system stability [79]. Hadoune et al. [80] proposed a scheme based on a classical PID controller and Lead/lag compensator in a double loop feedback for precise/point-to-point stabilization of the B&P system with a minimal tracking error.

Okafor et al. [81] developed a deep reinforcement learning-based PID controller for controlling and tracking the trajectory of a linearized B&P system, which used a customized deep deterministic policy gradient agent by altering the neural network architecture. However, these systems do not

guarantee the convergence of balancing and tracking errors. Oglah et al. [82] proposed a chicken swarm optimization-based multi-fuzzy control technique for 2D position control of the B&P system. However, the problem with fuzzy controllers is that they are difficult to tune with accurate system knowledge.

Khan et al. [83] proposed an integral sliding mode control (SMC) based linear parameter varying technique for stabilizing the dynamics of a laboratory-based ball and beam system. The switching controller i.e. vulnerable to Lyapunov stability theory, based on non-linearity analysis was used in classical control theory to follow the trajectory of a ball [84]. Mohammadi et al. [85] applied a neural network-based feedback controller on a B&P system in which two sub-controllers worked in parallel to reduce the dynamic errors in controller design.

2.5   REVIEW OF CONTROL TECHNIQUES FOR ROTARY INVERTED PENDULUM

An inverted pendulum (IP) is classified as an inherently unstable, non-linear and underactuated mechanical system in the control theory [86,87]. It has been used as a suitable benchmark system for training, testing and validating the effectiveness of different control and robotic systems for a long decade [88]. Cart-type IP, double IP and single-arm Rotary Inverted Pendulum (RotIP) are the most prevalent kinds of IP found in control laboratories. RotIP is commonly known as Furuta Pendulum which was initially developed by Katsuhisa Furuta in 1992 [89]. RotIP is a multivariable 4th-order nonlinear and open-loop dynamical system [90]. It is a modified version of the cart-type pendulum. Many real-life applications such as Segways [91], hoverboards, aircraft landing [92], rocket and spacecraft systems, robotics [93,94], industrial engineering systems like locomotives, marine systems and crane applications [95] work on the foundation of RotIP.

In order to deal with uncertainties and disruptions in the RotIP, a number of resilient control techniques such as linear quadratic controller [96,97], Lyapunov methods [98-100], PID control [101,102], Neural network [103,104], reinforcement learning [105,106] fuzzy logic controller (FLC) [107,108], SMC [109-111], genetic algorithm controller [112], adaptive controller [113,114] and many more [115-117] have been introduced in the last few decades to control and stabilize a RotIP in upright position. Stabilization control and tracking control have received the most attention due to their widespread use.

2.5.1   Traditional Control Techniques

Mehedi et al. [118] used a fractional order integral control scheme for stabilizing an extremely nonlinear rotary double inverted pendulum. This method used a state space fractional order integral

controller which was designed on the basis of Bode's transfer function. However, the procedure of tuning increases the complexity of the fractional order integral control scheme. The tuning process becomes more challenging and time-consuming when there is an increase in the number of inputs and outputs of the controller. A Lyapunov function-based backstepping LQG controller was introduced for balancing and controlling the angular displacement of the pendulum [119]. However, these controllers are not totally independent of the optimum parameter setting and are not entirely insensitive to model uncertainties and disruptions. Due to its simple architecture and dependability across numerous operating conditions, the standard PID controller performs very well for linear systems [120,121]. El-Sousy et al. [122] proposed an adaptive PID-SMC technique in combination with the super-twisting algorithm for the finite stabilization of RotIP in the presence of external disturbances. The state-space model of RotIP was achieved and the stability control was verified by using Lyapunov stability theory. However, PID controllers have inherent limitations like dependency on controller gains, latency in angular position sensing and the need for continuous tuning.

Various researchers have worked in the domain of nonlinear control algorithms like adaptive control, neural networks, backstepping control, fuzzy control and fractional order controllers to address the shortcomings of linear control methods in controlling the RotIP system. An adaptive neural network control technique was suggested for Furuta pendulum in steady state as a 2-DoF underactuated nonlinear system [123]. The non-linear oscillatory response of a RotIP was both analytically and experimentally investigated with a feedback-stabilized controller by Dolatabad et al. [124]. The measurement and 3-dimensional modelling of the actual system components were used to obtain the parameter values of a precise 2-DoF mathematical model that was derived using Lagrange's equations. However, feedback linearization requires a lot of complex computations to determine the ideal control input trajectory and sometimes removes the useful nonlinear components of the system.

2.5.2 Fractional Order Control Techniques

On the other hand, a lot of researchers are using fractional order controllers [125,126] to get the most robust and reliable system performance. A hybrid pole placement feedback controller was proposed in [127] for tracking and stabilizing input-output feedback linearized RotIP with an optimized PID and Fractional Order PID (FPID) controller using the PSO algorithm. This hybrid FPID controller was then compared with the Genetic Algorithm (GA) search to develop the subsequent model reference adaptive controllers (MRAC) with PID and linear quadratic regulator (LQR) controllers to analyse their tracking, stabilization and robust performance for adapting to different reference signals. However, the drawback is that this method only realized the ''virtual'' actuation of a 2-DOF RotIP system with only one actuator. Mondal et al. [128-130] proposed various versions of fractional order PID controllers to stabilize a cart-type pendulum system. The real-time implementation of cascaded structures of two different and distinct dual formations of fractional order PI-PD controllers has been

done in [128] using the classical control theory. In another work, an FPID controller was used to stabilize the controller Cart-IP System. The controller parameters were selected using an Integral time square error (ITSE) non-linear fitness function and evolutionary optimization techniques were used to tune the parameters [130]. This lacks the characteristics of robustness because of less accuracy and dependability. Balogh et al. [131] investigated an approach in which the feedback law was obtained by combining FOPD feedback with a single delay and PD feedback with two delays for the stabilization of the IP system. Even though these control strategies were successfully used to regulate the IP system's angular position with greater accuracy and oscillation dampening, they have problems such as higher-order nonlinearities, time delays, chattering and discontinuity.

2.5.3 Robust Control Techniques

Some researchers have worked on the concept of robust control of non-linear systems. The behavioural characteristics of the RotIP have been compared in the literature to show a robust performance. Saleem et al. [132] presented an optimized self-tuning Fractional-order Proportional-Derivative controller for improving attitude stabilization and minimizing the deviations in trajectories of a RotIP system. The PSO algorithm was used to determine the power of the fractional derivative operator for every controller and the hyperparameters of the nonlinear gain-adjustment functions. Mehedi et al. [133,134] implemented a constraint-based robust generalized dynamic inversion approach for the robust stabilization and tracking of 3-DoF rotary double IP system by realizing the Moore–Penrose generalized inversion-based constraint dynamics. Constraint differential equations and SMC-based switching elements were incorporated for the robust performance of the closed loop against any disturbance and uncertainties. These approaches not only use a lot of energy but do not eliminate fluctuations in the control input and output signals.

2.5.4 Optimization Algorithms-based Control Techniques

Parameter tuning can be done in different ways like trial-and-error method and using different evolutionary algorithms. Neha et al. [135] proposed an adaptive super-twisting SMC approach for the balancing and trajectory tracking of the RotIP system. Adaptive law was used to select the gains of SMC, and a modified GWO algorithm was used to adjust the parameters of the adaptation law. The overall stability control is verified by using the Lyapunov stability theory. ŞEN et al. [136] proposed a state feedback controller approach for the pole placement of RotIP to stabilize it at an upright position. The pendulum dynamics were used alone for designing the first state feedback controller, and a GA search was used to develop the subsequent controllers. Babushanmugham et al. [137] developed a sliding mode controller to stabilize an IP system by optimizing the parameters using GA and PSO techniques. Simulation results showed that PSO-SMC generates better responses as

compared to SMC and GA-SMC control strategies in time domain analysis. For balancing the rotary IP system in an upright unstable equilibrium state, Hamza et al. [138] presented a cascade interval type-2 fuzzy proportional derivative controller whose parameters are optimized using GA and PSO techniques. Blondin et al. [139] suggested a comprehensive optimization strategy that uses an Ant Colony Optimization algorithm in conjunction with a constrained Nelder-Mead algorithm and a cost function to simultaneously tune the swing-up, stability, and switching mode parameters. However, there are large variations in the control input signals that cause the system to become unstable.

2.6 SUMMARY

The literature review reveals a need for further research into enhancing investigations on automated and non-linear control systems using different control schemes. Current research in automated systems has focused mostly on industrial automation and control whereas non-linear systems have been used mainly for the improvement of linear control systems, analyzing hard nonlinearities and uncertainties in a lot of control benchmark systems. There is a need for further research on the supervision, monitoring and control of assembly line balancing, ratio control and temperature control of heat exchangers in process control industries. Finally, more research is needed to develop, implement and replace tones of hard-wired controllers like relays, timers, and traditional controllers. Furthermore, research is required to develop novel control schemes for the real-time balancing and control of underactuated systems like the inverted pendulum, and ball balancer systems.

Chapter 3

PLC and SCADA-Based Control Framework for Automating Real-Time Operations in Industry 4.0

3.1 INTRODUCTION

SCADA systems play an important role in tracking the behavior of critical process variables and connecting geographically dispersed subsystems at the industrial plant level. The majority of critical infrastructure networks like electricity production, mining deposits, natural gas, oil pipelines, heating systems and chemical product distribution use SCADA for monitoring, control and supervision. This chapter presents a PLC and SCADA-based control framework to automate the process industry plant and monitor all the processes using a single-screen HMI. This chapter aims to address a dynamic real-world problem for the mixing of raw materials, filling of final product composition, capping, labelling and sorting of containers based on both size (small and large) and types (metallic and non-metallic) using a single assembly line. In this context, a ratio control framework is proposed for adjusting the ratio and mixing of raw materials. The OMRON (NX1P2-9024DT1) PLC controls the entire process and programming of OMRON NX1P2-9024DT1 PLC is done using Sysmac studio automation software using the ladder programming language. Wonderware Intouch SCADA software is used for visualizing the two stages independently. A mathematical and simulation model is proposed to minimize the assembly line timings, the workforce and overall cost of production. The developed model is applied in a real-life case study of an assembly line from a chemical processing industry in north India. In addition, the results of a real-world case study verify the design for effectively balancing a real-world assembly line and show that the proposed system improves the productivity, efficiency, throughput, workforce, cost and time of the process industry.

3.2 RELATED WORK

The configuration planning of assembly lines is extremely important in industrial manufacturing systems for producing a large number of standardized commodities with the help of unique flow-line capacity and high capital requirements [140]. In the past, various researchers have worked on to overcome the difficulties like setup time between different operations in the balancing of assembly lines, particularly in process industries. Rossit et al. [141] introduced an approach for resequencing the workflow, analyzing and supporting the late customization strategies in assembly line production systems along with a method for solving the tolerance scheduling and non-permutation sequence problems. Pilati et al. [142] proposed a method for balancing multi-manned assembly lines and scheduling activities for highly customized manufacturing of products by organizing the accessories into clusters based on a certain similarity index and necessitating a significant mounting time to avoid overloads before assigning tasks and accessories to operators. Schmid et al. [143] proposed an optimization approach that simultaneously integrates the assembly line balancing and feeding decisions using a logic-based Benders' decomposition framework. Ling et al. [144] proposed a data-driven synchronous reconfiguration for assembly cell line workshops for monitoring and analyzing the real-time operation process within the conveyor line by using industry 4.0 technologies.

The most crucial procedure in process industries like beverage, chemical, pharmaceutical and paint industries is the mixing of raw ingredients and filling of final product composition. An acceptable raw material ratio must be chosen during the mixing of raw ingredients with adequate technology and without manual involvement. Various PLC and SCADA-based bottle filling, capping, warehouse management and lighting systems have been presented in [145-148]. An automatic liquid filling system was designed for small-scale industries with a robotic arm conveyor managed by gear motors and an Arduino controller that automatically fills containers to a desired level [149]. The system used an IR proximity sensor to sense the bottle and an ultrasonic sensor to identify the level of liquid. Kiangala et al. [150] developed a decentralization method for real-time monitoring, tracking and controlling the different stages of the bottling process in a small beverage plant by implementing Industry 4.0 concepts using a Siemens S7-1200 PLC and ZENON SCADA human-machine interface (HMI) for simulation.

The industrial communication systems also play an important role in the management and control of a process industry. Kannan et al. [151] highlighted the challenges and future directions in smart process measurement and automation. It also discussed the problem of multiple input-output and confined nature of the industrial processes and non-linearity compensation for sensors. It mainly focused on the measurement of smart process parameters, uncertainty and noises in automated industries. Gil et al. [152] introduced a method for the integration of various open communications protocols like MQTT, LoRaWAN, HTTP REST and OPC UA into an IoT platform and interoperable

architecture for automated industry applications. The OPC UA protocol integration allows for more data-driven applications in automated industrial plants. OPC UA has a Service Oriented Architecture (SOA) for automation networks that uses an appropriate data model to describe variables, objects procedures and services. Even though a lot of research has been done to overcome the difficulties in balancing of assembly lines, there is still a lack of research considering real-world case studies, especially in the process control industries.

3.3   PROBLEM STATEMENT

The throughput of production has a significant impact on the balancing and optimization of assembly lines which ensures a smooth flow of work with minimal bottlenecks and maximum profits. Currently, industries are using different production lines for producing different sizes or types of containers in the batch process which increase the assembly line setup cost and workforce cost. Containers are filled in batches with the same type of composition in them which takes huge idle time during the transition from one batch to another to produce different types of products within the same production line. There are various limitations in automation industries such as non-linearities, uncertainties, noise, large cycle time, etc. Therefore, centralized monitoring of critical production parameters is required to maintain a continuous flow of materials and avoid time delays between production regions.

The objective of this chapter is to envision or anticipate the automated process industry plant. This chapter is divided into two stages: the first stage shows the method for adjusting the ratio and mixing of raw materials, and the second stage shows the filling, sorting, capping and labelling operations of the proposed assembly line using a SCADA system. Each stage is controlled by two different OMRON NX1P2-9024DT1 PLC. The ladder logic of PLCs is designed using OMRON's Sysmac studio automation software and Wonderware Intouch SCADA software is used for visualizing the two stages independently. To the best of our knowledge, no other work in the literature has taken into account all of these constraints at the same time. The main contributions of this chapter are as follows:

- Developing a PLC and SCADA-based control framework to automate the process industry plant and monitor all the processes through a single-screen HMI.
- Presenting a ratio control framework for adjusting the ratio and mixing of raw materials.
- Considering/Addressing a dynamic real-world sequencing problem for the mixing of raw materials, filling of final product composition, capping, labelling and sorting of containers on the basis of both size (small and large) and type (metallic and non-metallic) using a single assembly line.

- Addressing the smooth and precise movement of the conveyor system based on highly accurate photoelectric sensors.

- Improving the overall productivity and throughput of the process industry plant with an improved assembly line design with proper fixtures/modifications in the existing design for eliminating the idle time between the batch processes by utilizing the proper resources.

- Developing a mathematical and simulation model to minimize the assembly line timings, the workforce and overall cost of production.

- Validation of the simulation and mathematical models, using a real-world problem from the process industry

- Comparing the effectiveness of the proposed methods in the real world by a case study.

3.4 EXPERIMENTAL ARCHITECTURE OF PROPOSED SYSTEM

This section provides the experimental architecture of the proposed system along with the software, hardware and communication protocol for OMRON NX1P2-9024DT1 PLC and SCADA.

3.4.1 OMRON NX1P2-9024DT1 PLC and SCADA

PLCs are extensively used in automation and manufacturing industries due to their ease of programmability, reliability, less scan cycle time, easy troubleshooting, and fewer hardware failures than tones of wired controllers such as timers and relays [153,154]. The proposed system uses OMRON (NX1P2-9024DT1) PLC, which can handle multiple input and output operations at a time. Table 3.1 shows the specifications of Omron NX1P2-9024DT1 PLC. PLCs are used for the control operations of a real-time control process so that the received voltage signals are not hindered. OMRON (NX1P2-9024DT1) PLC needs a regulated power source to operate, preferably one with a 24V DC output. A specially fabricated circuit known as a switched mode power supply (SMPS) produces a controlled DC power supply from an unregulated DC/AC voltage source. SCADA systems have witnessed enormous changes to their capabilities, architecture, and usefulness in industrial control systems (ICS) during the last three decades. The ICS networks/industrial automation system includes various types of embedded devices, field-level sensors and actuators, control-level PLCs, and human-machine interfaces for supervisory control. SCADA system collects the data, performs necessary control operations and then displays the information on the HMI screen for system monitoring. The whole operation of the proposed system is controlled by the SCADA server as shown in Fig. 3.1. To control automated processes, sensors, buttons, process state variables, and other devices are used by PLCs to monitor the status of inputs. The SCADA server receives periodic status updates from the PLC devices and stores those details in a database. The required tasks are completed by the PLC devices as directed by the SCADA server.
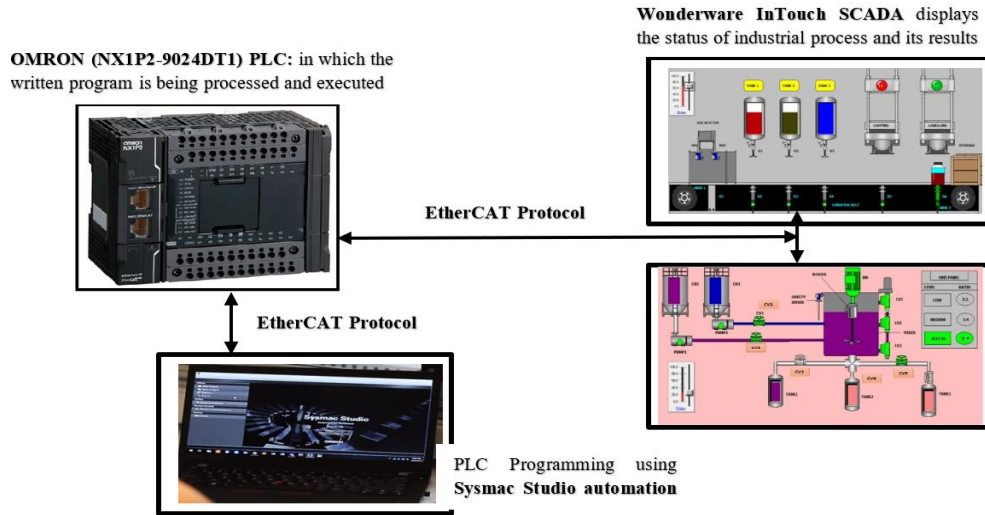
Figure 3.1. Experimental architecture of the proposed assembly line balancing and ratio control system

Table 3.1. Specifications of Omron NX1P2-9024DT1 PLC [155]

S. No.	Specifications of Omron NX1P2-9024DT1 PLC	
1.	DC Supply voltage	20.4V-28.8 V
2.	Scan cycle time	2ms
3.	Number of digital inputs	14
4.	Number of digital outputs	10
5.	Input type	NPN/PNP
6.	Output type	PNP
7.	Maximum number of expansion units	8
8.	Maximum number of remote I/O nodes	16
9.	Communication port(s)	EtherCAT Master, EtherNet/IP, Ethernet TCP/IP
10.	Number of Ethernet ports	2
11.	Communication option(s)	Serial RS-232C, Serial RS-422, Serial RS-485
12.	Real-time clock	✓

3.4.2 Communication Protocol for PLC and SCADA

The most crucial step in any industry is the communication between PLC & SCADA, which is now made possible with a PC and wireless devices. Communication with programmable logic controllers happens over industrial protocols. Earlier, the RS-485 standard was used for defining the electrical properties of drivers and receivers in serial communication systems. However, there are architectural cyberthreat flaws in the OPC series of industrial automation protocols [38]. The proposed system uses EtherCAT (Ethernet Control Automation Technology) protocol for connecting the PLC devices and SCADA server. For automation networks, the EtherCAT protocol offers an architecture that employs a suitable data-driven model to define objects, variables, services and procedures [156,157]. EtherCAT protocol is used in industrial control system networks because of its high speed, low hardware cost, wide range of products, low latency/delay, flexible topology support and incredible

synchronization than other real-time protocols. EtherCAT protocol supports UDP/IP-based routing, device level and factory-level communication in critical infrastructures.

3.4.3 Software System for Programming PLC and Interfacing with SCADA

The Sysmac studio automation software tools package from the OMRON portal is used to program, develop and configure OMRON NJ/NX-series PLCs. It is used to program NJ/NX-series machine automation controllers using the Ladder programming language. The OMRON (NX1P2-9024DT1) PLC is interfaced with the Wonderware InTouch SCADA system to gather data, carry out the necessary control operations, and display this data on the HMI screen. Wonderware InTouch SCADA system is used to develop HMI screens for supervision by offering an advanced visualization system with a variety of powerful functions for monitoring automation processes for all fields in the process control industry. The HMI interface is capable of reading values from system inputs like sensors, push buttons and regulating actuators using the program in the PLC. The extensive collection of objects and graphic components offered by the Wonderware InTouch library is used to build HMI panels for tracking and controlling production time and monitoring machine inputs and outputs. Push buttons, valves, conveyors, solenoid valves, and other installation components are represented by predefined objects.

3.5   DESIGNED PROTOTYPE OF THE PROPOSED SIMULATED PROCESS INDUSTRY PLANT

There are two divisions in the process industry. The first division is the assembly line where the raw ingredients undergo processing according to a predefined ratio to produce the end product. In the second division, the final product is filled into different containers depending on various factors like container type and size.

3.5.1 Overview of Assembly Line Division Strategy

The key assembly tasks like filling are completed in the section of the assembly line division. The proposed assembly line is designed on the basis of the factors shown in Fig. 3.2. Fig. 3.3 depicts the basic structure of the proposed assembly line division. There are several steps to the overall container filling and other assembling processes:

- **Sorting stage:** Containers moving over the conveyor are categorized basis of size (small and large) and type. Two capacitive proximity sensors (CPR) are placed at the top of the size detector unit to sort containers according to size, while an inductive proximity sensor (IPR) i.e. IME10/IME08 is utilized to sort metallic and non-metallic containers. While CPR sensors

can detect any kind of container but IPR sensors can only identify metallic containers. Sorting stage decides about which type of composition to be filled in which container.

- **Filling stage:** In this stage, containers are filled with a variety of material compositions. There are two material compositions in large non-metallic containers but three liquid compositions in small metallic base containers, with 1/3rd of each component present in each container. It is possible to use both photoelectric retroreflective sensors and laser beam sensors at this stage. In order to control the flow, solenoid valves are utilized.

- **Auxiliary Stage:** Capping, labelling, and storing processes are part of the auxiliary assembly line stage. Both photoelectric retroreflective and laser beam sensors can be employed in this situation.

- **Counting Stage:** Counting of both types of containers is done at this stage using PLC programming.
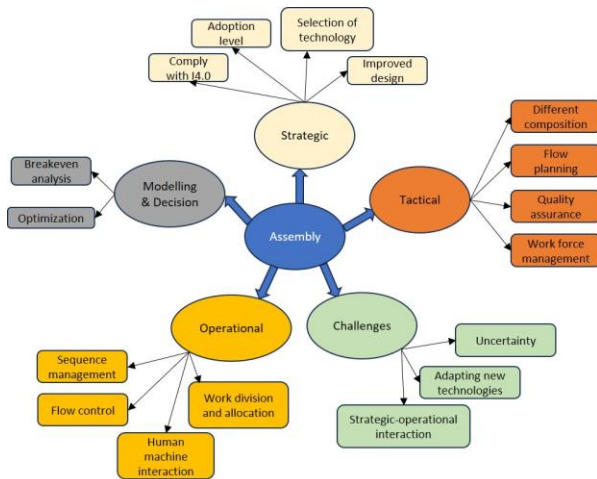
Figure 3.2. Important factors for designing assembly line division
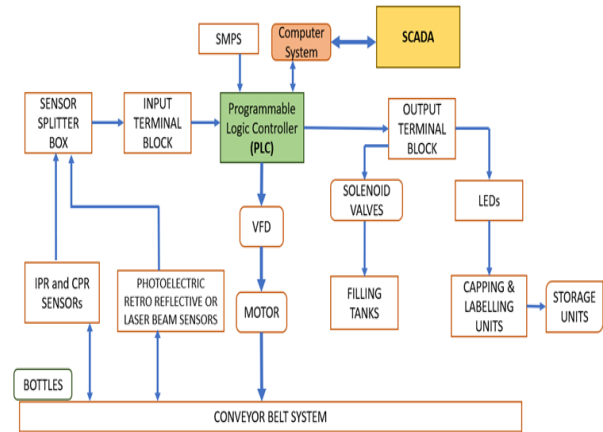
Figure 3.3. Framework for working of assembly line division

This entire assembly line division operation is headed by PLC as shown in Fig. 3.3. SCADA can connect with PLC using a variety of media. Sensors and push buttons function as input devices. A single PLC CPU module cannot read the signal directly. Therefore, each of these sensors is coupled with a sensor splitter to display the ON/OFF and defective/faulty status of each sensor before being connected to the PLC's I/P terminal block. IPR, CPR, photoelectric retroreflective, or laser beam sensors are mounted above the conveyor system to identify the types of containers by sending input signals to the PLC. The DC motor and Variable Frequency Drive (VFD) ensure precision and accuracy throughout the movement of the conveyor system. VFD can be used in both speed control and position control modes for the smooth movement of containers over the conveyor system.

The output terminal block connects the PLC to all output devices, including solenoid valves and LED indicators. The output terminal block then performs a logical action for output-related devices like drive→motor→conveyor belt, LEDs→capping & labelling units, solenoid valves→filling tanks,

based on the interpretation of the information from these sensors. Similarly, laser beam or photoelectric retroreflective sensors are used to control capping and labelling machines using signal conditioning via a PLC. Positioning of the sensors over the conveyor system below the filling tanks, the capping and labelling unit serves as the foundation of position control as shown in Fig. 3.4. Conveyor system stops when a sensor reads HIGH. Different final product compositions are filled into the containers under the control of solenoid valves that are connected to the filling tanks. The gap between the filling tanks ($Tank_1$, $Tank_2$ and $Tank_3$) is incredibly small. Therefore, the container must move relatively slowly between these tanks as compared to the movement between $Tank_3$, capping and labelling unit in the assembly line division. The list of components utilized in both ratio control division and assembly line division is displayed in Table 3.2.
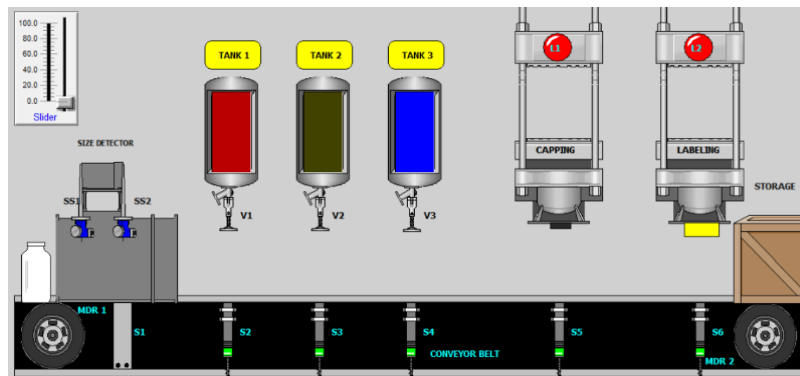
Figure 3.4. Simulated model of assembly line division in SCADA

Table 3.2. Components involved in Assembly line and Ratio Control Strategy

Input Elements/Constituents	Output Elements	Other Supplementary Elements
Start PUSH button	$Pump_1$ and $Pump_2$	Two PLC units; Wonderware InTouch SCADA software;
IPR Sensor (S_1)	Control valves ($CV_1, CV_2, CV_3, CV_4, CV_5$)	Conveyor belt system
One laser beam safety sensor	Solenoid Valves (V_1, V_2, V_3)	Overhead raw materials units (CH_1, CH_2)
Level sensors (LS_1-LS_3)	Conveyor system motor	Motor driver blender; Two Motor driven rollers (MDRs);
Photoelectric Retroreflective or laser beam sensors (S_2, S_3, S_4, S_5, S_6)	Blender DC motor	Mixer tank; Size detector unit
CPR sensors (SS_1 & SS_2)	LED indicators (L_1, L_2) for capping and labelling at assembly line division	$Tank_1$, $Tank_2$ and $Tank_3$ for filling different compositions of final products
		Assembly line unit for capping, labelling and storage of containers

3.5.2 Overview of Ratio Control Strategy

The ratio control method is a special type of feedforward control strategy that can be implemented in these industries to qualitatively and quantitatively maintain the desired ratio of raw materials [158]. The ratio control technique is used to maintain the appropriate ratio of raw materials in process industries. The ratio control approach has become popular in industry for the following purposes:

- To maintain a predetermined constant ratio for the streams in the reboiler.

- To maintain the flow rate of the feeding streams of the distillation column and the streams involving the reflux ratios of the distillation column.
- To maintain the ideal combustion ratio.
- To maintain a desired ratio of the purge stream and the recycle stream.
- To maintain the desired fixed composition of the blend by holding the fixed ratio of two blended streams.

The raw materials are measured using the ratio control technique in regard to the flow rates of wild and controllable streams. The stream whose flow rate can be measured but not controlled is known as a wild/disturbance stream, while the other is known as a controllable/manipulated stream because its flow rate can be both measured and controlled. Only one stream can be controlled at a time. There are different configurations for ratio control as follows:

1) In **configuration 1**, the ratio between the disturbance and manipulated streams is calculated by measuring the flow rate of both streams. The error induced between the predetermined and desired constant ratio provides a correction signal to the ratio controller. Afterward, this calculated ratio is contrasted with the fixed ratio or setpoint as shown in Fig. 3.5(a).
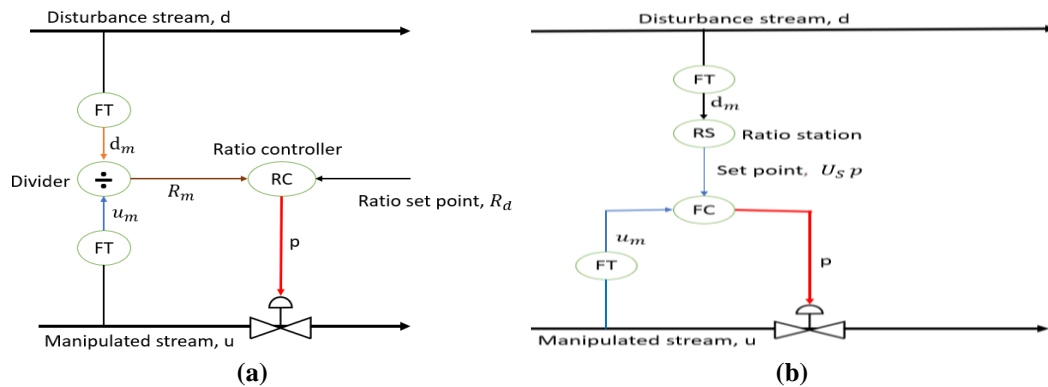
Figure 3.5. Different configurations for ratio control **(a)** Configuration 1 **(b)** Configuration 2

2) **Configuration 2** begins by measuring the wild stream's flow rate and then multiplies it by the chosen constant ratio. The outcome gives a setpoint and the flow rate value that are used by the controllable stream to maintain a predefined constant ratio. The measured value of the flow rate of the manipulated stream is compared to this setpoint as shown in Fig. 3.5(b). The PLC receives the actuation signal from the deviation from the true constant ratio and uses it to change the controllable stream flow rate through the control valve.

3) **Configuration 3** functions much like a ratio adjustment procedure to config. 2, operating as a compensation for the feed-forward ratio control. Here, the appropriate ratio is modified using the auxiliary measurement of the controlled stream.

Proportional Integral derivative (PID) controller is used in the programming of the ratio controller whose parameters are obtained using the auto-tuning approach as shown in Fig. 3.6. The

PID toolbox in Sysmac Studio programming software is used to program the ratio controller, where the inputs like transfer function, control valves and flow measurements for the final control element can be given.
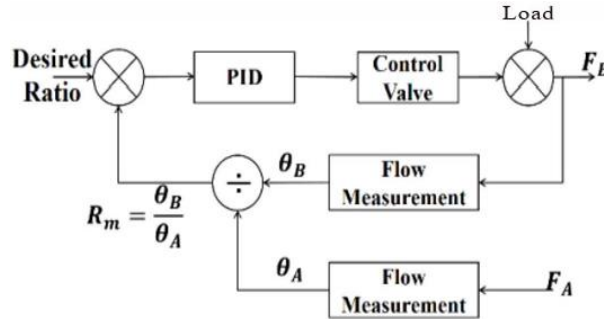
Figure 3.6. Block diagram for the working of ratio control strategy

Figure 3.7 shows the simulated model of the ratio control division process in Wonderware Intouch SCADA software. Here, $Chemical_1$ (CH_1) and $Chemical_2$ (CH_2) are the basic raw materials that are kept in a set ratio to one another in the reservoirs. The corresponding pumps and valves for the uncontrolled and controlled stream are $Pump_1$ and $Pump_2$ and valve CV_1 and CV_2. The ratio of quantities of raw materials in the wild stream and controlled stream are based on flow rates. The quantity is decided by the opening of the control valves for a particular time, which is directly proportional to the ratio of streams. PLC sends OPEN and CLOSE signals to these control valves on the basis of timers. The blender in the mixer is driven by a Blender DC motor (BM). Level sensors (LS_1-LS_3) and one safety sensor is used in the mixer to avoid overflow. Following the acquisition of the desired product, the associated tanks ($Tank_1$, $Tank_2$ and $Tank_3$) are filled. The control valves CV_3-CV_5 regulate the flow to these tanks.
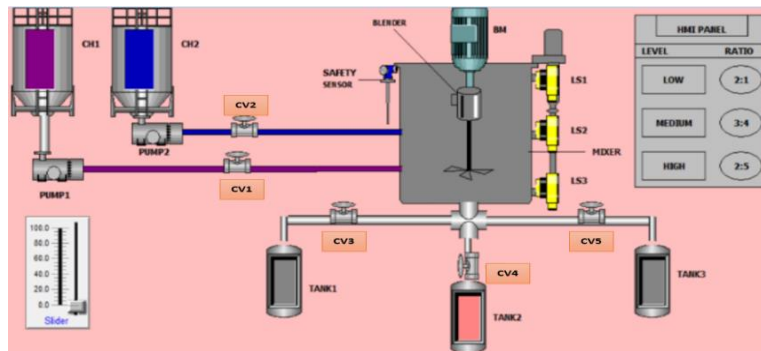
Figure 3.7. Simulated model of ratio control division in SCADA

In the ratio control division, the levels are defined inside the mixer and the ratio of the raw materials is through the HMI panel. HMI PANEL (Omron NB5QTW01B, 5.6 inches) regulates the ratio of wild and modified streams as well as the processed volume level. The Omron Sysmac Studio software is used to configure the defined ratios and levels, which are then displayed on the actual HMI panel. The ratios can be determined at the configuration level as well as the plant site but modification of the ratios is only possible using programming software.

3.6 OPERATION AND FUNCTIONALITY OF THE ASSEMBLY LINE DIVISION AND RATIO CONTROL DIVISION

This section explains the functionality of the assembly line division and ratio control division using flow charts. Figure 3.8 shows how a processing plant executes the ratio control division method. The safety sensor must first be determined to be ON or OFF. If the safety sensor is high, no further activity will be permitted. If the safety sensor is low, then the HMI panel will turn ON and further processes can be executed after that. There are two categories on the HMI panel. i.e. LEVEL and RATIO. The quantity of the products to be produced from the raw ingredients CH_1 and CH_2 are determined by the level indicator using levels LOW, MEDIUM and HIGH. The desired ratio of CH_1 to CH_2 is determined by the ratio indicator from a number of level and ratio combinations given in Eq. (1)-Eq. (3). After selecting the appropriate level and ratios, Pump_1, Pump_2 and blender DC motor turn ON and overhead raw materials units begin filling the mixer through the control valves. The amount and ratio of CH_1: CH_2 determine the length of time that these valves should be left open.

$$LOW\ Level\ and\ 3:4\ Ratio\ = [(CV_1 \times 30) + (CV_2 \times 40)] \times 0.3\ sec \tag{3.1}$$

$$MEDIUM\ Level\ and\ 2:1\ Ratio\ = [(CV_1 \times 70) + (CV_2 \times 35)] \times 0.6\ sec \tag{3.2}$$

$$HIGH\ Level\ and\ 2:5\ Ratio\ = [(CV_1 \times 20) + (CV_2 \times 50)] \times 0.8\ sec \tag{3.3}$$
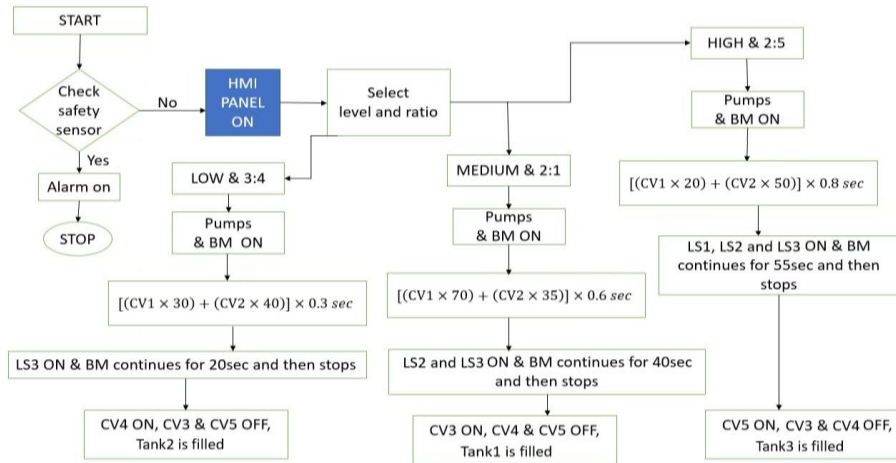
Figure 3.8. Functionality of ratio control division strategy

At this point, the level of the composition inside the mixer is indicated by the ON state of the Blender DC motor and level sensors LS_1-LS_3. The mixer timer for the composition is indicated by LS_3 to represent LOW level by staying ON for 20 seconds. Following this, CV_4 opens while CV_3 and CV_5 stay closed, and the Tank_2 is filled with the finished product. Indicating a MEDIUM level, both LS_3 and LS_2 turn ON for a mixer timer of 40 seconds. Following this, CV_3 opens while CV_4 and CV_5 stay closed and $Tank_1$ is filled with the final product. Accordingly, LS_1, LS_2 and LS_3 switch ON to signify HIGH level for a mixer timer of 55 sec. Following this, CV_5 opens while CV_3 and CV_4 stay

closed and the $Tank_3$ is filled with the final product. At the top of the mixer, there is a safety sensor that prevents composition overflow during the malfunctioning of level sensors and control valves.

In assembly line division, the containers are in motion as they go on the conveyor belt which makes it important to control the conveyor system's motion. This flowchart in Fig. 3.9 depicts the actions that must be taken in order to stop the conveyor motor, which remains ON even after the sensor inputs. The motor-driven rollers (MDRs) control the dynamics of the conveyor belt. The motor turns ON while measuring the container's size and material type and it will stop when any of the (S_2-S_6) sensors register a HIGH value. The container is filled with compositions from $Tank_1$, $Tank_2$ and $Tank_3$. The STOP time depends on the timer of filling, capping and labelling units. Once the timer is turned off, the conveyor system resumes its regular operation once the motor is turned ON.
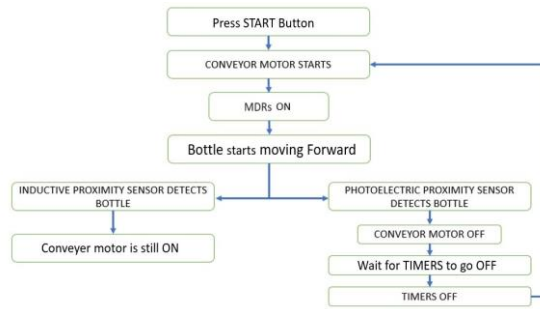
Figure 3.9. Events of the conveyor system

Figure 3.10 shows the more detailed working of the assembly line division along with various divisions such as sorting, filling, and supporting procedures like capping, labelling, and storage of containers. Sorting happens according to the size and type of containers, as they move along the conveyor belt. Both CPR sensors (SS_1, SS_2) are HIGH when a large metallic container travels along the belt. The IPR sensor also turns HIGH at the same time for a metallic container. However, SS_1 turns HIGH and SS_2 stays LOW when a small non-metallic container passes along the conveyor belt. The IPR sensor gives a continuous LOW reading for a non-metallic container.
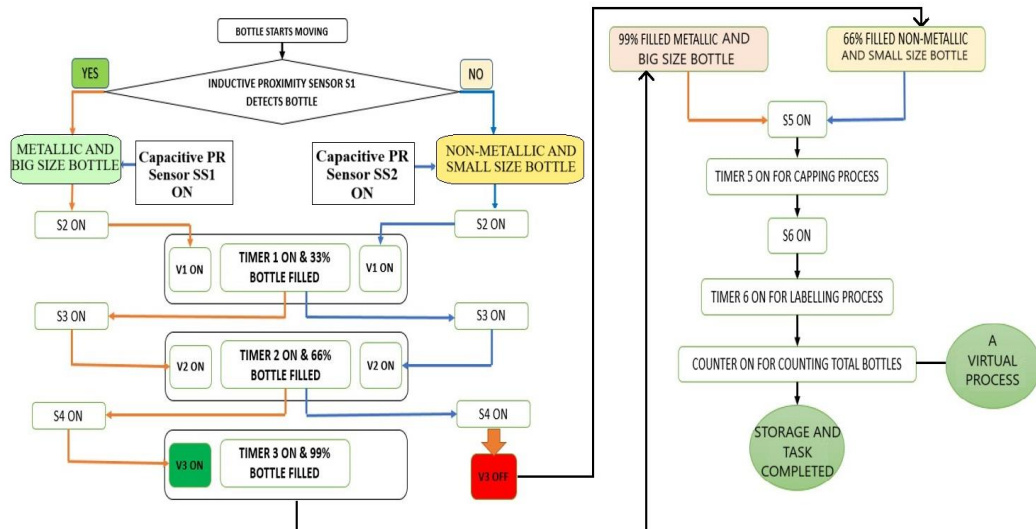
Figure 3.10. Detailed working of assembly line division

29

Afterward, both categories of containers continue to move down the conveyor system and are identified either by a photoelectric retroreflective sensor or a laser beam sensor (S_2) during the filling stage. The opening of the solenoid valve V_1 cause the motor to stop and the conveyor system comes to a complete stop. $Tank_1$ begins to fill the container with its composition and this process continues for the predetermined amount of time to fill the container up to one-third section. When the timer expires, the conveyor system's motion resumes and it keeps going until the next laser beam sensor S_3 detects a container so that the whole operation can be repeated again. Similarly, the opening of the solenoid valve V_2 causes the motor to stop and the conveyor system comes to a complete stop. As a feedback of this signal, $Tank_2$ begins to fill the container with its composition and this process continues for the predetermined amount of time to fill the container up to two-thirds section. When the timer expires, the conveyor system's motion resumes and it keeps going until the next laser beam sensor S_4 detects a container, so that the whole operation can be repeated.

The solenoid valve (V_3) opens when a large metallic container is present, causing the motor to stop and bringing the conveyor system to a complete halt. As a result of this signal, the $Tank_2$ begins to fill the container with its composition, continuing for the duration of the timer until the container is completely filled, or 99% full. However, the motor shuts off and the conveyor system comes to a complete halt for small non-metallic containers. The solenoid valve did not open at this instance due to the absence of feedback from HIGH level and metallic type signal from the IPR sensor S_1 and CPR sensor SS_2. This logical progression caused the small non-metallic container to fill with two-thirds of the composition of the large metallic container.

The auxiliary assembly phases like capping, labelling, and storing are performed after these stages. The labelling and storing of containers are done separately for easy identification. The motor stops and the conveyor system comes to a complete stop when the photoelectric retroreflective sensor S_5 detects any type of container. The caps are placed on the containers after the LED indicator L_1 of the capping device in the auxiliary stage turns HIGH. Then motor restarts again when the capping unit's timer is OFF. Again, when sensor S_6 detects any container, the motor stops and the conveyor system come to a complete halt. Various labels are applied to various types of containers after L_2 of the labelling unit turns HIGH. Then motor restarts again when the labelling unit's timer is OFF. The containers continue moving after being hand-selected and placed in various storage cartons.

3.7 IMPLEMENTATION AND RESULTS OBTAINED

This section displays and explains the SCADA simulation results of both ratio control and assembly line divisions.

3.7.1 Ratio Control Division

The predetermined ratio of CH_1 to CH_2 is determined by the ratio indicator using levels low, medium and high. There are three standard ratios taken as 3:4, 2:1 and 2:5 for $CH_1 : CH_2$. The level and ratio combinations are chosen with the help of Eq. (3.1-3.3). Figure 3.11 shows the different cases of level and ratio combinations in the ratio control division.

(a) Low Level and 3:4 ratio   **(b)** Medium Level and 2:1 ratio

(c) High Level and 2:5 ratio
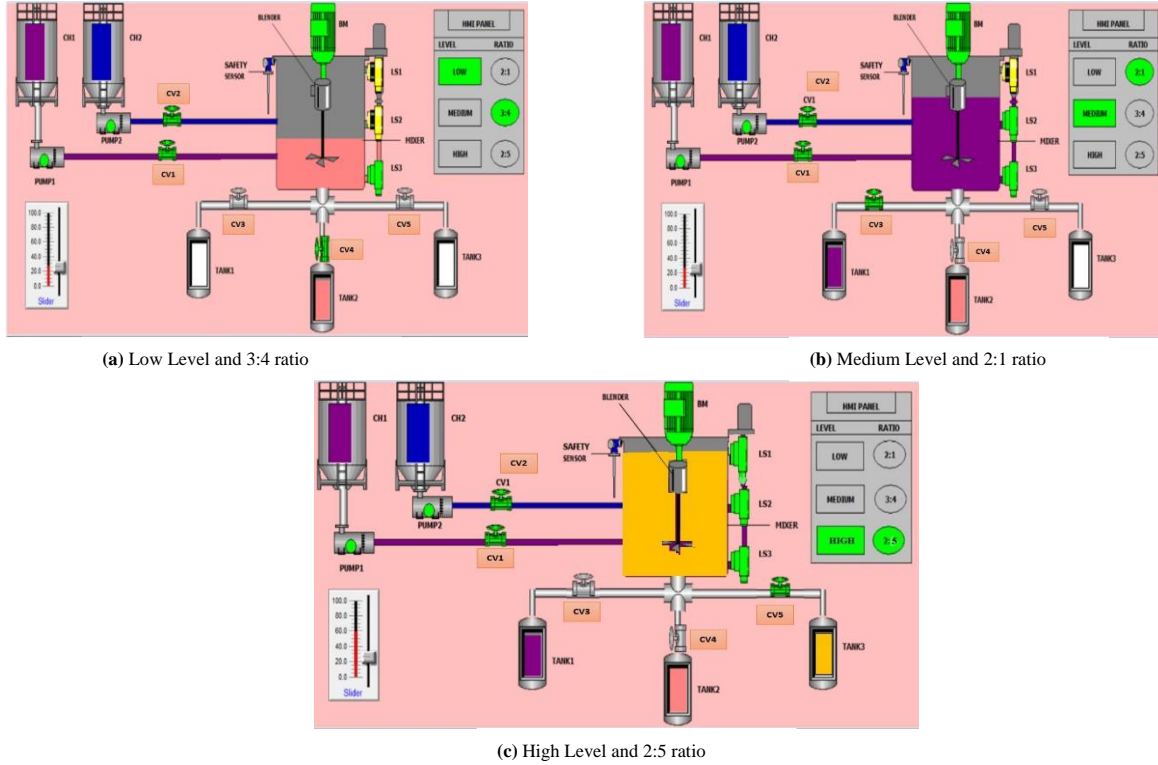
Figure 3.11. Different cases of level and ratio combinations in ratio control division

When the HMI panel is set at LOW level and $CH_1 : CH_2$ ratio is taken as 3:4 to start $Pump_1$ and $Pump_2$, CV_1 and CV_2 of disturbance and controllable streams are turned on. During the production stage, when BM is ON and LS_3 indicates the LOW level, then CV_4 opens and allows the composition to fill up into $Tank_2$ as shown in Fig. 3.11(a). When the HMI panel is set with the MEDIUM level and $CH_1 : CH_2$ ratio is taken as 2:1 to start $Pump_1$ and $Pump_2$, CV_1 and CV_2 of disturbance and controllable streams are turned on. During the production stage, when BM is ON and LS_3 & LS_2 indicates a MEDIUM level, then CV_3 opens and allows the composition to fill up into $Tank_1$ as shown in Fig. 3.11(b). Similarly, when the HMI panel is set with the HIGH level and $CH_1 : CH_2$ ratio is taken as 2:5 to start $Pump_1$ and $Pump_2$, CV_1 and CV_2 of disturbance and controllable streams are turned ON. During the production stage, when BM is ON and LS_3, LS_2 & LS_1 indicates a HIGH level, then CV_5 opens and allows the composition to fill up into $Tank_3$ as shown in Fig. 3.11(c).

3.7.2 Assembly Line Division

In this case, the color scheme selected for $Tank_1$, $Tank_2$ and $Tank_3$ differs from the ratio control division. This demonstrates that the ratio composition can be adjusted according to the requirements.

The metal-base and large containers are detected by CPR sensors (SS_1, SS_2) and inductive PR sensors (S_1 & S_2) as shown in Fig. 3.12(a). IPR sensor passes the non-metallic and small containers when SS_1 is HIGH and SS_2 is LOW as shown in Fig. 3.12(b).

(a)   **(b)**
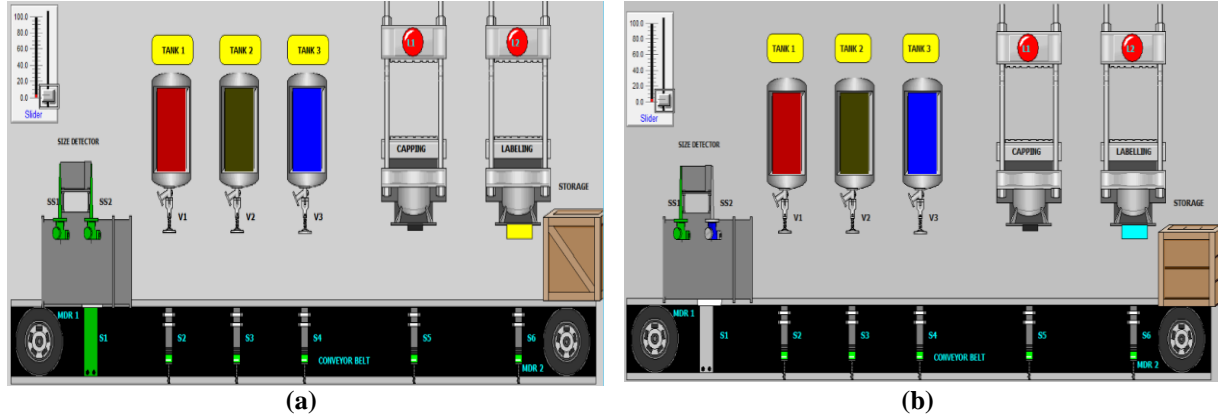
Figure 3.12. Identification of **(a)** Large metallic containers **(b)** small non-metallic containers

Both metallic and non-metallic containers are identified with photoelectric retroreflective or laser beam sensor S_2. Valve V_1 opens as a result of the conveyor motor stopping and both the containers get filled with the composition in $Tank_1$ up to one-third level as shown in Fig. 3.13(a). Both metallic and non-metallic containers are identified with photoelectric retroreflective or laser beam sensor S_3. Valve V_2 opens as a result of the conveyor motor stopping and both containers get filled with the composition in $Tank_2$ up to two-thirds level as shown in Fig. 3.13(b). Large-size metallic containers are identified with photoelectric retroreflective or laser beam sensor S_4. Valve V_3 opens as a result of the conveyor motor stopping and large size metallic containers are filled with the composition in $Tank_3$ up to the maximum or 99% level as shown in Fig. 3.13(c). Small non-metallic containers are identified with photoelectric retroreflective or laser beam sensor S_4 which results in the stopping of the conveyor motor. However, the solenoid valve is closed. As a result, small non-metallic containers are filled with two-thirds of the overall composition as shown in Fig. 3.13(d).

(a) Filling both type of containers by $Tank_1$ **(b)** Filling both type of containers by $Tank_2$
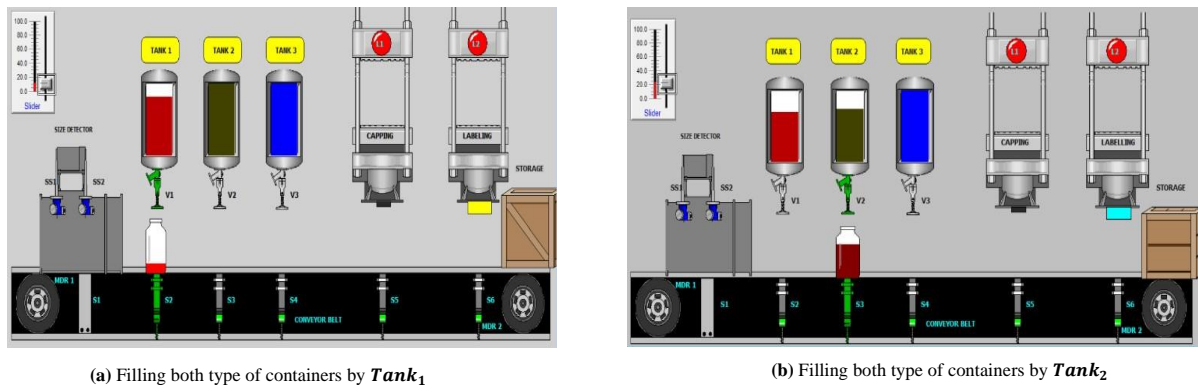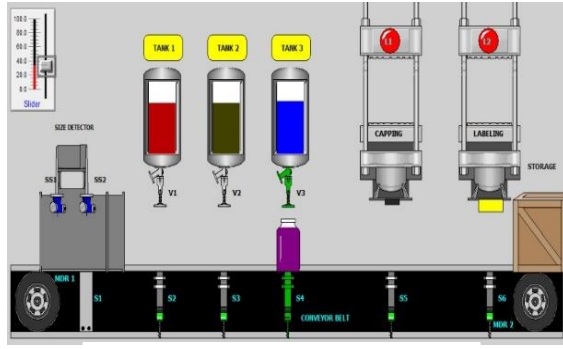
(c) Filling large metallic containers by $Tank_3$
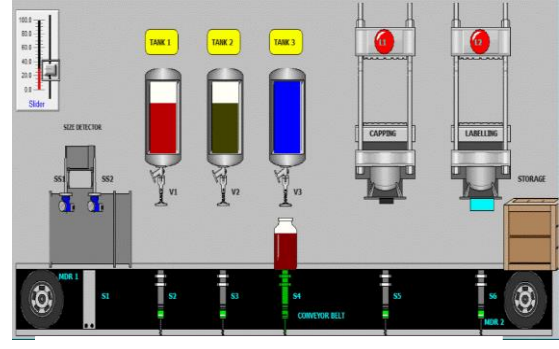
(d) Non-Filling small non-metallic containers by $Tank_3$

Figure 3.13. Filling of different containers by $Tank_1$, $Tank_2$ and $Tank_3$ in assembly line

Both metallic and non-metallic containers are identified with photoelectric retroreflective or laser beam sensor S_5. The LED indicator L_1 turns HIGH as the conveyor motor stops and both types of containers are capped by the capping unit as shown in Fig. 3.14(a-b). Both metallic and non-metallic containers are identified with photoelectric retroreflective or laser beam sensor S_6. The LED indicator L_2 turns HIGH as the conveyor motor stops and both types of containers are labelled with different colors by the labelling machine in order to them as shown in Fig. 3.14(c-d). After executing all these processes, the storage of containers is done as shown in Fig. 3.14(e). Table 3.3 depicts the comparison of the proposed work with the relevant literature.
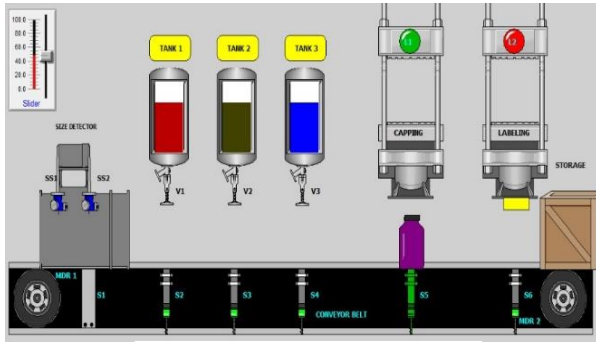
(a) Capping of large metallic containers
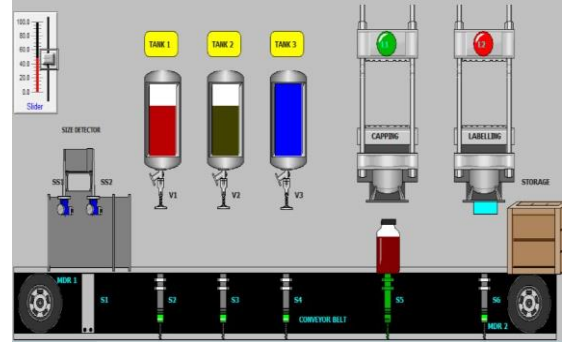
(b) Capping of small non-metallic containers
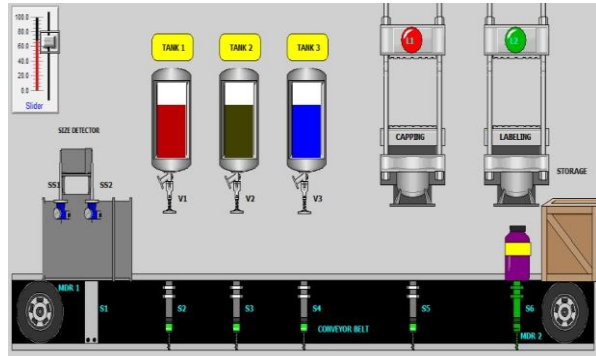
(c) Labelling of large metallic containers
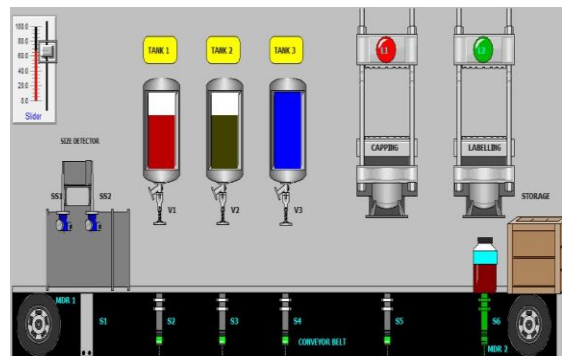
(d) Labelling of small non-metallic containers

33
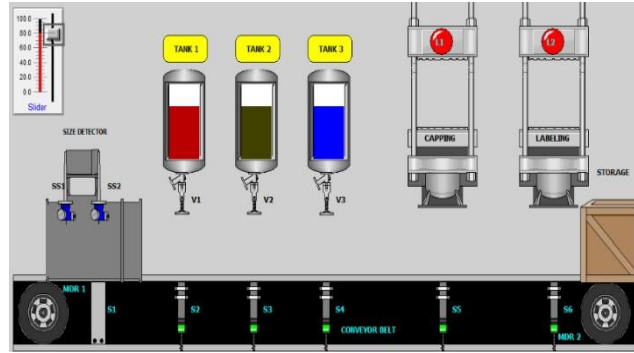
(**e**) Storage of Containers

Figure 3.14. Capping, Labelling and storing of containers in the auxiliary stage

3.8 A CASE STUDY ON IMPROVING PRODUCTIVITY IN PROCESS INDUSTRIES

An industrial case study is chosen to show and validate the proposed work. The case study was conducted in India's leading chemical industry process plant 'J' (name changed) situated in North India, which is engaged in full flagged production, packaging and servicing of the products. During the plant visit, there was a proper discussion with the automation and production departments for the proper operation study of the process plant to examine all the units. Currently, the plant 'J' is producing products in batch process. Containers are filled in batches and with the same type of composition in them. Different production lines are used for producing different sizes or different types of containers. This increases the assembly line setup cost and also the workforce cost.

If one intends to produce different types of products within the same production line as the batch process, it will create huge idle time during the transition from one batch to another. In some cases, it was reported to have around 27% idle time of the total production time. This will reduce the overall throughput of the plant. The different processes involved in the production are mentioned in Fig. 3.15.
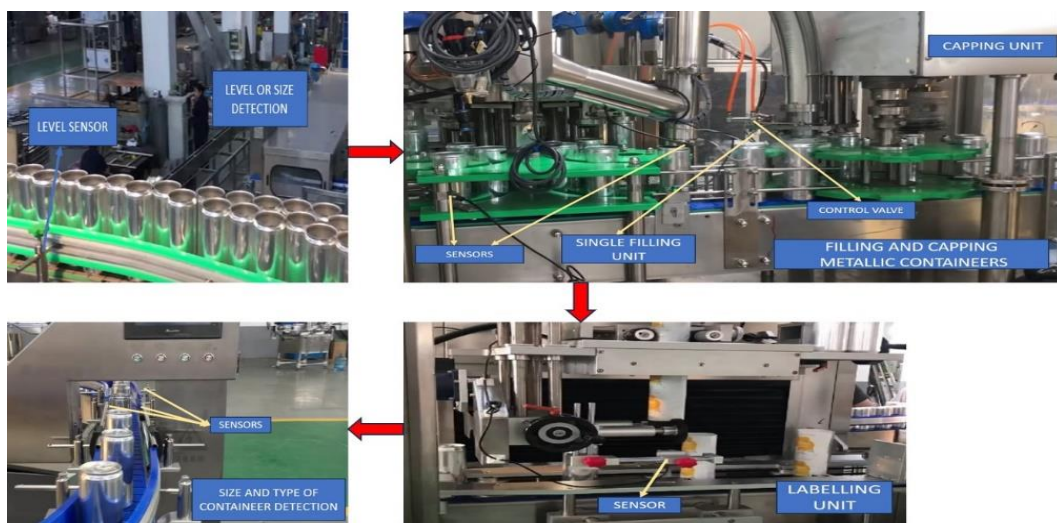
Figure 3.15. Different processes involved in the production

34

Table 3.3. Comparison of the proposed work with the current relevant literature

Authors	Ratio Control	Assembly Line		Mixing Process	Filling Process	Capping Process	Labelling Process	Sorting Process	Real-world implementation with Case study	Monitoring the whole plant	Solution Technique
		Different	Single								
Huo et al. [32]		For balancing the assembly line							✓		Type-1 & Type2 fuzzy control system to re-balance the assembly line
Geurtsen et al. [33]		For balancing the assembly line							Real-world data for experimentation		Deep Q-reinforcement learning technique and Markov decision process
Didden et al. [34]		For balancing the assembly line							✓	✓	Genetic algorithm for assembly line balancing
Schmid et al. [143]		For assembly line feeding and balancing problem							✓		Logic-based Benders' decomposition framework.
Ling et al. [144]		Designing of assembly system							Computer vision to monitor and analyze the real-time operation process		Data-driven synchronous reconfiguration
Aung et al. [145]					✓						PLCSIM and HMI
Win et al. [146]					✓	✓					PLC for filling and capping
Nadgauda et al. [147]					✓						PLC and SCADA for filling and packaging
Viraktamath et al. [148]					✓						PLC for filling
Ghita et al. [35]	✓										Theoretical framework for ratio control of material flows using impedance spectroscopy
Abubakar et al. [149]					✓						Robotic arm conveyor and Arduino controller to fill containers
Kiangala et al. [150]					✓	✓					Siemens S7-1200 PLC and ZENON SCADA-based Simulated prototype of bottling process
Sreejeth et al. [36]				✓	✓						PLC-based laboratory prototype
This work	✓	Single		✓	✓	✓	✓	✓	✓	✓	• PLC and SCADA-based control framework to automate the process industry plant and monitor all the processes using a single-screen HMI. • Address a dynamic real-world problem for the mixing of raw materials, filling of final product composition, capping, labelling and sorting of containers on the basis of both size and type using a single assembly line.

3.8.1 Current Scenario

The current scenario in the company 'J' is that it has only a single operational assembly line. It is used for filling only one type of container, which is of 500ml. This is coded in blue colour in Fig. 3.16(a). The assembly line is comprised of five processes namely, level or size detection (P_1), Filling (P_2), Capping (P_3), Labelling (P_4) and Packaging (P_5). Each person, workforce (w_1, w_2, ...w_5) is assigned at each process for supervision and handling. The maximum time required to complete each process at each assembly line is called process time, denoted with T_p and the time required by the container to shift from one process to another over the assembly line is called transition time, denoted with T_r. The transition time is taken to be equal between all the processes i.e., 5s. If there's a need to fill another size of container i.e. 750 ml, then a second assembly line is required as per the current scenario of the company 'J'. This is coded in orange colour as shown in Fig. 3.16(a). This will lead to an increase in workforce, transition time and processing time. Also, the cost of installation of these process units, the conveyor system and the workforce will increase. As a result, the overall production cost per unit of containers will increase.

In another scenario, shown in Fig. 3.16(b), it is required to fill a different material type 750ml container. So, another process (P_0) is used to identify the type of container increased. This again requires another unit (installation cost = 100) for type detection, which leads to more processing time ($T_p = 2.5s$), more initial transition time ($T_{r0} = 5s$) and more workforce which increases production cost per unit. If the workforce is increased, then the overall idle time of the industry 'J' will also increase.

3.8.2 Mathematical Modelling

Now, the objective is to minimize the assembly line timings, the workforce and overall cost of production. For these factors, some mathematical modelling is established as shown below.

Table 3.4 Parameters for the mathematical modelling of the assembly line

Workforce, w=1,2,3…...n
Assembly line, A_l=1,2,3……i
Process, p =1,2,3……. J
Time required for each process, at each Assembly line, to be completed, t_p
Cycles, C
Processes p available at assembly line $A_l = M_{pl}$
Workforce assigned for assembly line = W_{wl}

For a particular cycle time, the following constraints are to be followed:

$$\sum M_{pl} = 1 \tag{3.4}$$

$$\sum W_{wl} \leq C \tag{3.5}$$

It is ensured that the total time does not exceed the total cycle time.

In order to minimize the number of workforces, the constraints are chosen as

$$\sum_{w=1}^{n} W_{wl} \leq 1 \tag{3.6}$$

The objective function for minimizing the Assembly line time is formulated as

$$f_1 = \sum_{p}^{j} t_p \tag{3.7}$$

And the objective function for minimizing the number of workforces is formulated as

$$f_2 = \sum_{w=1}^{n} W_{wl} \tag{3.8}$$
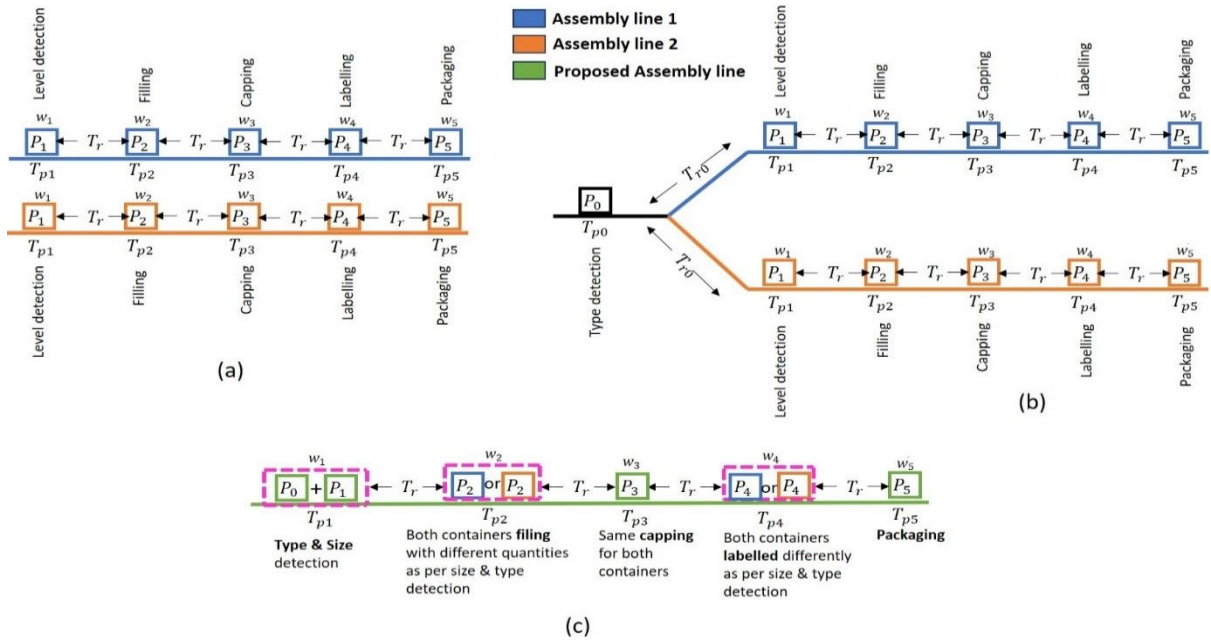
Figure 3.16. Different scenarios of Assembly lines in the industry 'J' and the proposed Assembly line

3.8.3 Test Case

In the proposed work, a single unit (based on sensors) incorporates both size and type detection process as shown in Fig. 3.16(c). A single workforce (w_1), is assigned at this level. There will be no case of initial transition time (T_{r0}) and processing time (T_{p0}). The proposed assembly line accommodates both scenarios of filling both type and sized (metallic 750ml and non-metallic 500ml) containers with the flexibility of choosing the ratios of the quantities of the composition of the material. A single workforce (w_2), is assigned at this level. Both containers are capped with single units and workforce (w_3), is assigned at this level. Similarly, the labelling unit also incorporates the labelling of both types of containers based on identification at the first level of size and type detection and a single workforce (w_4), is assigned at this level. The counting and packaging process will be similar to that of the earlier scenarios. All these amendments reduce the workforce at different processes, transition time and processing time. As a result, the production cost per unit of containers will decrease and throughput of the plant will increase. The idle time of the plant will be reduced significantly. A detailed representation showing different scenarios of Assembly lines in the industry 'J' and the proposed Assembly line is shown in Fig. 3.16. The process time and installation cost of two process units of company 'J' and the proposed work respectively are shown in Table 3.5. This type of data is chosen for proper understanding and easy calculation related to the whole work.

Table 3.5 Comparison of Process time and installation cost of different process units of company 'J' with proposed work

Processes	Process Time of 'J' ($T_p \times 2$) sec	Process Time of Proposed Work ($T_p \times 2$) sec	Installation Cost of Process Unit in 'J' ($\times 2$)	Installation Cost of Process Unit in Proposed Work ($\times 1$)
Size detection (P_1)	2.5	2.5 (Including type detection)	125	150 (Including type detection)
Filling (P_2)	5	5	200	200
Capping (P_3)	3	3	150	150
Labelling (P_4)	3	3	200	250
Counting & packaging (P_5)	5	5	150	300

3.8.4 Comparative Analysis of the Trends

The real-time trends of the proposed work in the SCADA software, depicted in Fig. 3.17(a) show the rate at which both containers are filled. The proposed assembly line filled both containers in a group of six containers each (metallic 750ml and non-metallic 500ml). It is important to note that there is no overlapping of the containers. A group of particular containers is chosen to make the packaging process

smooth. Similarly, the trends in Fig. 3.17(b) show the filling of both containers. The trend shows six spikes of each of 500ml and 750ml. These spikes indicate the smooth filling of these containers.
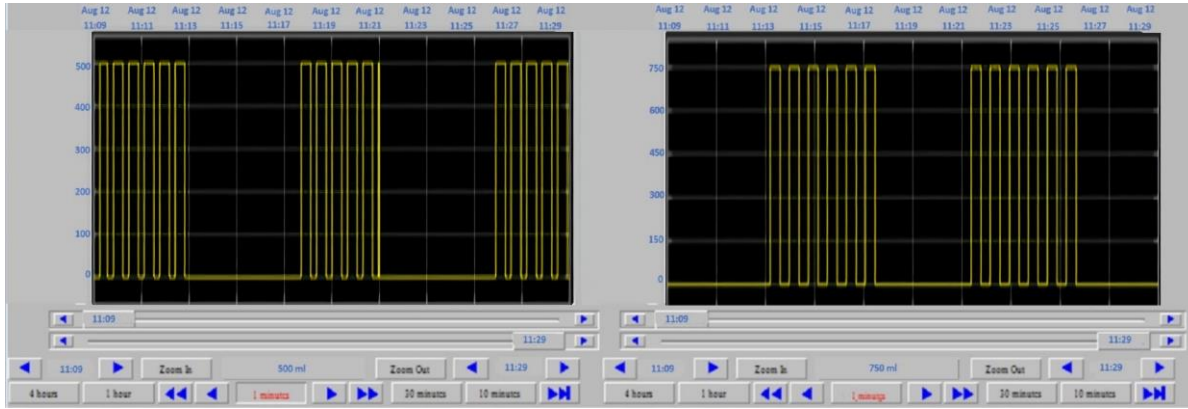
(a) Output rate of filling of both containers
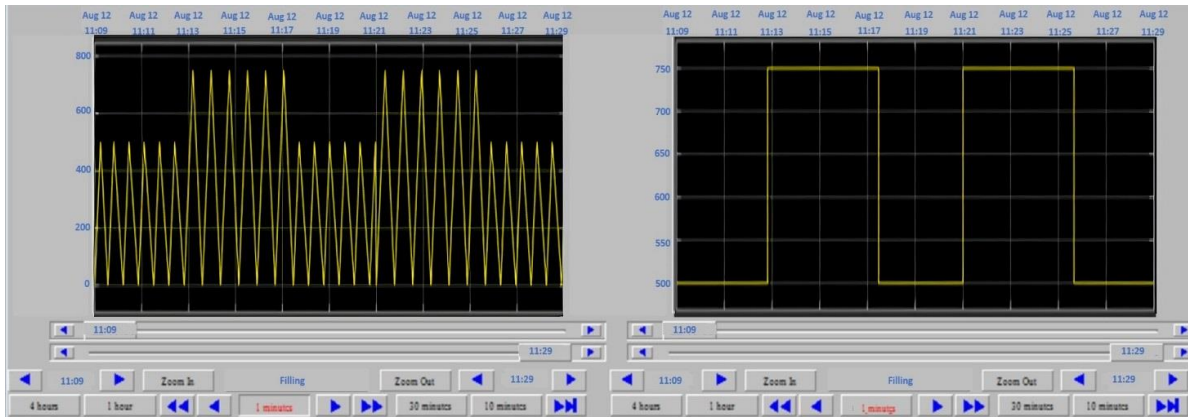
(b) Output spikes of smooth filling of containers in a batch of six each

Figure 3.17 Real-time trends of the proposed work in the SCADA software

The results in Fig. 3.18 show a significant improvement in all areas while adopting the proposed assembly line in comparison to the existing Assembly line in company 'J'. For analysis purposes, the production of two containers (each metallic 750ml and non-metallic 500ml) is considered. The workforce is reduced to half which directly contributes to lower expenses of the company. The cost analysis of the process units shows that the installation cost of the proposed assembly line is much lower than that of the existing assembly line. With the introduction of multiple assembly lines, the transition time between the processes also increases. However, with the proposed assembly line, transition time and the overall process time decreases. All these factors combined together provide a very significant improvement in the overall throughput of the industry. Table 3.6 presents the key features and contributions of the proposed study.
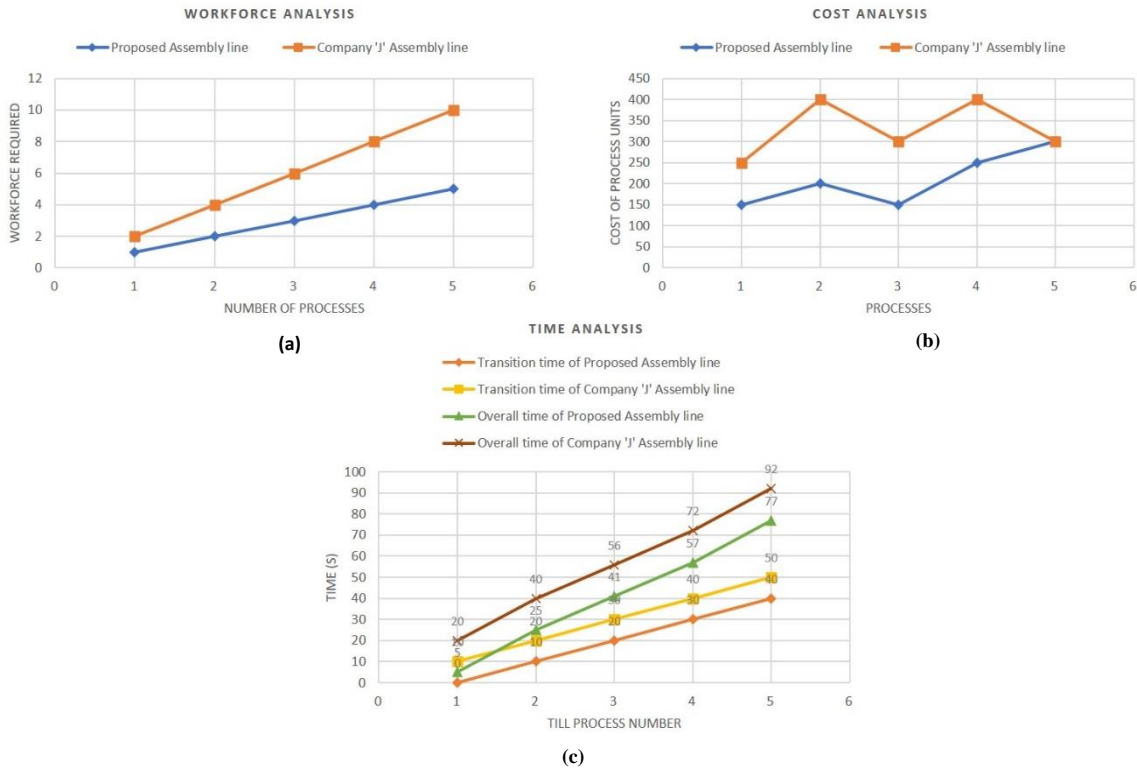
Figure 3.18. Comparative analysis of workforce, cost and time of the proposed assembly line with Company 'J' assembly line

Table 3.6. Key features and contribution of the proposed study

S. No.	Features	Contribution
1	Installation and Extendibility	• Easy installation and incorporation of additional devices with few modifications in the system. • Easiness of adoption
2	Cost	• Low estimated total costs • Higher resource utilization with mass customization
3	EtherCAT	• Anomaly detection in EtherCAT-based indusial control networks • Automatic data exchange and communication using EtherCAT
4	Operation sustainability and transparency	• Real-time data exchange and monitoring for transparency • Low interference with existing operations
5	Remote Control	• Provides continuous and secure monitoring of all the processes • Offers remote control, access and visualization of all process parameters using HMI on a single SCADA interface.
6	PLC and SCADA	• Increased flexibility, scalability and variety • Increasing system responsiveness • Real-time control and self-scheduling/balancing • Workforce planning: Reduces the workforce and avoid gathering of workers
7	Single Assembly line	• Product variation in assembly systems • Improving the efficiency of assembly line and increasing overall productivity
8	Throughput	Transition time and the overall process time decrease with the proposed assembly line. All these factors combined together provide a very significant improvement in overall throughput of the industry.
9	Maintenance	Easy maintenance to solve malfunctioning issues.

3.9 SUMMARY

In this chapter, a PLC and SCADA-based control framework has been proposed to automate the process industry plant and monitor all the processes using a single-screen HMI. First, a dynamic real-world problem is addressed for the mixing of raw materials, filling of final product composition, capping, labelling and sorting of containers on the basis of both size (small and large) and type (metallic and non-metallic) using a single assembly line inside a process industry plant. Then, a ratio control framework is proposed for adjusting the ratio and mixing of raw materials. The automated process operation of the two stages is visualized independently using Wonderware Intouch SCADA software and the entire operation is controlled by an OMRON (NX1P2-9024DT1) PLC. The OMRON (NX1P2-9024DT1) PLC is interfaced with the Wonderware InTouch SCADA system to gather data, create a simulated prototype of the assembly line and ratio control divisions, carry out the necessary control operations, and display this data on the HMI (Omron NB5Q-TW01B, 5.6 inches) screen within the process industry plant. Inductive and capacitive proximity sensors are used in assembly line division to separate the containers according to their size and material type. Moreover, the smooth and precise movement of the conveyor system is addressed using highly accurate photoelectric sensors. A mathematical and simulation model is proposed to minimize the assembly line timings, the workforce and the overall cost of production. Effective product sequencing enhances short-term balancing and production time by reducing waiting time. The developed model is applied in a real-life case study of an assembly line from a chemical processing industry in north India to investigate the efficacy of the proposed method. The results of a real-world case study verified the design for effectively balancing a real-world assembly line and showed that the proposed system improves the productivity, efficiency, throughput, workforce, cost and time of a process industry.

The proposed SCADA system allows the user and operators to get live video streaming from any of the sites on their HMI screens. This SCADA system achieves the automatic control and management of industrial processes, improves worker safety, and reduces manpower and physical resources instead of a distributed control system. The significance of investigating and implementing automated systems across multiple sectors is increased by this work.

Chapter 4

Temperature Control of Heat Exchanger System

4.1 INTRODUCTION

This chapter presents a PLC and SCADA-based control framework to automate and supervise the temperature control processes in the heat exchanger plant. The OMRON (NX1P2-9024DT1) PLC is interfaced with the Wonderware InTouch SCADA system to gather data, create a simulated temperature control prototype and carry out the necessary control operations within the heat exchanger plant. The PLC controls the entire process and programming of PLC is done using Sysmac studio automation software using the ladder programming language. The proposed system controls the temperature of the heat exchanger system through PID and Fractional Order PID ($PI^\lambda D^\mu$) controllers with Integral Anti-windup technique. Various control strategies like Cascade Control, Feedforward Control and Smith Predictor for time delayed process are discussed for controlling the temperature of the process. The performance of both PID and fractional order PID controllers is optimized using adaptive heuristic optimization techniques like Genetic Algorithm (GA), Ant Colony Optimization (ACO) and Particle Swarm Optimization (PSO). In control system design and analysis, the calculated performance indices are used as quantitative measures for evaluating the performance of a system. The combined form of temperature controller with Cascade control, Feedforward control and dead-time compensator is modelled and examined for simulation using MATLAB. Simulation and real-time experimentation analysis of the developed controllers are executed with metaheuristic optimization techniques based on different performance indices like ISE, IAE and ITAE.

4.2 RELATED WORK

High-precision temperature control technology is one of the most critical factors in industrial thermal processing systems. Temperature control is a process of automatically controlling the temperature of large systems to achieve an ideal value in the industrial processes. Temperature stability of heat exchangers is required for many biological, chemical production and industrial manufacturing processes [159,160]. Different industries use different forms of heat exchangers on the basis of construction type, transfer process, flow arrangement and phase of liquid as shown in Fig. 4.1 [161,162]. Shell and tube heat exchanger (STHEX) is the most prevalent type of heat exchanger in the process industries, mainly due to its flexible and robust design, and capability to operate at high pressure and temperature (cryogenic to high-temperature applications). STHEXs have a larger heat transfer surface-to-volume ratio, and ease of manufacturing in a variety of configurations than double-pipe heat exchangers. STHEX consists of parallel tubes/pipes enclosed in a cylindrical shell in which there is enough space between the tubes and the shell for the fluids to flow through. STHEX allows for easy disassembly for routine maintenance and cleaning and can handle very viscous or corrosive process streams with impurities [163,164]. STHEX are utilized in a wide range of applications like cooling of water, oil heaters, petrochemical industries, boilers and condensers in power plants [165,166].
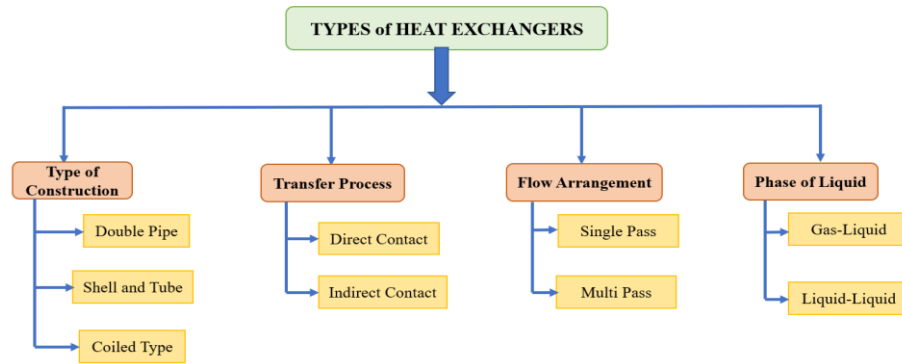
Figure 4.1. Types of heat exchangers

Numerous mathematical modelling approaches and control algorithms have been employed for studying the dynamic behaviour, response characteristics and controlling the temperature of heat exchangers [167-169]. Ouyang et al. [170] introduced a PID approach for controlling the temperature of a continuous stirred tank reactor process which used a sparrow search algorithm for optimizing the PID control parameters. Along with that, it used the Gauss Cauchy mutation technique for each iteration in order to enhance the local optimization capability. PID controllers can't resolve the time-varying control model parameters because of large lag and long adjustment time.

Thepmanee et al. [171] introduced an Allen Bradley PLC using WirelessHART for temperature control and device diagnostic by implementation of SCADA system along with Prosoft configuration builder and Studio 5000 software. Jamil et al. [172] discussed various fractional-order PID controllers for temperature control in different types of heating systems in industries. Instead of conventional feed-forward control methods, Li et al. [173] introduced an effective temperature-based predictive feedback control algorithm to improve the indoor temperature fluctuation, control flexibility, and anti-interference quality of large-scale district heating substations.

Maya-Rodriguez et al. [174] proposed a metaheuristic optimization-based neuro-fuzzy controller for the temperature control of a transesterification biodiesel reactor. This method increased the efficiency of a chemical reactor and minimised the error function and disturbances. Miao et al. [175] introduced a cascade feedforward control technique based on incremental PID and predictive functional control strategy to resolve the delay and anti-disturbance ability problem in the outlet temperature control system of a heat exchanger.

Hou et al. [176] introduced a linear active disturbance rejection controller parameter optimization based on a simultaneous heat transfer search algorithm for the cascade control of the main steam temperature control system. The conduction, convection and radiation phases of heat transfer are implemented in parallel during the optimization process to provide significant improvement toward negative effects caused by uncertainties and disturbances.

Temperature control is a common time delay issue that negatively impacts the performance and stability of controlled systems. Temperature overshooting or undershooting is difficult when there are rapid temperature changes with high precision and stability [177]. Therefore, it is important to design a control scheme to regulate the outlet temperature of a heat exchanger to a certain reference value and enhance the heat transmission efficiency.

4.3 PROBLEM STATEMENT

It is very difficult to control a heat exchanger system because of its complex and nonlinear nature due to unknown fluid characteristics i.e. fluid flow patterns and rates, non-causalities, temperature-dependent and time-varying qualities, contact resistance, leakages, ambiguous mechanics and friction [178,179]. Temperature control is challenging due to the complex thermal interactions in the traditional heater-controlled methods. The conventional control methods are not able to cope with difficulties like strong non-linearity, disturbance, uncertainties, large response and delay time of the controlled objects which further results in uncontrollable feedback efficiency for precise control [180,181]. In the presence of external interference, the current conventional control approaches exhibit high-temperature fluctuation,

44

longer stability correction times, and poor temperature stability. Therefore, an effective control strategy and hardware design is required to maintain a smaller temperature fluctuation amplitude around the desired temperature value for a fluid and heat transfer system.

This chapter proposes a novel cascade control strategy using PID and Fractional Order PID controller ($PI^\lambda D^\mu$) along with the Integral Anti-windup technique, feedforward control and Smith predictor to control and regulate the outlet temperature of a heat exchanger to a certain reference value and enhance the heat transmission efficiency. The main contributions of this chapter are as follows:

- For developing a real-time framework for the temperature control of a heat exchanger plant, this chapter proposes a PLC and SCADA-based control framework to automate and supervise the temperature control processes in a heat exchanger plant and monitor all the processes using SCADA.

- The OMRON PLC is interfaced with the Wonderware InTouch SCADA system to gather data and to create a simulated prototype of the temperature control system to monitor the entire process on a real-time basis in the SCADA screen and historize the data to its database. To the best of our knowledge, no other articles have taken into account all of these constraints at the same time.

- The primary objective is to maintain the outflow temperature of the fluid constant by manipulating the steam flow. These are two principle perturbances or disturbances i.e. fluid flow rate and fluid inflow temperature that need to be controlled with feedforward control.

- The proposed system will take the temperature feedback from the sensors installed in the field and automatically control the temperature by adjusting the hot and cold control valves using the logic written in the PLC.

- The SCADA server receives periodic status from sensors, buttons, process state variables, and other PLC-interfaced devices and stores those details in a database. PLC carries out the necessary control operations within the heat exchanger plant as directed by the SCADA server.

- The designed controller regulates the outlet fluid temperature of a heat exchanger to a certain reference value and enhances the heat transmission efficiency irrespective of external disturbances, non-linearity and delay characteristics.

- The parameters of the Fractional Order PID (FPID) controller are tuned by GA, ACO and PSO optimization techniques along with their comparative study to achieve an optimal and desired performance with the fastest steady-state regime and less percentage overshoot.

- These algorithms work with a fitness function for modifying and analyzing a set of potential solutions for evaluating the effectiveness of the model. The controller type may have an impact

on the stability of the system. Therefore, the IAE, ISE and ITAE cost function is designed to select the optimum parameters of the controller to improve the transient and steady-state response of the controller.

- This study uses both real-time experimental and simulation results to validate the effective performance of the proposed technique while guaranteeing both transient and steady-state response of the controller and rejection of external disturbances in comparison to the existing literature.

4.4 SYSTEM DESCRIPTION

The temperature process control setup consists of a combination of heat exchanger and boiler as the main process. Temperature sensors, signal conditioning units, control values and other associated components are also incorporated in the system. The hardware setup is shown in Fig. 4.2(a) and the block diagram is shown in Fig. 4.2(b).
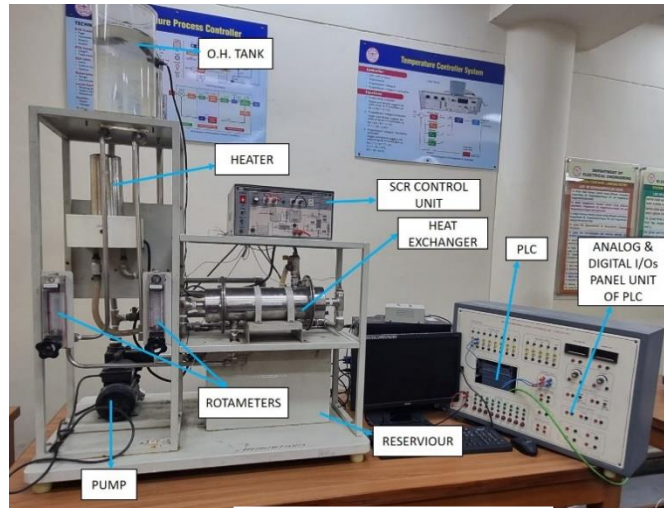
(a) Hardware Setup
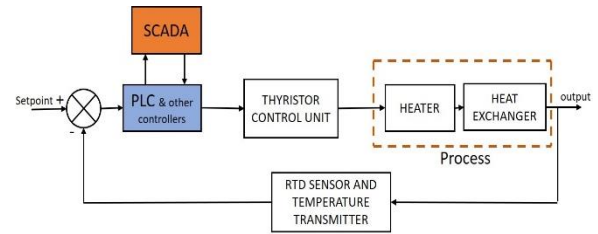
(b) Block diagram of the proposed system

Figure 4.2. Experimental architecture of the proposed temperature control system

The rotameter is one of the types of flow sensors used in process industries. In a rotameter, the obstruction is a float of various shapes (tapered in this process) that rises in a vertical tapered column. The rotameter housed here is mainly used for introducing disturbance or perturbation and also to measure the inlet flow rate. Resistance temperature detectors (RTDs) are used as the temperature sensors in the process. RTD exhibits a change in resistance with temperature. The electric power dissipation must be regulated to avoid errors due to the heating of sensing elements. Typically, 10mW of energy dissipation

will raise the temperature to 0.3°C, which corresponds to low values of current (< 4mA) and voltage (< 1V) in industries. For signal conditioning, the temperature is sensed by RTD and it gets converted into (4-20) mA corresponding to the temperature range of (0-100°C) in the temperature control setup. This current signal is used by the main controller i.e. Programmable Logic Controller (PLC), which fires the final control element, the SCR control unit.

4.4.1 Mathematical Modelling

The process has to be mathematically modelled for designing the controllers. Almost all industrial processes have non-linear characteristics along with some kind of lag. Generally, these processes are approximated as first-order plus time delay (FOPTD) and second-order plus time delay (SOPTD) models.

Generally, FOPTD can be expressed as

$$G_f(s) = \frac{K_f e^{-t_d s}}{\tau s + 1} \tag{4.1}$$

SOPTD can be expressed as follows in the general form

$$G_{ff}(s) = \frac{K_{ff} e^{-t_d s}}{(\tau_1 s + 1)(\tau_2 s + 1)} \tag{4.2}$$

where, K_f is process gain and τ is the time constant of FOPTD, K_{ff} is the process gain and τ_1 and τ_2 are time constants of SOPTD, t_d is the time delay.

Now, the heat exchange transfer function along with the process time delay can be expressed as

$$G_P = \frac{A_P e^{-t_d s}}{\tau_P s + 1} \tag{4.3}$$

where A_P is process gain, t_d is process time delayed and τ_P is the process time constant.
Disturbance transfer function can be expressed as

$$G_d = \frac{A_d}{\tau_D s + 1} \tag{4.4}$$

where A_d is disturbance gain and τ_D is disturbance time constant.
Considering A_d as unity, the disturbance transfer function can be expressed as

$$G_d = \frac{1}{\tau_D s + 1} \tag{4.5}$$

Valve and sensing element transfer functions can be expressed as

$$G_v = \frac{A_v}{\tau_v s + 1}, G_H = \frac{A_H}{\tau_H s + 1} \tag{4.6}$$

where A_v is valve constant, τ_v is the valve time constant, A_H is sensing element gain constant and τ_H is sensor time constant.

So, the overall transfer function of the whole process is formulated as

$$G_{ff}(s) = \frac{5e^{-1s}}{90s^2 + 33s + 1} \qquad (4.7)$$

For reference purposes, the values of the constants which have been considered here are shown in Table 4.1.

Table 4.1. Description of the parameters used in mathematical modelling of the temperature control process

DESCRIPTION	CONSTANTS	VALUES (units)
Heat exchange transfer function along with process time delay	G_P	50
Process time constant	τ_P	30 sec
Disturbance gain	A_d	1
Disturbance time constant	τ_D	10 sec
Valve constant	A_v	0.13
Valve time constant	τ_v	3 sec
Sensing element gain constant	A_H	0.16
Sensor time constant	τ_H	10 sec
Process time delay	t_d	1 sec

4.4.2 Development of SCADA for Temperature Control System

The OMRON (NX1P2-9024DT1) PLC is interfaced with the Wonderware InTouch SCADA system to gather data and create a simulated prototype of the temperature control system for monitoring the entire process on a real-time basis in the SCADA screen and historize the data to its database. The ladder logic of PLCs is designed using Sysmac studio automation software and Wonderware Intouch SCADA software is used for visualizing the plant independently. A user can enter the temperature set point through SCADA. SCADA screen displays the temperature at various points, the direction of the motion, operator caution alarms, auto mode failure, high-temperature alarms, safety alarms, safety shutdown alarms and trends, etc. PLC uses sensors, buttons, process state variables, and other devices to control automated processes and monitor the status of inputs. The SCADA server receives periodic status updates from the PLC-interfaced devices and stores those details in a database under the trends section. PLC carries out the necessary control operations within the heat exchanger plant as directed by the SCADA server. By implementing the proposed system, the operator can easily start the system by setting the temperature set point from SCADA and clicking the start button. The system will take the temperature feedback from the sensors installed in the field and automatically control the temperature by adjusting the hot and cold water valves using the logic written in the PLC.

Figure 4.3 shows the prototype of the developed SCADA system for temperature control of heat exchanger system. The water from the reservoir is pumped to the overhead tank (O.H. Tank), as shown in

48

Fig. 4.3(a). The O.H. Tank is equipped with a safety sensor for preventing overflowing from the tank. A level transmitter (LT) is installed for level measurement in the O.H. Tank unit. The water flow from the O.H. Tank to the heater is measured by rotameter (ROT_1) and it is controlled with a control valve (CV_1). Initially, the SCR unit is triggered by starting the controller and then the internal switch to the heater is turned ON. The increasing temperature can be measured by the temperature-sensing element RTD. The change in resistance from the RTD is fed into the Wheatstone's bridge circuit and converted into the appropriate voltage signal (0-10)Volt and its corresponding current signal (4-20)mA by using the temperature transmitter. This current signal is coupled with controllers. This control action is used to drive the SCR unit which acts as a final control element unit and is triggered according to the control voltage. The directions of the flow in the plant are shown with the arrows in Fig. 4.3(b).

(b)
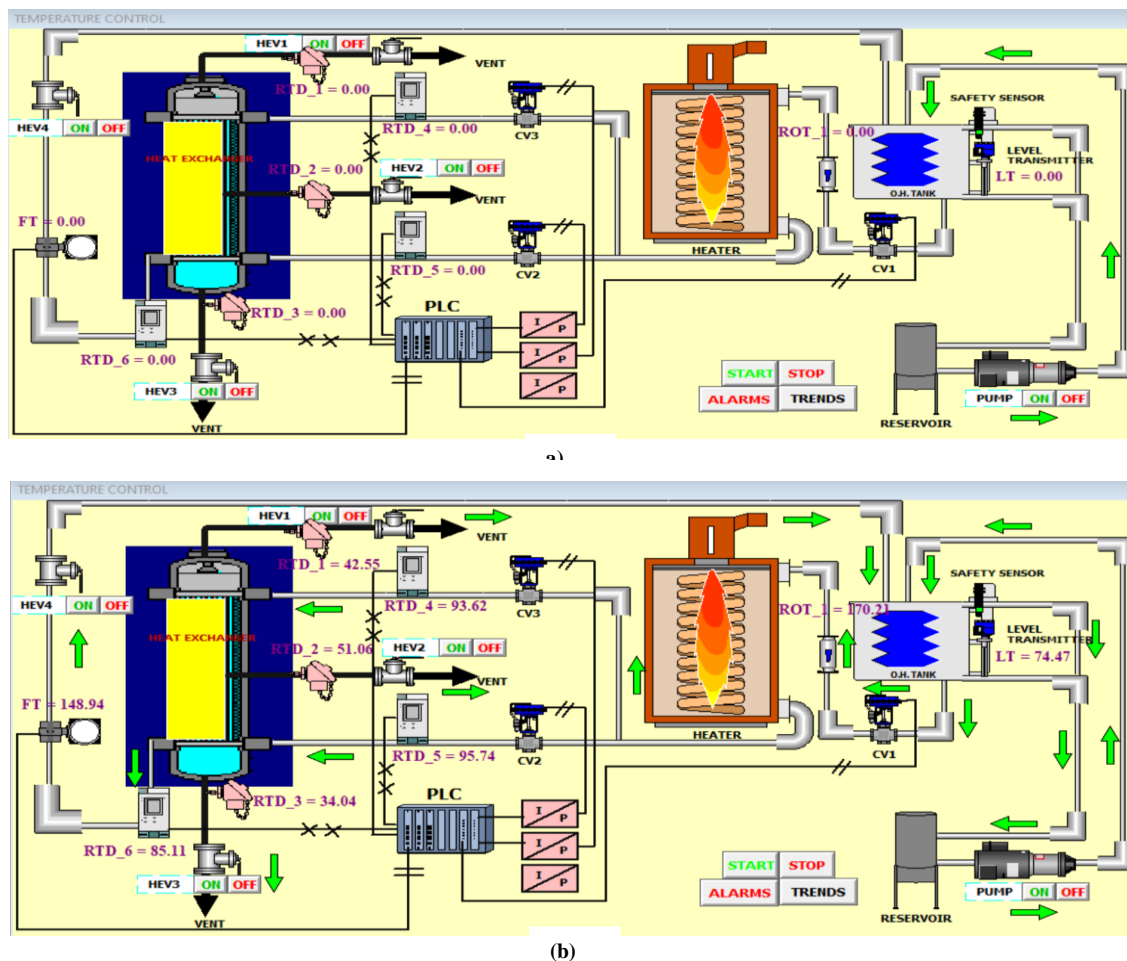
Figure 4.3. Prototype of the developed SCADA system for temperature control of heat exchanger system

4.5   CONTROLLERS DESIGN

In this section, various control strategies like cascade control, feedforward control and Smith predictor for time-delayed process are discussed for controlling the temperature of the process.

4.5.1   Cascade Control Strategy using PID and FPID Controller along with Integral Anti-windup Technique and Velocity Setpoint

PID and Fractional Order Proportional Integral Derivative ($PI^\lambda D^\mu$) controller with the Integral Anti-windup technique is proposed here. In the cascade control configuration, there is more than one measurement for the single manipulated variable. In this configuration, there's a primary or master loop that provides the reference setpoint and the other one is the secondary or slave loop which uses the output of the master loop as its setpoint. The dynamics of the slave loop are much faster than that of the master loop. So, the phase lag of the slave loop is much smaller than that of the master loop. Also, the crossover frequency of the slave loop is much higher than that of the master loop which allows it to accommodate higher gains in the slave loop for regulating the disturbances in the secondary loop without affecting the overall stability of the system. Generally, a proportional control is used in slave loops but Integral control action is also introduced to eliminate the offset error. So, a Proportional Integral (PI) controller is used in the secondary loop. Since flow disturbance is a quick process, therefore, there is no need to increase the proportional gain too much. It will cause too many oscillations. The temperature control process is generally very slow as compared to other control processes like flow and pressure. Usually, PID controller action is preferred for the temperature control process. It accommodates high gains for faster response without affecting the stability of the process. The block diagram of the cascade control strategy using PID and FPID controller is shown in Fig 4.4.
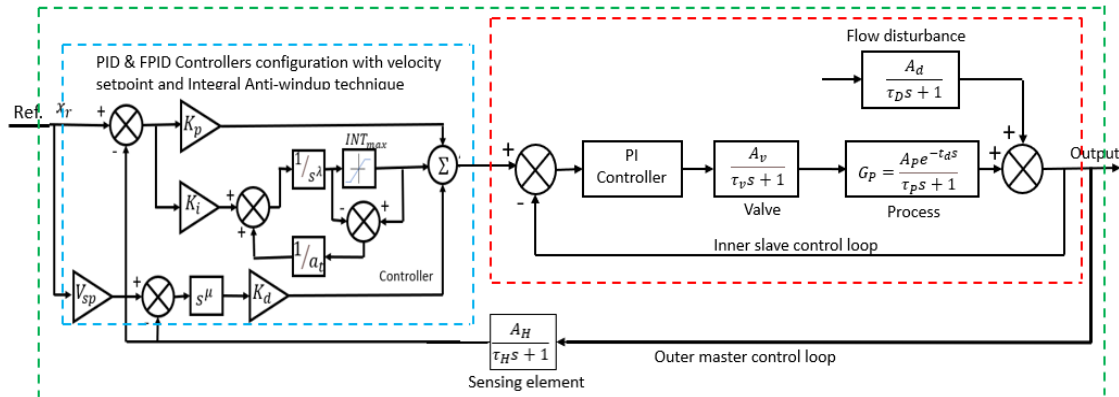
Figure 4.4. Block diagram of cascade control strategy using PID and FPID controller

50

The PID compensator in the time domain, when λ, μ of $PI^\lambda D^\mu$ controller is considered as a unity, as shown in Fig. 4.4 and the expression is given as

$$K_c(t) = K_p\{x_r(t) - r(t)\} + K_d\left[V_{sp}\left\{\frac{d}{dt}x_r(t)\right\} - \frac{d}{dt}r(t)\right] + K_i \int (x_r(t) - r(t))dt \qquad (4.8)$$

where K_p, K_i, K_d are proportional, integral and derivative constants respectively. V_{sp} is the velocity setpoint and it is considered between 0 and 1.

When λ and μ are considered as non-integer orders, then it is said to be FPID controller. FPID features two additional fractional parameters, integral order (λ) and derivative order (μ) to boost the system's flexibility and enable a more effective implementation than a standard PID controller. The generalized equation of $PI^\lambda D^\mu$ controller is formulated as

$$K_c(t) = K_p\{x_r(t) - r(t)\} + K_d D^{-\lambda}\left[V_{sp}\left\{\frac{d}{dt}x_r(t)\right\} - \frac{d}{dt}r(t)\right] + K_i D^\mu \int (x_r(t) - r(t))dt \qquad (4.9)$$

where both λ and μ are as: $0 < \lambda < 1$ and $0 < \mu < 1$.

D is the fractional operator and is defined as

$$D^{-n}f(t) = \frac{1}{\Gamma(n)}\int_0^t f(x)(t-x)^{n-1}dx \qquad (4.10)$$

where, n is non-integer order and Γ is the gamma function. The $PI^\lambda D^\mu$ controller is the generalization of the PID controller.

The active region of $PI^\lambda D^\mu$ and PID controllers are shown in Fig. 4.5.
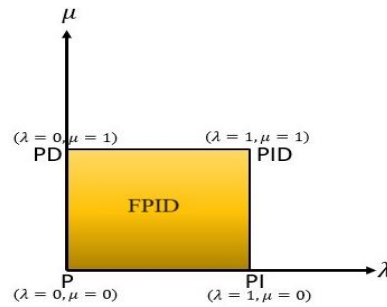
Figure 4.5. Point-to-point representation of active regions of $PI^\lambda D^\mu$ and PID controllers

Figure 4.4 also displays the design of controllers with Integral ANTI-WINDUP. This design incorporates an additional loop around the Integrator, in contrast to the conventional PID controller. By lowering the integrator input, this extra loop inhibits the integrator from reaching saturation and intensifying excessively. At parameter INT_{max}, the Integrator is intended to reach saturation. The integral control action is defined as

$$m_i = \begin{cases} -INTG_{max} & n_i < -INTG_{max} \\ n_i & n_i < -INTG_{max} < 0 \text{ and } -INTG_{max} - n_i < 0 \\ INTG_{max} & INTG_{max} < n_i \end{cases} \qquad (4.11)$$

where $\text{INTG}_{\max}$ is the upper limit of integrator, a_t is the time constant of the anti-windup loop which gets activated only in case of Integrator saturation. The reset time of Integrator depends on a_t. The Integrator is in normal control action when $m_i = n_i$. But the anti-windup controller makes the saturation error zero in case of Integration saturation and then Integrator output becomes saturation limits, i.e. $\text{INTG}_{\max}$ and $-\text{INTG}_{\max}$.

4.5.2 Feedforward Control for Slave Loop

Feedback slave control loops are not able to achieve perfect control of a chemical industrial process. They react only after detecting any deviation in the output value from the desired value. Unlike feedback control loops, feedforward control loops directly measure the perturbances or disturbances and then anticipate the effect that they will have on the main process output. The control action starts when any change is detected in the disturbance. It changes the manipulated variable precisely to eliminate the disturbance impact on the process-controlled output. The main objective is to maintain the outflow temperature of the fluid constant by manipulating the steam flow. Fluid flow rate and fluid inflow temperature are the two principal perturbances or disturbances that need to be controlled with feedforward control. The block diagram of the feedforward control with feedback control loop is shown in Fig. 4.6. From the block diagram, we have

$$y = G_P \bar{m} + G_d d \tag{4.12}$$

The manipulated variable is given as

$$\bar{m} = G_v G_{c1}(\bar{y}_{sp} - G_{m1}y) + G_v G_{c2}(\bar{y}_{sp} - G_{m2}d) \tag{4.13}$$

From Eq. (4.12) and Eq. (4.13), we get

$$y = \frac{G_P G_v (G_{c1} + G_{c2} G_{sp})}{1 + G_P G_v G_{c1} G_{m1}} \bar{y}_{sp} + \frac{G_d - G_p G_v G_{m2} G_{c2}}{1 + G_P G_v G_{c1} G_{m1}} d \tag{4.14}$$

The transfer functions of the feedforward loop are

$$G_{c2} = \frac{G_d}{G_p G_v G_{m2}} \quad and \quad G_{sp} = \frac{G_{m2}}{G_d} \tag{4.15}$$
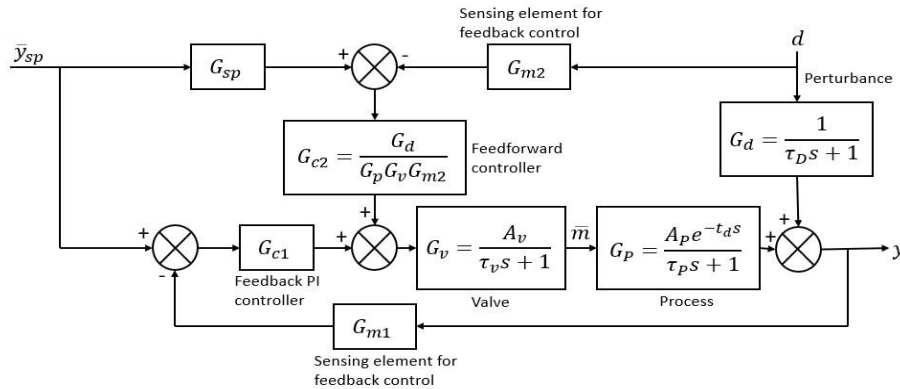
Figure 4.6. Block diagram of the feedforward control with feedback control loop

If G_p, G_d, G_v and G_{m2} are known to be true, then this feedforward loop will compensate for the whole disturbance. While any of the G_p, G_d, G_v and G_{m2} are known by approximation, then

$$G_p G_{c2} G_v G_{sp} \neq 1 \quad and \quad G_d - G_v G_{c2} G_p G_{m2} \neq 0 \tag{4.16}$$

As a result, the feedforward loop will not compensate the whole disturbance perfectly but the feedback loop offers the required compensation.

4.5.3 Smith Predictor for Time Delay Process

In the earlier discussions, it was assumed that whenever there is any change in the perturbance and manipulated variables, the effects are observed instantly in the controlled output variable. However, in real physical experience, there is always a time interval (duration depends on the complexity of the process) during which no effect is observed on the output-controlled variable. This is termed as dead time or transportation lag. Smith predictor or dead-time compensator is defined as a modification in the classical feedback control system to incorporate the transportation lag as shown in Fig. 4.7.

$$G_P = \frac{A_P e^{-t_d s}}{\tau_P s + 1} \quad or \quad G_P = G_s e^{-t_d s} \tag{4.17}$$
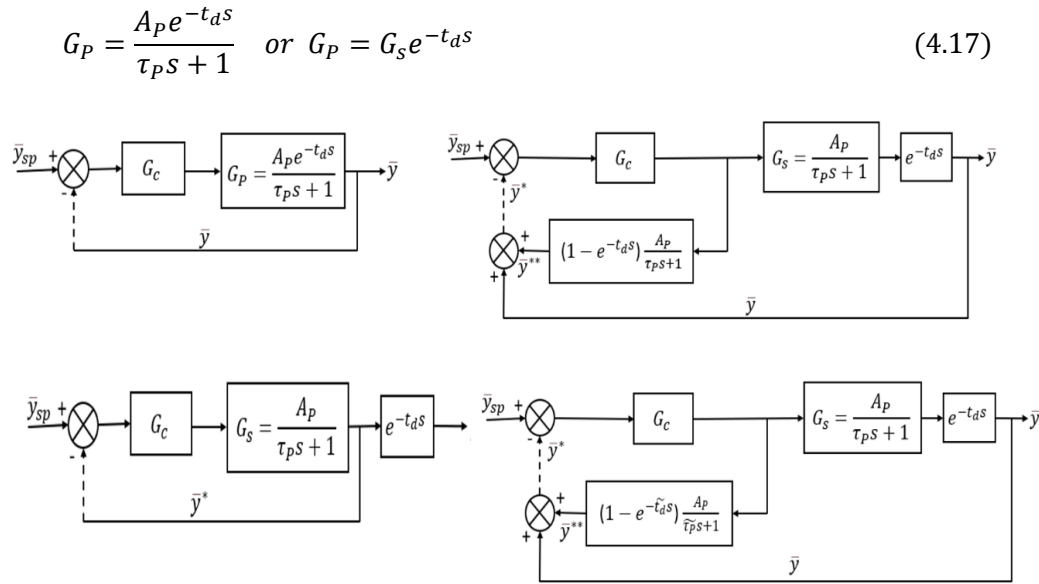
Figure 4.7. Block diagram of Smith predictor or dead-time compensator for the time delay process

Now, the open loop response for Fig. 4.7 will be equal to

$$\bar{y} = \bar{y}_{sp}[G_s e^{-t_d s}] G_c \tag{4.18}$$

For undesired effects elimination, it is required to have a feedback signal that does not carry any transportation lag information, such as

$$\bar{y}^* = \bar{y}_{sp}[G_s] G_c \tag{4.19}$$

This is only possible if a certain quantity is added in $\bar{y}^*$, such that

$$\bar{y}^{**} = \bar{y}_{sp}[G_s] G_c [1 - e^{-t_d s}] \tag{4.20}$$

which implies

$$\bar{y} + \bar{y}^{**} = \bar{y}^* \qquad (4.21)$$

Usually, in process control, the process and dead time are obtained by approximation. So, let us assume that G_s and t_d are true process characteristics and $\widetilde{G_s} = \frac{A_P}{\widetilde{\tau_P} s + 1}$ and $\tilde{t}_d$ are their respective approximation. In this case, the improved Smith predictor is

$$\bar{y}^* = \bar{y}_{sp}\left[\widetilde{G_s} + \left(G_s e^{-t_d s} - \widetilde{G_s} e^{-\tilde{t}_d s}\right)\right]G_c \qquad (4.22)$$

Eq. (4.22) implies that $G_c = \widetilde{G_s}$ and $t_d = \tilde{t}_d$ for the perfect dead-time compensation. Greater the modelling error $[G_c - \widetilde{G_s}$ and $t_d - \tilde{t}_d]$, lower the effectiveness of the compensation. But, the term $(t_d - \tilde{t}_d)$ is more crucial because of the exponential factor.

The combined form of the temperature controller with cascade control, feedforward control and dead-time compensator is shown in Fig. 4.8.
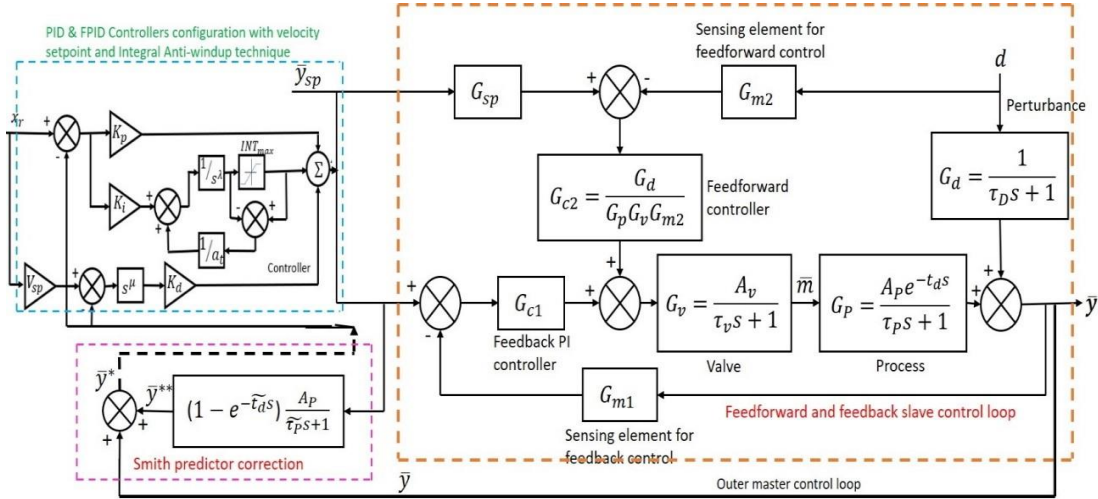
Figure 4.8. Temperature controller with cascade control, feedforward control and dead-time compensator

4.6 METAHEURISTIC OPTIMIZATION TECHNIQUES

The performance of both PID and $\text{PI}^\lambda \text{D}^\mu$ controllers are optimized using adaptive heuristic optimization techniques. Genetic algorithm (GA), Ant Colony Optimization (ACO) and Particle Swarm Optimization (PSO) are used for optimizing the parameters of both controllers. In control system design and analysis, the calculated performance indices are utilized as a quantitative matrix for evaluating the performance of a system. The parameters of a control system are adjusted such that the design index reaches its lowest value while respecting the constraints of the controlled system. Integral square error (ISE), Integral absolute error (IAE) and Integral time absolute error (ITAE) are the commonly used indices. These indices are defined as

$$ISE = \int_0^t e^2(t)dt \qquad (4.23)$$

$$IAE = \int_0^t |e(t)| dt \qquad (4.24)$$

$$ITAE = \int_0^t t|e(t)|\, dt \qquad (4.25)$$

The selection of these criteria depends on the type of characteristics to be controlled. For suppressing large errors, ISE is preferred and IAE is preferred for suppressing small errors. ITAE is preferred to suppress the errors that persist for a long time. The flow charts of GA, ACO and PSO algorithms are shown in Fig. 4.9. These algorithms are a little time-consuming but give better accuracy and precision after a series of experiments and better parameter selection as shown in Table 4.2.

(a)

(b)

(c)
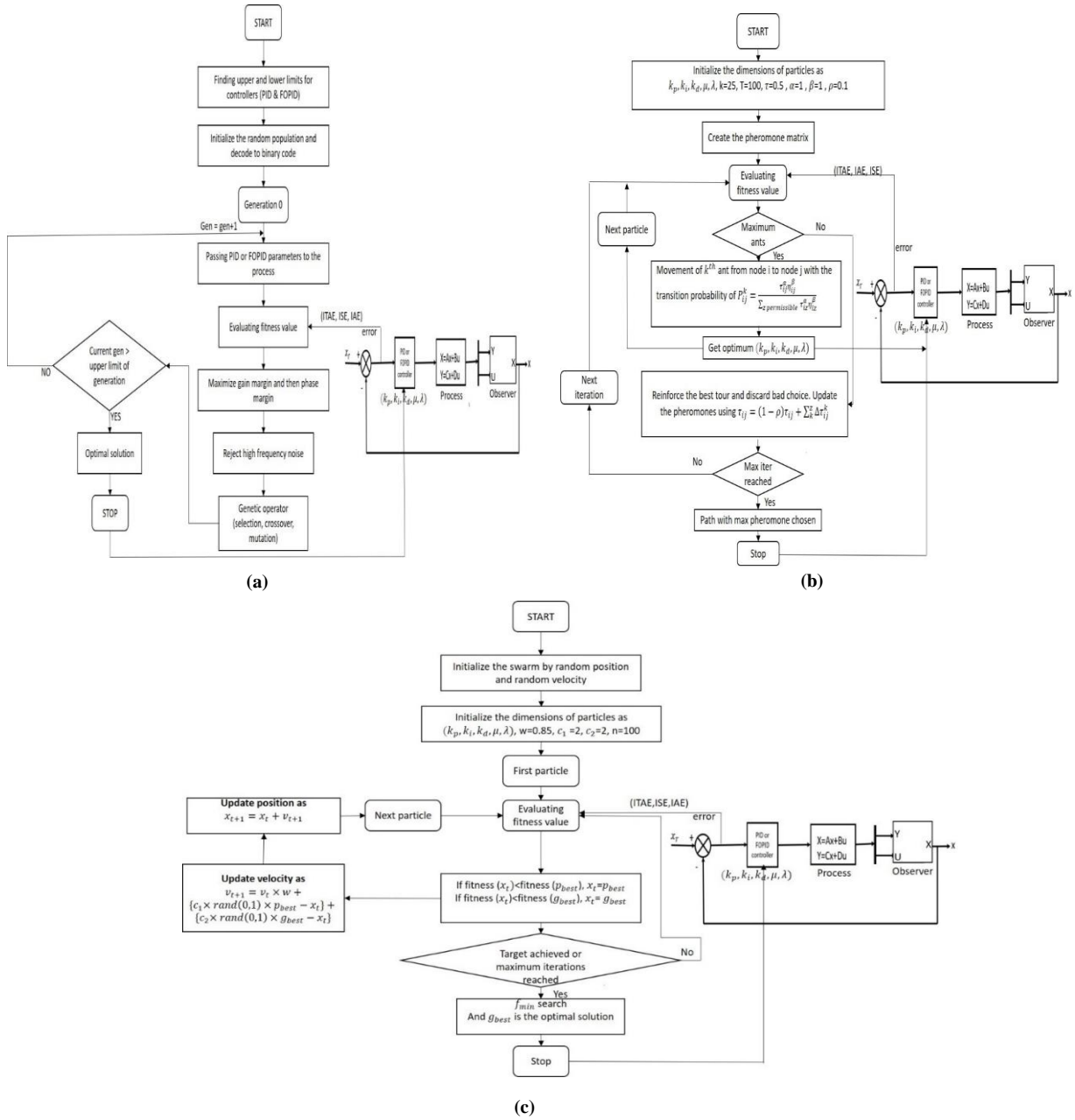
Figure 4.9. Flow chart of the proposed **(a)** Genetic Algorithm **(b)** Ant Colony Optimization **(c)** Particle Swarm Optimization

Table 4.2. Parameters of GA, PSO and ACO algorithm

PARAMETERS of GA		PARAMETERS of ACO		PARAMETERS of PSO	
Parameters	**Values**	**Parameters**	**Values**	**Parameters**	**Values**
Number of generations	100	Max iterations (T)	100	Number of iterations	100
Population size	50	Pheromone (τ)	0.5	Number of participles	50
Length of chromosomes	35	Number of ants (k)	50	Inertia	0.85
Probability of crossover	0.85	Pheromone exponential weight (α)	1	Cognitive component (c_1)	2
Probability of mutation	0.3	Pheromone heuristic weight (β)	1	Social component (c_2)	2
		Evaporation parameter (ρ)	0.1		

4.7 RESULTS AND DISCUSSIONS

This section discusses the simulation and real-time experimental results of PID and FPID controllers along with optimization techniques for studying temperature control system. Different performance indices like ISE, IAE and ITAE are implemented for simulation and only ITAE is used for real-time experimentation. The combined form of temperature controller with Cascade control, Feedforward control and dead-time compensator is examined after modelling for simulation using MATLAB 2022a. To keep the computational time measurements consistent, all the experiments were run on a computer with an Intel I7-3770, 3.4 GHz CPU with 32GB of memory with no GPU acceleration. Verification of results after the implementation of various indices on the simulated model is to be considered on a momentary basis. After that, real-time experimentation is carried out with these controllers over the temperature control setup where $V_{sp} = 0.95$.

4.7.1 Comparison of simulated results using PID controller with Metaheuristic Optimization Techniques based on ISE, IAE and ITAE

Fig. 4.10(a-c) shows the comparison of simulated results using PID controller with metaheuristic optimization techniques based on different indices ISE, IAE and ITAE respectively. Values of all the parameters (P, I, D, N) are optimized on the basis of different indices as shown in Table 4.3. Table 4.4 depicts the performance analysis of PID and PID with optimization techniques based on different indices. It is observed that all three optimization techniques provide much better results in comparison to non-optimized PID controllers. Among optimization techniques, ACO provides the best settling time and GA provides the least overshoot. Among performance indices, ITAE provides overall balanced results.
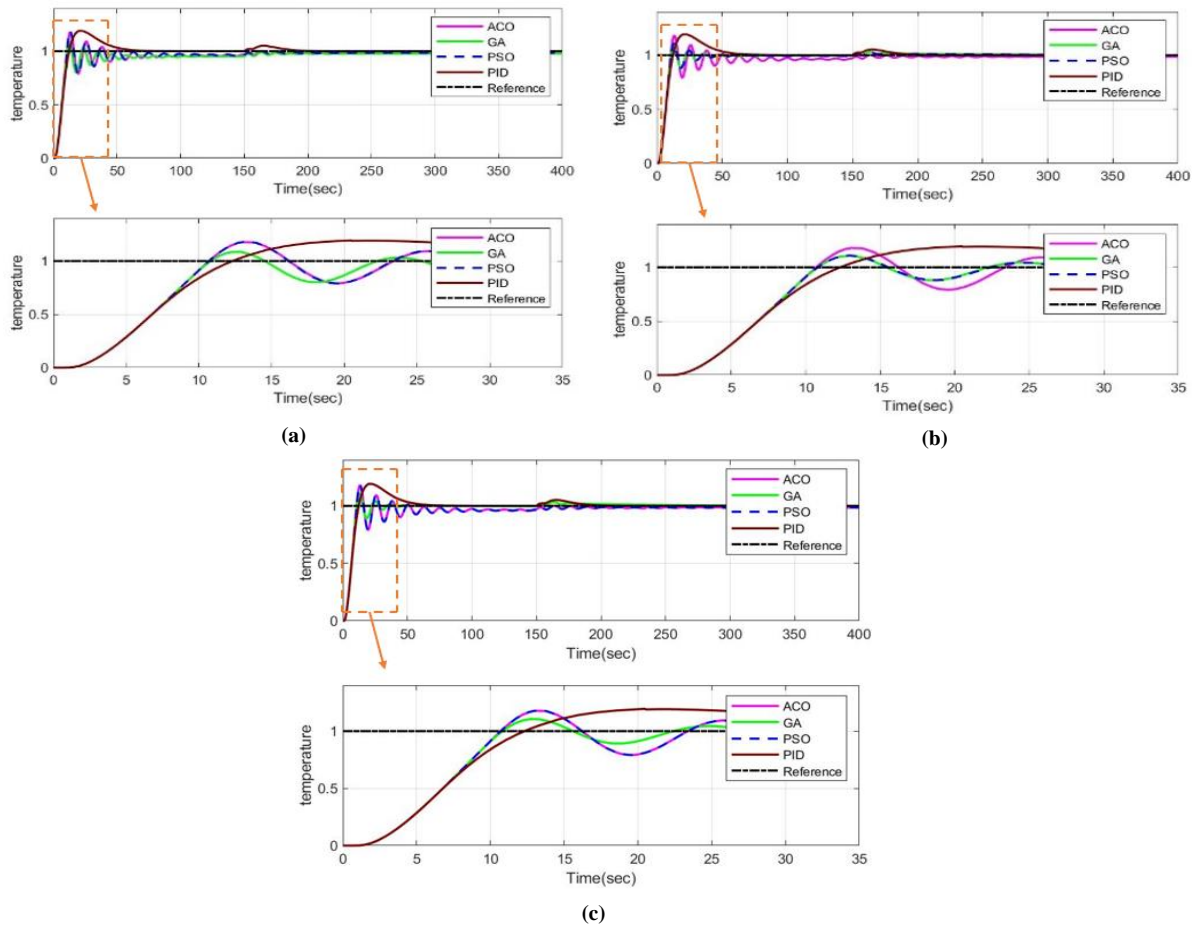
Figure 4.10. Comparison of simulated results using PID controller with metaheuristic optimization techniques based on different indices **(a)** ISE **(b)** IAE and **(c)** ITAE

Table 4.3. Optimized values of all the parameters (P, I, D, N) on the basis of different indices

INDICES →	ISE				IAE				ITAE			
CONTROLLER & OPTIMIZATION TECHNIQUES → PARAMETERS ↓	PID	GA	PSO	ACO	PID	GA	PSO	ACO	PID	GA	PSO	ACO
P	1.694	1.858	1.143	1.116	1.694	1.402	1.012	1.116	1.694	1.658	1.716	1.114
I	0.093	0.002	0.044	0.001	0.093	0.083	0.099	0.003	0.093	0.096	0.099	0.001
D	5.664	4.491	4.089	4.082	5.664	4.193	4.084	4.084	5.664	4.232	4.023	4.083
N	30.42	28.26	28.29	28.12	30.42	28.001	28.18	28.13	30.42	28.51	28.48	28.67

Table 4.4. Performance analysis of PID and PID with optimization techniques based on different indices

INDICES →	ISE			IAE			ITAE		
PARAMETERS → CONTROLLER & OPTIMIZATION TECHNIQUES ↓	RISE TIME (s)	SETTLING TIME (s)	OVERSHOOT	RISE TIME (s)	SETTLING TIME (s)	OVERSHOOT	RISE TIME (s)	SETTLING TIME (s)	OVERSHOOT
PID	25.02	276.98	19.48	25.02	276.98	19.48	25.02	276.98	19.48
GA	15.19	269.20	10.82	16.10	267.29	10.53	15.86	263.21	10.74
PSO	13.01	245.65	20.03	12.97	241.34	19.41	15.84	256.56	11.03
ACO	12.97	238.71	19.2	12.39	238.73	19.56	12.97	238.70	19.45

4.7.2 Comparison of simulated results using FPID controller with Metaheuristic Optimization Techniques based on ISE, IAE and ITAE

Fig. 4.11(a-c) shows the comparison of simulated results using the FPID controller with metaheuristic optimization techniques based on different indices ISE, IAE and ITAE respectively. Values of all the parameters (P, I, D, μ, λ) are optimized on the basis of different indices as shown in table 4.5. The performance analysis of FPID and FPID with optimization techniques based on different indices is shown in Table 4.6. Among optimization techniques, ACO provides the best settling time and the least overshoot. Among performance indices, ITAE provides the best-balanced results. As compared to PID and PID with optimization techniques, FPID and FPID with optimization techniques provide much better performance results.
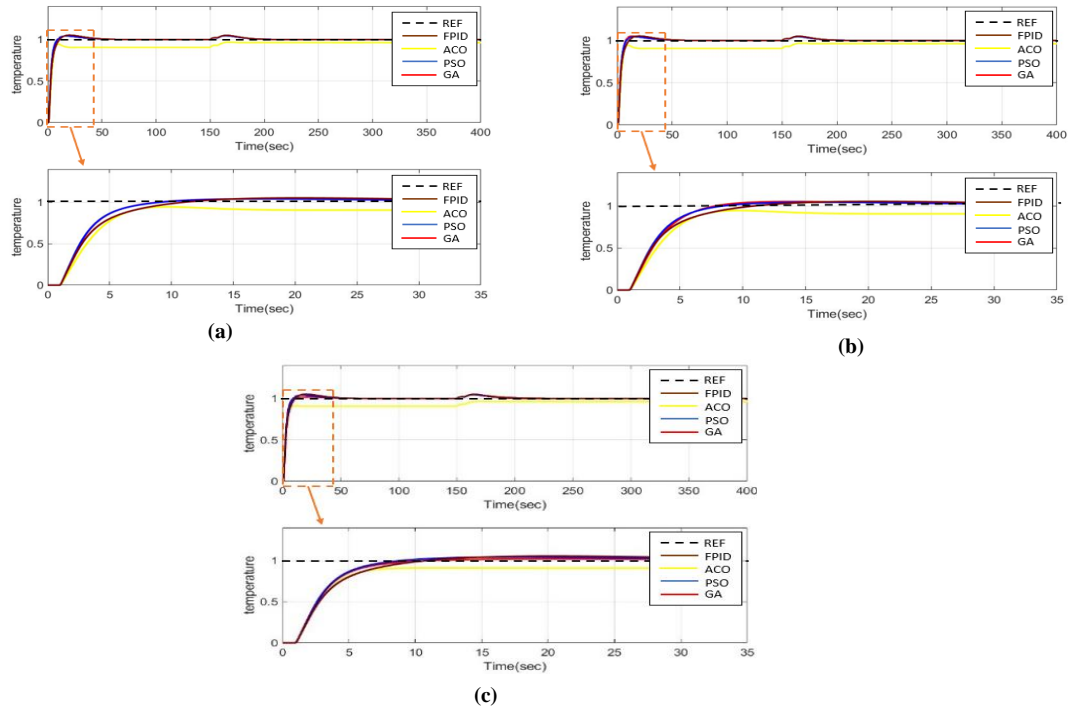
Figure 4.11. Comparison of simulated results using FPID controller with metaheuristic optimization techniques based on different indices **(a)** ISE **(b)** IAE and **(c)** ITAE

Table 4.5. Optimized values of all the parameters (P, I, D, μ, λ) on the basis of different indices

INDICES →	ISE				IAE				ITAE			
CONTROLLER & OPTIMIZATION TECHNIQUES → PARAMETERS ↓	FPID	GA	PSO	ACO	FPID	GA	PSO	ACO	FPID	GA	PSO	ACO
P	1.694	1.998	1.979	1.955	1.694	1.982	2.011	1.955	1.694	1.989	2.001	1.953
I	0.093	0.099	0.100	0.001	0.093	0.110	0.101	0.001	0.093	0.077	0.110	0.023
D	5.664	5.923	6.021	4.181	5.664	5.183	5.692	4.187	5.664	5.923	5.992	5.582
μ	0.998	0.129	0.001	0.001	0.989	0.183	0.751	0.001	0.999	0.198	0.672	0.001
λ	0.989	0.184	0.011	0.011	0.970	0.839	0.534	0.011	0.998	0.701	0.491	0.010

Table 4.6. Performance analysis of FPID and FPID with optimization techniques based on different indices

INDICES →	ISE			IAE			ITAE		
PARAMETERS → CONTROLLER & OPTIMIZATION TECHNIQUES ↓	RISE TIME (s)	SETTLING TIME (s)	OVERSHOOT	RISE TIME (s)	SETTLING TIME (s)	OVERSHOOT	RISE TIME (s)	SETTLING TIME (s)	OVERSHOOT
FPID	49.78	1692	5.35	49.78	1691	5.35	49.78	1691	5.35
GA	33.80	1534	4.58	35.05	1536	5.21	34.76	1611	4.77
PSO	32.67	1555	4.56	34.22	1535	4.60	34.22	1565	4.57
ACO	39.34	1366	0.41	39.36	1362	0.40	41.23	1392	0.23

4.7.3 Comparison of real-time experimentation results using PID and FPID controllers with Metaheuristic Optimization Techniques based on ITAE

During simulation, it has been observed that ITAE provides balanced results among all performance indices. So, only ITAE is considered for the real-time analysis of the system. The parametric values of the controllers are decided on the basis of the simulated results discussed above. The results of both PID and FPID controllers with different optimization techniques based on ITAE are shown in Fig. 4.12 respectively and the performance analysis is shown in table 4.7.
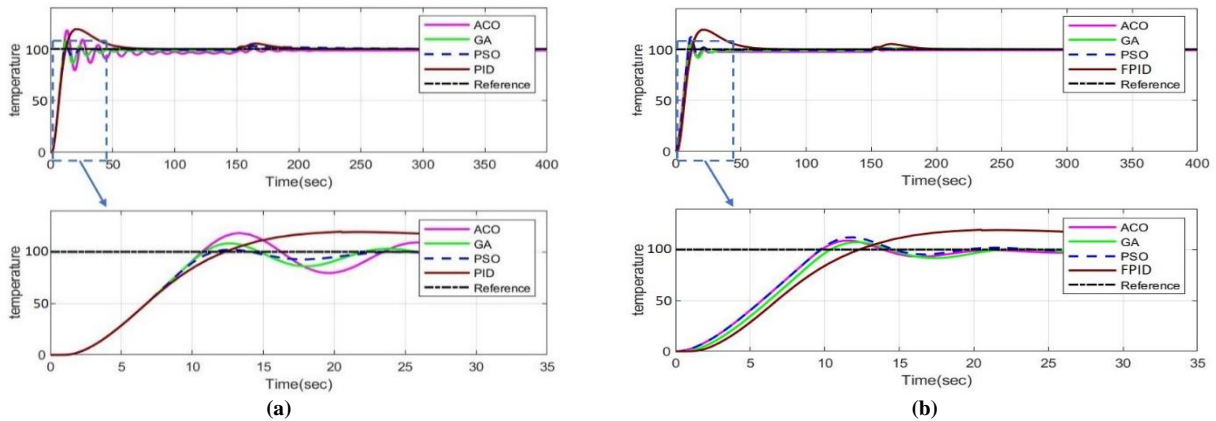
Figure 4.12. Real-time analysis of the system using PID and FPID controllers with different optimization techniques based on ITAE

Table 4.7. Performance analysis of results of both PID and FPID controllers with different optimization techniques based on ITAE

CONTROLLER →	PID			FPID		
PARAMETERS → CONTROLLER & OPTIMIZATION TECHNIQUES ↓ (based on ITAE)	RISE TIME (s)	SETTLING TIME (s)	OVERSHOOT	RISE TIME (s)	SETTLING TIME (s)	OVERSHOOT
PID/FPID	25.02	276.98	19.48	23.12	276.97	19.48
GA	16.86	245.76	8.14	17.56	137.14	7.27
PSO	20.74	231.96	3.04	14.04	118.18	12.31
ACO	17.03	245.51	19.94	11.09	92.34	9.29

4.8 SUMMARY

This chapter proposed a novel cascade control strategy using PID and Fractional Order PID ($PI^\lambda D^\mu$) controller along with an integral anti-windup technique and velocity setpoint to control and regulate the outlet temperature of a heat exchanger to a certain reference value and enhance the heat transmission efficiency irrespective of the external disturbances, non-linearity and delay characteristics. Various control strategies like cascade control, feedforward control and Smith predictor for the time-delayed process (dead-time compensator) are discussed for controlling the temperature of the process. The parameters of both PID and $PI^\lambda D^\mu$ controllers are tuned using adaptive heuristic optimization techniques like GA, ACO and PSO to achieve an optimal and desired performance with the fastest steady-state regime and less percentage overshoot. IAE, ISE and ITAE cost functions are designed to select optimum parameters of the controllers to improve the transient and steady-state response of the controllers.

For developing a real-time framework for the temperature control of a heat exchanger plant, this chapter used a PLC and SCADA-based control framework to automate and supervise the temperature control processes in a heat exchanger plant and monitor all the processes using SCADA. The OMRON (NX1P2-9024DT1) is interfaced with the Wonderware InTouch SCADA system to gather data and create a simulated prototype of the temperature control to monitor the entire process on a real-time basis in the SCADA screen and historize the data to its database. PLC carries out the necessary control operations within the heat exchanger plant as directed by the SCADA server. The programming of PLC is done using Sysmac studio automation software using the ladder programming language and Wonderware Intouch SCADA software is used for visualizing the whole plant operations.

In control system design and analysis, the calculated performance indices are used as quantitative measures for evaluating the performance of the system. This study used both real-time experimental and simulation results to demonstrate the effective performance of the developed controllers using MATLAB with metaheuristic optimization techniques based on different performance indices like ISE, IAE and ITAE while guaranteeing both transient and steady-state response of the controller and rejection of external disturbances in comparison to the existing literature. The outcomes of simulation and experimental assessment implies that the Fractional Order PID controller provides overall better control performances as compared to the PID compensator for the temperature control of a heat exchanger plant. During simulation, the optimized PID controller with ACO algorithm provides the best setting time and the optimized PID controller with GA algorithm provides the minimum peak overshoot. However, the optimized FPID controller with the ACO algorithm provides the least settling time and the least peak overshoot. ITAE performance index provides overall balanced results both in the case of optimized PID and $PI^\lambda D^\mu$ controllers

respectively. As compared to the PID controller, $PI^{\lambda}D^{\mu}$ controller provide better performance results. During real-time experimentation, PID optimized with PSO algorithm provides balanced results and FPID optimized with ACO provides the most balanced results and FPID controller provides better performance results as compared to PID controller.

The proposed temperature control system used the EtherCAT protocol which offers high speed, low hardware cost, a wide range of products, low latency/delay, flexible topology support and incredible synchronization than other real-time protocols in industrial control systems. The proposed SCADA system achieves automatic control and management of industrial processes, improves worker safety, and reduces manpower and physical resources instead of a distributed control system. This work increases the significance of investigating and implementing automated systems across multiple sectors.

Chapter 5

Real-Time Control of 2-DOF Ball Balancer using Intelligent Controllers

5.1 INTRODUCTION

The ball balancer system is an electromechanical non-linear system which innates unstable and underactuated behaviour that can be helpful in the realisation of both position tracking and balancing control problems in robotic systems analysis. This chapter presents the modelling, design, control and affirmation of various controllers over the 2-DOF Ball balancer system. Different compensators like Proportional-Derivative (PD), Proportional-Integral-Derivative (PID), PID with Integral ANTI-WINDUP with different velocity setpoint values along with different inputs and Neuro-fuzzy with PID (NiF-PID) controller are implemented over the system. The modelling of different controllers is done using MATLAB/Simulink and the Quarc system is used for interfacing. After simulation, the designed control law is applied to a physical (real-time) Quanser experimental setup of the ball balancer system. The overhead camera tracks the ball's position and controllers predicts the precise position and provides the planar position of the ball as an output. Both transient and steady-state response analyses are done to evaluate the performance of these compensators. The comparisons for variation in ball position, applied input voltage to the servo motor and plate angle are executed with different compensators for both simulation and real-time experimentation purposes. Position and plate angle control with load variation are also executed in real-time with NiF-PID compensator. A comparative analysis of the simulation and experimental results is done to see which controller provides overall better control performances, best adaptability and best relevancy among all the designed controllers for the ball balancer system. NiF-PID compensator provides 18.55% better result in case of steady-state error and 10 times less overshoot in case of real-time experimentation as compared to the PID controller.

5.2 RELATED WORK

Nonlinear systems with underactuated actuators are approximated with intelligent control and autonomous decision-development techniques [182]. The position tracking and balance control in robotic ball balancer systems is a widely researched problem because of its nonlinearity and instability. Generally, these systems find their application as benchmark systems for testing control laws and developing control strategies for problems related to the movement of robotic manipulators. Researchers have investigated the behaviour of numerous controllers to achieve self-balancing control and steady-state operation because of the structural complexity of these systems. Several linear and nonlinear controller architectures like optimal controller [183], PID [184], sliding mode controller (SMC) [185], neural network [186,187], model predictive control [188,189], fuzzy logic control, fractional control [190] and different optimization algorithms [191] have been studied in the literature for the stabilization control, trajectory tracking and position control of a B&P system.

Conventionally, classical controllers like PD and PID made their way to be implemented with the B&P system for closed-loop system stability [192]. However, conventional PIDs cannot produce satisfactory eliminated outcomes in the presence of more intense external disturbance. Borah et al. [193] presented a study which used integer and fractional order PD controllers for tracking various trajectories of a B&P system using gravitational search, BAT and firefly algorithm. Srivastava et al. [194] implemented PSO with GSA and GWO hybrid optimization algorithms on the PID controller to tune controller parameters in order to control the angle of the beam and the position of the ball. However, the unwanted chattering in the actuators causes harm to the mechanical and electronic components of the system.

To eliminate coordinate transformation and minimise complexity, Zheng et al. [195] suggested a parallel thinning and window-searching approach which used a sensing camera for tracking the position and movement of the B&P system with both fuzzy and PID control. When external disturbance is more intense, the main problem with conventional PID is that it cannot produce satisfactory eliminated outcomes. With differential feedback, these systems have a drawback that they can't intensify measurement noise.

Similar to the forward-stepping controller, a backstepping controller was proposed to generate a distinct control law for achieving better control performance more quickly [196]. Ma et al. [197] presented an observer-integrated backstepping control technique for a cascaded B&P system which used a linear extended state observer and tracking differentiator to measure the uncertainties and derivatives of the virtual controls with Lyapunov theory. However, these systems result in unwanted chattering entering the actuators of the system, harming both its mechanical and electronic components.

Fuzzy and sliding mode controllers have been widely discussed to overcome the chattering phenomenon in a B&P system. Zaare et al. [198] implemented an adaptive fuzzy sliding mode controller based on the state disturbance observer to control the position of the ball and beam system with different uncertainties. Elshamy et al. [199] proposed a hybrid pseudo-PD controller (fuzzy logic) for improving the stabilization and tracking the trajectory of the B&P system which used different machine learning algorithms like random forest, decision tree and support vector regression to detect the servo motor angle for correcting the ball plate position. While utilizing the simplified model, some degree of control error is unavoidable.

Jang et al. [200] proposed an adaptive observer control technique based on a virtual angle to solve the under-actuation problem without velocity measurements and local minima issues. It estimated the velocity information of robots with uncertainty using a neural network-based observer. Haddad et al. [201] presented a study by implementing different model-based controllers such as PID, LQR, linear model predictive control, state feedback control and linear quadratic tracker using ATmega328P microcontroller to control and stabilize a laboratory prototype of a B&P system. However, the greatest shortcoming of these traditional methods is the significant increase in peak overshoot and settling time.

Zakeri et al. [202] presented a type-2 fuzzy fractional order twisting algorithm for fully-actuated and second-order SMC for under-actuated nonlinear systems. A comparison of different control algorithms for balancing the B&P system with the 6-DOF Stewart platform has been done in [203,204]. Further, an innovation in disturbance observer using active disturbance rejection control (ADRC) methodology was devised in [205] to avoid harmful frictional effects for balancing and controlling the ball on the plate.

Different complex control challenges were accomplished and implemented using perplexed and self-perceptive neuro-fuzzy systems were examined by researchers in different areas like electrical and electronic systems, unidentified nonlinear control systems [206,207], NFS enhancements [208], image processing, feature extraction, technical diagnostics and measurement [209]. Chavez et al. [210] designed a PD controller based on a spiking neural network for the laboratory testbed of a B&P prototype. Kravets et al. [211] introduced a neural network controller based on a field-programmable gate array device for stabilizing the ball balancer system.

Hadoune et al. [212] used a 3-DOF parallel robot based on an adaptive neuro-fuzzy inference system technique for controlling the stability, oscillation and smoothening of the movement of the ball in the B&P system. However, these systems are non-robust and less accurate. A power-reaching law-based radial basis function network adaptive control approach was proposed by Li et al. [213] to reduce the chattering problems of the ball balancer system. However, the high nonlinearities introduced by the pneumatic actuators overcomplicate the controller design.

5.3 PROBLEM STATEMENT

After doing a thorough analysis of the literature, it was determined that the development of robust controllers for the B&P system could be seen as a potential research work for improving the dynamic nature of ball position and plate angle. The B&P system is highly nonlinear and underactuated because of the electromagnetic actuators and susceptibility to external perturbations than the actuated systems [214]. The nonlinear and underactuated behaviour of the ball balancer system significantly impacts the steady-state operation and position tracking. The B&P system is inherently unstable because a small disturbance can cause the ball to roll off to the edges from an equilibrium or predetermined position on the plate. Therefore, it is important to have an appropriate strategy to control the ball's motion on a plate to direct it along a predetermined path.

The ball balancer system has not yet utilized (to the best of our knowledge) hybrid algorithms like neural-fuzzy (NiF) or neural-fuzzy PID (NiF-PID) controllers for controlling the ball balancer system. Therefore, this chapter proposes the development and implementation of different controllers including PD, PID, PID with Integral ANTI-WINDUP and Neuro integrated Fuzzy with PID controller on a 2-DOF ball balancer system with different velocity setpoints (V_{sw}) values along with different inputs in order to tackle the non-linear disturbances and uncertainties efficiently. Most of the studies on controllers in the literature are primarily supported by simulation results only. On the other hand, real-time experimental results also validate the effective performance of the proposed technique, while guaranteeing both reference tracking and rejection of external disturbances in comparison to the existing literature. This study uses the QUARC target libraries in MATLAB to provide a hardware-in-loop structure to enable a real-time controller interface. As a result, it is possible to implement these PID and NiF-PID controllers in real-time on a highly unstable B&P system, achieving good performance even in the presence of external perturbations.

5.4 2-DOF BALL BALANCER SYSTEM

The 2DBB system is an electromechanical, second-order multi-input, and multi-output system which is highly nonlinear and unstable [215]. 2DOFBB is the more sophisticated version of one DOF ball and beam system. The system's two inputs are servo input commands for the x and y axes, and its two outputs are ball position along the x and y axes. To keep the system stable, it needs a feedback closed-loop controller. The 2DoF ball balancer system addresses two control issues:

   a) Controlling the plate's inclination (i.e., the plate angle)
   b) Controlling the ball's position on the moving plate.

As voltage is applied to the system, the rigid plate's slope changes, thus affecting the ball's movement as the plate's inclination changes. The servo motor's movement alters the plate's angle,

which causes the ball to drop from the plate [216]. Therefore, a controller is required with this system for balancing the ball's movement on the plate.

5.4.1 Hardware Setup of the 2-DOF Ball Balancer System

The real-time hardware model of the 2-DoF ball balancer system used for designing of Simulink model is manufactured by QUANSER [217]. A little plastic ball, two rotating servo motors, a power amplifier, a USB camera to record the image of the ball's location, a data-gathering device, and a computer system with a feedback controller make up the hardware needed to conduct the experiment. A metallic plate with four quadrants is fixed to the 2-DOF ball balancer system with a gimbal joint in the middle that features a two-degree range of flexibility in rotation for tilting in the x and y axes. The two servo motors that are part of the 2DBB system are mechanically attached to the plate's axis and connected perpendicularly in the x and y directions. The two servo motors operate independently of one another. The block diagram architecture of the B&P system is shown in Fig. 5.1(a). The laboratory setup of a 2DoF B&P system is depicted briefly in Fig. 5.1(b).

Through the employment of a Faulhaber series DC micromotor, the plate rotates in order to balance the system in both directions [218]. This keeps the ball balanced on the metallic plate's quadrangular surface and prevents it from slipping off. The servo input voltage (SRV02) unit has a standard servo motor incorporated with a potentiometer, which is being used to balance the ball in both axes. The standard control problem of this set-up focuses mainly on balancing the ball on the square plate.

(a)   (b)
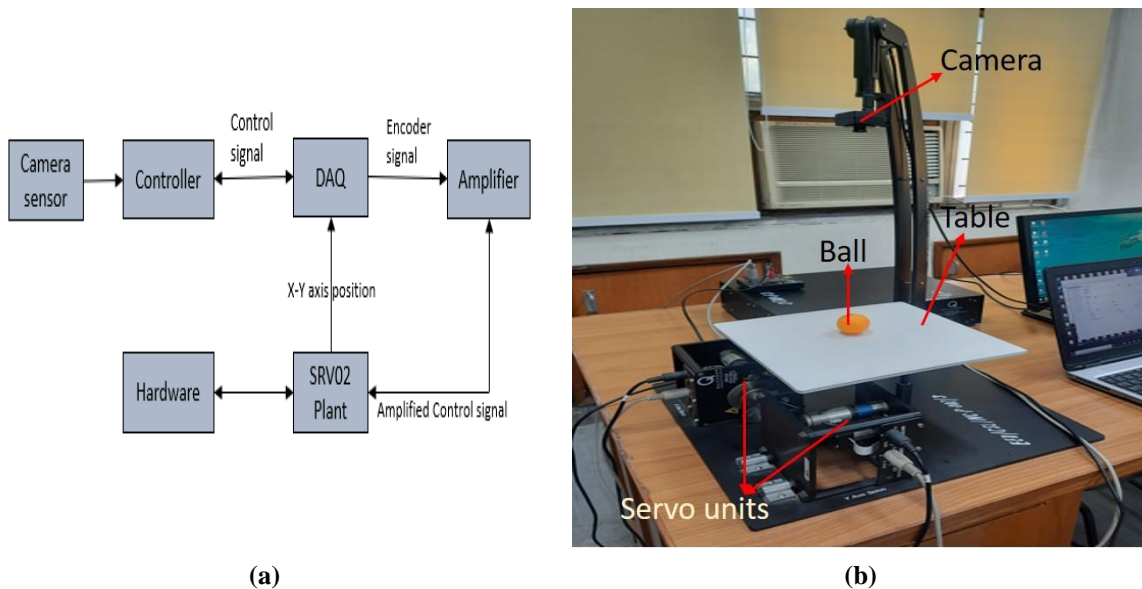
Figure 5.1. (a) Block diagram of 2-DOF Ball Balancer system **(b)** Hardware setup of 2DBB in laboratory

In order to obtain the ball movement with respect to voltage, a control signal, or plate inclination, is initially given to the Data Acquisition (DAQ) device from the hardware configuration, depicted in

Fig. 5.1(a). Using the Q2-USB data acquisition board, a longer period of time is spent in measuring the control signal related to the plate's disposition. The information about the movement of the ball on the plate regarding the voltage change is provided by the measured signal. Additionally, the received signal is relayed to the controller along with the ball coordinates that were recorded using the camera. The controller performs the required steps to keep the ball balanced, and the DAQ repeats the process until the plate's stabilising angle is reached. The controller receives the signal from DAQ and then coordinates with the camera signal from the overhead camera with the help of signal processing technique and then this controlled output signal is sent to the DAQ again, which delivers this encoded signal to the power amplifier for signal amplification and then this amplified control signal is fed back to the hardware setup or SRV02 plant and this process repeat itself. The SRV02 plant unit, which is accomplished currently for position and balance control, may be implemented for further applications like vibrations and self-erecting controls in other setups like solar energy tracker, inverted pendulum etc. which makes this system unit applications feasible and economical. Figure 5.2 depicts the taxonomy of required steps used for balancing and position tracking control of a 2-DoF ball balancer system.
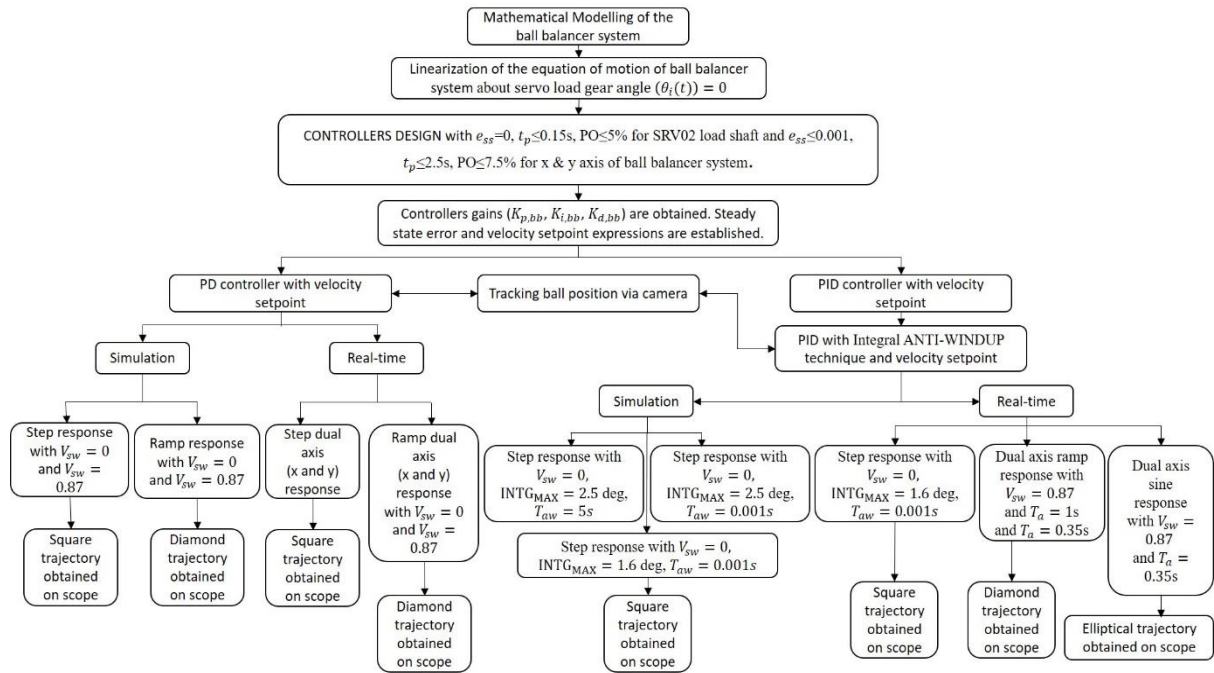
Figure 5.2. Flow chart depicting the taxonomy of required steps used for balancing and position tracking control of 2-DoF ball balancer system

5.4.2 Mathematical Modelling

Figure 5.3 displays the open loop transfer function of the ball balancer system. The transfer function $T_s(s)$ represents the dynamics between the resulting load gear angle $\theta_i(s)$ and input servo motor voltage $V_m(s)$. The transfer function $T_{ss}(s)$ represents the dynamics between the position of the ball R(s) and servo load gear angle $\theta_i(s)$.

Figure 5.3. Open loop transfer function of ball balancer system

Since this is a decoupled system in which the actuator dynamics of both SRV02 unit and 1DBB system are independent and will not affect each other. Thus, the SRV02 device is considered to be symmetrical for both the x and y-axis. Therefore, the modelling of the 2D Ball Balancer is presented only for a single axis 1DBB.

The complete transfer function is 1DBB + SRV02 unit is $T(s)$ as given in Eq. (5.1)

$$T(s) = T_s(s)T_{ss}(s) \tag{5.1}$$

where, $T_s(s)$ and $T_{ss}(s)$ are the transfer functions of the SRV02 unit and 1DBB system.

$$T_s(s) = \theta_i(s)/V_m(s) \tag{5.2}$$

$$T_{ss}(s) = R(s)/\theta_i(s) \tag{5.3}$$

The ball's motion with respect to the plate angle is calculated using the second-order differential equation of motion (EoM). Thus, the EoM with respect to the angle of the beam (δ) is formulated as

$$\frac{d^2}{dt^2}x(t) = f\big(\delta(t)\big) \tag{5.4}$$

where $\delta(t)$ is a non-linear function. Figure 5.4 depicts the front view of the B&P system. The side view of the B&P system is identical in both x and y-directions. Table 5.1 describes the parameters of the Ball and plate system.

Figure 5.4. Illustration of the schematic layout of the Ball and Plate system along with Free body diagram

Table 5.1. Description of the parameters of the B&P system

Symbol	Description/Quantity	Units
x	Displacement	m
M_{ball}	Mass of ball	kg
τ_{ball}	Torque of ball	N-m
r_{ball}	Radius of ball	m
θ_i	Servo load gear angle	Rad
δ	Angle of beam	rad
J_{ball}	Moment of inertia of ball	kg-m^2
R_{arm}	Radius of Arm	m
H	Height of beam	m
g	Acceleration due to gravity	m/s^2
$\emptyset_{ball}$	Angle of ball	rad
L_p	Length of the plate	m
K	Steady-state gain	rad/A-s

Neglecting both viscous damping and friction, the ball forces can be represented as

$$\Sigma F = F_{x,t} - F_{x,r} = M_{ball}g \tag{5.5}$$

$$\Sigma F = M_{ball} \left\{ \frac{d^2}{dt^2} x(t) \right\} \tag{5.6}$$

When the inclination is positive, the two forces acting in the positive x-direction are

$$F_{x,t} = M_{ball}\, g\, \sin(\delta)\,, F_{x,r} = \tau_{ball}/r_{ball} \tag{5.7}$$

where, $F_{x,t}$ is the translational force due to the gravity, $F_{x,r}$ is the rotational inertia force of the ball, M_{ball} is the mass of the ball, δ is the angle of the beam, g is the acceleration due to gravity, τ_{ball} is the torque of the ball and r_{ball} is the radius of the ball.

Now, the torque applied over the ball, in terms of the moment of inertia and ball angle is given by

$$\tau_{ball} = J_{ball} \left\{ \frac{d^2}{dt^2} \emptyset_{ball}(t) \right\} \tag{5.8}$$

where, J_{ball} is the moment of inertia of the ball and $\emptyset_{ball}$ is the angle of the ball.

Substituting the value of τ_{ball} in Eq. (5.7), the rotational inertia force of the ball in terms of the moment of inertia and radius is represented as

$$F_{x,r} = J_{ball} \left\{ \frac{d^2}{dt^2} x(t)/r_{ball}^2 \right\} \tag{5.9}$$

Substituting the values of $F_{x,t}$ from Eq. (5.7) and $F_{x,r}$ from Eq. (5.9) into Eq. (5.5), the overall forces applied over the ball in terms of the moment of inertia are given as

$$\Sigma F = M_{ball} \left\{ \frac{d^2}{dt^2} x(t) \right\} = M_{ball}\, g \sin(\delta) - J_{ball} \left\{ \frac{d^2}{dt^2} x(t)/r_{ball}^2 \right\} \tag{5.10a}$$

$$M_{ball} \left\{ \frac{d^2}{dt^2} x(t) \right\} = M_{ball}\, g \sin(\delta) - \frac{J_{ball} \left\{ \frac{d^2}{dt^2} x(t) \right\}}{r_{ball}^2} \tag{5.10b}$$

Now, solving for the final equation of motion in terms of acceleration of the B&P system, the equation of motion is formulated as

$$\frac{d^2}{dt^2}x(t) = \frac{M_{ball}\, g\, \sin(\delta(t))\, r_{ball}{}^2}{M_{ball}.\, r_{ball}{}^2 + J_{ball}} \tag{5.11}$$

The above Eq. (5.11) gives the final ball and plate system equation of motion. It is quite difficult to design a stabilizing controller for a non-linear system model. So, it is important to linearize the non-linear system about a desired operating point to analyze the system's behaviour such as stability, reference tracking, etc. In this work, Eq. (5.11) is linearized about the servo load gear angle $(\theta_i(t)) = 0$ in order to use the model for Laplace-based PID controller design.

5.4.3 Inclusion of SRV02 Dynamics

To obtain the position of the ball with respect to the servo load gear angle and beam angle

$$\sin(\delta(t)) = 2H/L_p\, ,\, \sin(\theta_i(t)) = H/R_{arm} \tag{5.12}$$

So, the relation between beam angle and servo load gear angle is formulated as

$$\sin(\delta(t)) = 2\sin(\theta_i(t))\, R_{arm}/L_p \tag{5.13}$$

where, δ is the angle of the beam, H is the height of the beam, L_p is the length of the plate, θ_i is the servo load gear angle, R_{arm} is the radius of the arm.

Designing a stabilizing controller for a non-linear system model is a challenging task. Therefore, it is important to linearize the non-linear system about a desirable operating point in order to study the behaviour of the system. In this study, Eq. (5.11) is linearized about $\theta_i(t) = 0$ to use the model for Laplace-based PID controller design.

$$\frac{d^2}{dt^2}x(t) = \frac{2M_{ball}\, g\, \sin(\theta_i(t))\, R_{arm}r_{ball}{}^2}{(M_{ball}.\, r_{ball}{}^2 + J_{ball}\,)L_p} \tag{5.14}$$

At $\theta_i(t) = 0$, $\sin(\theta_i(t)) = \theta_i(t)$. By approximating the value, the Linear equation of motion for the 1DBB plant is formulated as

$$\frac{d^2}{dt^2}x(t) = \frac{[2M_{ball}\, g.\, \theta_i(t)\, R_{arm}r_{ball}{}^2}{(M_{ball}.\, r_{ball}{}^2 + J_{ball}\,)L_p} \tag{5.15}$$

Eq. (5.14) is a non-linear equation as discussed above and Eq. (5.15) represents the linear equation of motion for 1DBB plant. Lumping the coefficient parameters of $\theta_i(t)$ to get the parameter model gain (K_m) Of 1DBB system

$$K_m = \frac{[2M_{ball}\, g.\, R_{arm}]\, r_{ball}{}^2}{(M_{ball}.\, r_{ball}{}^2 + J_{ball}\,)L_p} \tag{5.16}$$

Eq. (5.15) becomes a nonlinear equation of motion for 1DBB plant as formulated below

$$\frac{d^2}{dt^2} x(t) = K_m . \theta_i(t) \tag{5.17}$$

All the initial conditions are assumed to be zero to get the transfer function for 1DBB plant. The Laplace transform of Eq. (5.17) is formulated as

$$s^2 X(s) - D(x(0)) - sx(0) = K_m . \theta_i(s) \tag{5.18}$$

$$X(s) = K_{bb} \theta_i(s) / s^2 , T_{ss}(s) = K_m / s^2 \tag{5.19}$$

where, K_m is the parameter model gain, K_{bb} is the velocity gain, $T_{ss}(s)$ is the transfer function of the 1DBB system.

The transfer function of SRV02 is formulated as

$$T_s(s) = K / s(1 + \tau s) \tag{5.20}$$

So, the complete transfer function of 1DBB and SRV02 unit and ball position becomes

$$T(s) = K \frac{K_m}{s^3(1 + \tau s)} , \qquad R(s) = V_m k \frac{K_m}{s^3(1 + \tau s)} \tag{5.21}$$

where, $T(s)$ is the transfer function of 1DBB and SRV02 unit, K is the steady-state gain, $R(s)$ is the ball position, V_m is the input servo motor voltage.

5.5 DESIGNING CONTROLLERS FOR BALL BALANCER SYSTEM

In this section, the PID controller with velocity setpoint (V_{sw}) and Neuro-Fuzzy with PID (NiF-PID) controllers are designed for position tracking and balancing of the ball balancer system. The cascade control for the x-axis of the SRV02+2DBB system is depicted in Fig. 5.5. 2DBB is a decoupled system. So, the x-axis actuator will not affect the response of the y-axis response. SRV02 device is considered to be symmetrical for both the x and y-axis. Therefore, the modelling is represented only for a single axis. 2DBB single axis (x-axis) is represented as 1DBB.
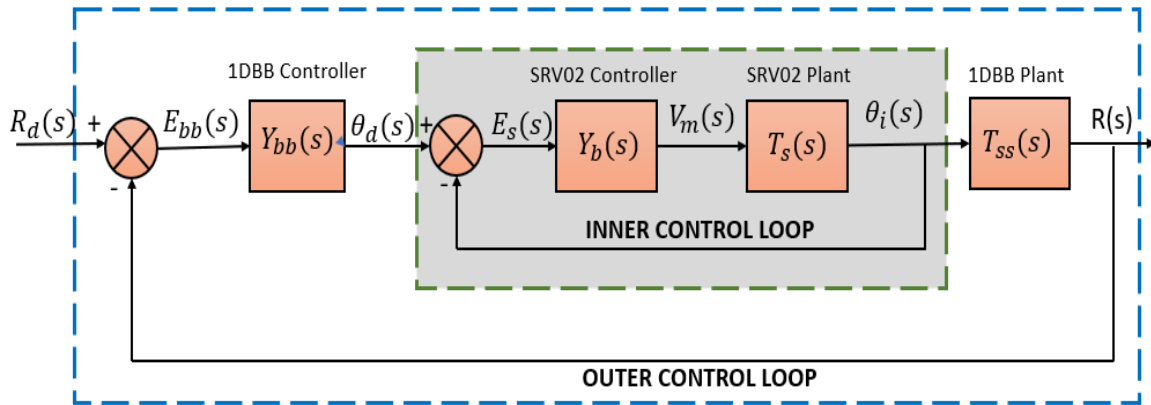
Figure 5.5. Cascade control for the x-axis of the SRV02+2DBB system

In Fig. 5.5, R_d is the desired ball position, $Y_{bb}(s)$ is the ball balancer compensator, $E_s(s)$ is the error signal transfer function, Y_b is the servo compensator, V_m is the input servo motor voltage, $T_s(s)$ is the transfer function of the SRV02 unit, θ_i is the servo load gear angle, $T_{ss}(s)$ is the transfer function of the 1DBB system and $R(s)$ is the ball position. Depending upon the ball position R(s), the ball balancer compensator $Y_{bb}(s)$ computes the required servo load angle $\theta_d(s)$ to get the desired ball position $R_d(s)$. The servo position control is described by an inner loop where a servo compensator $Y_b(s)$ calculates the required motor voltage $V_m(s)$ for the desired load angle. Later on, the compensator for the outer loop is designed. The desired specifications for the SRV02 load shaft and the x and y-axis of the ball balancer system are as follows:

- e_{ss}=0, $t_p \leq$0.15s, PO≤5% for SRV02 load shaft
- $e_{ss} \leq$0.001, $t_p \leq$2.5s, PO≤7.5% for the x & y axis of ball balancer system

where, e_{ss} is the steady-state error, t_p is the peak time and PO is the peak overshoot.

For designing the inner control loop, the proportional velocity controller gains are obtained when SRV02 is in a high-gear configuration. The nominal SRV02 model parameters are model steady-state gain ($K = 1.78$ rad/s) and time constant ($\tau = 0.0288$s). To meet the above specifications, the desired damping ratio is 0.693 and the minimum natural frequency is 28.82 rad/s. Using nominal model parameters, the proportional control gain (K_p) is 13.57 V/rad and velocity control gain (K_v) is 0.0788 Vs/rad. The outer control loop controls the ball position along the x-axis.

5.5.1 PID Control Design

The PID compensator with cascade control in the time domain for the outer control loop (illustrated in Fig. 5.6) is provided as

$$\theta_d(t) = K_{p,bb}\{r_d(t) - r(t)\} + K_{d,bb}\left[V_{sw}\left\{\frac{d}{dt}r_d(t)\right\} - \frac{d}{dt}r(t)\right] + K_{i,bb}\int(r_d(t) - r(t))dt \quad (5.22)$$

where, θ_d is the required servo load angle, $K_{p,bb}$ is the gain of proportional control action, $K_{i,bb}$ is the gain of integral control action and $K_{d,bb}$ is the derivative control action gain.
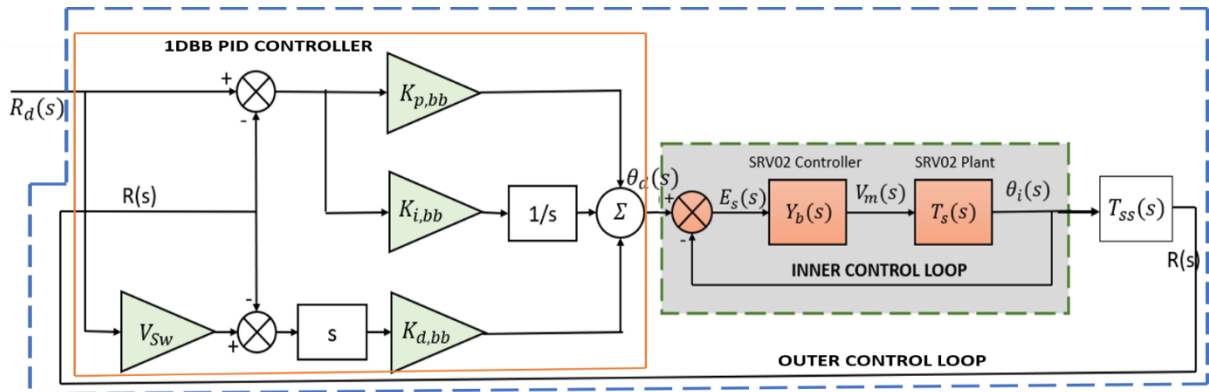
Figure 5.6. Overall architecture of the PID compensator with cascade control

72

With no servo dynamics, the outer-loop controller in the Laplace domain is formulated as

$$\theta_d(s) = \{K_{p,bb} + K_{i,bb}/s\}\,(R_d(s) - R(s)) + K_{d,bb}s(V_{sw}R_d(s) - R(s)) \qquad (5.23)$$

In case of no servo dynamics, $\theta_d(s) = \theta_i(s)$. Therefore, the control loop equation becomes

$$\frac{R(s)}{R_d(s)} = \frac{K_m\left(s^2 K_{d,bb}V_{sw} + sK_{p,bb} + K_{i,bb}\right)}{s^3 + s^2 K_m K_{d,bb} + sK_m K_{p,bb} + K_m K_{i,bb}} \qquad (5.24)$$

The prototype third-order characteristic equation is formulated as

$$(s^2 + 2\zeta\omega_n s + \omega_n{}^2)(s + a_0) \qquad (5.25)$$

$$s^3 + (2\zeta\omega_n + a_0)s^2 + (2\zeta\omega_n a_0 + \omega_n{}^2)s + (\omega_n{}^2 + a_0) \qquad (5.26)$$

Comparing the characteristic equations Eq. (5.24) and Eq. (5.26), PID control action gains are formulated as

$$K_{p,bb} = \frac{\omega_n(2\zeta a_0 + \omega_n)}{K_m} \qquad (5.27)$$

$$K_{i,bb} = \frac{\omega_n{}^2 a_0}{K_m} \qquad (5.28)$$

$$K_{d,bb} = \frac{2\zeta\omega_n + a_0}{K_m} \qquad (5.29)$$

where, ω_n is natural frequency, ζ is the damping ratio and a_0 is pole location.

These parameters decide the response of the third-order system. The natural frequency and damping ratio are calculated on the basis of predefined specifications. After solving Eq. (5.27)-Eq. (5.29) under the pre-defined specifications, $\omega_n = 2.195\left(\frac{rad}{s}\right)$ and $\zeta = 0.638$.

❖ <u>Controller Gains</u>

To meet the desired specifications, PD and PID controller gains are estimated. For the PD controller, pole location is considered as $a_0 = 0$ and for the PID controller, pole location is considered as $a_0 = 1$. The decay time constant (T_a) is taken as 1s. The velocity setpoint is zero for the PD controller and varies from 0 to 1 in the case of the PID controller. Table 5.2 shows the calculated controller gains.

Table 5.2. Parameters and Gains of PD and PID Controller

Parameters→ Controllers ↓	Pole location, a_0 (rad/s)	Steady-state gain, K (rad/Vs)	Time constant, τ (s)	V_{sw}	$K_{p,bb}$ (rad/m)	$K_{i,bb}$ (rad s/m)	$K_{d,bb}$ (rad s/m)
PD	0	8.837	0.051	0	3.72	0	2.148
PID	1	8.837	0.051	0-1	5.819	3.693	2.967

❖ **Steady State Error**

The error in the x-axis of the 2DBB system is formulated as

$$E(S) = R_d(s) - R(s) \tag{5.30}$$

After solving Eq. (5.24), the closed-loop PID response is formulated as

$$R(s) = \frac{K_m\big(s^2 K_{d,bb} V_{sw} + sK_{p,bb} + K_{i,bb}\big)}{s^3 + s^2 K_m K_{d,bb} + sK_m K_{p,bb} + K_m K_{i,bb}} R_d(s) \tag{5.31}$$

Substituting the value of $R(s)$ from Eq. (5.31) in Eq. (5.30), the error transfer function of the PID controller is obtained as

$$E(s) = \frac{s^2\big(s + K_m K_{d,bb} - K_m K_{d,bb} V_{sw}\big)}{s^3 + s^2 K_m K_{d,bb} + sK_m K_{p,bb} + K_m K_{i,bb}} R_d(s) \tag{5.32}$$

If $K_{i,bb}=0$, the error transfer function of PD is formulated as

$$E(s) = \frac{s\big(s + K_m K_{d,bb} - K_m K_{d,bb} V_{sw}\big)}{s^2 + sK_m K_{d,bb} + sK_m K_{p,bb}} R_d(s) \tag{5.33}$$

When a step reference with amplitude a_0 is applied to the error transfer function of the PD controller, then steady-state error (e_{ss}) is zero, which is less than the required specification of 0.1mm. Similarly, when a ramp reference with slope $a_0 = 0.012 \left(\frac{m}{s}\right)$ and $V_{sw} = 0$ is applied to the error transfer function of the PD controller, then $e_{ss}=0.7$, which is more than the required specification. In order to meet the desired specifications of $e_{ss}<0.1$mm, it is required to design a velocity set-point weight (V_{sw}).

When a ramp input with a slope a_0 is applied to PD controller, the steady-state error is given as

$$e_{ss} = \frac{a_0 K_{d,bb}(V_{sw} - 1)}{K_{p,bb}} \tag{5.34}$$

Solving this further to get velocity setpoint,

$$V_{sw} = \frac{a_0 K_{d,bb} - K_{p,bb}.e_{ss}}{a_0 K_{d,bb}} \tag{5.35}$$

By substituting the specifications of steady-state error, PD gains and all the constant values in Eq. (5.35), the desired velocity set-point weight is obtained as 0.863.

5.5.2 PID Compensator with Integral ANTI-WINDUP Technique

The actuator limits should be considered while implementing an integral control action in any control system loop. This is due to the actuator's inherent property to achieve maximum amplifier supply

voltage. Due to the inclusion of large set points, the actuator gets saturated because the integral value keeps increasing to compensate for the error. This phenomenon is known as integral windup. As a result, the system becomes unstable with large overshoots.

The Integral term in the PID controller makes the output to change continuously until there is zero error. But sometimes the error cannot be eliminated quickly and within a particular time frame, larger and larger Integral terms are produced and it continues to happen until saturation is achieved. This leads to the bad performance of the system in terms of peak overshoot. Therefore, a PID compensator with an Integral ANTI-WINDUP technique is implemented over the ball balancer system for simulation and real-time experimentation in order to reduce these unnecessary oscillations.

Figure 5.7 shows the architecture of the proposed PID controller with the Integral ANTI-WINDUP technique. Contrary to the traditional PID controller, this design includes another loop around the integrator. In the case of integrator saturation, this additional loop prevents it from building up too much intensity by decreasing the integrator input. The integrator is designed to saturate at parameter INTG_{MAX}.
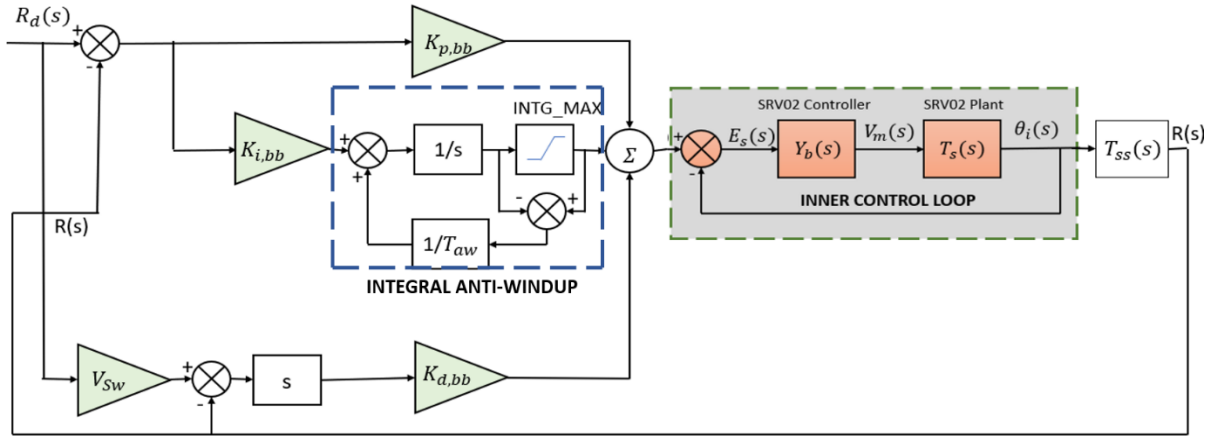
Figure 5.7. Block architecture of PID compensator with Integral ANTI-WINDUP

The integral control action is defined as

$$m_i = \begin{cases} -\text{INTG}_{\text{MAX}} & n_i < -\text{INTG}_{\text{MAX}} \\ n_i & n_i < -\text{INTG}_{\text{MAX}} < 0 \text{ and } -\text{INTG}_{\text{MAX}} - n_i < 0 \\ \text{INTG}_{\text{MAX}} & \text{INTG}_{\text{MAX}} < n_i \end{cases} \qquad (5.36)$$

where $\pm\text{INTG}_{\text{MAX}}$ represents the limits of the integrator. The Integrator reset time depends on the time-constant (T_{aw}) of the anti-windup loop which gets activated only in case of integrator saturation. If $m_i=n_i$, then the Integrator is in normal control action. i.e. no integral saturation. However, in the case of Integral saturation, the anti-windup controller makes the saturation error zero and the saturation limits (INTG_{MAX} and $-\text{INTG}_{\text{MAX}}$) becomes the output of the Integrator.

5.5.3 Neuro-integrated Fuzzy with PID (NiF-PID) Controller

Neuro-fuzzy controller (NiF) includes the highlights of artificial neural networks and fuzzy logic under a single architecture. As a result, NiF has the ease in interpreting the control action via fuzzy logic and learning through neural optimization techniques. Neural networks adapt the events and then train data according to the previous values and fuzzy provides liberty in the system formation without the availability of a system model. The hybrid adaptive neuro-fuzzy inference system (ANFIS) is formulated by training the adaptive neural network optimization techniques and then generating the fuzzy model. neural learnings adapt to environmental conditions and then adjust activation function accordingly and thus minimize error while fuzzy formation. NiF control is the combination of five layers as follows:

- Layer 1: Linear transfer function layer
- Layer 2: Logical operations
- Layer 3: Fuzzification process
- Layer 4: Fuzzy inference layer, having parameters that can be changed over time
- Layer 5: Defuzzification process

Neuro-fuzzy controller represents the Takagi-Sugeno (T-S) model which is the amalgamation of gradient descent and estimation of the least squares approach. This is known as a hybrid learning algorithm which is used to update the data from pre-defined fuzzy rules and fuzzified neuron activation functions.

The neural network architecture is shown in Fig. 5.8. Let us assume M and N be two inputs with $x_1, x_2, \ldots x_n$ be the linguistic variables for defining membership functions of M and similarly $y_1, y_2, \ldots y_n$ be the linguistic variables for defining N. The formation of rules is as depicted below:

Rule 1: if M is x_1 and N is y_1 then f_1 is $A_1 M + B_1 N + O_1$

Rule 2: if M is x_2 and N is y_2 then f_2 is $A_2 M + B_2 N + O_2$

……

……

Rule N^{th}: if M is x_n and N is y_n then f_n is $A_n M + B_n N + O_n$
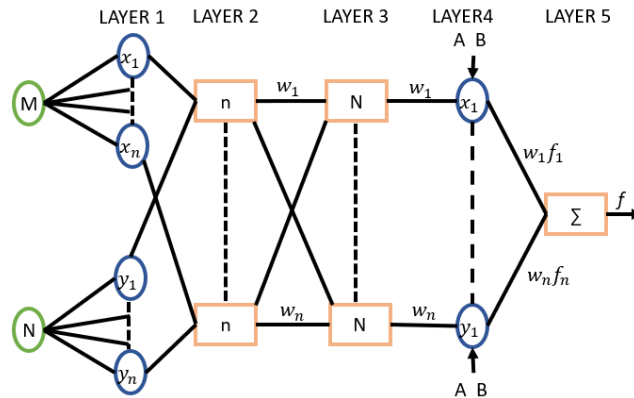
Figure 5.8. Neural network architecture

The output function f in Fig. 5.8 is formulated as

$$f = \frac{w_1}{w_1 + w_2}f_1 + \frac{w_2}{w_1 + w_2}f_2$$

$$f = \overline{w_1}f_1 + \overline{w_2}f_2$$

$$f = (\overline{w_1}M)A_1 + (\overline{w_1}N)B_1 + (\overline{w_2}M)A_2 + (\overline{w_2}N)B_2 + (\overline{w_1}O_1) + (\overline{w_1}O_2) \qquad (5.37)$$

In order to design the NiF-PID controller, the initial work is to integrate all relevant inputs that can be used for training purposes. The next step is to choose a proper I/O data set for training with the help of a hybrid optimization technique. The error $e(t)$ in ball position and change in error of ball position, $\frac{de(t)}{dt}$ are considered as two inputs whose different combinations within a particular range are used for training the NiF-PID controller. The fuzzy control signal $u(t)$ is provided as the desired targeted output. Figure 5.9 depicts the architecture of the proposed NiF-PID controller.
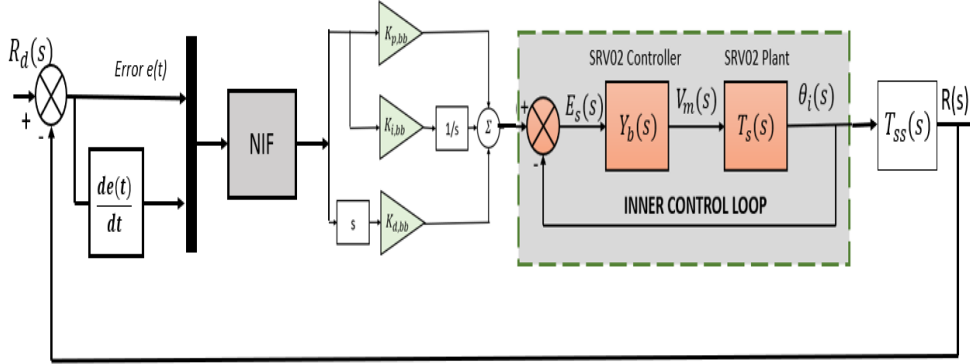
Figure 5.9. Illustration of the proposed NiF-PID controller

The discourse universe is set to be [−0.2, 0.2] for the desired plate angle and [−30, 30] for the error in ball position and change in position because the Saturation block limits the SRV02 angle to ±30 degrees, desired by the manufacturer. 200 epochs are taken to train the NiF-PID controller as shown in Fig. 5.10(a). This training approach employs a hybrid training algorithm that combines least squares with the back-propagation gradient descent method. Nine linguistic variables very high negative (VHN), high negative (HN), medium negative (MN), small negative (SN), zero error (ZE), small positive (SP), medium positive (MP), high positive (HP), very high positive (VHP) are taken for each input so that the experimentation can be based on a large number (9×9 = 81) of fuzzy rules set, which provides better chances of getting the desired output. As a result, input space is divided among 81 fuzzy subspaces and each of these subspaces follows the fuzzy if-then rules. (AM + BN + O) is the first-order polynomial for these functions where A, B and O are movable variables. The fuzzy neural network's output scaling factor is obtained as $A_{e(t)} = n/e(t) = B_{de(t)/dt} = n/\frac{de(t)}{dt} = 40$ for input scaling and $O_{u(t)} = \frac{U}{n} = 0.08$ for output scaling. The learning coefficient system starts at $\vartheta = 2.0624e - 05$ with minimal training Root Mean Squared Error (RMSE) = 0.000020. Figure 5.10(b) depicts the trained data for the fuzzy output.

77

Figure 5.10 (a) Epochs vs training error **(b)** Training data and output of the fuzzy interference system
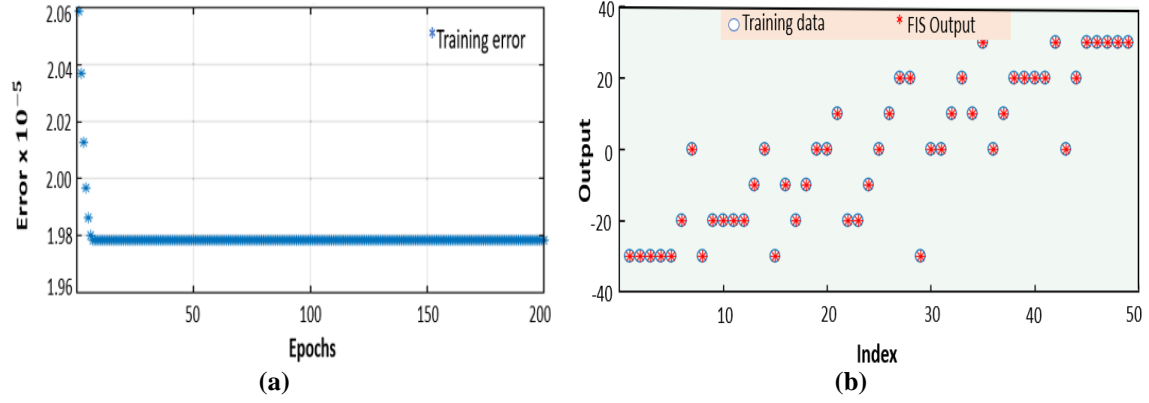
The symmetric ANFIS, depicted in Fig. 5.11(a), is known when the membership function of both inputs is uniformly distributed. Figure 5.11(a) shows that all the nine linguistic variables of both membership functions are distributed uniformly. For example, linguistic variable ZE lies in the range of [-0.05 to +0.05] with a peak at 0 for both membership functions. Conversely, the asymmetric ANFIS, depicted in Fig. 5.11(b), is known when any input's membership function is not uniformly distributed. Figure 5.11(b) shows that all the nine linguistic variables of both membership functions are not distributed uniformly. For example, the linguistic variable ZE lies in the range of [-0.035 to +0.06] with a peak at -0.04 for error membership function and in the range of [-0.05 to +0.05] with a peak at 0 for change in error, i.e. $\frac{de(t)}{dt}$ membership function.

Figure 5.11. (a) Symmetric membership function **(b)** Asymmetric membership function
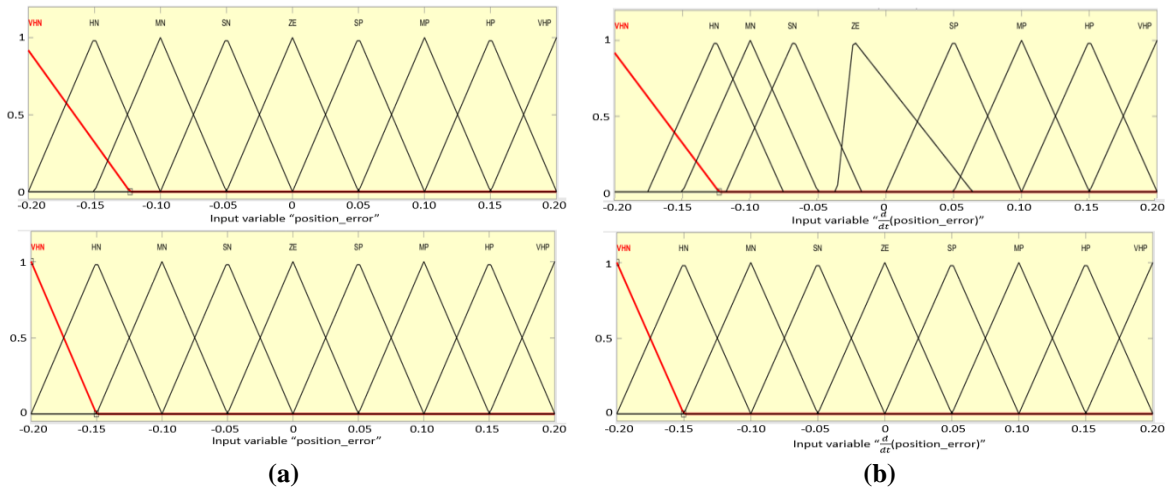
The neural network has a distribution of 2 neurons in Layer 1 for error e(t) and change in error $\frac{de(t)}{dt}$, 18 neurons (9 each for error and change in error) in Layer 2, 81 neurons (9 linguistic variables each for error and change in error) in each of Layer 3 and Layer 4, and 1 neuron (output) in Layer 5 with fuzzy implementation (structure is displayed in Fig. 5.12). Table 5.3 gives a description of the fuzzy rules. Following the training of fuzzy interface system data, the control signal's surface is formed as depicted in Fig. 5.13 and quiver surfaces are depicted in Fig. 5.14.
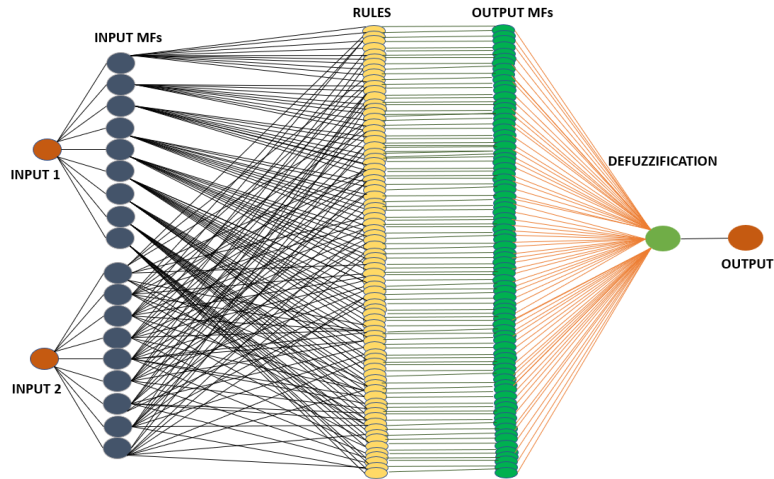
Figure 5.12. Structure of Neuro integrated Fuzzy controller

Table 5.3. Description of the fuzzy rules

error / Δ error	VHN	HN	MN	SN	ZE	SP	MP	HP	VHP
VHN	VHN	VHN	VHN	VHN	VHN	HN	MN	SN	ZE
HN	VHN	HN	HN	VHN	HN	MN	SN	ZE	SP
MN	VHN	HN	MN	HN	MN	SN	ZE	SP	MP
SN	VHN	HN	MN	MN	SN	ZE	SP	MP	HP
ZE	VHN	HN	MN	SN	ZE	SP	MP	HP	VHP
SP	HN	MN	SN	ZE	SP	SP	MP	HP	VHP
MP	MN	SN	ZE	SP	MP	MP	MP	HP	VHP
HP	SN	ZE	SP	MP	HP	HP	HP	HP	VHP
VHP	ZE	SP	MP	HP	VHP	VHP	VHP	VHP	VHP

CONTROL SIGNAL SURFACE OF SYMMETRIC INFERENCE SYSTEM

CONTROL SIGNAL SURFACE OF ASYMMETRIC INFERENCE SYSTEM
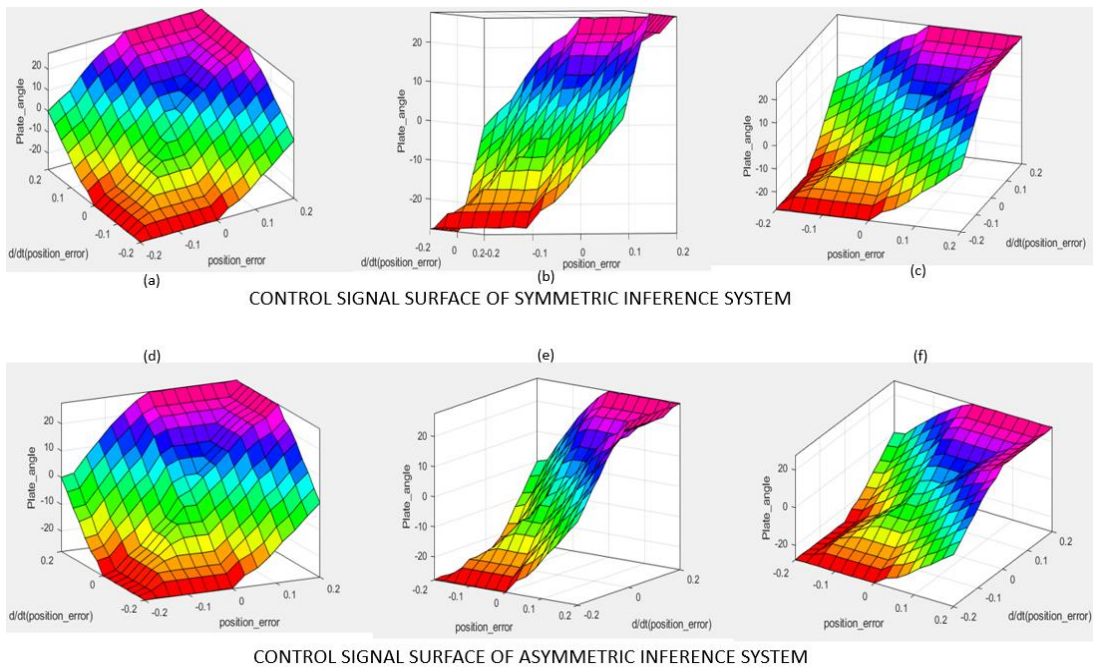
Figure 5.13. Comparison of different angled surfaces of symmetric and asymmetric inference system

79
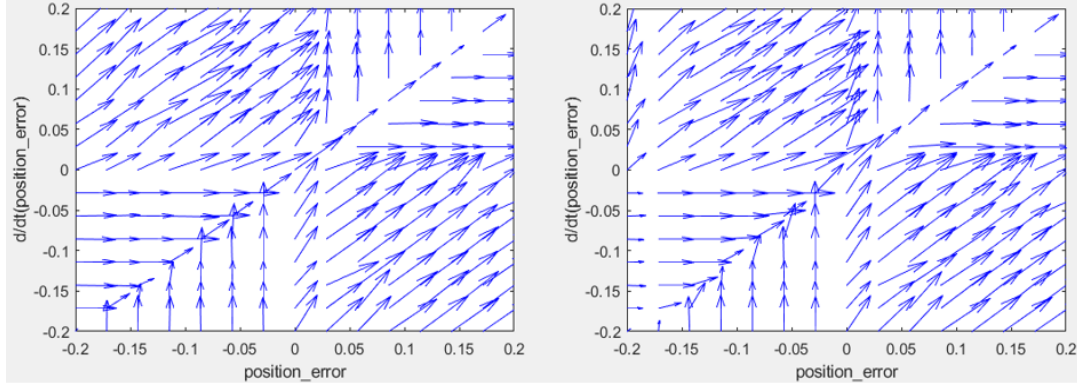
(a) Symmetric inference system   (b) Asymmetric inference system

Figure 5.14. Comparison of quiver surfaces of symmetric and asymmetric inference system

5.5.4 Tracking Ball Position via Camera

The controllers predict the precise position and provide the planar position of the ball as an output. The ball's position is tracked via the overhead camera within a square viewing area whose width and height resolutions are equal as shown in Fig. 5.15. The position of the ball is detected and converted into pixel coordinates P_{ix} & P_{iy} (pixels of the x-axis and y-axis) within the square viewing area. These pixel coordinates are then used to determine the ball's position in the coordinate system as $[X_{co}, Y_{co}]$.
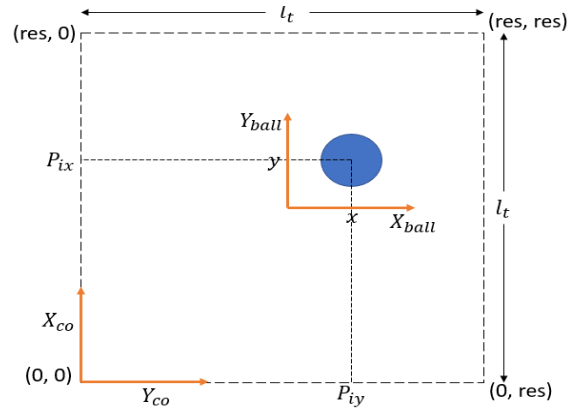
Figure 5.15. Mapping of the ball's position onto the coordinate system for the raw camera measurement of the ball position

The functions describing the ball position from camera pixels relative to ball coordinates $[X_{ball}, Y_{ball}]$ are x & y and can be expressed as

$$x = \left\{\frac{P_{ix}}{res} - 0.5\right\} l_t, \quad y = \left\{\frac{P_{iy}}{res} - 0.5\right\} l_t \tag{5.38}$$

where, P_{ix} and P_{iy} are the camera pixels related to the ball coordinates $[X_{ball}, Y_{ball}]$, res is the resolution and l_t is the length of the table.

5.6 RESULTS AND DISCUSSIONS

The closed-loop response of the 2D ball balancer system is initially simulated using Proportional Derivative (PD), NiF-PID controller and Proportional Integral Derivative (PID) controllers with different V_{sw} values and with different kinds of inputs. Modeling for Simulink is done using MATLAB and Quarc for interfacing. Along with simulation, a real-time experimentation study is carried out on hardware setup with these different controllers and load variation on ball balancer setup as shown in Fig. 5.1(b). The closed-loop responses show the signatures of the input servo motor voltage V_m(v), controlled output ball position x(cm) and servo load gear angle θ_i(degree). The X-Y figures are obtained on the scope with respect to different applied inputs and V_{sw} values. For both simulation and real-time experimental processes, direct derivative computation of the ball velocity can't be obtained because of some inherent noise in the measurement of ball position. If the derivative of this noise is taken, it would result in the amplification of the high-frequency signal which is being fed to the motor. The saturation block limits the SRV02 angle to ±30 degrees.

5.6.1 System Specifications and Configuration

The modeling of different controllers is designed using MATLAB/Simulink R2022a. After modeling the ball balancer system by defining the system dynamics using the mathematical model, the model is implemented in Simulink. The neuro-fuzzy PID controller is designed using the PID controller block from the Simulink library and then the neuro-fuzzy logic is incorporated. After that, the Neuro-Fuzzy PID controller is integrated with the ball balancer system model in Simulink. After simulation, the designed control law is applied to a physical (real-time) Quanser experimental setup of the ball balancer system as shown in Fig. 5.1(b). The components of this system are shown in Table 5.4. QUARC version 2.3.355 software is used for hardware-in-the-loop simulations to provide a powerful platform for validating the controller's performance in real time [229]. Fig. 5.16 depicts the block representation of the real-time implementation of the 2-DOF ball balancer system.

Table 5.4. Hardware equipment of 2-DoF ball balancer along with the system specifications

Equipment	System Specifications
Power amplifier	VoltPAQ-X2
Data acquisition device	Q2 USB DAQ control board
Rotary Servo Base units	Quanser SRV02
Optical encoders	Autonics optical rotary encoders
CPU	Intel Core i7 4Ghz
RAM	32 GB
MATLAB Version	MATLAB R2022a

Implementing these controllers in real-time using QUARC and MATLAB means that:

- **Real-time Interface**: The control algorithms are executed on a computer (i.e. connected to the physical system) in real-time, allowing for immediate feedback and adjustment based on actual system behavior.

- **Hardware-in-the-Loop Simulation**: The physical system (i.e. the B&P system) is connected to the simulation environment through QUARC, enabling the controller to interact with the actual system hardware. This setup ensures that the controllers' performance can be tested and validated under realistic conditions, including external perturbations and system uncertainties.

- **Achieving Stability and Performance**: Despite the inherent instability of the B&P system and the presence of external disturbances, this study demonstrates that the NiF and NiF-PID controllers can effectively stabilize the system and achieve desired performance metrics (such as reference tracking and disturbance rejection).

In order to balance the ball on the plate, two Rotary Servo Base units i.e. Quanser SRV02 are mounted to the plate to rotate it along the x and y axes. The overhead camera is used to measure the ball position which provides the visual input. MATLAB analyzes the square plate image to find the ball position. A Quanser VoltPAQ-X2 power amplifier is used to amplify the voltage and then send it to the servo system to generate the requisite torque. The attached optical encoders are used to measure the angles. The personal computer can access sensor measurements and control the amplifier's voltage with the help of a Q2-USB DAQ device. The Q2 USB DAQ board gathers data from the optical encoders and serves as an interface between hardware and software. It also measures the control signal related to the plate's disposition. In order to obtain the movement of the ball with respect to voltage, the controller receives signals from DAQ and the overhead camera. The DAQ board sends the control signal to the amplifier in order to generate and transfer control signals to servo motors incorporated with a potentiometer to balance the ball in both axes.
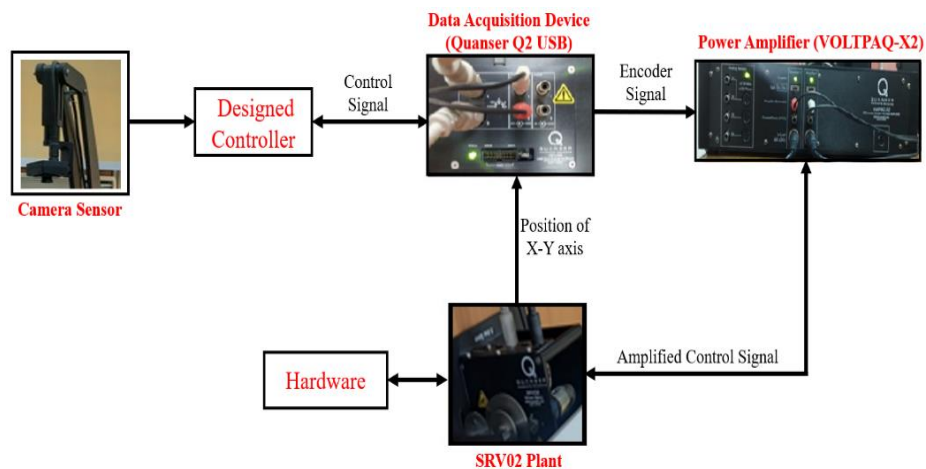
Figure 5.16. Block representation of the real-time implementation of 2-DOF Ball Balancer system

5.6.2 Simulation-based Position Control of Ball Balancer with PD and PID Controllers

This section shows the simulated closed-loop response of the 2D ball balancer system using PD and PID controllers with different velocity setpoint weights (V_{sw}) and with different kinds of inputs like step input, ramp input and sinusoidal input.

5.6.2.1 Step and Ramp Response of PD Controller

The step and ramp input response of the PD controller is simulated with $V_{sw} = 0$ & $V_{sw} = 0.87$ as shown in Fig. 5.17(a-d) respectively meet the specifications. It is noticed that as V_{sw} increases, the peak overshoot increases abruptly but the steady-state error remains the same for both values of V_{sw} in case of step input response. In the case of ramp response, steady-state error is the main concern. It is observed that there is no major effect on steady-state error with an increase in V_{sw} value. Steady-state error is 0.692 cm and 0.13 cm for $V_{sw} = 0$ and $V_{sw} = 0.87$ respectively, which is under the required criteria and very close to theoretical values for both cases. The X-Y figures obtained on scope in case of step response with $V_{sw} = 0$ and ramp response with $V_{sw} = 0.87$ are shown in Fig. 5.17(e) and Fig. 5.17(f) respectively. When $V_{sw} = 0$, it is noticed that the desired trace and simulated trace overlap with each other. Whereas, a small steady-state error is observed in the diamond-shaped response in the case of $V_{sw} = 0.87$ for ramp response, which is less than the required specifications.

(a) PD Step response with $V_{sw} = 0$

(b) PD Step response with $V_{sw} = 0.87$

(c) PD Ramp response with $V_{sw} = 0$

(d) PD Ramp response with $V_{sw} = 0.87$
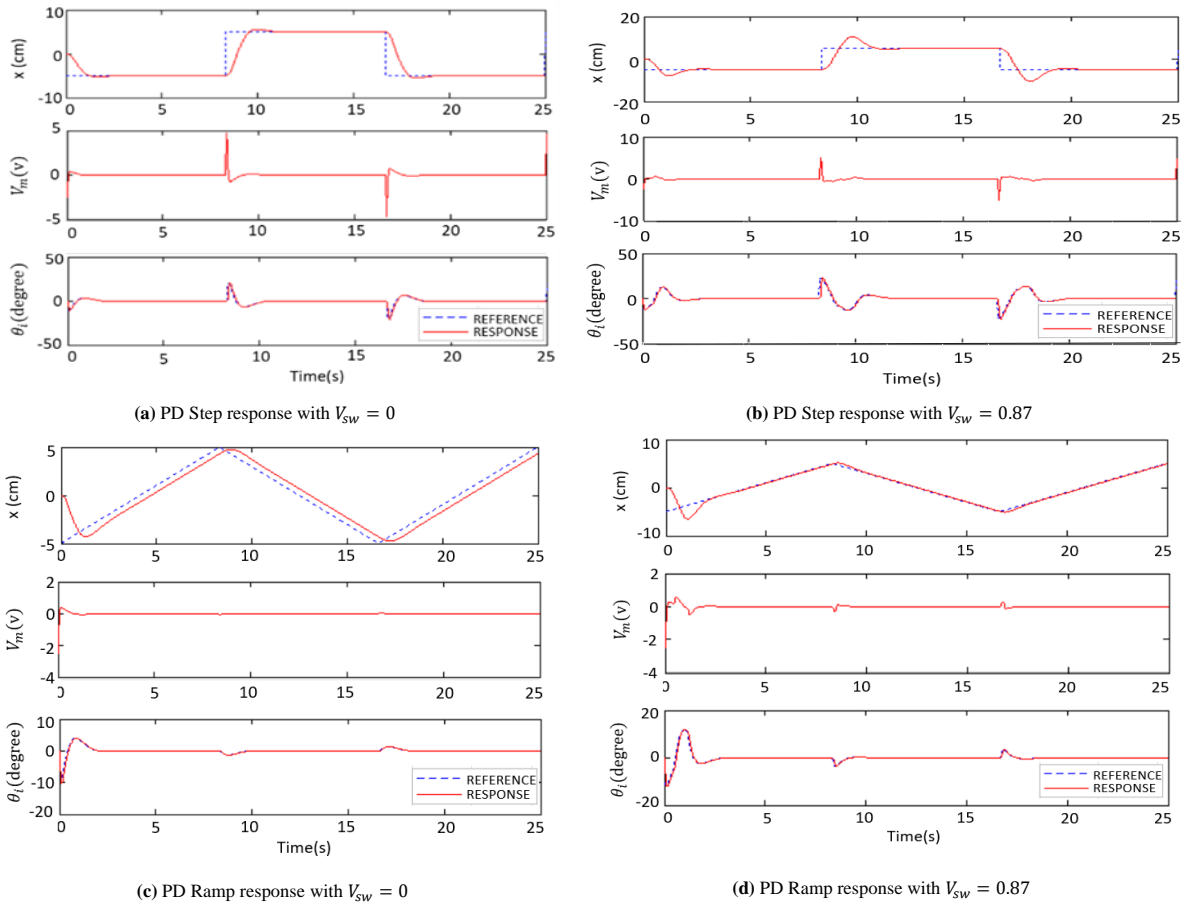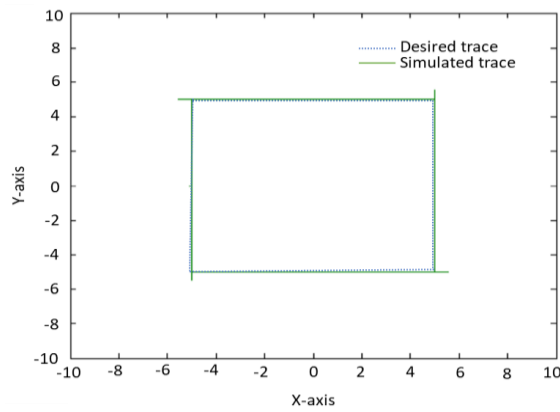
(e) Scope simulation of the PD controller with $V_{sw} = 0$
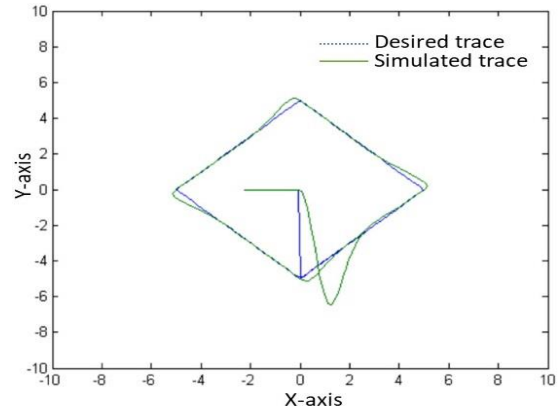
(f) Scope simulation of the PD controller with $V_{sw} = 0.87$

Figure 5.17. Simulated step response, ramp response and X-Y scope of the PD controller

5.6.2.2 Step Response of PID Controller

While implementing an additional integral controller to the PD controller, $V_{sw} = 0$ is taken because $V_{sw} = 1$ would create too many oscillations. The PID controller is simulated for $\text{INTG}_{MAX} = 2.5$ degrees, anti-windup time constant $T_{aw} = 5s$; $\text{INTG}_{MAX} = 2.5$ degrees, $T_{aw} = 0.001s$ and $\text{INTG}_{MAX} = 1.6$ degrees, $T_{aw} = 0.001s$ as shown in Fig. 5.18(a-c) respectively. The integral reset time decreases with a decrease in the anti-windup time. As a result, the integral does not get any windup chance and the settling time decreases significantly as shown in Fig. 5.18(b-c). A decrease in the INTG_{MAX} value also decreases the peak overshoot value. However, the servo angle gets saturated but it doesn't create any instability due to the proper tuning of windup control. As a result, there is no saturation to the servo motor. The X-Y figure obtained on scope when $\text{INTG}_{MAX} = 1.6$ degrees, $T_{aw} = 0.001s$ and $V_{sw} = 0$, in Fig. 5.18(d) shows almost a perfect square where both desired and simulated traces overlapped after tuned windup. Table 5.5 shows the comparison of outputs of PD & PID simulations.

Table 5.5. Comparison of peak overshoot, settling time and steady-state error of PD & PID simulations

S. No.	PARAMETERS → DESCRIPTION ↓	PEAK OVERSHOOT (PO) %	SETTLING TIME (t_s) sec	STEADY-STATE ERROR (e_{ss}) cm
1.	Step response of PD controller with $V_{sw} = 0$, Fig. 5.17(a)	5.62	2.39	0
2.	Step response of PD controller with $V_{sw} = 0.87$, Fig. 5.17(b)	51.7	2.501	0
3.	Step response of PID controller with $V_{sw} = 0$, $\text{INTG}_{MAX} = 2.5$ deg, $T_{aw} = 5s$, Fig. 5.18(a)	8.12	6.1	0.0149
4.	Step response of PID controller with $V_{sw} = 0$, $\text{INTG}_{MAX} = 2.5$ deg, $T_{aw} = 0.001s$, Fig. 5.18(b)	7.4	2.45	0.0086
5.	Step response of PID controller with $V_{sw} = 0$, $\text{INTG}_{MAX} = 1.6$ deg, $T_{aw} = 0.001s$, Fig. 5.18(c)	5.46	2.28	0.000119

(a) PID Step response with $\text{INTG}_{\text{MAX}} = 1.6$ deg, $T_{aw} = 5s$

(b) PID Step response with $\text{INTG}_{\text{MAX}} = 2.5$ deg, $T_{aw} = 0.001s$

(c) PID Step response with $\text{INTG}_{\text{MAX}} = 1.6$ deg, $T_{aw} = 0.001s$

(d) X-Y figure on scope simulation of PID response
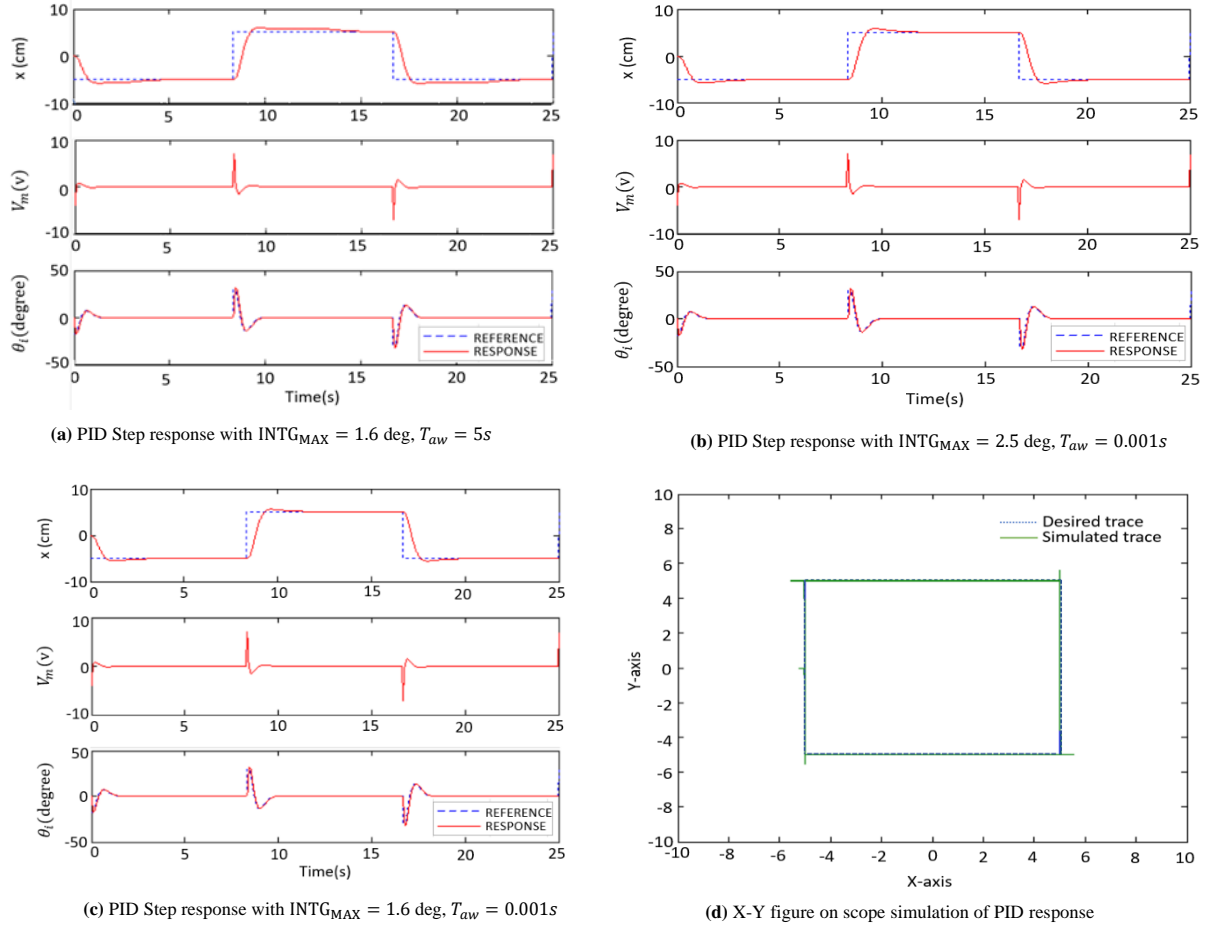
Figure 5.18. Simulated step input response of the PID controller with different cases

During simulation, the PID compensator provides better results in terms of both transient and steady-state response. Taking reference to Table 5.5, the step response of the PD controller with $V_{sw} = 0$ gives a peak overshoot (PO%) of 5.62 and settling time of 2.39s as shown in Fig. 5.17(a) whereas, the step response of the PID controller with $V_{sw} = 0, \text{INTG}_{\text{MAX}} = 1.6$ deg, $T_{aw} = 0.001s$ gives a peak overshoot (PO%) of 5.46 and settling time of 2.28s as shown in Fig. 5.18(c). The steady-state error is also negligible in the case of the PID compensator.

5.6.3 Real-time Experimentation based Position Control of Ball Balancer with PD and PID Controllers

This section shows the real-time experimentation of the closed-loop response of the 2D ball balancer system, carried out on hardware setup, shown in Fig. 5.1(b), using PD and PID controllers with different velocity setpoint weights (V_{sw}) and with different kinds of inputs like step input, ramp input and sinusoidal input.

5.6.3.1 Step Response of PD Controller along x and y Axis

Figure 5.19(a-b) shows the PD step responses along the x and y-axis. Along the x-axis, t_s is 113s, peak overshoot is 5.11% and e_{ss} is 0.61 cm, which doesn't meet the required specifications. While measuring the response along the y-axis, the setpoint is chosen only in the x direction. However, it is observed that the y-axis servo also performs the control action due to the coupling difference between both axes. When the x-axis servo tries to control the ball position along the x-axis, there is a change in the direction of the plate angle in the y-direction. Therefore, the ball tracks the step inputs in both directions simultaneously. The step response of the PD controller in both axes is shown in Fig. 5.19(c). $V_{m,x}$ and $V_{m,y}$ show the input servo motor voltage along the x and y-axis respectively. Similarly, x(cm) and y(cm) show the controlled output ball position along height and width respectively. Each axis causes disturbances on the other axis while tracking the setpoint. The scope simulation of the step response of the PD controller in Fig. 5.19(d) does not show a perfect square due to a large steady-state error.

(a) Step response of PD controller along the x-axis

(b) Step response of PD controller along the y-axis

(c) Dual-axis step response of PD controller

(d) X-Y scope of the step response of PD controller
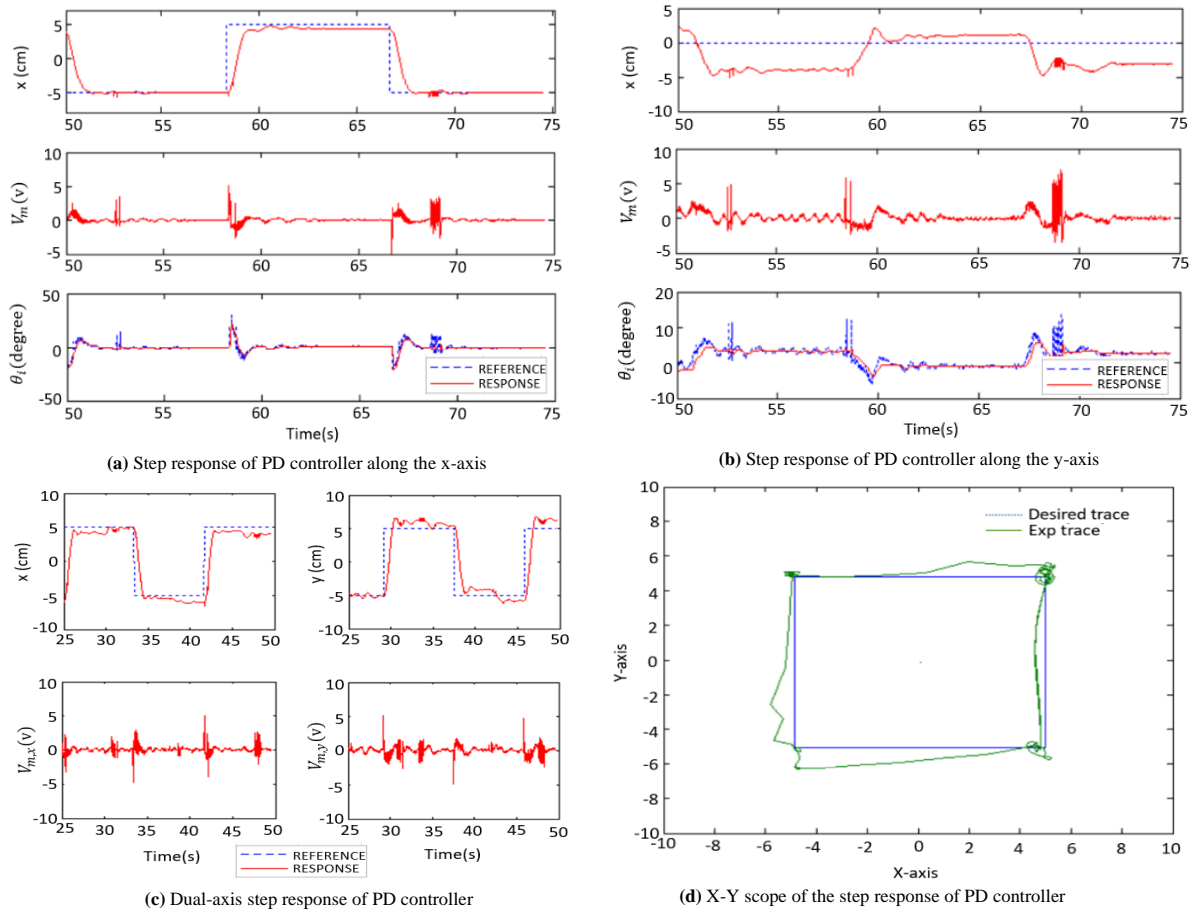
Figure 5.19. Experimental results of step response and X-Y scope of the step response of the PD controller

5.6.3.2 Step Response of PID Controller

Figure 5.20(a) shows the step responses of the PID controller with $V_{sw} = 0$, $INTG_{MAX} = 1.6$ deg and $T_{aw} = 0.001s$. Peak overshoot is 5.65% and $e_{ss} = 0.082$cm. It is observed that there is a significant improvement in steady-state error while using the PID controller. The x-y scope in Fig. 5.20(b) shows a better response in the case of the PID controller in comparison to the PD controller.

(a) Step response of PID controller along the x-axis

(b) X-Y scope of the step response of PID controller
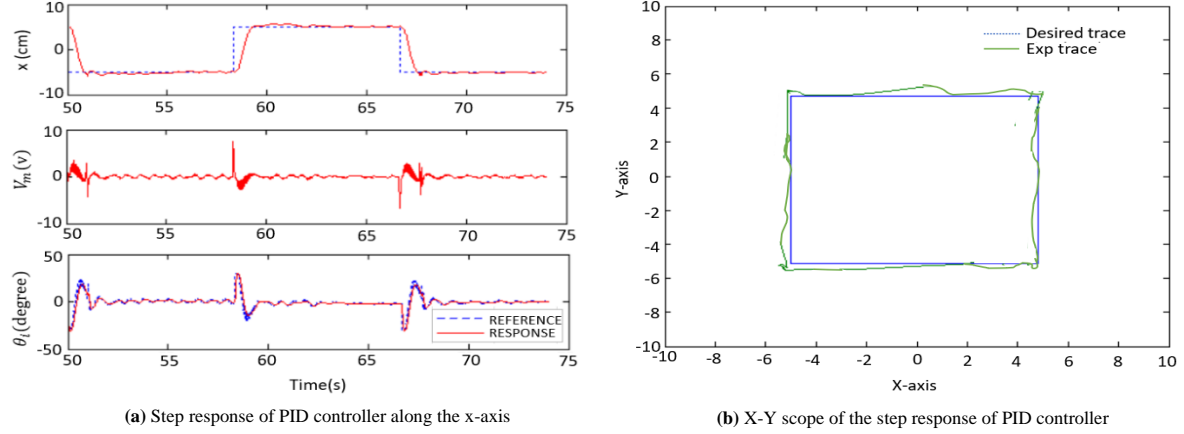
Figure 5.20. Experimental results of step response and X-Y scope of the step response of the PID controller

5.6.3.3 Ramp Response of PD Controller

The dual-axis ramp response of the PD controller with $V_{sw} = 0$ & $V_{sw} = 0.87$ are shown in Fig. 5.21(a) and Fig. 5.21(b). $V_{m,x}$ and $V_{m,y}$ show the input servo motor voltage along the x and y axis respectively. Similarly, x(cm) and y(cm) show the controlled output ball position along height and width respectively. However, the responses are quite similar by varying V_{sw} also. This is due to the unmodelled effects like cross-axis coupling and friction which have a much bigger effect on the response.

(a)

(b)
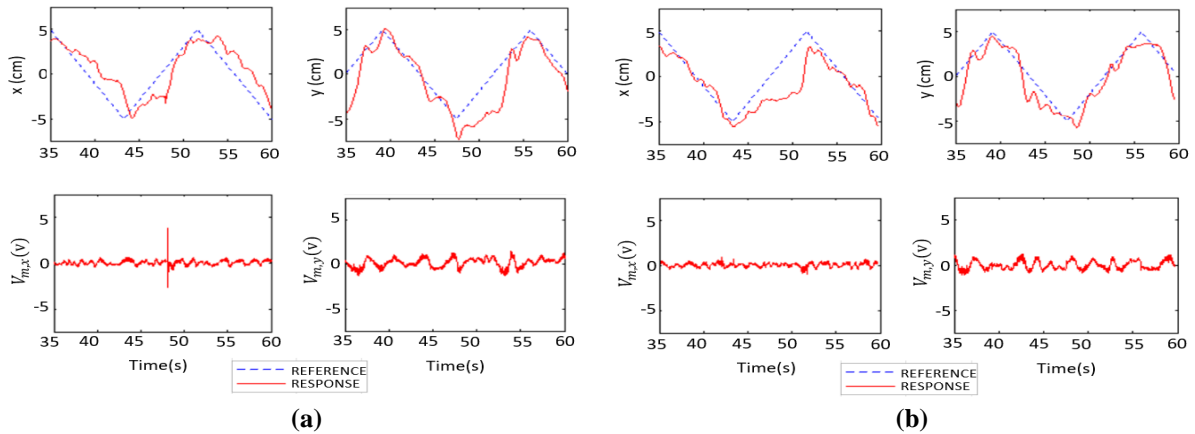
Figure 5.21. Experimental results of dual-axis ramp response of PD controller with **(a)** $V_{sw} = 0$ **(b)** $V_{sw} = 0.87$

87

5.6.3.4 Ramp and Sinusoidal Response of PID Controller

The PID controller is tested for ramp input after the step input response. Figure 5.22(a) shows the dual-axis ramp response of the PID controller with $V_{sw} = 0.87$ and $T_a = 1$s. It is observed that tracking of ramp input response requires less control effort than step input. Therefore, proper tuning of T_a is required to get a better response. Figure 5.22(b) shows the dual-axis ramp response of the PID controller with $V_{sw} = 0.87$ and $T_a = 0.35$s where the desired pole location shifts more towards the left plane leading to an increase in the controller gain values, i.e. $K_{p,bb} = 14.2$ rad/m, $K_{i,bb} = 18.9$ rad/m. s, $K_{d,bb} = 5.987$ rad. s/m. The X-Y figure obtained on scope, corresponding to the ramp input of the PID controller for $T_a = 0.35$s and $V_{sw} = 0.87$, is shown in Fig. 5.22(c). For the same controller values, the dual-axis sinusoidal response of the PID controller with $V_{sw} = 0.87$ and $T_a = 0.35$s, is shown in Fig. 5.22(d). The X-Y figure obtained on scope, corresponding to the sinusoidal response of the PID controller for $T_a = 0.35$s and $V_{sw} = 0.87$, is shown in Fig. 5.22(e). With decrease in T_a values, the responses get better.

(a) Ramp response of PID controller with $T_a = 1s$

(b) Ramp response of PID controller with $T_a = 0.35s$

(c) X-Y scope of PID controller with ramp input

(d) Dual-axis sinusoidal response of the PID controller

(e) X-Y scope of PID controller with sinusoidal input
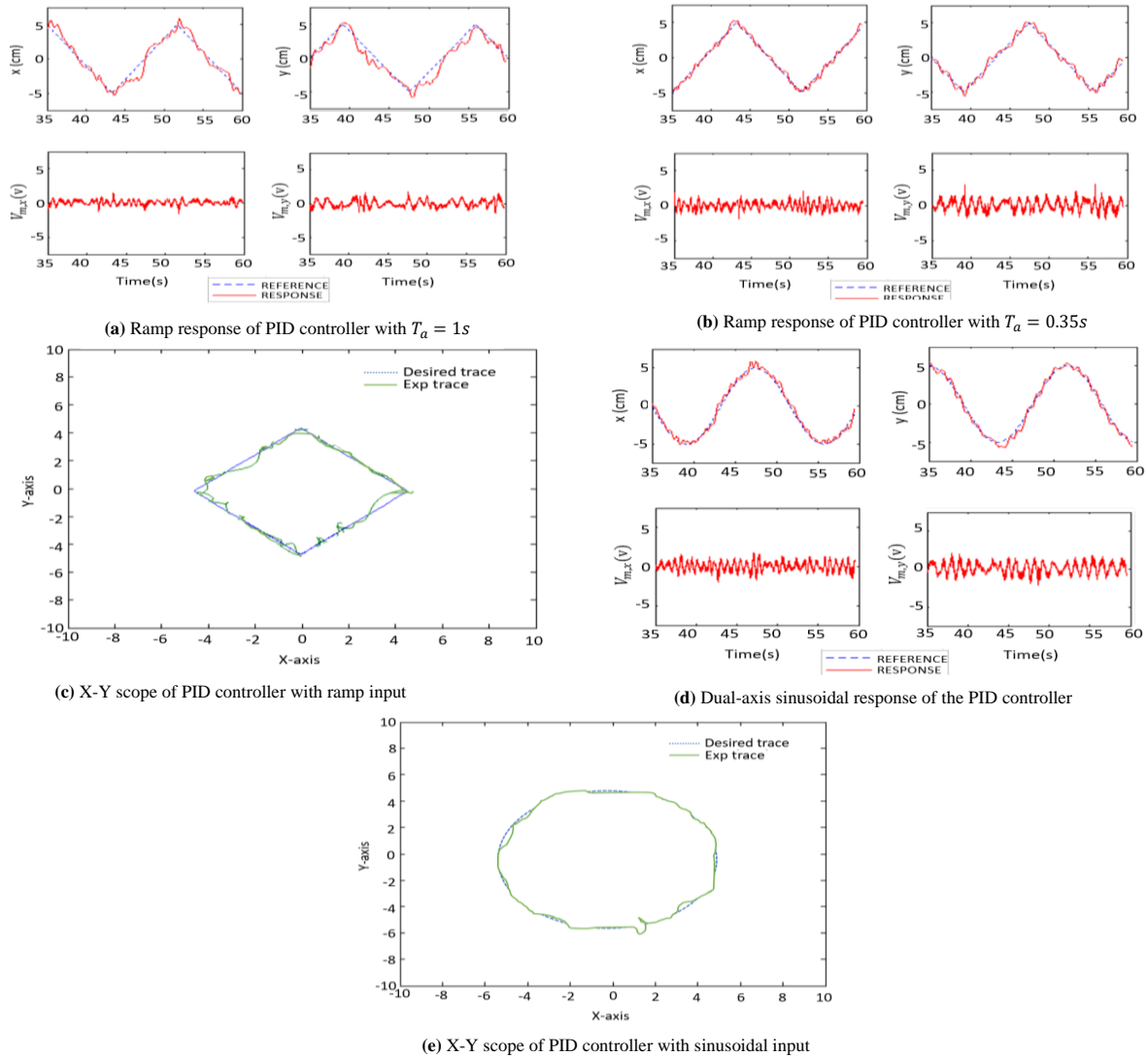
Figure 5.22. Experimental results of ramp response and diamond-shape X-Y scope of the PID controller

During real-time experimentation, e_{ss} is 0.61 cm for the step response of the PD controller along the x-axis, which doesn't meet the requirements. But, e_{ss} is greatly improved in the case of step response of the PID controller (e_{ss}=0.082 cm) as compared to the step response of the PD controller. The square response of the PID controller in Fig. 5.20(b) is smoother than the square response of the PD controller in Fig. 5.19(d). Also, the trajectories of ramp PID responses in Fig. 5.22(a-b) are much smoother than the ramp response of the PD controller in Fig. 5.21(a-b). All these observations make PID compensator better than the PD compensator.

5.6.4 Comparison of Simulation and Experimentation results using different Controllers

A comparison has been made with PD, PID and NiF-PID controllers for both simulation and experimentation purposes as shown in Fig. 5.23 and Fig. 5.24 respectively. Verification of results after the implementation of various controllers on simulated models and later in the real-time experimentation stage, are to be considered on a momentary basis. During simulation and real-time experimentation, the system is more oscillatory in the case of the PD controller and it becomes unstable after increasing the gain, which can be seen in the peak overshoot of the system. However, with the proper tuning of PID and NiF-PID controllers, it is observed that the present oscillations die out to a great extent. A comparison of simulated and experimental parameters of controllers on a ball balancer model is illustrated in Table 5.6 and Table 5.7 respectively. Pie charts in Fig. 5.25 show the comparison of settling time and peak overshoot for PD, PID, and NiF-PID controllers on simulation and experimentation.
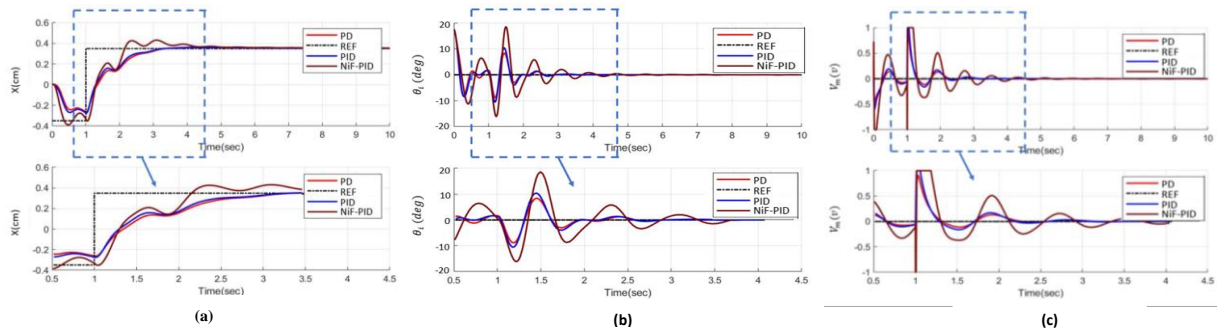
Figure 5.23. PD, PID, and NiF-PID responses on simulation for **(a)** Ball position comparison **(b)** Input voltage comparison **(c)** Plate angle comparison

Table 5.6. Comparative analysis of simulated parameters of controllers on a ball balancer model

S. No.	PARAMETERS → CONTROLLERS ↓	SETTLING TIME (t_s) s	PEAK OVERSHOOT (PO) %	STEADY-STATE ERROR (e_{ss}) cm
1.	PD	4.78	11.89	0.0426
2.	PID	2.21	1.23	0.00039
3.	NiF-PID	1.53	9.4e-06	7.92e-05
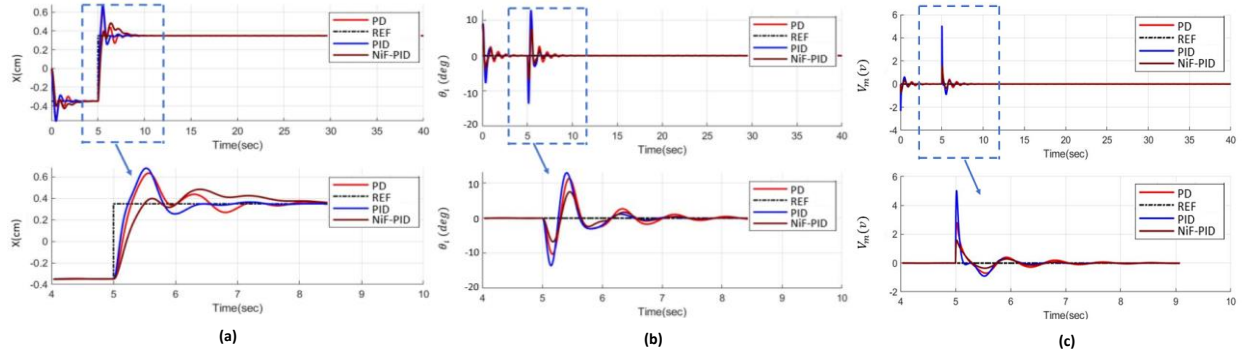
Figure 5.24. PD, PID, and NiF-PID responses on real-time experimentation for **(a)** Ball position comparison **(b)** Input voltage comparison **(c)** Plate angle comparison

Table 5.7. Comparative analysis of experimental parameters of controllers on a ball balancer model

S. No.	PARAMETERS → CONTROLLERS ↓	SETTLING TIME (t_s) s	PEAK OVERSHOOT (PO) %	STEADY-STATE ERROR (e_{ss}) cm
1.	PD	4.97	31.6	1.83
2.	PID	1.99	34.7	0.97
3.	NiF-PID	1.61	3.86	0.79

In the case of the PID controller, the steady-state error is 0.97cm and for the NiF-PID controller, the steady-state error is 0.79cm (refer to Table 5.7).

Now,

$$\% \left(e_{ss}\right) = \left\{\frac{e_{ss}(\text{PID}) - e_{ss}(\text{NiF\_PID})}{e_{ss}(\text{PID})}\right\} \times 100\%$$

$$\% \left(e_{ss}\right) = \left\{\frac{0.97 - 0.79}{0.97}\right\} \times 100\%$$

$$\% \left(e_{ss}\right) = 18.556 \%$$

It is evident from Table 5.7 that the peak overshoot is 34.7% in the case of the PID controller and 3.86% in the case of the NiF-PID controller, which is approximately 10 times less than the PID controller. This shows that the NiF-PID compensator provides 18.55% better results in the case of steady-state error and 10 times less overshoot in the case of real-time experimentation as compared to the PID controller.

According to the responses, NiF-PID controller has the most appropriate response among all with an acceptable overshoot, and lowest steady-state error, and proves to be the excellent controller without many oscillations. For the NiF-PID controller, steady state error, peak overshoot, and settling time are each 1.08 cm, 4.16%, and 1.62 s. Controlled voltage signal varies between ±5v in the case of the NiF-PID controller which is best among all controllers. Angle variation is also ±15 degrees in the case of NiF-PID controller for the stable and smooth movement of the ball.

SETTLING TIME

NiF-PID 18%

PID 26%

PD 56%

PEAK OVERSHOOT

NiF-P 1% PD 14%

PID 85%

(a)

SETTLING TIME

NiF-PID 19%

PID 23%

PD 58%

PEAK OVERSHOOT

NiF-P 6%

PD 45%

PID 49%

(b)
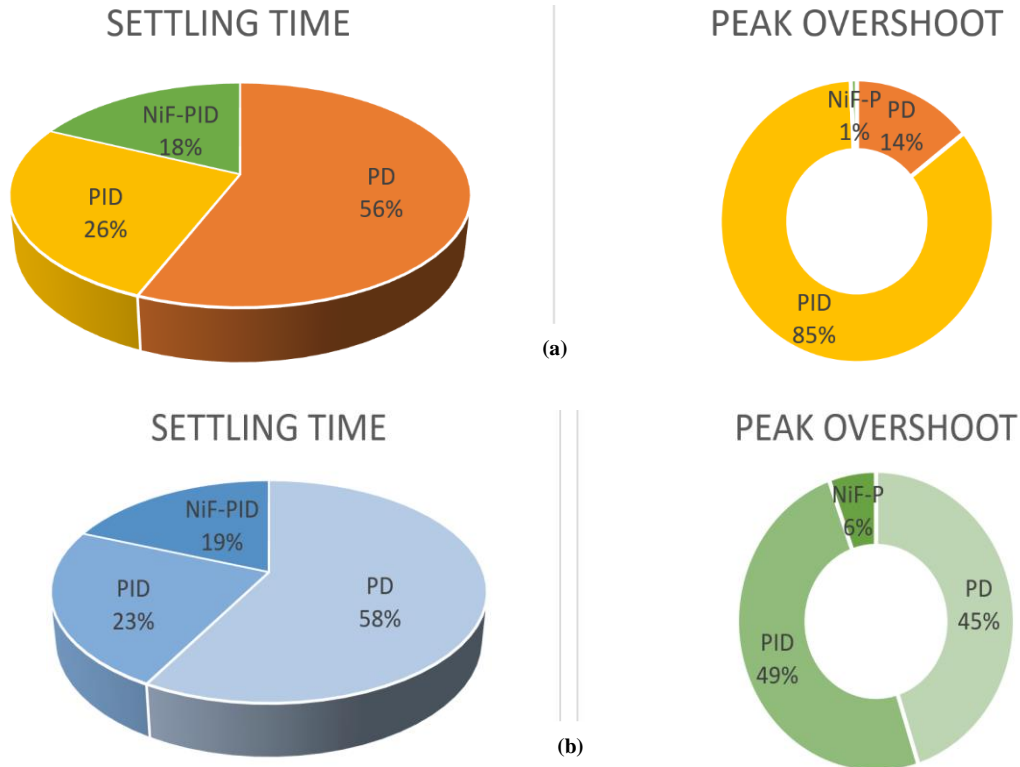
Figure 5.25. Comparison of settling time and peak overshoot of PD, PID and NiF-PID controllers on **(a)** simulation **(b)** experimentation

5.6.5 Position and Plate Angle Control With Load Variation

The integration of NiF-PID controller produces good results for controlling the ball location and plate angle. So, NiF-PID controller is implemented for load variation over the ball balancer system to check the efficacy and adaptability of the controller. Table 5.8 shows the specifications of different balls of different mass, radius and moment of inertia that have been taken for the implementation of NiF-PID controller. Figure 5.26 illustrates the performance of NiF-PID for varying ball locations and plate angles for different balls having different dimensions and weights. Pie charts in Fig. 5.27 shows the comparison of settling time and peak overshoot of different balls.

(a)

(b)
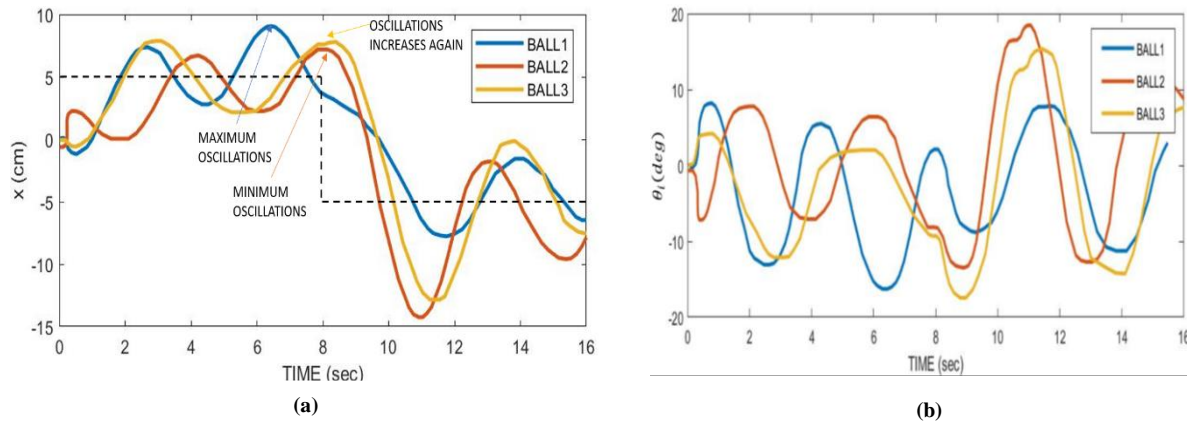
Figure 5.26. (a) Variation in the position of $Ball_1$, $Ball_2$ and $Ball_3$ **(b)** Plate angle comparison of $Ball_1$, $Ball_2$ and $Ball_3$ for different loads

91

Table 5.8. Specifications of load variation

LOAD PARAMETERS	$BALL_1$	$BALL_2$	$BALL_3$
MASS (kg)	0.110	0.003	0.085
RADIUS (m)	0.02	0.0196	0.026
MOMENT OF INERTIA (kg-m^2)	1.77e-05	0.0462e-05	2.125e-05

Evidently from the results shown in Fig. 5.26, $Ball_1$ has the maximum oscillations, $Ball_2$ has the least oscillations and in the case of $Ball_3$, oscillations increase again. Peak overshoot is 3.7, 2.9 and 3.4 for $Ball_1$, $Ball_2$ and $Ball_3$ respectively. Similarly, settling time is 2.29s, 1.53s and 2.05s for $Ball_1$, $Ball_2$ and $Ball_3$ respectively. It is found that as the mass of the ball decreases, the settling time also decreases and the ball balances the plate efficiently due to the controller's ability.
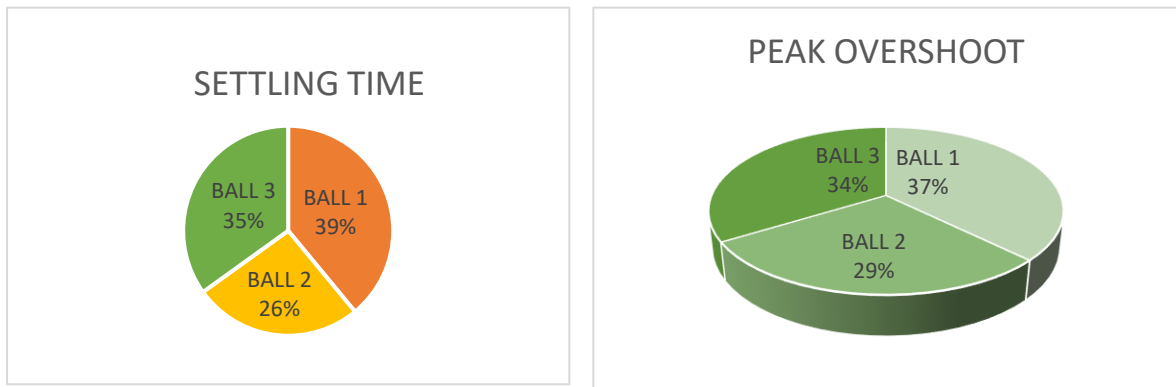
Figure 5.27. Comparison of settling time and peak overshoot of different balls

5.7 SUMMARY

This chapter investigated the implementation of various controllers like PD, PID, PID with Integral ANTI-WINDUP with different velocity setpoint (V_{sw}) values and Neuro-fuzzy with PID (NiF-PID) controller over the 2-DOF ball balancer system. The comparisons for variation in ball position, applied input voltage to servo motor and plate angle are executed with the developed control schemes for both simulation and real-time experimentation purposes. Peak overshoot, settling time and steady-state error analysis have been carried out for these controllers. Based on these performances, load variation on the ball balancer system has been carried out with NiF-PID controller.

The outcomes of simulation and experimental assessment imply that PID with Integral ANTI-WINDUP controller has overall better control performances for the ball balancer system. PID controller showed a better performance because of its ability to reduce the steady-state error that occurs between reference and generated output. NiF-PID controller provides reduced and improved settling time, peak overshoot and steady-state error as compared to PD and PID controllers. The proposed controllers can stabilize the system even in the presence of high-frequency disturbances. NiF-PID controller provides considerable performance along with traditional control structure framework.

For future prospects, relatively more advanced hybrid control strategies such as type-2 NiF-PID, and wavelet NiF-PID, along with optimization algorithms can be implemented for control. Much more extensive analysis may be carried out for robustness analysis and thus allowing the system to withstand external disturbances. The SRV02 unit may also be investigated further for performing vibration analysis of the system.

Chapter 6

Optimal control of Rotary Inverted Pendulum Using Continuous Linear Quadratic Gaussian Controller

6.1 INTRODUCTION

This chapter presents a continuous Linear Quadratic Gaussian (LQG) controller based on the optimal control strategy for swinging up the rotary inverted pendulum and maintaining an equilibrium in the vertical upward position, both using simulation and experimentation. The trajectories and optimal control with sufficient weights are approximated using a numerical method. Gradient descent and algebraic descent are the numerical methods used for obtaining optimal control functions. Experimentally, swing-up is to be controlled with ad hoc strategies: energy shaping and exponentiation of the pendulum position. The equilibrium at the upward position, achieved by the linear controller, can be easily disturbed by a small perturbation. So, the region of stability where equilibrium can be maintained for the maximum input voltage is found on the basis of a binary search algorithm.

6.2 RELATED WORK

Various control techniques have been proposed in the past for stabilizing and swinging up the pendulum. A nonlinear optimal H-infinity control technique was suggested in [219,220] for the wheeled inverted pendulum (IP) model under the conditions of model uncertainty and outside disturbances. It used Lyapunov analysis to demonstrate the stability characteristics of the wheeled IP. But they do not discuss the challenges and robustness in handling the uncertainties. A variant of the grey wolf optimization using PSO based on adaptive constants was presented in [221]. This variant was tested using 23 benchmark functions to ensure its viability. Additionally, the Reduced Linear

Quadratic Regulator (RLQR) was used in conjunction with Variable Structure Adaptive Fuzzy (VSAF) to balance the inverted pendulum. Mai-Phuong et al. [222] proposed a PD-like fuzzy logic methodology integrated with a modified GA optimization technique to balance a cart-type practical inverted pendulum model. The modified GA was used for the fast optimization of the six scaling factors/coefficients of the FLC. Simulation and practical experiment results showed the effectiveness of this approach in accelerating global convergence and improving the control quality in comparison to conventional PID controllers and single FLC.

An adaptive fuzzy logic proportional integral control design based on machine learning was presented in [223] for balancing and controlling the motion of a mobile IP robot with variable load. A robust control against time-varying uncertainties was achieved using an adaptive optimal controller in [224] at any point of time. Sahnehsaraei et al. [225] presented a feedback linearization-based optimum control technique for handling/addressing the stabilization issue of a cart-type IP system having time-varying uncertainties. An approach to discrete-time nonlinear model predictive control based on Taylor series expansion for prediction, discrete-time state-space models, and performance index optimization was suggested by Sotelo et al. [226]. Since both the unstable under-actuated state variables and fully-actuated state variables are stabilized simultaneously, therefore, the stabilization of the Rotary Inverted Pendulum (RotIP) system becomes more challenging.

Alvarez-Hidalgo et al. [227] presented a state space feedback control approach for gain scheduling of an IP system with two operating modes i.e. static balancing mode and a velocity control mode. A velocity and position controller based on the state-space model of the linear dynamic system was used to simulate the pendulum system in MATLAB to examine the difference in behaviour. In contrast to the velocity control mode, the control was more responsive and resilient to disturbances in static equilibrium mode.

A modified optimal adaptive fuzzy logic control approach was presented in [228] for the inverted pendulum model using Fractional-Order derivatives that were optimally chosen using PSO without disturbance to build the adaptive laws. The stability of this method was proven mathematically using the Lyapunov approach. For the stabilization control of RotIP, a hybrid control technique was presented in [229] based on fuzzy logic controllers, LQR controllers and energy balance. In order to provide robust control performance, the state feedback gains based on fuzzy logic were dynamically modified by minimizing the error between actual and desired states. However, the problem with fuzzy controllers is that they are difficult to tune without accurate system knowledge.

Llama et al. [230] proposed an adaptive full-state feedback fuzzy controller for tracking the trajectory of a cart-type IP system. The stability, position and velocity of the pendulum for the closed-loop system were verified using the Lyapunov synthesis approach. This controller was heuristically tuned via evolutionary algorithms like PSO, firefly algorithm and differential evolution for optimizing the performance via simulation and real-time experiments. Bejarbaneh et al. [231] introduced a

technique to optimize a PID-MRAC in order to balance a nonlinear IP in a vertical-upright position. Constriction coefficient PSO and differential evolution algorithms were used to determine the controller's parameters. Then, the efficiency of these approaches has been evaluated in terms of time response, transient response and peak overshoot characteristics.

6.3 PROBLEM STATEMENT

Even though a lot of control strategies have been used to regulate the IP system's angular position with greater accuracy and oscillation dampening, but they have problems such as higher-order nonlinearities, time delays, chattering and discontinuity. This chapter presents a continuous Linear Quadratic Gaussian controller based on the optimal control strategy for swinging up the RotIP and maintaining an equilibrium in the vertical upward position, using both simulation and practical experiments. The proposed LQG controller determines the stable boundary regions of the rotary inverted pendulum and maintains the equilibrium quickly when the system is subjected to any external perturbations.

6.4 OPTIMAL CONTROL OF ROTARY INVERTED PENDULUM

A rotary inverted pendulum system is an improved optimal control technique that can manage challenging and limited linear and non-linear dynamic systems [232]. RotIP is a crucial control system in contemporary control theory due to its unstable, non-linear and state coupling characteristics [233]. The RotIP system comprises a pendulum that rotates freely in the vertical direction. The pendulum would then reach its upright equilibrium position by the use of a swing-up motion employing a pivot arm in the horizontal plane.

This section presents the mathematical modelling for the optimum control of RotIP. This work uses a Rotary Servo Base Unit coupled Quanser RotIP module [234] as displayed in Fig. 6.1. The hardware consists of a VoltPAQ-X2 power amplifier, Q2 USB DAQ control board, and the single IP installed on the Quanser SRV02 based device. Quanser offers the QUARC control environment in MATLAB/Simulink for real-time implementation. Two optical shaft encoders are also included in this system for measuring the rotary arm and pendulum angles. The data acquisition device (Q2 USB DAQ) is used to gather data from the encoders and deliver it to the computer. The control signal is received by the DAQ device from the computer, amplified by the VoltPAQ-X2 power amplifier, and then fed to the motor.
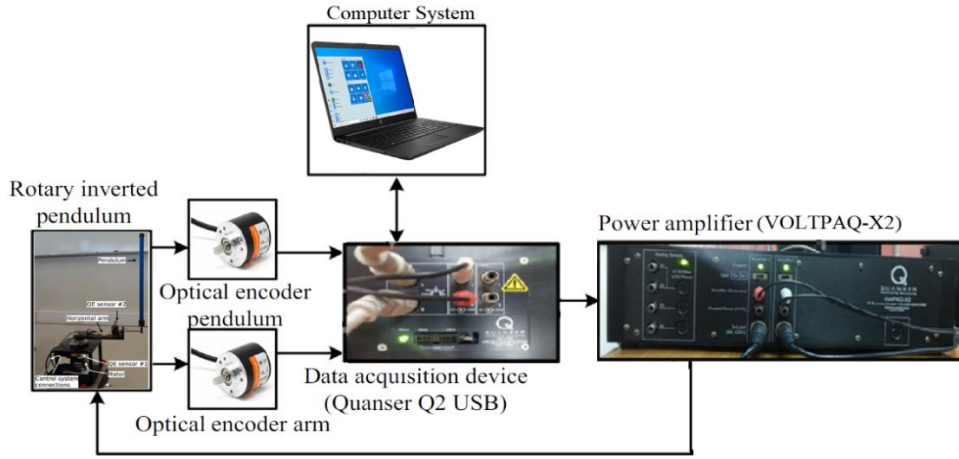
Figure 6.1. Experimentation setup of RotIP with LQG controller

Let the trajectory, $x(t)$ be defined as

$$\dot{x} = f[x(T), u(t)] \tag{6.1}$$

And cost function $O[u(t)]$ is defined in the form

$$O[u(t)] = \int_{t_1}^{t_2} \lambda[x(T), u(t)] \, dt + \chi[x(T)] \tag{6.2}$$

where, $\chi[x(T)]$ is cost term, $\lambda[x(T), u(t)]$ is the running cost function indicating the transient cost and u is the input variable. Minimizing the Hamiltonian at every instant, the cost function can be rewritten in the form

$$O[u(t)] = \frac{1}{2} w_1 x(T)^T Q_1 x(T) + \int_0^T \left\{ \frac{1}{2} w_2 x(t)^T Q_2 x(t) + \frac{1}{m} w_3 |u(t)|^m \right\} dt \tag{6.3}$$

where $w_i \in R$, $Q_i \in R^{n \times n}$ is by convention normalization. w_i are the relative weights.

In this form, the following set of 2n first-order differential equations hold

$$\chi[x(T)] = \frac{1}{2} w_1 x(T)^T Q_1 x(T), \chi_x[x(T)] = w_1 x(T)^T Q_1 \tag{6.4}$$

$$\lambda[x(T), u(t)] = \frac{1}{2} w_2 x(t)^T Q_2 x(t) + \frac{1}{m} w_3 |u(t)|^m$$

$$\lambda_x[x(T), u(t)] = w_2 x(t)^T Q_2 \tag{6.5}$$

If m=1, the cost function is said to be optimized from L_1 norm and if m=2, the cost function is said to be optimized from L_2 norm. The trajectories and optimal control with sufficient weights are approximated using a numerical method.

In the case of L_1 norm, the Hamiltonian can be expressed as

$$H(u) = \frac{\lambda_5}{Z_m} u + \chi_3 |u| \tag{6.6}$$

97

And the optimal control input (u^*), can be expressed as

$$u^* = \begin{cases} u_{sat-}, & \chi_3 Z_m < \lambda_5 \\ 0, -\chi_3 Z_m < \lambda_5 < \chi_3 Z_m \\ u_{sat+}, & -\chi_3 Z_m > \lambda_5 \end{cases} \tag{6.7}$$

Similarly, in the case of L_2 norm, the Hamiltonian and u^* can be expressed as

$$H(u) = \frac{\lambda_5}{Z_m} u + \frac{\chi_3 |u^2|}{2} \tag{6.8}$$

$$u^* = \frac{-\lambda_5(t)}{\chi_3 Z_m} \tag{6.9}$$

Gradient descent and algebraic descent are the numerical methods used for obtaining the optimal control functions. The piece-wise optimal control function by Gradient descent is expressed as

$$u^{(j+1)}(t_n) = u^j(t_n) - \tau \nabla_u H(t_n) \tag{6.10}$$

In the case of algebraic descent, the Hamiltonian is optimized at every instant. At a particular time, u^* is expressed as

$$u^*(t_n) = u^{(i+1)}(t_n) \tag{6.11}$$

Hamiltonian time function with 100, 400 and 1000 iterations for both L1 norm and L2 norm are shown in Fig. 6.2. Cost function vs number of iterations for optimizing the rotary inverted pendulum with both L1 norm and L2 norm are shown in Fig. 6.3.
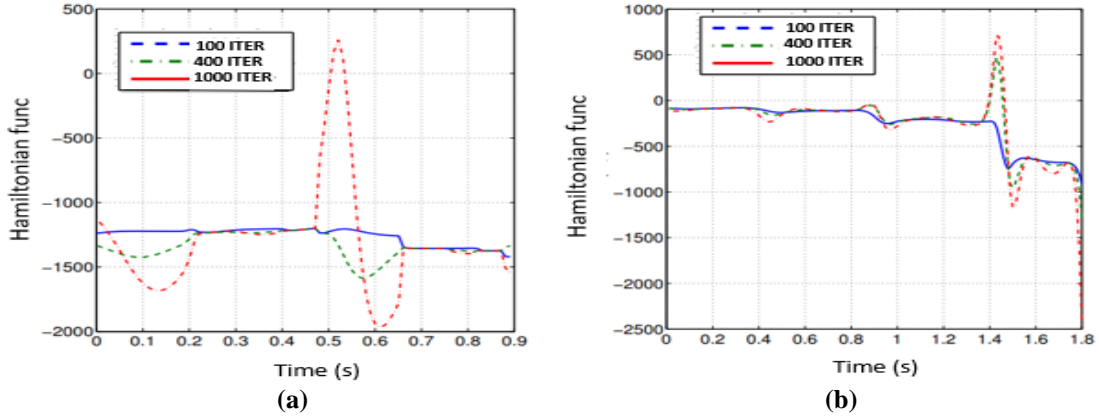
Figure 6.2. Hamiltonian time function with different iterations in **(a)** L1 norm **(b)** L2 norm
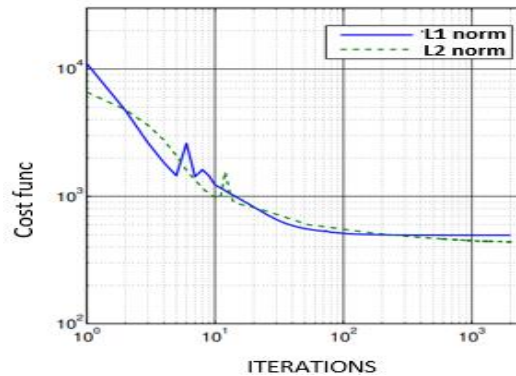
Figure 6.3. Cost function of L1 and L2 norm

98

6.5 TRAJECTORY CONTROL OF INVERTED PENDULUM USING LQG CONTROLLER

A Continuous Linear Quadratic Gaussian controller is designed for non-linear systems on the basis of optimum control theory. Here, the superposition theorem is valid, so designing of LQG controller can be done separately for both the regulator and estimator.

6.5.1 Designing Linear Quadratic Regulator

The primary objective of the Linear Quadratic Regulator (LQR) is to find the gain vector (K_f) for state space feedback law as shown in Eq. (6.12).

$$u = -K_f x \qquad (6.12)$$

which is applied to the system to minimize the cost function.

$$J_r = \int_0^\infty x x^T Q_r + u u^T W_r \qquad (6.13)$$

After applying Pontryagin's minimum principle to LQR, the Algebraic Riccati equation will be

$$A^T P + A P - P B B^T W_r^{-1} P + Q_r \qquad (6.14)$$

And the feedback gain (K_f) is given by

$$K_f = W_r^{-1} P B \qquad (6.15)$$

Figure 6.4 displays the block diagram representation of the state space feedback controller when it is subjected to D=0.
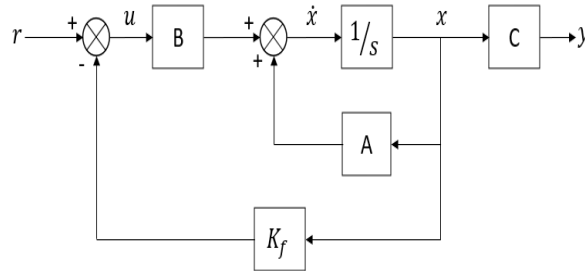
Figure 6.4. Block representation of Linear Quadratic Regulator controller

6.5.2 Designing Linear Quadratic Estimator

It is also known as the Kalman Filter approach which provides an estimation for the state space model of the system when both the model and measurements are subjected to uncertainties. Figure 6.5 displays the block representation of the state space feedback controller with an Estimator when subjected to D=0.

Let the system be subjected to Gaussian noise

$$\begin{cases} \dot{x} = Ax + By + w \\ y = Cx + Du + v \end{cases} \qquad (6.16)$$

And covariances be

$$Q_e = Eww^T \text{ \& } W_e = Evv^T \qquad (6.17)$$
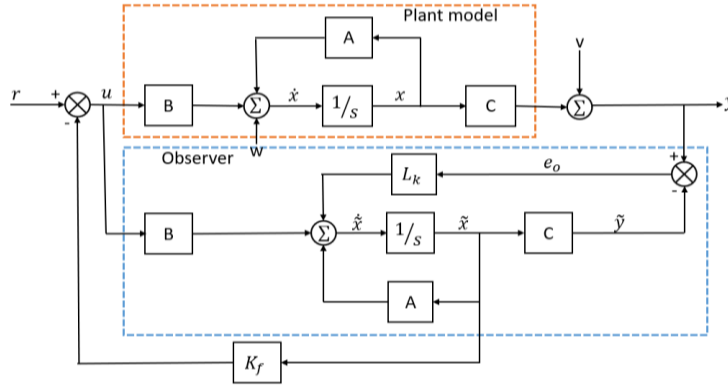
Figure 6.5. Block diagram of Linear Quadratic Estimator controller

The optimal estimator is the Kalman Filter with gain (L_k) is

$$L_k = \Sigma C^T W_e^{-1} \qquad (6.18)$$

where, Σ is the solution of the Riccati equation.

The state estimation is dynamic and is given as Eq. (6.19).

$$\dot{\tilde{x}} = (A - L_k C)\tilde{x} + Bu + L_k y \qquad (6.19)$$

6.5.3 Designing Linear Quadratic Gaussian Controller

LQR and Linear Quadratic Estimator (LQE) are simply combined to create the LQG processor. Figure 6.6 displays the block representation of the Linear Quadratic Gaussian controller.

$$\begin{cases} \dot{\tilde{x}} = \left(A - BK_f - L_k C\right)\tilde{x} - L_k(x_r - y) \\ \qquad\qquad u = -K_f x \end{cases} \qquad (6.20)$$
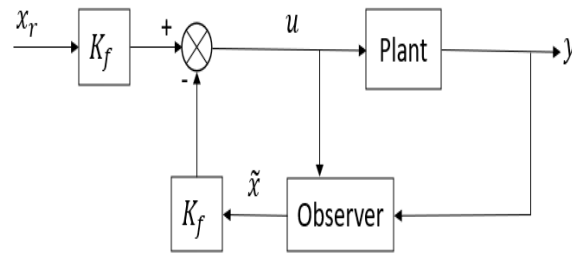
Figure 6.6. Full block representation of Linear Quadratic Gaussian Controller

6.5.4 Determining Stability Region

The equilibrium at the upward position, achieved by the linear controller, can be easily disturbed by a small perturbation. So, there should be a region of stability where equilibrium can be maintained for maximum input voltage. The stability region can be found on the basis of a binary search algorithm.

100

The algorithm is as follows:

Step 1: Initially, a known point is taken inside the stability region.

Step 2: The binary search, having 'n' number of iterations, is conducted within a line segment with $2 - 2^{-(n-1)}$ steps. At every iteration, the stability of the point is determined. By doing this, the stable region can be determined with an error of $\leq \frac{step}{2^n}$.

Step 3: After getting the stable boundary, an angular binary search with 'n' number of iterations is performed. The points that lie on a circle, are examined for stability and the angle is updated for the best estimation. By doing this, the angle estimation can be determined with an error of $\leq \frac{step}{2^n}$. This stable point is considered the centre of the next angular binary search operation.

Step 4: This method advances by recursively applying step 3 until we get a $360°$ angled boundary around that initial point.

6.6 RESULTS AND DISCUSSIONS

The generated trajectories of swing-up control of RotIP, based on both energy shaping and exponentiation approach are discussed here. Both simulated and experimental results are shown. LQG controller tries to maintain the quick equilibrium position in the upward position after a sudden perturbation.

6.6.1 Control Function and Trajectories Generated with L1 and L2 Norm

The trajectories generated and optimal control functions based on proper weights with L1 norm and L2 norm are approximated by a numerical method as illustrated in Fig. 6.7. The number of iterations increases in the direction of the arrow. The direction of the arrow signifies the increase in number of iterations. As the number of iterations increases, the deviation decreases.
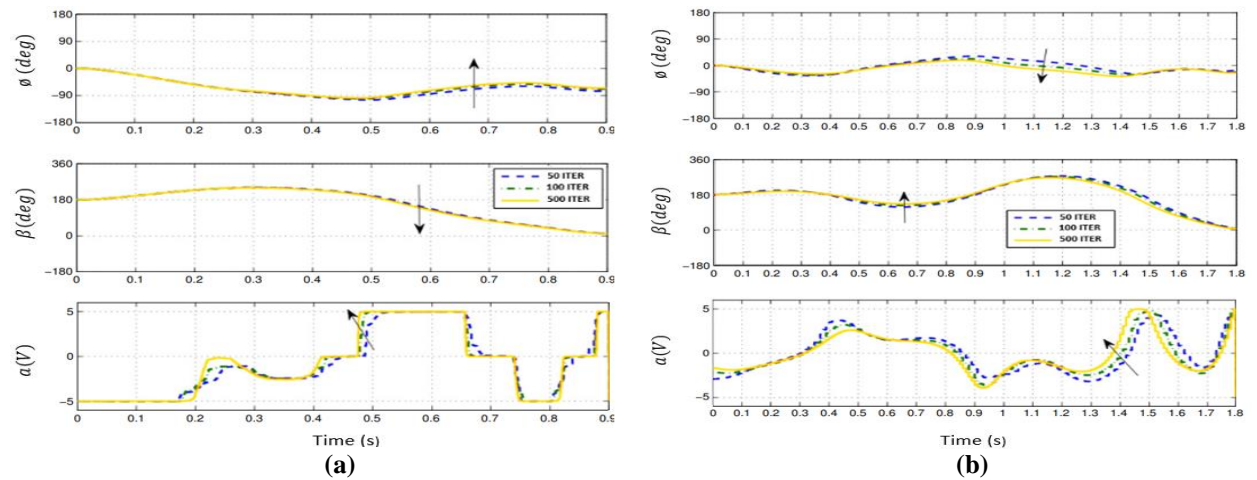
Figure 6.7. Control function and trajectories generated with **(a)** L1 norm **(b)** L2 norm, where arrows indicate an increase in the number of iterations.

6.6.2 Region of Convergence with Different Conditions

Simulation of the non-linear model using LQG controller is illustrated in Fig. 6.8. The Equilibrium state of the pendulum for having the maximum initial angle, is achieved using $'u'$. The lines represent the region of convergence with conditions $x_1(0) = 0, x_2(0) = 0$ and $x_5(0) = 0$ in the case of Fig. 6.8(a) and $x_1(0) = 0$ and $x_5(0) = 0$ in the case of Fig. 6.8(b). The state space is of 5 dimensions. These boundaries signify the region where RotIP can be stabilized by the linear controller.

(a)   **(b)**
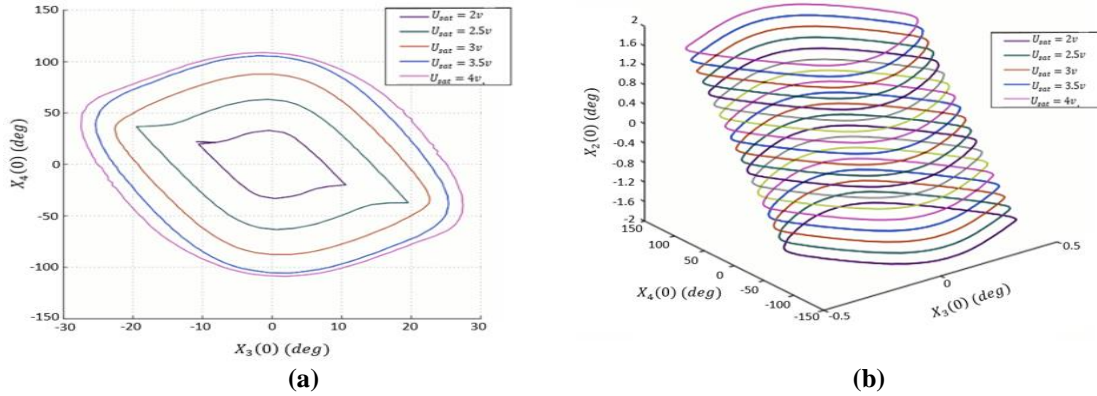
Figure 6.8. Region of convergence in case of **(a)** $x_1(0) = 0, x_2(0) = 0$ and $x_5(0) = 0$ **(b)** $x_1(0) = 0$ and $x_5(0) = 0$

6.6.3 Trajectories of Swing-Up Control with L1 and L2 Norm

The trajectories of swing-up control of the pendulum, performed with optimal control L1 norm and L2 norm are shown in Fig. 6.9. The reference inputs are set to zero at t=0.9s and t=1.8s, in case of L1 norm and L2 norm respectively and the sampling time of 1ms is considered in both cases.

(a)   **(b)**
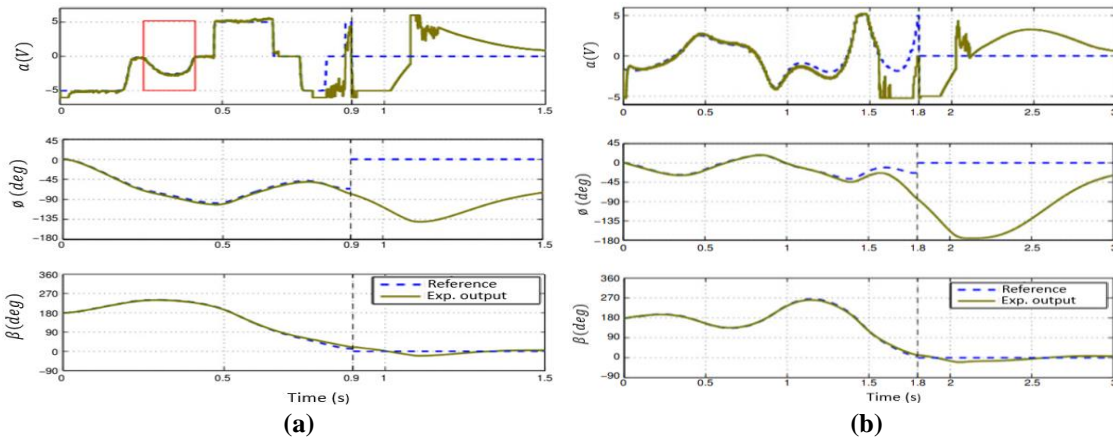
Figure 6.9. Swing-up performed with **(a)** L1 norm **(b)** L2 norm

6.6.3 Trajectories of Swing-Up Control with Energy Shaping and Exponential Approaches

The trajectories of swing-up of the RotIP, performed with energy shaping and exponential approaches are illustrated in Fig. 6.10. For both cases, the open-loop simulation, closed-loop simulation and

closed-loop experimental results are compared. For open-loop simulation, experimental data input is applied to the device model with no feedback control. In closed-loop simulation and experimentation, the energy shaping method is used for controlling with a sampling time of 1ms.
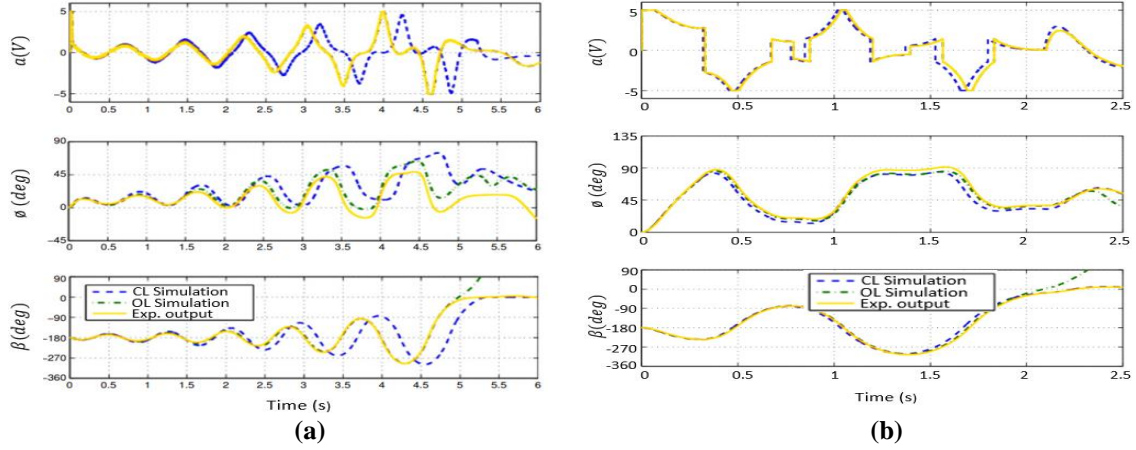
Figure 6.10. Swing-up trajectories with **(a)** energy shaping approach **(b)** exponential approach

6.6.5 Trajectories of Swing-Up Control with Energy Control

The trajectories of the swing-up control of the RotIP, performed with energy control are shown in Fig. 6.11(a) and equilibrium is maintained with the LQG controller after t = 1.7s. An external perturbation is applied to the pendulum at t=14.8s, shown by an arrow in Fig. 6.11(b). After the perturbation, there is a sudden spike in the response but the designed LQG controller tries to maintain the equilibrium quickly.
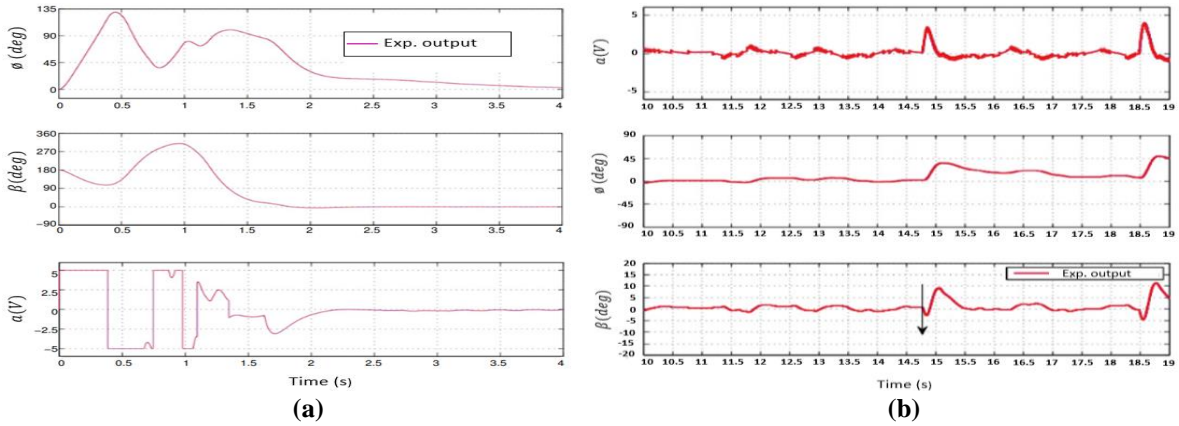
Figure 6.11. Swing-up trajectories with **(a)** energy control **(b)** energy control and equilibrium maintained with the LQG controller.

6.7 SUMMARY

This chapter proposed an effective control method using a continuous Linear Quadratic Gaussian (LQG) controller based on the optimal control strategy for swinging up the rotary inverted pendulum and maintaining an equilibrium in the vertical upward position, using both simulation and

experimentation analysis. While following the trajectories, the deviation decreases with an increase in the number of iterations. The stable boundary regions of the inverted pendulum can be determined by the LQG controller. The designed LQG controller tries to maintain the equilibrium quickly when the system is subjected to any external perturbations.

Chapter 7

Robust Control of Rotary Inverted Pendulum using Metaheuristic Optimization Techniques Based PID and Fractional Order PID Controller

7.1 INTRODUCTION

Rotary inverted pendulum (RotIP) innates unstable and underactuated behaviour that is helpful in the realisation of many real-world problems. It is very challenging to identify and control the dynamics of the RotIP system due to its nonlinear, complex, underactuated and unpredictable nature. The primary objective of this chapter is to improve the swing-up and stabilization performances of RotIP in comparison to the existing approaches. This chapter aims to propose the modelling and optimal design of a PID and Fractional Order $PI^{\lambda}D^{\mu}$ Controller with Integral ANTI-WINDUP technique along with variable velocity setpoints for the robust stabilization and control of the RotIP system using metaheuristic optimization techniques. The parameters P, I, λ, D and μ of the Fractional Order $PI^{\lambda}D^{\mu}$ Controller are tuned by two optimization techniques i.e. Genetic Algorithm and Particle Swarm Optimization based on Integral Time Absolute Error (ITAE). The pendulum angle, rotary arm angle and controlled input voltage comparisons are executed with the developed control schemes for both simulation and real-time experimentation purposes. The analysis of transient response and steady-state response of both simulation and real-time experimentation implies that Fractional Order $PI^{\lambda}D^{\mu}$ compensator provides overall better control performances as compared to conventional PID controllers for the RotIP system. PSO provides much better-optimized results for both PID and $PI^{\lambda}D^{\mu}$ controllers as compared to the results provided by GA.

7.2 RELATED WORK

Rotary inverted pendulum serves as a testbed for the class of underactuated mechanical systems and many other complex nonlinear engineering applications including balancing of two-wheelers [235], ankle joint control, crane mechanisms, the orbital motion of satellites, quad-rotor helicopters [236] and many others along with large-scale uses like military, transportation, and medical applications etc [237,238]. However, due to the significant underactuation and high nonlinearities of the system, the control of RotIP becomes a very challenging problem in the field of control and robotics. The literature review of RotIP identifies four general control issues:

a) Swing-up control involves moving the pendulum from a stable downward position to an unstable upward position.

b) Stabilisation control involves keeping the pendulum in its upward position.

c) Switching control involves the switching between swing-up and stabilisation control.

d) Trajectory tracking control directs the arm to follow a specific time-varying trajectory while keeping the pendulum in its upward-pointing orientation.

Different kinds of control algorithms have been used in the past to achieve these control objectives. In most cases, both stabilization control and swing-up control objectives are implemented together because a stabilization controller is needed to stabilize the pendulum when it swings closer to the upright equilibrium position. To improve control performance for stabilisation control, various controller approach designs have been proposed. A Fast hybrid dual-mode non-linear model predictive control method was introduced for the stabilisation and swing-up control of a parallel double inverted pendulum (IP) using a control parameterisation [239,240]. Pratheep et al. [241] proposed a PID controller with a genetic algorithm (GA) to hold the IP in its upright position from the downward direction by optimizing the controller's parameters. This controller enhanced the performance indexes in comparison to the conventional PID controller by holding minimum settling time and peak overshoot. The effectiveness of an optimised fuzzy logic controller was investigated in [242] using genetic algorithms for the swing-up and stabilisation control of a twin-arm IP system. The black-box method was used for the controller design and Lyapunov criteria was utilized by the fuzzy controller to ensure system stability.

Chawla et al. [243] proposed an LQR-based adaptive neuro-fuzzy inference system controller to address the real-time stabilization problem of the RotIP. The problem with LQR-based schemes is that some unusual computational modelling errors and parametric uncertainties tend to degrade their performance. Although these control systems function very well, but they are both intricate and challenging to put into practice. A robust $H\infty$ controller with μ-synthesis architecture has been designed in [244] to control a RotIP in its upright equilibrium position within a tolerable desired angle margin. Robust stability and performance analysis was done along with rudimentary pole placement

analysis for a given degree of the actuator and modelled uncertainties. Zakeri et al. [245] proposed a hierarchical sliding surface with an interval type-2 fuzzy fractional order super twisting algorithm which utilized a multi-tracker optimization technique to optimize the controller's parameters for reducing chattering, improving tracking accuracy, and decreasing the control effort in the presence of uncertainty in different underactuated systems.

An FPID controller and a fractional order MRAC were proposed in [246] for the stability analysis of the IP system. A PID controller and Find minimum of constrained nonlinear multivariable function (FMINCON) numerical optimization algorithm was utilized to optimize the FPID controller using a scaler objective function called Integral time square error (ITSE). A fractional-order sliding mode control (SMC) approach under the Smith predictive method was proposed in [247] for the second-order IP system with delay. The efficacy of the approach was validated using numerical simulations through MATLAB software and stability was proved through the Lyapunov theorem. Wang et al. [248] introduced a hierarchical SMC approach for the modelling and trajectory tracking of spatial IP which used a heterogeneous comprehensive learning PSO algorithm to optimize the control parameters for the hierarchical SMC. However, these approaches have additional fluctuations and steady-state errors.

Pandey et al. [249] introduced a robust control framework for a RotIP using an optimal control approach which used the Lyapunov stability technique with regards to a cost function for incorporating the maximum limit on the uncertainties. A non-quadratic term was also added to solve the bounded robust control issue based on the Hamilton–Jacobi–Bellman equation. Dwidei et al. [250] investigated a fractional controller approach for stabilizing a RotIP in an upright position by minimizing the deviations in the rotational arm. The parameters of the fractional controller were tuned using dynamic PSO and a frequency response graphical tuning method. The saturation non-linearity is compensated by incorporating a back-calculation anti-windup technique.

Masrom et al. [251] proposed a PSO and spiral dynamic algorithm (SDA) based interval type-2 FLC mechanism to reduce noise/vibration and cater for uncertainties in a triple-link IP system. SimWise 4D software environment was used to develop the IP model and then integrated with MATLAB/Simulink. The PSO and SDA were used to find optimal values for controller gains and parameter values of the interval type-2 FLC membership function. However, the rule explosion issue with fuzzy controllers for multivariable systems is challenging. Gutarra et al. [252] implemented a cascade fuzzy controller on a non-linear RotIP system which used GA for tuning the parameters of the FLC membership functions. Comparative analysis showed that a fuzzy controller covers a larger range of operating points even in the presence of typical disturbances than a conventional LQR controller.

Alimoradpour et al. [253] proposed an optimal FLC to control a real-time IP system by optimizing its parameters like fuzzy rules, membership function and the learning process length using

a genetic evolutionary algorithm. The integration of GA and Mamdani fuzzy controller solved the inverse pendulum control problem. Vishnu et al. [254] proposed an approach to stabilize an IP using PID and fuzzy modelling which used PSO to optimize the control system parameters. The simulation results showed an improvement in speeding up the convergence process and achieving control over non-linear and unstable processes in comparison to GA. Nagarajan et al. [255] suggested a coherently tuned control approach to resolve the non-linearity issues of the underactuated RotIP systems which used a modified Manhattan distance updated whale optimization algorithm to optimize the controller parameters.

7.3   PROBLEM STATEMENT

A system is said to be efficient when it overcomes the limitations such as fluctuations in control input and output signals, steady-state errors, latency in angular position sensing, computational complexity, higher order nonlinearities, time delays, chattering and discontinuity while also maintaining a low cost. Therefore, there is a need to design and develop a more stable, reliable, robust and high-performance controller to control the dynamics of the RotIP system. This chapter proposes the modelling and optimal design of a PID and Fractional Order $PI^\lambda D^\mu$ (FPID) controller with Integral ANTI-WINDUP technique along with variable velocity setpoints (V_{sw}) and optimization using GA and PSO techniques for the robust stabilization and control of the RotIP system by allowing more degrees of freedom in comparison to its integer-order counterparts. The proposed system aims to accomplish two objectives in particular:

- To keep the pendulum balanced and to preserve some degree of tolerance for a vertical upright position.
- To bring the pendulum out of its state of passive equilibrium and into its upright posture so that the balancing controller can achieve balance.

The primary feature of the proposed controller is that it resolves the issues of robustness, accuracy, dependability and complexity in comparison to many existing algorithms.

7.4   MATHEMATICAL MODELLING AND DESIGN

The hardware setup consists of a QUANSER-made RotIP which is fixed on the ground. So, the system can neither be moved forward nor backwards. The rotary arm pivot is connected to the rotary servo system and the pendulum link is connected to the rotary arm as displayed in Fig. 7.1. The pendulum is designed to move upright from the downward inverted position, and the rotary arm can move freely in both clockwise and anti-clockwise direction. It is very challenging to keep the pendulum in the vertical upright position with very little vibrations despite having only two degrees of

freedom. The RotIP system is a SIMO system comprising multiple outputs controlled by a single input. Disturbances affecting one output can interfere with the control of the other output. The non-linear nature of the RotIP system makes it very critical to control the pendulum dynamics. Figure 7.1 shows the model of RotIP. The model has the following conventions. The pendulum has length L_P, mass M_P and centre of mass at $L_p/2$. J_P is the moment of inertia about its centre of mass. β is defined as the angle of the inverted pendulum but β is zero when the pendulum is in an upright vertical position. The rotary arm, that is attached to the SRV02 system has length L_R, moment of inertia J_R and its angle is $\emptyset$, and it will be positive when the servo is moved in the anti-clockwise direction.
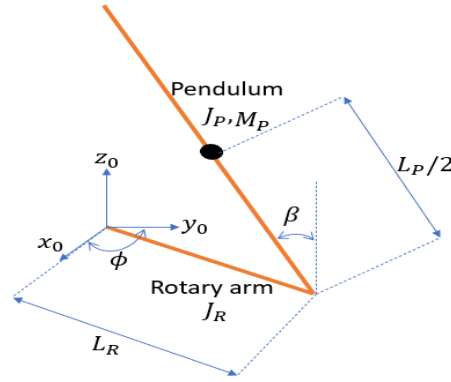
Figure 7.1. Model of rotary inverted pendulum system

The dynamics of the rotary arm and inverted pendulum are described by the Euler-Lagrange equation.

$$\frac{\partial^2 L}{\partial t \partial \dot{q}_i} - \frac{\partial L}{\partial q_i} = Q_i \qquad (7.1)$$

where, Q_i are generalised coordinates. For this system, suppose

$$q(t)^T = [\emptyset(t)\beta(t)] \qquad (7.2)$$

So,

$$q(\dot{t})^T = \left[\frac{\partial}{\partial t}\emptyset(t).\frac{\partial}{\partial t}\beta(t)\right] \qquad (7.3)$$

After defining the generalized coordinates, the Euler-Lagrange equation of the system becomes

$$\frac{\partial^2 L}{\partial t \partial \dot{\emptyset}} - \frac{\partial L}{\partial \emptyset} = Q_1 \qquad (7.4)$$

$$\frac{\partial^2 L}{\partial t \partial \dot{\beta}} - \frac{\partial L}{\partial \beta} = Q_2 \qquad (7.5)$$

The Lagrange is of the form

$$L = TE - PE \qquad (7.6)$$

where TE, PE are total energy and potential energy respectively. The generalized forces on the rotary arm and pendulum are

$$Q_1 = -B_R \dot{\emptyset} + \tau, \qquad Q_2 = -B_P \dot{\beta} \qquad (7.7)$$

So, the RotIP can be described by the following non-linear equations of motion

$$\left\{M_P L_R^2 + \frac{1}{4} M_P L_P^2 (1 - cos^2\beta) + J_R\right\} \ddot{\phi} - \left(\frac{1}{2} M_P L_P L_R \cos\beta\right) \ddot{\beta} + \left(\frac{1}{2} M_P L_P L_R \sin\beta\right) \dot{\beta}^2 +$$

$$\frac{1}{2}(M_P L_P^2 \sin\beta \cos\beta)\dot{\beta}\dot{\phi} = -B_R\dot{\phi} + \tau \qquad (7.8)$$

$$\left(J_P + \frac{1}{4} M_P L_P^2\right) \ddot{\beta} - \frac{1}{2} M_P L_P L_R \cos\beta \, \ddot{\phi} - \frac{1}{4} M_P L_P^2 \sin\beta \cos\beta \, \dot{\phi}^2 - \frac{1}{2} M_P L_P \sin\beta \, g = -B_P\dot{\beta} \qquad (7.9)$$

The torque generated by the servo arm at the base of the rotary arm is given by

$$\tau = \frac{K_G \eta_G \eta_M K_t \left(V_M - K_G K_M \dot{\phi}\right)}{R_M} \qquad (7.10)$$

However, the torque cannot be controlled directly. Instead of this, there's a need to control the servo input voltage. For controlling the torque and for implementation of PID and FPID controller, it is necessary to linearize the model first. So, the Eq. (7.8) and Eq. (7.9) are linearized at $\phi_0 = 0, \dot{\phi}_0 = 0, \beta_0 = 0$ and $\dot{\beta}_0 = 0$ to get the linearized function as shown in Eq. (7.13) and Eq. (7.14).

Now, linearizing Eq. (8) at, $\phi_0 = 0, \dot{\phi}_0 = 0, \beta_0 = 0$ and $\dot{\beta}_0 = 0$.

Let variable z be $z^T = [\phi, \beta, \dot{\phi}, \dot{\beta}, \ddot{\phi}, \ddot{\beta}]$

$$f(z) = \left\{M_P L_R^2 + \frac{1}{4} M_P L_P^2 (1 - cos^2\beta) + J_R\right\} \ddot{\phi} - \left(\frac{1}{2} M_P L_P L_R \cos\beta\right) \ddot{\beta} + \left(\frac{1}{2} M_P L_P L_R \sin\beta\right) \dot{\beta}^2$$

$$+ \frac{1}{2}(M_P L_P^2 \sin\beta \cos\beta)\dot{\beta}\dot{\phi} \qquad (7.11)$$

The linearized forms for Eq. (7.8) are

$$\frac{\partial}{\partial\phi} f(z)|z = z_0 = 0, \; \frac{\partial}{\partial\beta} f(z)|z = z_0 = 0, \; \frac{\partial}{\partial\dot{\phi}} f(z)|z = z_0 = 0, \; \frac{\partial}{\partial\dot{\beta}} f(z)|z = z_0 = 0, \; \frac{\partial}{\partial\ddot{\beta}} f(z)|z =$$

$$z_0 = -\frac{1}{2} M_P L_P L_R, \; \frac{\partial}{\partial\ddot{\phi}} f(z)|z = z_0 = J_R + M_P L_R^2 \qquad (7.12)$$

The final linearized function for Eq. (7.8) becomes

$$f(z)_{lin}(8) = J_R + M_P L_R^2 - \frac{1}{2} M_P L_P L_R = -B_R\dot{\phi} + \tau \qquad (7.13)$$

Similarly, the final linearized function for Eq. (7.9) becomes

$$f(z)_{lin}(9) = \left(J_P + \frac{1}{4} M_P L_P^2\right) \ddot{\beta} - \frac{1}{2} M_P L_P L_R \ddot{\phi} - \frac{1}{2} M_P L_P g\beta = -B_P\dot{\beta} \qquad (7.14)$$

The linear state-space model is described by Eq. (7.15)

$$\dot{x} = Ax + Bu, \qquad \dot{y} = Cx + Du, \qquad (7.15)$$

In this case, only link angles and servo position are measured. So, the state and output are defined as

$$x^T = [\phi \; \beta \; \dot{\phi} \; \dot{\beta}] \; \& \; y^T = [x_1 \; x_2] \qquad (7.16)$$

and

$$C = \begin{bmatrix} 1 & 0 & 0 & 0 \\ 0 & 1 & 0 & 0 \end{bmatrix} \ \& \ D = \begin{bmatrix} 0 \\ 0 \end{bmatrix} \tag{7.17}$$

The linearized equations in matrix form become

$$\begin{bmatrix} M_P L_R^2 + J_R & -\frac{1}{2} M_P L_P L_R \\ -\frac{1}{2} M_P L_P L_R & J_P + \frac{1}{4} M_P L_P^2 \end{bmatrix} \begin{bmatrix} \ddot{\emptyset} \\ \ddot{\beta} \end{bmatrix} + \begin{bmatrix} B_R & 0 \\ 0 & B_P \end{bmatrix} \begin{bmatrix} \dot{\emptyset} \\ \dot{\beta} \end{bmatrix} + \begin{bmatrix} 0 \\ -\frac{1}{2} M_P L_P g \beta \end{bmatrix} = \begin{bmatrix} \tau \\ 0 \end{bmatrix} \tag{7.18}$$

Solving the above matrix in Eq. (7.18) for acceleration, we get

$$\ddot{\emptyset} = \frac{\frac{1}{2} M_P L_P L_R B_R \dot{\emptyset} - (M_P L_R^2 + J_R) B_P \dot{\beta} + \frac{1}{2} M_P L_P g (J_R + M_P L_R^2) \beta + \frac{1}{2} M_P L_P L_R \tau}{J_P M_P L_R^2 + \frac{1}{4} M_P J_R L_P^2 + J_R J_P} \tag{7.19}$$

Let $E = J_P M_P L_R^2 + \frac{1}{4} M_P J_R L_P^2 + J_R J_P$ \hfill (7.20)

So, the linear state-space model of the rotary pendulum is represented as

$$A = \frac{1}{E} \begin{bmatrix} 0 & 0 & 1 & 0 \\ 0 & 0 & 0 & 1 \\ 0 & \frac{1}{4} M_P^2 L_P^2 L_R g & -B_R \left(\frac{1}{4} M_P L_P^2 + J_P \right) & -\frac{1}{2} M_P L_P L_R B_P \\ 0 & \frac{1}{2} M_P L_R g (J_R + L_R^2 M_P) & \frac{1}{2} M_P L_P L_R B_R & -B_P (J_R + M_P L_R^2) \end{bmatrix},$$

$$B = \frac{1}{E} \begin{bmatrix} 0 \\ 0 \\ \frac{1}{4} M_P L_P^2 + J_P \\ \frac{1}{2} M_P L_P L_R \end{bmatrix}, C = \begin{bmatrix} 1 & 0 & 0 & 0 \\ 0 & 1 & 0 & 0 \end{bmatrix} \ \& \ D = \begin{bmatrix} 0 \\ 0 \end{bmatrix} \tag{7.21}$$

7.5 BALANCING CONTROL

For balancing control, the desired specifications of QUANSER-made RotIP are Natural frequency $(\omega_n) = 5 \ rad/s$, damping ratio $(\zeta) = 0.707$, maximum angle of deflection for the pendulum, $|\beta| < 20$ (deg) and maximum control effort, $(a_m) = 10v$.

The linear state-space model of the rotary pendulum, described in Eq. (7.21), is used to investigate the stability. If any of the poles lie in the right-hand plane or if there are multiple poles on the hypothetical axis, then it is an unstable system. A system is deemed controllable if the control input $'u'$ the system includes all state variables, $x_{j}, j = 1 \dots n$, from the initial state to the final; otherwise, it is uncontrollable and the controllable matrix is represented as

$$T_c = [B \ AB \ A^2 B \ \dots \dots \dots A^n B] \tag{7.22}$$

The system is controllable if $rank(T_c) = n$. The control loop structure for balancing the rotary inverted pendulum is depicted in Fig. 7.2.
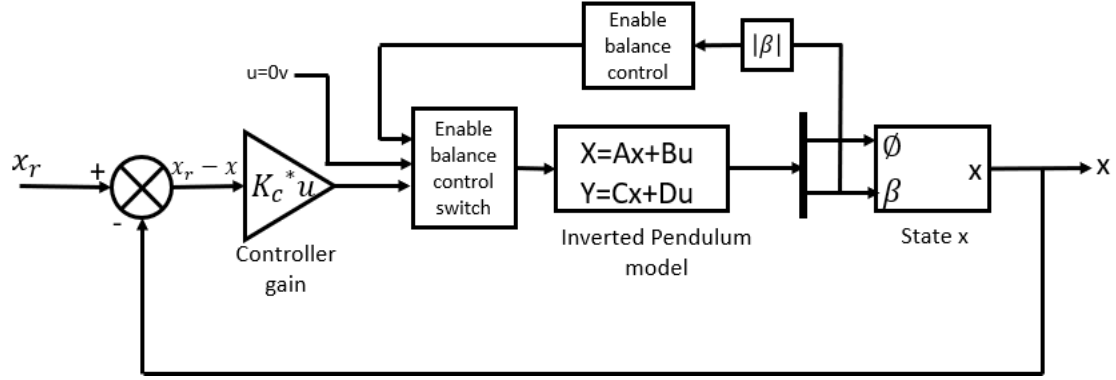
Figure 7.2. Control loop structure for balancing the rotary inverted pendulum

Let us define the reference state as $x_r = [\emptyset_d \ 0 \ 0 \ 0]$, where the desired rotary arm angle is $\emptyset_d$.

The controller is

$$u = \begin{cases} K_c(x_r - x) & |x_2| < \delta \\ 0 & otherwise \end{cases} \tag{7.23}$$

where, δ is the controller engaging angle. The balance control must be enabled only when the pendulum is brought up in an upright vertical position and no action is taken in the hanging downward position.

The open loop poles of the rotary pendulum system are -17.11, 8.345, -2.87 & 0. The one pole in the right-hand plane indicates that the system is unstable. It is obvious that an inverted pendulum cannot be inverted by itself. It will eventually fall without any controlling effect.

The characteristic equation of the system using open loop poles is

$$s^4 + 11.6s^3 - 117.3s^2 - 408.3s = 0 \tag{7.24}$$

The companion matrices are

$$\tilde{A} = \begin{bmatrix} 0 & 1 & 0 & 0 \\ 0 & 0 & 1 & 0 \\ 0 & 0 & 0 & 1 \\ 0 & 408.3 & 117.3 & -11.6 \end{bmatrix} \& \tilde{B} = \begin{bmatrix} 0 \\ 0 \\ 0 \\ 1 \end{bmatrix} \tag{7.25}$$

Using the desired specifications, the desired location of the closed loop poles is -2.81±j2.859, -40 and -30. Using these desired poles, the characteristic equation becomes

$$s^4 + 75.61s^3 + 1608s^2 + 7840s + 19200 = 0 \tag{7.26}$$

While applying control action, $u = -\widetilde{K_c}x$, the companion form becomes $\tilde{A} - \tilde{B}\tilde{K}, \tilde{B}$, where $\widetilde{K_c} = [k_1 \ k_2 \ k_3 \ k_4]$ and correspondingly the characteristic equation is

$$s^4 + (11.6 + k_4)s^3 + (k_3 - 117.3)s^2 + (k_2 - 408.3)s + k_1 = 0 \tag{7.27}$$

Comparing Eq. (7.26) & Eq. (7.27), we get

$$\widetilde{K_c} = [19200 \ 8248 \ 1725 \ 64] \tag{7.28}$$

For controller gain K_c, we need to calculate the transformation matrix $W = T_c\widetilde{T_c^{-1}}$, where T_c is the oscillatory time period. The resultant matrices are

$$T_c = \begin{bmatrix} 0 & 83.5 & -930.7 & 16989 \\ 0 & 80.3 & -974.6 & 20780 \\ 83.5 & -930.7 & 16989 & -272898 \\ 80.3 & -974.6 & 20780 & -323519 \end{bmatrix}$$

$$\widetilde{T_c} = \begin{bmatrix} 0 & 0 & 0 & 1 \\ 0 & 0 & 1 & -11.7 \\ 0 & 1 & -11.7 & 253.1 \\ 1 & -11.7 & 253.1 & 3906 \end{bmatrix}$$

$$\widetilde{T_c^{-1}} = \begin{bmatrix} -410.4 & -117.4 & 11.7 & 1 \\ -117.4 & 11.7 & 1 & 0 \\ 11.65 & 1 & 0 & 0 \\ 1 & 0 & 0 & 0 \end{bmatrix}$$

$$W = \begin{bmatrix} -3649 & 41.8 & 83.5 & 0 \\ 0 & -38.8 & 80.3 & 0 \\ 0 & -3649 & 41.8 & 83.5 \\ 0 & 0 & -38.8 & 80.3 \end{bmatrix} \tag{7.29}$$

Now, the balanced controller gain, $K_c = \widetilde{K_c}W^{-1}$.

Finally, the generated controller gain, $K_c = [-5.267\ \ 30.07\ -2.651\ \ 3.549]$

Simulated and experimental responses of state feedback balance control are displayed in Fig. 7.3 respectively. It is clear from the responses and parametric data shown in Table 7.1 that when the rotary arm angle ($\emptyset$) is tracking a $\pm20°$ angle square wave, maximum pendulum angle (β_{max}) and maximum controlled input voltage (a_{max}) for both simulated and experimental responses are within the specified limits of $|\beta| < 20$ (deg) and maximum control effort $(a_{max}) = 10v$.

(a)   **(b)**
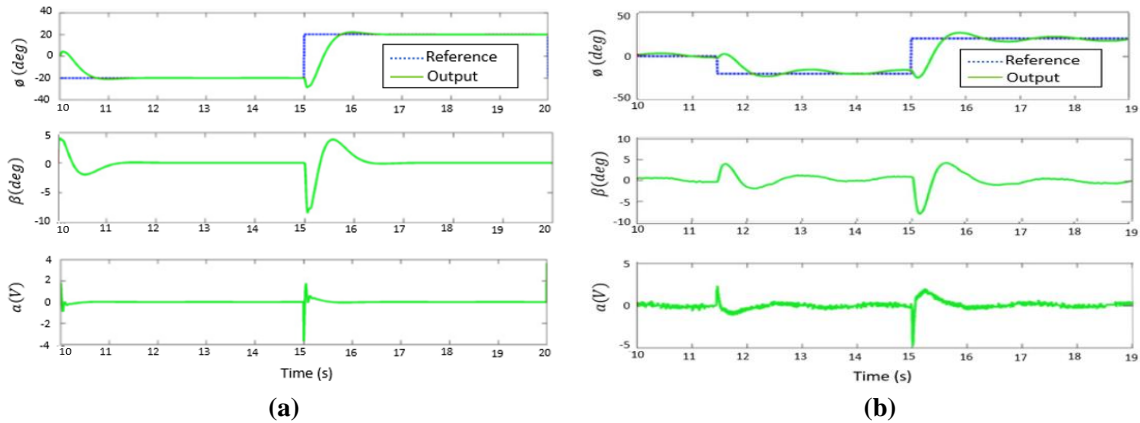
Figure 7.3. State feedback balance control of **(a)** Simulated response **(b)** Experimental response

Table 7.1. Parametric data of both simulation and experimental responses of state feedback balance control

S. No.	PARAMETERS	Simulation Response	Experimental Response
1.	β_{max}(deg)	8.4	8.1
2.	a_{max} (v)	3.8	4.82

113

7.6 SWING-UP CONTROL

For swinging up the pendulum to an upright vertical position from its downward hanging position, an energy-based control strategy is used. The pendulum dynamics are defined as

$$J_P\ddot{\beta} + \frac{1}{2}M_P L_P g \sin\beta = \frac{1}{2}M_P L_P \cos\beta\, a_p \tag{7.30}$$

where $'a_p'$ is the linear pivot acceleration of the link base of the pendulum. And torque in terms of $'a_p'$ can be expressed as

$$\tau = M_R L_R a_p \tag{7.31}$$

The total energy (TE) of the pendulum can be expressed as

$$TE = \frac{1}{2}J_P\dot{\beta}^2 + \frac{1}{2}M_P L_P g(1 - \cos\beta) \tag{7.32}$$

Taking the time derivative of TE, we get

$$\dot{TE} = \dot{\beta}\left(J_P\ddot{\beta} + \frac{1}{2}M_P L_P g \sin\beta\right) \tag{7.33}$$

Solving for $\sin\beta$, we get

$$\sin\beta = \frac{M_P L_P a_p \cos\beta - 2J_P\ddot{\beta}}{M_P L_P g} \tag{7.34}$$

And

$$\dot{TE} = \frac{1}{2}M_P L_P a_p \dot{\beta} \cos\beta \tag{7.35}$$

The proportional control action that will swing the pendulum to the desired reference energy (TE_r) is

$$a_p = (TE - TE_r)\dot{\beta} \cos\beta \tag{7.36}$$

The control action magnitude should be large enough for a quick change in energy and it should be implemented as

$$a_p = sat_{a_{max}}\{\sigma(TE - TE_r)sign(\dot{\beta} \cos\beta)\} \tag{7.37}$$

where, $sat_{a_{max}}$ is the saturated control signal at maximum acceleration, σ represents the tuneable control gain and taking the $sign(\dot{\beta} \cos\beta)$ allows us to switch quickly.

The servo voltage (V_M) in terms of torque is expressed as

$$V_M = \frac{\tau R_M}{K_G \eta_G K_t \eta_M} + K_G K_M \dot{\emptyset} \tag{7.38}$$

From Eq. (7.31) and Eq. (7.38), the servo voltage (V_M) is formulated as

$$V_M = \frac{R_M M_R L_R a_p}{K_G \eta_G K_t \eta_M} + K_G K_M \dot{\emptyset} \tag{7.39}$$

Both balancing control and swing-up control can be combined with the same control law by just some changes. When balancing control is not engaged, swing-up control can be enabled. Thus, the final controller becomes

$$a_p = \begin{cases} K_c(x_r - x) & |x_2| < \delta \\ sat_{a_{p(max)}}\{\sigma(TE - TE_r)sign(\dot\beta\cos\beta)\} & otherwise \end{cases} \tag{7.40}$$

The term $\cos\beta$ determines whether the current position is horizontal or below and above the horizontal position. If $\cos\beta = 0$, it implies the horizontal position and at this position the system is uncontrollable. Horizontal arm angle ($\emptyset$) does not affect this energy. Thus, this variable cannot be controlled during swing-up. A slight modification in the above controller in Eq. (7.40) makes a smooth transition between the non-linear and stabilizing controllers. Thus, the modified controller is formulated as

$$a_p = \begin{cases} K_c(x_r - x) & |x_2| < \delta \\ sat_{a_{p(max)}}\{\sigma\beta^n sign(\dot\beta\cos\beta)\} & otherwise \end{cases} \tag{7.41}$$

7.7 PID AND FRACTIONAL ORDER PID CONTROLLER DESIGN

The PID compensator in the time domain, when λ, μ of $PI^\lambda D^\mu$ are considered as unity, is shown in Fig. 7.4 and the expression is given as

$$K_c(t) = K_p\{x_r(t) - r(t)\} + K_d\left[V_{sp}\left\{\frac{d}{dt}x_r(t)\right\} - \frac{d}{dt}r(t)\right] + K_i\int(x_r(t) - r(t))dt \tag{7.42}$$

where K_p, K_i, K_d are proportional, integral and derivative constants respectively. V_{sp} is the velocity setpoint and it is considered between 0 and 1. When λ and μ are considered as non-integer orders, it is said to be an FPID controller. In comparison to a typical PID controller, FPID has two additional parameters: integral order (λ) and derivative order (μ), both of which are fractions. This increases the system's flexibility and makes the implementation more effective than a standard PID controller. The block diagram of a combination of balancing control and swing-up control with PID and $PI^\lambda D^\mu$ controller with Integral ANTI-WINDUP is shown in Fig. 7.4.
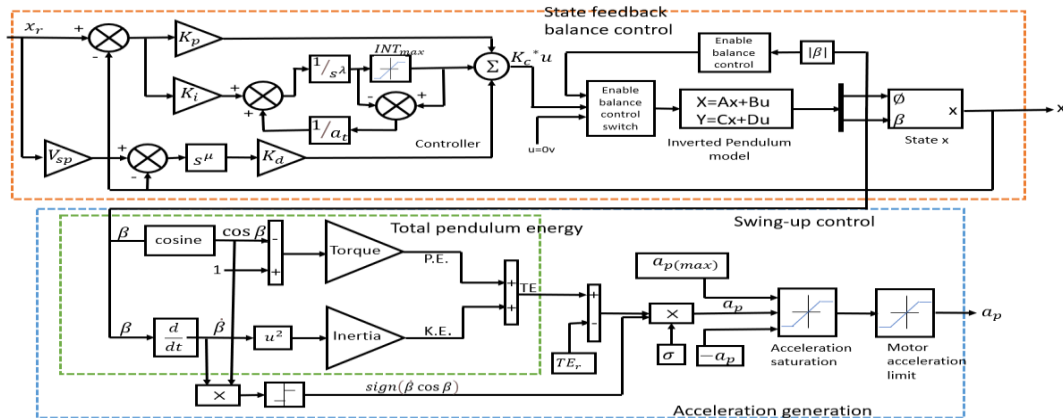
Figure 7.4. Combination of balancing control and swing-up control

The generalized equation of PI$^\lambda$D$^\mu$ controller, corresponding to Fig. 7.4 is

$$K_c(t) = K_p\{x_r(t) - r(t)\} + K_d D^{-\lambda}\left[V_{sp}\left\{\frac{d}{dt}x_r(t)\right\} - \frac{d}{dt}r(t)\right] + K_i D^\mu \int(x_r(t) - r(t))dt \quad (7.43)$$

where both λ and μ are as: $0 < \lambda < 1$ and $0 < \mu < 1$. D is the fractional operator and is defined as

$$D^{-n}f(t) = \frac{1}{\Gamma(n)}\int_0^t f(x)(t-x)^{n-1}dx \quad (7.44)$$

where, n is non-integer order and Γ is the gamma function.

The PI$^\lambda$D$^\mu$ controller is the generalization of the PID controller. The active region of PI$^\lambda$D$^\mu$ and PID controllers are shown in Fig. 7.5.
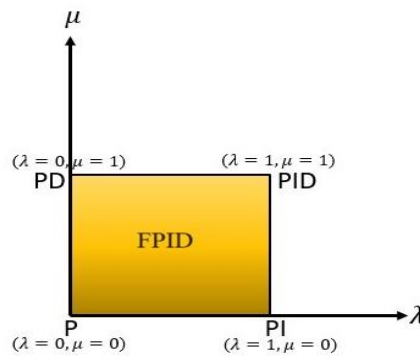
Figure 7.5. Point-to-point representation of active regions of PID and Fractional order PID controllers

This design incorporates an additional loop around the Integrator, in contrast to the conventional PID controller. By lowering the integrator input, this extra loop inhibits the integrator from reaching saturation and intensifying excessively. At parameter INT$_{max}$, the Integrator is intended to reach saturation. The integral control action is defined as

$$m_i = \begin{cases} -\text{INTG}_{max} & n_i < -\text{INTG}_{max} \\ n_i & n_i < -\text{INTG}_{max} < 0 \text{ and } -\text{INTG}_{max} - n_i < 0 \\ \text{INTG}_{max} & \text{INTG}_{max} < n_i \end{cases} \quad (7.45)$$

where INTG$_{max}$ is the upper limit of integrator, a_t is the time constant of the anti-windup loop which gets activated only in the case of Integrator saturation. The reset time of Integrator depends on a_t. The Integrator is in normal control action when $m_i = n_i$. But the anti-windup controller makes the saturation error zero in case of Integration saturation and then Integrator output becomes saturation limits, i.e. INTG$_{max}$ and $-$INTG$_{max}$.

7.8 METAHEURISTIC OPTIMIZATION TECHNIQUES

The performances of both PID and PI$^\lambda$D$^\mu$ controllers are optimized by adaptive heuristic optimization methods. Generally, the control parameters are selected using a trial and error approach which takes a significant amount of time and effort for tuning the parameters. The controller type may have an impact on the stability of the system. Therefore, it is essential to finely tune the controller settings.

Therefore, evolutionary search algorithms like GA and PSO are used to attain the desired performance with the fastest steady-state regime and less percentage overshoot by tuning the parameters of Fractional Order $PI^\lambda D^\mu$ controller. The performance of evolutionary search algorithms is ideal for determining a global optimal solution for a non-linear, underactuated and unstable process with various local optimal solutions. Genetic algorithm and Particle Swarm Optimization techniques are used for the optimization of both controllers' parameters. Integral time Absolute error (ITAE) is used for generating the cost functions and it is defined as

$$ITAE = \int_0^t t|e(t)| \, dt \tag{7.46}$$

The values of the set parameters of GA and PSO are shown in Table 7.2. The flow charts of the genetic algorithm and particle swarm optimization methods are shown in Fig. 7.6 respectively. The convergence rates of the objective function in GA and PSO techniques are shown in Fig. 7.7 respectively. The mean computational time was 207.83 sec for GA and 175.23 sec for PSO.
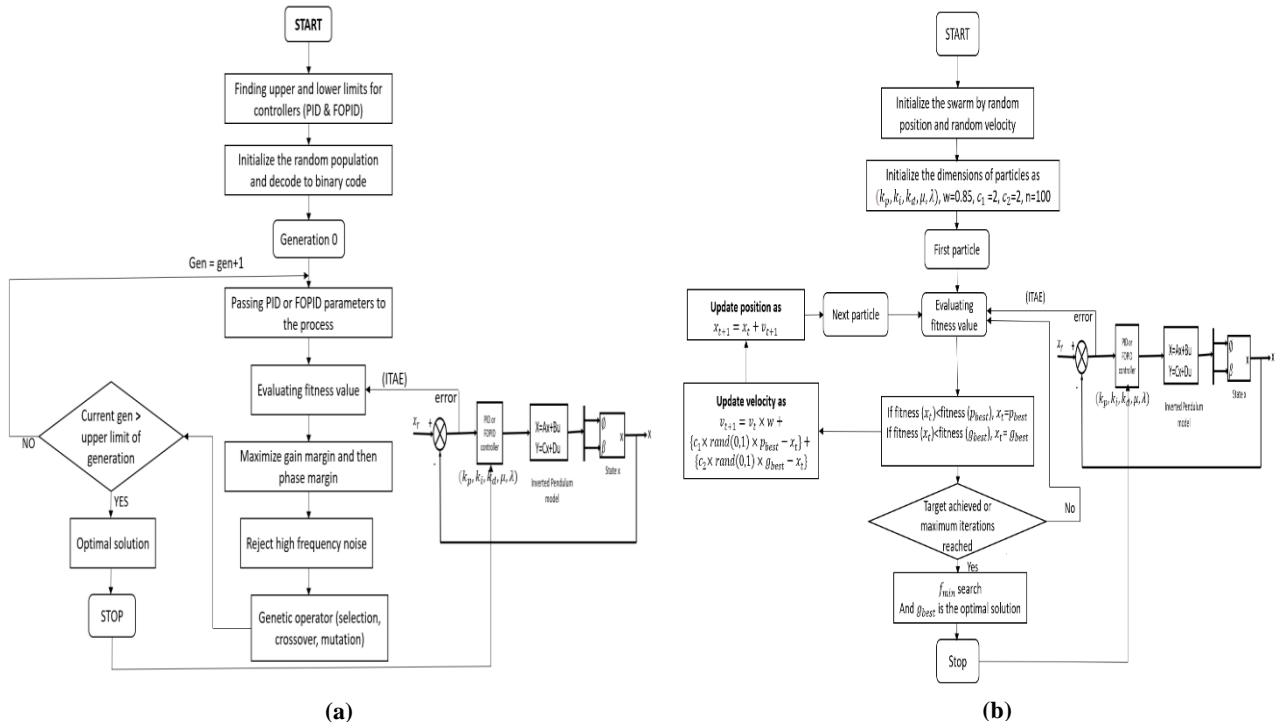
Figure 7.6. Flow chart of the proposed **(a)** Genetic Algorithm and **(b)** Particle Swarm Optimization

Table 7.2. Parameters of Genetic Algorithm and Particle Swarm Optimization

S. No.	Parameters of GA		Parameters of PSO	
	PARAMETERS	VALUES	PARAMETERS	VALUES
1.	Number of generations	100	Number of iterations	100
2.	Population size	20	Number of participles	50
3.	Length of chromosomes	35	Inertia	0.85
4.	Probability of crossover	0.85	Cognitive component (c_1)	2
5.	Probability of mutation	0.3	Social component (c_2)	2

117
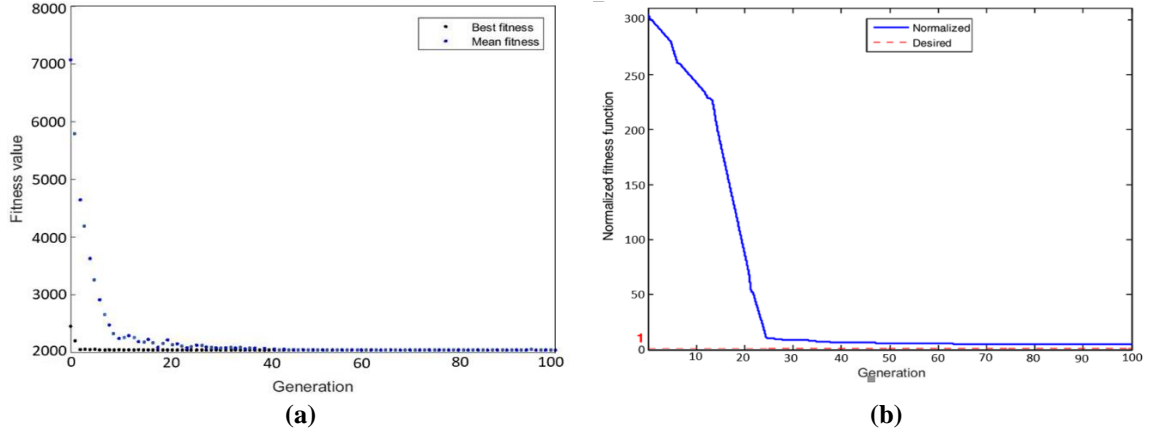
Figure 7.7. Convergence rates of the objective function of **(a)** GA **(b)** PSO algorithm

7.9 RESULTS AND DISCUSSIONS

The Fractional Order $PI^\lambda D^\mu$ controller is designed using MATLAB/Simulink. After simulation, the designed control law is applied to a physical (real-time) Quanser experimental setup of the RotIP system as depicted in Fig. 7.8. The components of this system are shown in Table 7.3. QUARC version 2.3.355 software serves as an interface between MATLAB and hardware for real-time implementation. RotIP is the primary component of this experimental setup. The angular motion of the pendulum is controlled by a Rotary Servo Base unit i.e. Quanser SRV02 for tracking [234]. A voltage amplifier VoltPAQ-X2 is used to amplify the voltage and then send it to the servo system to generate the requisite torque. The Q8 USB DAQ data acquisition device gathers the data from the optical rotary encoders and serves as an interface between the hardware and software.
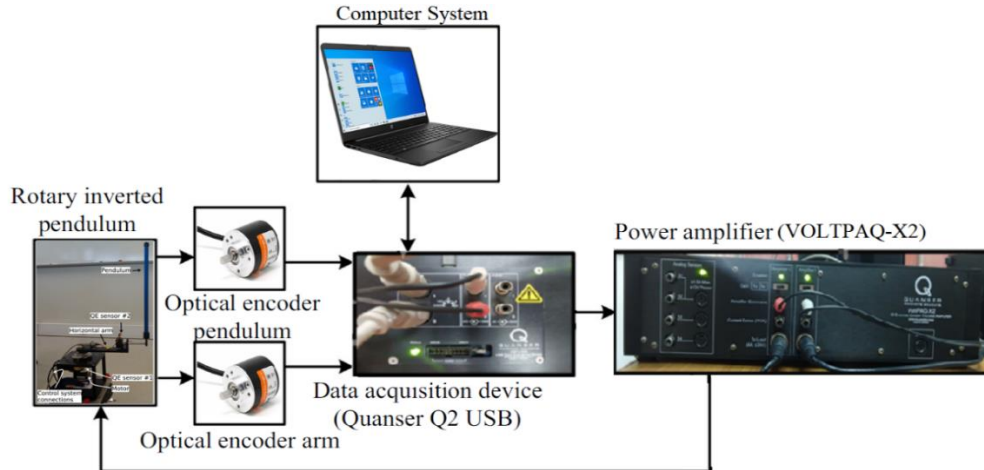
Figure 7.8. Experimental platform viewing connection diagram of RotIP model

During the implementation of swing-up and self-erecting or balancing control, the following parametric values are considered. Reference energy, $TE_r = 0.42$; maximum controlled acceleration, $a_{p(max)} = 8v$ and gain, $\sigma = 2.3$. For Integral anti-windup control, $\text{INTG}_{max} = 2.5\ deg$ and Integral anti-windup time, $a_t = 0.001s$. The simulation of PID controller for transient and steady-state

response with adaptive heuristic algorithms is carried out in MATLAB. For the implementation of FPID controller in MATLAB, the FOMCON (Fractional-Order Modelling and Control) toolbox is required that facilitate the research of fractional-order systems, their modelling and control design. The basic functionality of the FOMCON toolbox is the identification of fractional-order system and designing of Fractional Order $PI^\lambda D^\mu$ controller. With the inclusion of Simulink blocks, this toolbox aims at a more sophisticated modelling and control approach. The work is divided into three steps i.e. Analysis of the fractional order system; identification of the system in both time and frequency domain; Fractional Order $PI^\lambda D^\mu$ design, tuning and its optimization.

Table 7.3. Hardware equipment of RotIP along with the system specifications

Equipment	System Specifications
Power amplifier	VoltPAQ-X2
Data acquisition device	Q8 USB DAQ control board
Rotary Servo Base unit	Quanser SRV02
Optical encoders	Two Autonics optical rotary encoders
CPU	Intel Core i7 4Ghz
RAM	32 GB
MATLAB Version	MATLAB R2022a

7.9.1 Comparison of Simulation and Real-Time Results of PID and Optimization Algorithms

Swing-up and balancing responses of the inverted pendulum in simulation and real-time with PID controller and optimization using GA and PSO are displayed in Fig. 7.9(a-c). Figure 7.9 showcases the responses of rotary arm angle ($\emptyset$), pendulum angle (β) and controlled input voltage responses in simulation and real-time operation respectively. PID parameters and tuned PID parameters in the case of adaptive heuristic algorithms are shown in Table 7.4. Transient and steady-state responses in the case of simulation and real-time experimentation for PID, GA and PSO are shown in Table 7.5. For both simulation and real-time operation, GA & PSO provide better-optimized responses as compared to PID response but PSO reduced the peak overshoot very significantly as compared to PID and GA. In the case of settling time, both GA & PSO give somewhat similar results as evident from Table 7.5.

Table 7.4. PID parameters and tuned PID parameters in case of adaptive heuristic algorithms

OPERATION → PARAMETERS ↓	PID	GA	PSO
P	1.605	0.0377	-0.0281
I	1.415	0.9276	0.927
D	-0.2206	-0.123	-2.078
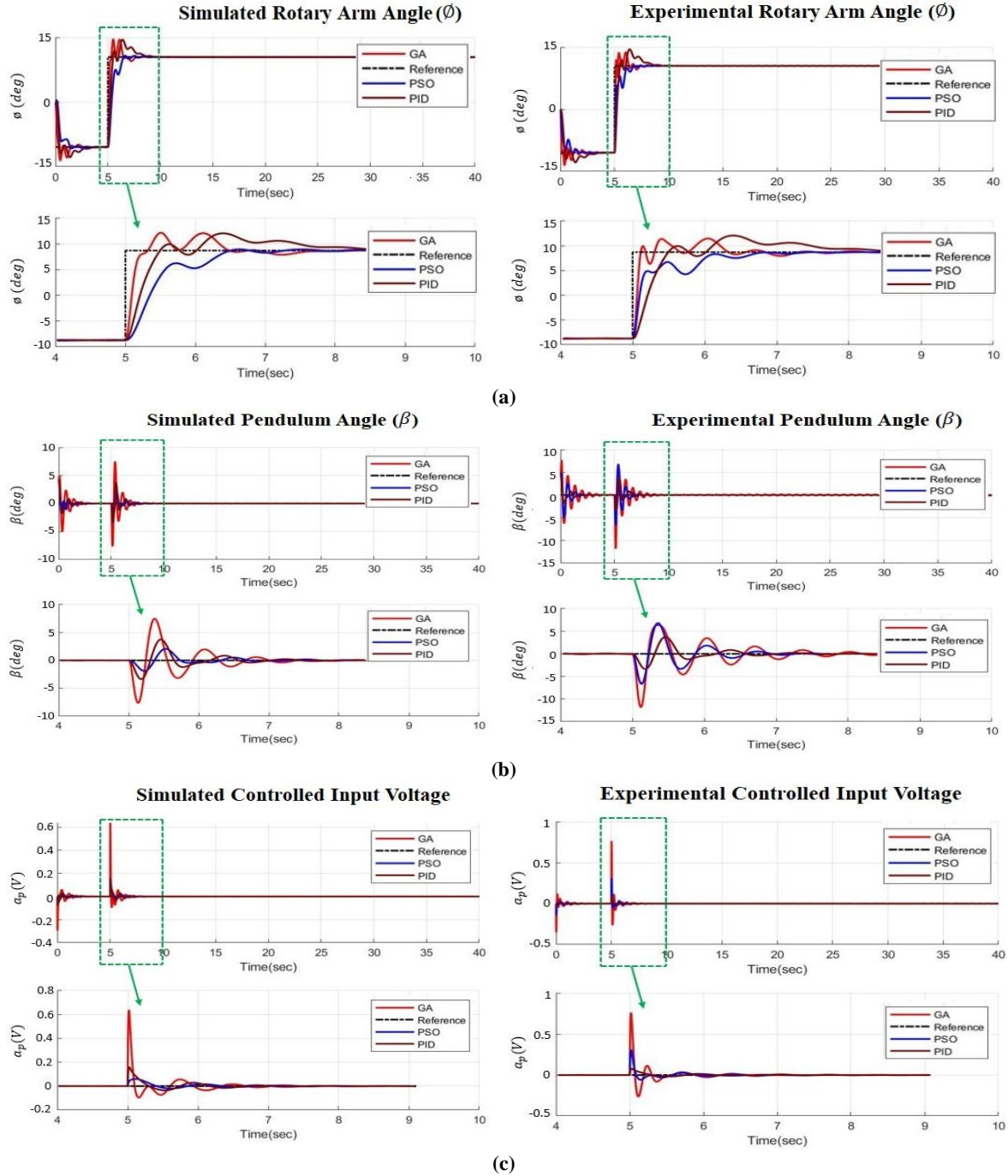
Figure 7.9. PID, GA and PSO responses of inverted pendulum in simulation and in real-time for **(a)** rotary arm angle (∅), **(b)** pendulum angle (β) and **(c)** controlled input voltage (a_p).

Table 7.5. Transient and steady state response in case of simulation and real-time for PID, GA and PSO

	SIMULATED RESULTS				EXPERIMENTAL RESULTS				
PARAMETERS → / OPERATION ↓	RISE TIME (s)	OVERSHOOT	SETTLING TIME (s)	ITAE	PARAMETERS → / OPERATION ↓	RISE TIME (s)	OVERSHOOT	SETTLING TIME (s)	ITAE
PID	5.4367	38.55	8.91	0.34907	PID	5.6408	36.64	9.17	0.34384
GA	5.2443	37.678	8.94	0.34936	GA	5.154	31.72	9.58	0.3905
PSO	6.437	3.422	8.59	0.34668	PSO	6.867	0.1262	8.77	0.34913

120

7.9.2 Comparison of Simulation and Real-Time Results of FPID and Optimization Algorithms

Swing-up and balancing responses of the inverted pendulum in simulation and real-time with FPID controller and optimization using GA and PSO are shown in Fig. 7.10(a-c). Figure 7.10 shows the responses of rotary arm angle ($\emptyset$), pendulum angle (β) and controlled input voltage responses in simulation and real-time operation respectively. FPID parameters and tuned FPID parameters in the case of adaptive heuristic algorithms are shown in Table 7.6. Transient and steady-state responses in the case of simulation and real-time operation for FPID, GA and PSO are shown in Table 7.7. For both simulation and real-time experimentation results, GA & PSO reduced the peak overshoot and settling time very significantly as compared to the FPID controller. Between optimization algorithms, PSO provides overall better-optimized results as evident from results in Table 7.7.
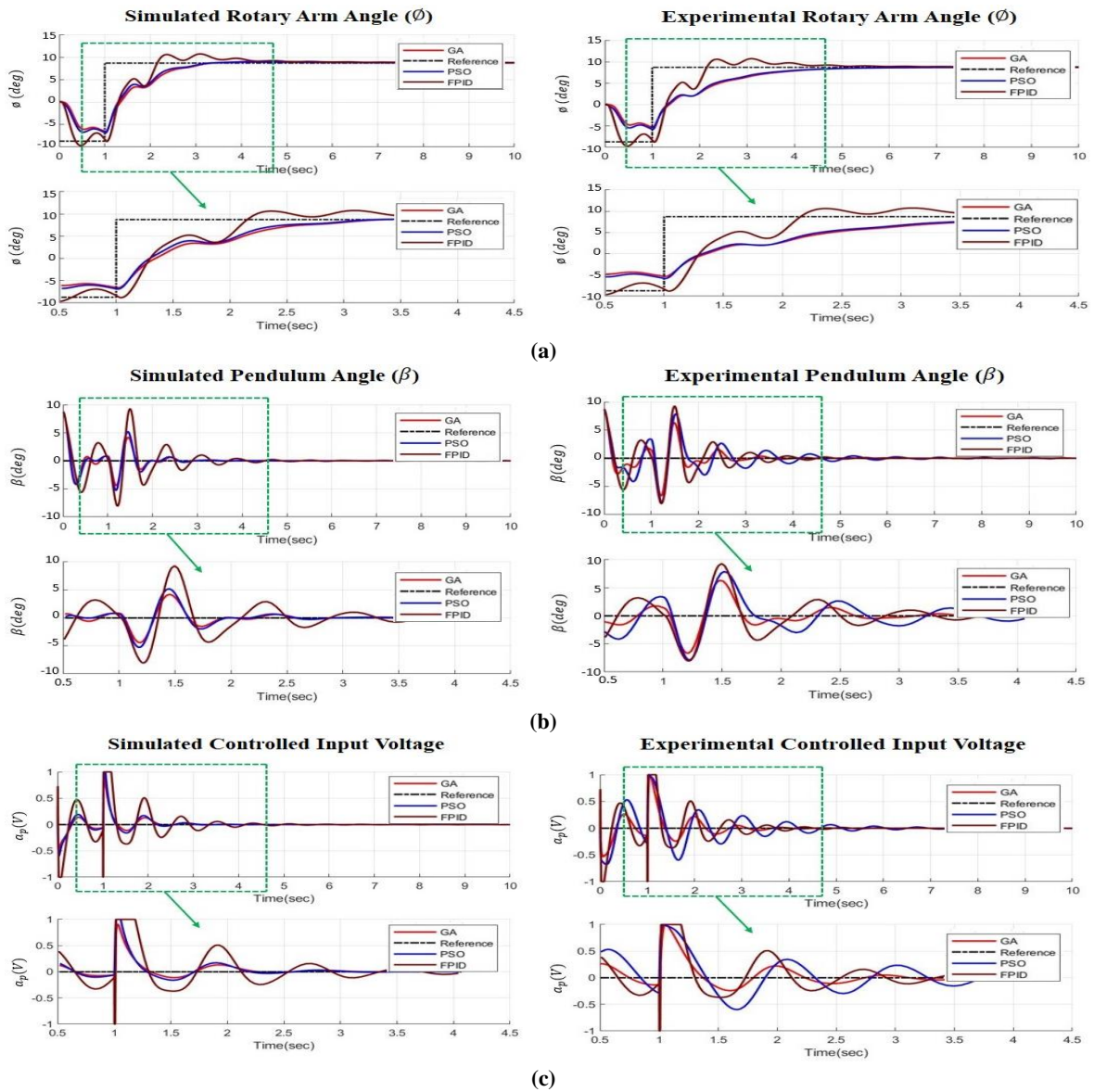
Figure 7.10. FPID, GA and PSO responses of inverted pendulum in simulation and real-time for **(a)** rotary arm angle ($\emptyset$), **(b)** pendulum angle (β) and **(c)** controlled input voltage.

Table 7.6. FPID parameters and tuned FPID parameters in case of adaptive heuristic algorithms

OPERATION → / PARAMETERS ↓	FPID	GA	PSO
P	1.605	1.1039	1.2453
I	1.415	9.9873	0.0133
D	-0.2206	0.06673	0.26872
λ	0.52	0.10938	0.0027
μ	0.45	0.1937	0.0515

Table 7.7. Transient and steady-state response in case of simulation and real-time for FPID, GA and PSO

SIMULATED RESULTS					EXPERIMENTAL RESULTS				
PARAMETERS → / OPERATION ↓	RISE TIME (s)	OVERSHOOT	SETTLING TIME (s)	ITAE	PARAMETERS → / OPERATION ↓	RISE TIME (s)	OVERSHOOT	SETTLING TIME (s)	ITAE
FPID	2.15	21.88	7.13	0.355	FPID	2.23	24.88	7.68	0.35354
GA	3.21	3.41	4.56	0.332	GA	5.81	0.17112	5.11	0.35051
PSO	3.245	2.345	5.04	0.347	PSO	5.947	0.012	4.95	0.34924

7.10 SIGNIFICANT FEATURES & ADVANTAGES OF FRACTIONAL ORDER PID CONTROLLER

The significant features and advantages of the proposed Fractional Order $PI^\lambda D^\mu$ Controller in comparison with the other control methods in the literature are as follows:

- Providing a novel Fractional Order $PI^\lambda D^\mu$ Controller to improve the trajectory tracking, decrease control effort and chattering level in the presence of uncertainties by two additional parameters in fractional operators i.e. integral order (λ) and derivative order (μ) which successfully attains the Fundamental characteristics of a classical PID controller in addition to a careful design process for parameter selection.

- Fractional Order $PI^\lambda D^\mu$ controller permits the modelling of complex and non-linear relations between the input and outcome variables. In addition, the proposed robust controller has the ability to learn from the data by adapting the corresponding parameters.

- The parameters of the FPID controller are tuned by evolutionary and swarm-based optimization techniques along with their comparative study to achieve an optimal and desired performance with the fastest steady-state regime and less percentage overshoot.

- The fine-tuning of the controller's parameters using GA and PSO improves the overall performance and generalization capacity of the entire model. These algorithms work with a fitness function for modifying and analyzing a set of potential solutions for evaluating the effectiveness of the model.

- The controller type may have an impact on the stability of the system. Therefore, the ITAE cost function is designed to select the optimum parameters of the controller to minimize swing-up time and achieve high stabilization performance.

- Most of the studies on PID and FPID controllers in the literature are primarily supported by simulation results only. On the other hand, real-time experimental results also validate the effective performance of the proposed technique, while guaranteeing both reference tracking and rejection of external disturbances in comparison to the existing literature.

- This study uses the QUARC target libraries in MATLAB to provide a hardware-in-loop structure to enable a real-time controller interface. As a result, it is possible to implement these PID and Fractional Order $PI^\lambda D^\mu$ controllers in real-time on a highly unstable RotIP system, achieving good performance even in the presence of external perturbations.

- Real-time experimental results and MATLAB simulation both demonstrate the effectiveness of the claims presented and their excellence. A detailed comparative analysis was conducted for each case taking into account alternative controllers and control methodologies found in existing literature.

- The proposed controller can stabilize the pendulum under external perturbations by observing the system response to change parameters, multiplicative gain variations, and externally induced perturbations.

7.11 SUMMARY

In this chapter, a PID and Fractional Order $PI^\lambda D^\mu$ Controller with Integral ANTI-WINDUP technique has been proposed for the robust stabilization and control of the rotary inverted pendulum system by using metaheuristic optimization techniques. Genetic Algorithm and Particle Swarm Optimization techniques are used for tuning the parameters of controllers on the basis of Integral Time Absolute Error (ITAE). The pendulum angle, rotary arm angle and controlled input voltage comparisons are executed with the developed control schemes for both simulation and real-time experimentation purposes. The responses and parametric data of State feedback Balance control, PID and FPID controllers implied that when rotary arm angle ($\emptyset$) is tracking a $\pm 20^\circ$ angle square wave in case of State feedback Balance control and $\pm 8^\circ$ angle square wave in case of PID and FPID, maximum pendulum angle (β_{max}) and maximum controlled input voltage (a_{max}) for both Simulated and experimental responses are within the specified limits of $|\beta| < 20$ (deg) and maximum control effort ($a_{max}) = 10v$. Simulation and real-time experimentation results shows that GA & PSO tuned PID provides better optimized responses as compared to PID response but PSO tuned PID reduced the peak overshoot very significantly as compared to PID and GA tuned PID. In the case of settling time,

both GA & PSO tuned controllers give somewhat similar results. GA & PSO tuned FPID reduced the peak overshoot and settling time very significantly as compared to FPID. Between optimization algorithms, PSO-tuned FPID provides overall better-optimized results. PSO provides much better optimized results for both PID and $PI^{\lambda}D^{\mu}$ controllers as compared to the results provided by GA.

Chapter 8

Conclusions, Future Scope and Social Impact

In this thesis, various techniques have been formulated for improving the performance of automated and non-linear control systems. PLC and SCADA-based techniques along with sensors have been used to balance and control assembly lines in process industries. Also, a PLC and SCADA-based framework is used to automate and supervise the temperature control processes in the heat exchanger plant through a Fractional Order PID Controller using metaheuristic optimization techniques. Various controllers like PID with integral ANTI-WINDUP controller and neural-fuzzy PID controllers have been implemented for the balancing and position tracking control of the 2-DOF ball balancer. Additionally, continuous Linear Quadratic Gaussian controller and Fractional Order PID ($PI^{\lambda}D^{\mu}$) controller is implemented for the optimal and robust control of a rotary inverted pendulum. All these methods have been objectively/quantitatively evaluated and compared with respective state-of-the-art methods to show that the proposed techniques have desirable output performances. We discuss the summary of the work done in the thesis through Section 8.1. It is followed by future scope/directions and the social impact of the work done in Section 8.2 and Section 8.3.

8.1 SUMMARY OF THE WORK DONE IN THE THESIS

To automate the process industry plant, a dynamic real-world problem was addressed for the mixing, filling, capping, labelling and sorting process (using inductive and capacitive proximity sensors) in the assembly line division with an effluent ratio control strategy. The OMRON (NX1P2-9024DT1) PLC was interfaced with the Wonderware InTouch SCADA system to gather data, create a simulated prototype of the assembly line and ratio control divisions, carry out the necessary control operations,

125

and display this data on the HMI screen within the process industry plant. A mathematical and simulation model of a single assembly line was proposed to minimize the assembly line timings, the workforce and the overall cost of production. The developed model was applied in a real-life case study of an assembly line to investigate the efficacy of the proposed method. The results of the real-world case study verified the design for effectively balancing a real-world assembly line and showed that the proposed design improves the overall productivity and throughput of the process industry plant with an improved assembly line design with proper fixtures/modifications in existing design for eliminating the idle time between the batch processes.

A novel cascade control strategy was developed to control and regulate the outlet temperature of a heat exchanger system using PID and Fractional Order PID ($PI^\lambda D^\mu$) controller along with integral anti-windup technique, feedforward control and Smith predictor for the time-delayed process. GA, PSO and ACO techniques were used to optimize the parameters of both PID and FPID controllers. Simulation and real-time experimentation analysis of the developed controllers were executed with metaheuristic optimization techniques based on different performance indices like ISE, IAE and ITAE. Also, a PLC and SCADA-based control framework was proposed to automate and supervise the temperature control processes in the heat exchanger plant. PLC carries out the necessary control operations within the heat exchanger plant as directed by the SCADA server. The proposed technique enhanced the heat transmission efficiency, irrespective of the external disturbances, non-linearity and delay characteristics while guaranteeing both transient and steady-state response of the controller in comparison to the existing literature.

Different compensators like PD, PID, PID with Integral ANTI-WINDUP with different velocity setpoint values and neural-fuzzy PID controllers were implemented over the 2-DOF Ball balancer system to resolve the position tracking and balance control problem. The ball balancer system's model was developed in MATLAB Simulink and the QUARC system was used for interfacing. Both transient and steady-state response analysis were executed to evaluate the performance of these compensators in the presence of high-frequency disturbances. The Ball position, input voltage and plate angle comparisons were executed with different compensators for both simulation and real-time experimentation purpose. Position and plate angle control with load variation was also executed in real time with the NiF-PID compensator. NiF-PID controller provided overall better control performances and best adaptability because of its tendency to minimize the steady-state error between the reference and generated output. NiF-PID compensator provides 18.55% better result in case of steady-state error and 10 times less overshoot in case of real-time experimentation as compared to the PID controller. NiF-PID controller provides reduced and improved settling time, peak overshoot and steady-state error as compared to the PD and PID controllers.

Lastly, a continuous Linear Quadratic Gaussian controller based on the optimal control strategy was proposed for swinging up the rotary inverted pendulum and maintaining an equilibrium in the

vertical upward position. Along with that, PID and Fractional Order PID controllers with integral ANTI-WINDUP technique were introduced for the robust swing-up and stabilization control of the rotary inverted pendulum using metaheuristic optimization techniques. The parameters P, I, λ, D and μ of the $PI^\lambda D^\mu$ controller was tuned by GA and PSO techniques based on ITAE. The pendulum angle, rotary arm angle and controlled input voltage comparisons were executed with the developed control schemes for both simulation and real-time experimentation purposes The analysis of the transient response and steady-state response of both simulation and real-time experimentation implied that the FPID compensator provides overall better control performance as compared to conventional PID controller. PSO provided much better optimized results for both PID and $PI^\lambda D^\mu$ controllers as compared to the results provided by GA.

8.2 CONTRIBUTIONS

Automated and non-linear control systems are used to improve the performance of many control benchmark problems. The work in the thesis helps in the realization of problems in process industries, temperature control of a heat exchanger, and underactuated mechanical systems like inverted pendulum and ball balancer systems. Following are the contributions of the thesis:

- Development of a smart PLC and SCADA-based control framework for an automated assembly line in the process industry with an effluent ratio control strategy.
- PLC and SCADA-based temperature control of heat exchanger system through Fractional Order PID controller using metaheuristic optimization techniques.
- Real-time balancing and position tracking control of 2-DOF ball balancer using PID with integral ANTI-WINDUP controller and Neural-Fuzzy PID controllers.
- Optimal control of rotary inverted pendulum using continuous Linear Quadratic Gaussian controller.
- Robust control of rotary inverted pendulum using metaheuristic optimization techniques based PID and Fractional Order $PI^\lambda D^\mu$ controller.

8.3 FUTURE SCOPE

The potential future scope of the research work done in the thesis is as follows:

1. Enhancing the PLC and SCADA-based system for advanced fault-tolerant control process in Industry 4.0

2. Improving the tracking efficiency of underactuated systems with multiple degrees of freedom.

3. Implementing more learning-based optimization algorithms, evolutionary methods and other metaheuristic approaches with the nonlinear control systems.

4. Implementation of more advanced hybrid control strategies such as type 2 NiF-PID, and wavelet NiF-PID along with optimization algorithms for the position tracking and balancing control of ball balancer systems.

8.4 SOCIAL IMPACT

In this thesis, effective control design methods have been developed for automated and non-linear control systems. The specific problems addressed in this thesis are related to the following systems:

(a) Automated Control Systems
- Assembly line balancing and ratio control in process industries
- Temperature control of a heat exchanger

(b) Non-linear Control Systems
- Underactuated mechanical systems like inverted pendulum and ball balancer system

The social impact of the contributions of the work done related to automated and non-linear control systems in this thesis are as follows:

1. The proposed PLC and SCADA-based control framework automate the process industry plant by monitoring all the processes using a single-screen HMI. The proposed assembly line architecture improves the productivity, efficiency, throughput, workforce, overall cost of production and time of a process industry plant. Effective product sequencing enhances short-term balancing and production time by reducing waiting time. The SCADA system achieves automatic control and management of industrial processes, improves worker safety, and reduces manpower and physical resources instead of a distributed control system. This SCADA system allows users and operators to get live video streaming from any of the sites on their HMI screens. This PLC and SCADA-based control framework will bring a digital transformation in Industry 4.0 by increasing equipment efficiency, process quality, interoperability, and overall productivity.

2. The proposed PLC and SCADA-based real-time control framework automates and supervises the temperature control processes in the heat exchanger plant. Heat exchangers are utilized in applications like cooling of water, oil heaters, petrochemical industries, boilers and condensers in power plants. The proposed GA, ACO and PSO optimized PID and Fractional Order PID controllers control the temperature of a heat exchanger system and resolve

difficulties like non-linearity, uncertainties, high-temperature fluctuations, large response and delay time of the controlled objects.

3. The nonlinear and underactuated behaviour of the ball balancer system significantly impacts the steady-state operation and position tracking. Therefore, the developed controllers are helpful in reducing tracking errors and tackling non-linear disturbances and uncertainties efficiently. The designed controllers for the 2-DOF ball balancer system control the ball's motion on a plate to direct it along a predetermined path and improve the dynamic nature of the ball's position and plate angle. These controllers can be used with the ball balancer systems for position tracking and balance control applications related to the movement of robotic manipulators, vehicle balancing and position control, trajectory tracking, vertical take-off aircraft, path planning, vertical thrust control in rockets, etc.

4. The proposed LQG and Fractional Order PID ($PI^{\lambda}D^{\mu}$) Controllers can be used to swing the rotary inverted pendulum upward from its stationary downward position and maintain an equilibrium in the upward vertical position. Rotary Inverted Pendulum is a suitable benchmark in non-linear dynamics for testing and validating different control and robotic systems in real-life applications such as Segways, hoverboards, aircraft landing, rocket launches, marine systems and crane applications, etc. where a pendulum has to be controlled against its natural equilibrium position. The proposed controllers keep the pendulum balanced while maintaining both reference tracking and rejecting external disturbances compared to the existing literature.

REFERENCES

[1] R. Bars, P. Colaneri, C.E. de Souza, L. Dugard, F. Allgöwer, A. Kleimenov and C. Scherer, "Theory, algorithms and technology in the design of control systems," *Annual Reviews in Control*, vol. 30, no. 1, pp. 19-30, 2006.

[2] R.M. Murray, "Future directions in control, dynamics, and systems: Overview, grand challenges, and new courses," *European Journal of Control*, vol. 9, no. 2-3, pp. 144-158, 2003.

[3] C. Brecher, A. Müller, Y. Dassen and S. Storms, "Automation technology as a key component of the Industry 4.0 production development path," *The International Journal of Advanced Manufacturing Technology*, vol. 117, pp. 2287-2295, 2021.

[4] T. Pardi, "Fourth industrial revolution concepts in the automotive sector: performativity, work and employment," *Journal of Industrial and Business Economics*, vol. 46, no. 3, pp. 379-389, 2019.

[5] McKinsey & Company, "Transforming advanced manufacturing through Industry 4.0." Accessed: June 27, 2022. [Online]. Available: https://www.mckinsey.com/capabilities/operations/our-insights/transforming-advanced-manufacturing-through-industry-4-0.

[6] A. Christler, E. Felföldi, M. Mosor, D. Sauer, N. Walch, A. Dürauer and A. Jungbauer, "Semi-automation of process analytics reduces operator effect," *Bioprocess and biosystems engineering*, vol. 43, pp. 753-764, 2020.

[7] A. Jena and S.K. Patel, "Analysis and evaluation of Indian industrial system requirements and barriers affect during implementation of Industry 4.0 technologies," *The International Journal of Advanced Manufacturing Technology*, vol. 120, no. 3, pp. 2109-2133, 2022.

[8] S. Phuyal, D. Bista and R. Bista, "Challenges, opportunities and future directions of smart manufacturing: a state of art review," *Sustainable Futures*, vol. 2, p. 100023, 2020.

[9] M. Dulău, M. Karoly and T.M. Dulău, "Fluid temperature control using heat exchanger," *Procedia Manufacturing*, vol. 22, pp. 498-505, 2018.

[10] P. Laszczyk, "Simplified modeling of liquid-liquid heat exchangers for use in control systems," *Applied Thermal Engineering*, vol. 119, pp. 140-155, 2017.

[11] A. Dolgui, F. Sgarbossa and M. Simonetto, "Design and management of assembly systems 4.0: systematic literature review and research agenda," *International Journal of Production Research*, vol. 60, no. 1, pp. 184-210, 2022.

[12] B. Wang, J.J. Klemeš, N. Li, M. Zeng, P.S. Varbanov and Y. Liang, "Heat exchanger network retrofit with heat exchanger and material type selection: A review and a novel method," *Renewable and Sustainable Energy Reviews*, vol. 138, p. 110479, 2021.

[13] J.J. Klemeš and Z. Kravanja, "Forty years of heat integration: pinch analysis (PA) and mathematical programming (MP)," *Current Opinion in Chemical Engineering*, vol. 2, no. 4, pp. 461-474, 2013.

[14] I. Kaur and P. Singh, "State-of-the-art in heat exchanger additive manufacturing," *International Journal of Heat and Mass Transfer*, vol. 178, p. 121600, 2021.

[15] A. Safaei, A.H. Nezhad and A. Rashidi, "High temperature nanofluids based on therminol 66 for improving the heat exchangers power in gas refineries," *Applied Thermal Engineering*, vol. 170, p. 114991, 2020.

[16] L.G. Tugashova and A.V. Zatonskiy, "Comparison of Methods for Heat Exchanger Control," *Theoretical Foundations of Chemical Engineering*, vol. 55, no. 1, pp. 53-61, 2021.

[17] A. Kheddar, S. Caron, P. Gergondet, A. Comport, A. Tanguy, C. Ott, B. Henze, G. Mesesan, J. Englsberger, M.A. Roa and P.B. Wieber, "Humanoid robots in aircraft manufacturing: The airbus use cases," *IEEE Robotics & Automation Magazine*, vol. 26, no. 4, pp. 30-45, 2019.

[18] Y. Wang, Q. Zhu, R. Xiong, and J. Chu "Standing balance control for position control-based humanoid robot," *IFAC Proceedings Volumes*, vol. 46, no. 20, pp. 429-436, 2013.

[19] B.K. Patle, A. Pandey, D.R.K. Parhi and A.J.D.T. Jagadeesh, "A review: On path planning strategies for navigation of mobile robot," *Defence Technology*, vol. 15, no. 4, pp. 582-606, 2019.

[20] B. Zhang, Q. Zong, L. Dou, B. Tian, D. Wang, X. and Zhao, "Trajectory optimization and finite-time control for unmanned helicopters formation," *IEEE Access*, vol. 7, pp. 93023-93034, 2019.

[21] J. Zhao, X. Ding, B. Jiang, G. Jiang F. and Xie, "A novel control strategy for quadrotors with variable mass and external disturbance," *International Journal of Robust and Nonlinear Control*, vol. 31, no. 17, pp. 8605-8631, 2021.

[22] C. Liu, B. Jiang, K. Zhang and S.X. Ding, "Hierarchical structure-based fault-tolerant tracking control of multiple 3-DOF laboratory helicopters," *IEEE Transactions on Systems, Man, and Cybernetics: Systems*, vol. 52, no. 7, pp. 4247-4258, 2021.

[23] O. Boubaker, "The inverted pendulum: A fundamental benchmark in control theory and robotics," In *International Conference on Education, e-Learning and Innovations,* pp. 1-6, 2012.

[24] G. Rigatos, P. Siano, M. Abbaszadeh, S. Ademi and A. Melkikh, "Nonlinear H-infinity control for underactuated systems: the Furuta pendulum example," *International Journal of Dynamics and Control*, vol. 6, pp. 835-847, 2018.

[25] U.N.L.T. Alves, R. Breganon, L.E. Pivovar, J.P.L.S. de Almeida, G.V. Barbara, M. Mendonça, and R.H.C. Palácios, "Discrete-time H∞ integral control via LMIs applied to a Furuta pendulum," *Journal of Control, Automation and Electrical Systems*, vol. 33, no. 3, pp. 1-12, 2022.

[26] I.M. Mehedi, U.M. Al-Saggaf, R. Mansouri and M. Bettayeb, "Two degrees of freedom fractional controller design: Application to the ball and beam system," *Measurement*, vol. 135, pp. 13-22, 2019.

[27] L. Yan, B. Ma and W. Xie, "Robust practical tracking control of an underactuated hovercraft," *Asian Journal of Control*, vol. 23, no. 5, pp. 2201-2213, 2021.

[28] Ali, H.I., Jassim, H.M. and A.F. Hasan, "Optimal nonlinear model reference controller design for ball and plate system," *Arabian Journal for science and Engineering*, vol. 44, no. 8, pp. 6757-6768, 2019.

[29] G. Rigatos, G. Cuccurullo, K. Busawon, Z. Gao and M. Abbaszadeh, "Nonlinear optimal control of the ball and plate dynamical system," In *AIP Conference Proceedings*, vol. 2425, no. 1, AIP Publishing, 2022.

[30] W.M. Chow, "Assembly line design: methodology and applications," *CRC Press,* 2020.

[31] Y.L. Jiao, H.Q. Jin, X.C. Xing, M.J. Li and X.R. Liu, "Assembly line balance research methods, literature and development review," *Concurrent Engineering*, vol. 29, no. 2, pp. 183-194, 2021.

[32] J. Huo, J. Zhang and F.T. Chan, "A fuzzy control system for assembly line balancing with a three-state degradation process in the era of Industry 4.0," *International Journal of Production Research*, vol. 58, no. 23, pp. 7112-7129, 2020.

[33] M. Geurtsen, I. Adan and Z. Atan, "Deep reinforcement learning for optimal planning of assembly line maintenance," *Journal of Manufacturing Systems*, vol. 69, pp. 170-188, 2023.

[34] J.B. Didden, E. Lefeber, I.J. Adan and I.W.F. Panhuijzen, "Genetic algorithm and decision support for assembly line balancing in the automotive industry," *International Journal of Production Research*, vol. 61, no. 10, pp. 3377-3395, 2023.

[35] M. Ghita, I. Birs, D. Copot, I. Nascu and C.M. Ionescu, "Impedance spectroscopy sensing material properties for self-tuning ratio control in pharmaceutical industry," *Applied Sciences*, vol. 12, no. 1, p. 509, 2022.

[36] M. Sreejeth and S. Chouhan, "PLC based automated liquid mixing and bottle filling system," In *2016 IEEE 1st International Conference on Power Electronics, Intelligent Control and Energy Systems (ICPEICES)*, pp. 1-5, 2016.

[37] B. Rahmani, "Internet-based control of industrial automation systems," *Journal of Intelligent & Robotic Systems*, vol. 83, pp. 71-83, 2016.

[38] D.P. Zegzhda, M.O. Kalinin and M.V. Levykin, "Actual vulnerabilities of industrial automation protocols of an open platform communications series," *Automatic Control and Computer Sciences*, vol. 53, pp. 972-979, 2019.

[39] N.I. Aristova, "Ethernet in industrial automation: Overcoming obstacles," *Automation and Remote Control*, vol. 77, no. 5, pp. 881-894, 2016.

[40] A. Afram and F. Janabi-Sharifi, F., "Theory and applications of HVAC control systems–A review of model predictive control (MPC)," *Building and Environment*, vol. 72, pp. 343-355, 2014.

[41] P. Laszczyk, "Simplified modeling of liquid-liquid heat exchangers for use in control systems," *Applied Thermal Engineering*, vol. 119, pp. 140-155, 2017.

[42] M. Dulău, M. Karoly and T.M. Dulău, "Fluid temperature control using heat exchanger," *Procedia Manufacturing*, vol. 22, pp. 498-505, 2018.

[43] T.K. Palaniyappan, V. Yadav, V.K. Tayal and P. Choudekar, "PID control design for a temperature control system," In *2018 International Conference on Power Energy, Environment and Intelligent Control (PEEIC),* pp. 632-637, 2018.

[44] N. Cervantes-Escorcia, OJ. Santos-Sánchez, L. Rodríguez-Guerrero, H. Romero-Trejo and A. González-Facundo, "Optimal PI and PID temperature controls for a dehydration process," *Arabian Journal of Science and Engineering,* vol. 44, pp. 2519–2534, 2019.

[45] D. Pamela and M.S. Godwin Premi, "Wireless control and automation of hot air temperature in oven for sterilization using fuzzy PID controller and adaptive smith predictor," *Wireless Personal Communications*, vol. 94, pp. 2055-2064, 2017.

[46] H. Zou and H. Li, "Improved PI-PD control design using predictive functional optimization for temperature model of a fluidized catalytic cracking unit," *ISA Transactions*, vol. 67, pp. 215-221, 2017.

[47] A. Aldemir and H. Hapoğlu, "Comparison of PID tuning methods for wireless temperature control," *Journal of Polytechnic*, vol. 19, no. 1, pp. 9–19, 2016.

[48] A. Aldemir, "PID Controller Tuning Based on Phase Margin (PM) for Wireless Temperature Control," *Wireless Personal Communications*, vol. 103, pp. 2621–2632, 2018.

[49] J. Oravec, M. Bakošová, M. Trafczynski, A. Vasičkaninová, A. Mészáros and M. Markowski, "Robust model predictive control and PID control of shell-and-tube heat exchangers," *Energy*, vol. 159, pp.1-10, 2018.

[50] D. Tiwari, N. Pachauri, A. Rani and V. Singh, "Fractional order PID (FOPID) controller based temperature control of bioreactor," In *2016 International Conference on electrical, electronics, and optimization techniques (ICEEOT)*, pp. 2968-2973, 2016.

[51] Y.A.K. Utama and Y. Hari, "Design of PID disturbance observer for temperature control on room heating system," In *2017 4th International Conference on Electrical Engineering, Computer Science and Informatics (EECSI)*, pp. 1-6, 2017.

[52] M.D. Mohanty and M.N. Mohanty, "Design of fuzzy logic-based PID controller for heat exchanger used in chemical industry," In *New Paradigm in Decision Science and Management: Proceedings of ICDSM 2018*, pp. 371-379, Springer Singapore, 2020.

[53] A. Vasičkaninová and M. Bakošová, "Control of a heat exchanger using neural network predictive controller combined with auxiliary fuzzy controller," *Applied Thermal Engineering*, vol. 89, pp. 1046-1053, 2015.

[54] M. Al-Dhaifallah, "Fuzzy fractional-order PID control for heat exchanger," *Alexandria Engineering Journal*, vol. 63, pp. 11-16, 2023.

[55] K. Lu, L. Xu, Q. Fu, X. Yin and X. Yuan, "Composition-temperature cascade control of vapor recompression assisted dividing wall column with side heat exchanger," *Chemical Engineering Research and Design*, vol. 177, pp. 24-35, 2022.

[56] M. Bobič, B. Gjerek, I. Golobič and I. Bajsić, "Dynamic behaviour of a plate heat exchanger: Influence of temperature disturbances and flow configurations," *International Journal of Heat and Mass Transfer*, vol. 163, p. 120439, 2020.

[57] N.C. Damasceno, "PI controller optimization for a heat exchanger through metaheuristic bat algorithm, particle swarm optimization, flower pollination algorithm and cuckoo search algorithm," *IEEE Latin America Transactions*, vol. 15, no. 9, pp. 1801-1807, 2017.

[58] S. Xu, S. Shi, W. Jiang and S. Hashimoto, "Cooperative Control of Recurrent Neural Network for PID-based Single Phase Hotplate Temperature Control Systems," *IEEE Access*, vol. 11, pp. 105557-105569, 2023.

[59] M.M. Hussein, S. Alkhalaf, T.H. Mohamed, D.S. Osheba, M. Ahmed, A. Hemeida and A.M. Hassan, "Modern Temperature Control of Electric Furnace in Industrial Applications Based on Modified Optimization Technique," *Energies*, vol. 15, no. 22, p. 8474, 2022.

[60] Z. Zeng, W. Zhang, H. Yu, D. Cao and X. Li, "Dynamic thermal model and control performance analysis over frequency domain of temperature control unit," *Case Studies in Thermal Engineering*, vol. 45, p. 102975, 2023.

[61] S. Jenhani, H. Gritli, and G. Carbone, "LMI-based optimization for the position feedback control of underactuated robotic systems via an affine PD controller: Case of the pendubot," In *2022 International Conference on Data Analytics for Business and Industry (ICDABI)*, pp. 729-735, 2022.

[62] K. Rsetam, Z. Cao, L. Wang, M. Al-Rawi and Z. Man, "Practically robust fixed-time convergent sliding mode control for underactuated aerial flexible joint robots manipulators," *Drones*, vol. 6, no. 12, p. 428, 2022.

[63] Z. Chen, F. Gao, Q. Sun, Y. Tian, J. Liu and Y. Zhao, "Ball-on-plate motion planning for six-parallel-legged robots walking on irregular terrains using pure haptic information," *Mechanism and Machine Theory*, vol. 141, pp. 136-150, 2019.

[64] A. de Carvalho Junior, B.A. Angelico, J.F. Justo, A.M. de Oliveira and J.I. da Silva Filho, "Model reference control by recurrent neural network built with paraconsistent neurons for trajectory tracking of a rotary inverted pendulum," *Applied Soft Computing*, vol. 133, p. 109927, 2023.

[65] F. Wiebe, S. Kumar, L.J. Shala, S. Vyas, M. Javadi and F. Kirchner, "Open Source Dual-Purpose Acrobot and Pendubot Platform: Benchmarking Control Algorithms for Underactuated Robotics," *IEEE Robotics & Automation Magazine,* 2023.

[66] C. Pan, C. Cui, L. Zhou, P. Xiong and Z. Li, "A model-free output feedback control approach for the stabilization of underactuated TORA system with input saturation," In *Actuators*, vol. 11, no. 3, p. 97, 2022.

[67] H. Zhao, W. Liu, X. Chen and H. Sun, "Adaptive robust constraint-following control for underactuated unmanned bicycle robot with uncertainties," *ISA transactions*, vol. 143, pp. 144-155, 2023.

[68] F. ur Rehman and A. Mahmood, "Adaptive sliding mode-based full-state stabilization control of an underactuated hovercraft," *International Journal of Dynamics and Control*, vol. 12, pp. 1512–1521, 2024.

[69] A.K. Kashyap, D.R. Parhi and A. Pandey, "Multi-objective optimization technique for trajectory planning of multi-humanoid robots in cluttered terrain," *ISA transactions*, vol. 125, pp. 591-613, 2022.

[70] G. Kulathunga, D. Devitt and A. Klimchik, "Trajectory tracking for quadrotors: An optimization-based planning followed by controlling approach," *Journal of Field Robotics*, vol. 39, no. 7, pp. 1001-1011, 2022.

[71] F. Barato, E. Toson and D. Pavarin, "Variations and control of thrust and mixture ratio in hybrid rocket motors," *Advances in Astronautics Science and Technology*, vol. 4, pp. 55-76, 2021.

[72] M.R. Elshamy, E. Nabil, A.S. Abdelmageed and B. Abozalam, "Stabilization enhancement of the ball on the plate system (BOPS) based on Takagi-Sugeno (TS) fuzzy modelling," In *2021 International Conference on Electronic Engineering (ICEEM)*, pp. 1-8, 2021.

[73] H. Bang and Y.S. Lee, "Implementation of a ball and plate control system using sliding mode control," *IEEE Access*, vol. 6, pp. 32401-32408, 2018.

[74] H. Bang and Y.S. Lee, "Embedded model predictive control for enhancing tracking performance of a ball-and-plate system," *IEEE Access*, vol. 7, pp. 39652-39659, 2019.

[75] A. Umar, M.B. Mu'azu, A.D. Usman, U. Musa, O.O. Ajayi and A.M. Yusuf, "Linear quadratic Gaussian (LQG) control design for position and trajectory tracking of the ball and plate system," *Computing & Information Systems*, vol. 23, no. 1, 2019.

[76] D. Núñez, G. Acosta, and J. Jiménez, "Control of a ball-and-plate system using a State-feedback controller," *Ingeniare: Revista Chilena de Ingenieria*, vol. 28, no. 1, pp. 6-15, 2020.

[77] F.I.R. Betancourt, S.M.B. Alarcon and L.F.A. Velasquez, "Fuzzy and PID controllers applied to ball and plate system," In *2019 IEEE 4th Colombian Conference on Automatic Control (CCAC)*, pp. 1-6, 2019.

[78] D.F. Yépez Ponce and W.M. Montalvo López, "Development of a Hybrid Optimization Strategy Based on a Bacterial Foraging Algorithm (BFA) and a Particle Swarming Algorithm (PSO) to Tune the PID Controller of a Ball and Plate System," In *XV Multidisciplinary International Congress on Science and Technology*, pp. 15-29, Cham: Springer International Publishing, 2021.

[79] A.T. Azar, N. Ali, S. Makarem, M.K. Diab and H.H. Ammar, "Design and implementation of a ball and beam PID control system based on metaheuristic techniques," In *Proceedings of the International Conference on Advanced Intelligent Systems and Informatics 2019*, pp. 313-325, Springer International Publishing, 2020.

[80] O. Hadoune, M. Benouaret, A. Zeghida and H. Saker, "Tracking control of a ball on plate system using PID controller and Lead/Lag compensator with a double loop feedback scheme," *Avrupa Bilim ve Teknoloji Dergisi*, vol. 28, pp. 375-380, 2021.

[81] E. Okafor, D. Udekwe, Y. Ibrahim, M. Bashir Mu'azu and E.G. Okafor, "Heuristic and deep reinforcement learning-based PID control of trajectory tracking in a ball-and-plate system," *Journal of Information and Telecommunication*, vol. 5, no. 2, pp. 179-196, 2021.

[82] A.A. Oglah and M.M. Msallam, "Real-time implementation of Fuzzy Logic Controller based on chicken swarm optimization for the ball and plate system," *International Review of Applied Sciences and Engineering,* vol. 13, no. 3, pp. 263–271, 2021.

[83] I.K. Yousufzai, F. Waheed, Q. Khan, A.I. Bhatti, R. Ullah and R. Akmeliawati, "A linear parameter varying strategy based integral sliding mode control protocol development and its implementation on ball and beam balancer," *IEEE Access*, vol. 9, pp. 74437-74445, 2021.

[84] M.J. Mahmoodabadi and M. Andalib Sahnehsaraei, "Parametric uncertainty handling of under-actuated nonlinear systems using an online optimal input–output feedback linearization controller," *Systems Science & Control Engineering*, vol. 9, no. 1, pp. 209-218, 2021.

[85] A. Mohammadi and J.C. Ryu, "Neural network-based PID compensation for nonlinear systems: ball-on-plate example," *International Journal of Dynamics and Control*, vol. 8, no. 1, pp. 178-188, 2020.

[86] Y.F. Chen, and A.C. Huang, "Controller design for a class of underactuated mechanical systems," *IET control theory & applications*, vol. 6, no. 1, pp. 103-110, 2012.

[87] C. Aguilar-Avelar and J. Moreno-Valenzuela, "A composite controller for trajectory tracking applied to the Furuta pendulum," *ISA transactions*, vol. 57, pp. 286-294, 2015.

[88] O. Boubaker, "The inverted pendulum benchmark in nonlinear control theory: a survey," *International Journal of Advanced Robotic Systems*, vol. 10, no. 5, p. 233, 2013.

[89] K. Furuta, M. Yamakita and S. Kobayashi, "Swing-up control of inverted pendulum using pseudo-state feedback," *Proceedings of the Institution of Mechanical Engineers, Part I: Journal of Systems and Control Engineering*, vol. 206, no. 4, pp. 263-269, 1992.

[90] J.A. Acosta, "Furuta's Pendulum: A conservative nonlinear model for theory and practise," *Mathematical Problems in Engineering*, vol. 2010, pp. 1-29, 2010.

[91] W. Younis and M. Abdelati, "Design and implementation of an experimental segway model," In *AIP Conference Proceedings*, vol. 1107, no. 1, pp. 350-354, American Institute of Physics, 2009.

[92] P.C. Hughes, "Spacecraft attitude dynamics," *Courier Corporation*, 2012.

[93] A. Elhasairi and A. Pechev, "Humanoid robot balance control using the spherical inverted pendulum mode," *Frontiers in Robotics and AI*, vol. 2, p. 21, 2015.

[94] O. Boubaker and R. Iriarte, "The inverted pendulum in control theory and robotics: from theory to new innovations," *IET: The Institution of Engineering and Technology*, no. 137822, 2017.

[95] M. Szuster and Z. Hendzel, "Intelligent optimal adaptive control for mechatronic systems," p. 387, Berlin, Germany: Springer, 2018.

[96] E.V. Kumar and J. Jerome, "Robust LQR controller design for stabilizing and trajectory tracking of inverted pendulum," *Procedia Engineering*, vol. 64, pp. 169-178, 2013.

[97] A. Rojas-Moreno, J. Hernandez-Garagatti, O. Pacheco-De La Vega and L. Lopez-Lozano, "FO based-LQR stabilization of the rotary inverted pendulum," In *2016 Chinese Control and Decision Conference (CCDC)*, pp. 4292-4297, 2016.

[98] J. Wen, Y. Shi and X. Lu, "Stabilizing a rotary inverted pendulum based on logarithmic Lyapunov function," *Journal of Control Science and Engineering*, vol. 2017, no. 1, p.4091302, 2017.

[99] T. Türker, H. Görgün and G. Cansever, "Lyapunov's direct method for stabilization of the Furuta pendulum," *Turkish Journal of Electrical Engineering and Computer Sciences*, vol. 20, no. 1, pp. 99-110, 2012.

[100] J.J. Wang, "Simulation studies of inverted pendulum based on PID controllers," *Simulation Modelling Practice and Theory*, vol. 19, no. 1, pp. 440-449, 2011.

[101] T.F. Tang, S.H. Chong and K.K. Pang, "Stabilisation of a rotary inverted pendulum system with double-PID and LQR control: experimental verification," *International Journal of Automation and Control*, vol. 14, no. 1, pp. 18-33, 2020.

[102] T. Abut and S. Soyguder, "Real-time control and application with self-tuning PID-type fuzzy adaptive controller of an inverted pendulum," *Industrial Robot: the International Journal of robotics research and application*, vol. *46*, no. 1, pp. 159-170, 2019.

[103] J. Moreno-Valenzuela, C. Aguilar-Avelar, S.A. Puga-Guzmán and V. Santibáñez, "Adaptive neural network control for the trajectory tracking of the Furuta pendulum," *IEEE Transactions on cybernetics*, vol. 46, no. 12, pp. 3439-3452, 2016.

[104] A. de Carvalho, J.F. Justo, B.A. Angélico, A.M. de Oliveira and J.I. da Silva Filho, "Rotary inverted pendulum identification for control by paraconsistent neural network," *IEEE Access*, vol. 9, pp. 74155-74167, 2021.

[105] J.B. Kim, H.K. Lim, C.M. Kim, M.S. Kim, Y.G. Hong and Y.H. Han, "Imitation reinforcement learning-based remote rotary inverted pendulum control in openflow network," *IEEE Access*, vol. 7, pp. 36682-36690, 2019.

[106] Y. Dai, K. Lee and S. Lee, "A real-time HIL control system on rotary inverted pendulum hardware platform based on double deep Q-network," *Measurement and Control*, vol. 54, no. 3-4, pp. 417-428, 2021.

[107] E. Susanto, A.S. Wibowo and E.G. Rachman, "Fuzzy swing up control and optimal state feedback stabilization for self-erecting inverted pendulum," *IEEE Access*, vol. 8, pp. 6496-6504, 2020.

[108] Z.B. Hazem, M.J. Fotuhi and Z. Bingül, "Development of a Fuzzy-LQR and Fuzzy-LQG stability control for a double link rotary inverted pendulum," *Journal of the Franklin Institute*, vol. 357, no. 15, pp. 10529-10556, 2020.

[109] A. Wadi, J.H. Lee and L. Romdhane, "Nonlinear sliding mode control of the Furuta pendulum," In *2018 11th International Symposium on Mechatronics and its Applications (ISMA)*, pp. 1-5, 2018.

[110] İ. Yiğit, "Model free sliding mode stabilizing control of a real rotary inverted pendulum," *Journal of Vibration and Control*, vol. *23*, no. 10, pp. 1645-1662, 2017.

[111] O. Mofid, K.A. Alattas, S. Mobayen, M.T. Vu and Y. Bouteraa, "Adaptive finite-time command-filtered backstepping sliding mode control for stabilization of a disturbed rotary-inverted-pendulum with experimental validation," *Journal of Vibration and Control*, vol. 29, no. 5-6, pp. 1431-1446, 2023.

[112] B. Wu, C. Liu, X. Song and X. Wang, "Design and implementation of the inverted pendulum optimal controller based on hybrid genetic algorithm," In *2015 International Conference on Automation, Mechanical Control and Computational Engineering*, pp. 1480-1486, Atlantis Press, 2015.

[113] Y.F. Chen and A.C. Huang, "Adaptive control of rotary inverted pendulum system with time-varying uncertainties," *Nonlinear Dynamics*, vol. 76, pp. 95-102, 2014.

[114] J. Huang, T. Zhang, Y. Fan and J.Q. Sun, "Control of rotary inverted pendulum using model-free backstepping technique," *IEEE Access*, vol. 7, pp. 96965-96973, 2019.

[115] X. Yang and X. Zheng, "Swing-up and stabilization control design for an underactuated rotary inverted pendulum system: Theory and experiments," *IEEE Transactions on Industrial Electronics*, vol. 65, no. 9, pp. 7229-7238, 2018.

[116] M. Waszak and R. Łangowski, "An automatic self-tuning control system design for an inverted pendulum," *IEEE Access*, vol. 8, pp. 26726-26738, 2020.

[117] L. Zhang and R. Dixon, "Robust nonminimal state feedback control for a Furuta pendulum with parametric modeling errors," *IEEE Transactions on Industrial Electronics*, vol. 68, no. 8, pp. 7341-7349, 2020.

[118] I.M. Mehedi, U.M. Al-Saggaf, R. Mansouri and M. Bettayeb, "Stabilization of a double inverted rotary pendulum through fractional order integral control scheme," *International Journal of Advanced Robotic Systems*, vol. 16, no. 4, p. 1729881419846741, 2019.

[119] A.K. Patra, S.S. Biswal and P.K. Rout, "Backstepping linear quadratic gaussian controller design for balancing an inverted pendulum," *IETE Journal of Research*, vol. 68, no. 1, pp. 150-164, 2022.

[120] T.F. Tang, S.H. Chong and K.K. Pang, "Stabilisation of a rotary inverted pendulum system with double-PID and LQR control: experimental verification," *International Journal of Automation and Control*, vol. 14, no. 1, pp. 18-33, 2020.

[121] T. Abut and S. Soyguder, "Real-time control and application with self-tuning PID-type fuzzy adaptive controller of an inverted pendulum," *Industrial Robot: The International Journal of robotics research and application*, vol. 46, no. 1, pp. 159-170, 2019.

[122] F.F. El-Sousy, K.A. Alattas, O. Mofid, S. Mobayen and A. Fekih, "Robust adaptive super-twisting sliding mode stability control of underactuated rotational inverted pendulum with experimental validation," *IEEE Access*, vol. 10, pp. 100857-100866, 2022.

[123] S.H. Zabihifar, A.S. Yushchenko and H. Navvabi, "Robust control based on adaptive neural network for Rotary inverted pendulum with oscillation compensation," *Neural Computing and Applications*, vol. 32, pp. 14667-14679, 2020.

[124] M.R. Dolatabad, A. Pasharavesh and A.A.A. Khayyat, "Analytical and experimental analyses of nonlinear vibrations in a rotary inverted pendulum," *Nonlinear Dynamics*, vol. 107, no. 3, pp. 1887-1902, 2022.

[125] R. Shalaby, M. El-Hossainy and B. Abo-Zalam, "Fractional order modeling and control for under-actuated inverted pendulum," *Communications in Nonlinear Science and Numerical Simulation*, vol. 74, pp. 97-121, 2019.

[126] A.F. Ghaleb, A.A. Oglah, A.J. Humaidi, A.S.M. Al-Obaidi and I.K. Ibraheem, "Optimum of fractional order fuzzy logic controller with several evolutionary optimization algorithms for inverted pendulum," *International Review of Applied Sciences and Engineering*, vol. 14, no. 1, pp. 1-12, 2023.

[127] Y. Yang, H.H. Zhang and R.M. Voyles, "Optimal fractional-order proportional–integral–derivative control enabling full actuation of decomposed rotary inverted pendulum system," *Transactions of the Institute of Measurement and Control*, vol. 45, no. 10, pp. 1986-1998, 2023.

[128] R. Mondal and J. Dey, "A novel design methodology on cascaded fractional order (FO) PI-PD control and its real time implementation to Cart-Inverted Pendulum System," *ISA transactions*, vol. 130, pp. 565-581, 2022.

[129] R. Mondal and J. Dey, "Performance analysis and implementation of fractional order 2-DOF control on cart–inverted pendulum system," *IEEE transactions on industry applications*, vol. 56, no. 6, pp. 7055-7066, 2020.

[130] R. Mondal, A. Chakraborty, J. Dey and S. Halder, "Optimal fractional order $PI\lambda D\mu$ controller for stabilization of cart-inverted pendulum system: Experimental results," *Asian Journal of Control*, vol. 22, no. 3, pp. 1345-1359, 2020.

[131] T. Balogh and T. Insperger, "Extending the admissible control-loop delays for the inverted pendulum by fractional-order proportional-derivative controller," *Journal of Vibration and Control*, vol. 30, no. 11-12, pp. 2596-2604, 2024.

[132] O. Saleem and K. Mahmood-ul-Hasan, "Robust stabilisation of rotary inverted pendulum using intelligently optimised nonlinear self-adaptive dual fractional-order PD controllers," *International Journal of Systems Science*, vol. 50, no. 7, pp. 1399-1414, 2019.

[133] I.M. Mehedi, U. Ansari and U.M. AL-Saggaf, "Three degrees of freedom rotary double inverted pendulum stabilization by using robust generalized dynamic inversion control: Design and experiments," *Journal of Vibration and Control*, vol. 26, no. 23-24, pp. 2174-2184, 2020.

[134] I.M. Mehedi, U. Ansari, A.H. Bajodah, U.M. AL-Saggaf, B. Kada and M.J. Rawa, "Underactuated rotary inverted pendulum control using robust generalized dynamic inversion," *Journal of Vibration and Control*, vol. 26, no. 23-24, pp. 2210-2220, 2020.

[135] N. Gupta and L. Dewan, "Modified grey wolf optimised adaptive super-twisting sliding mode control of rotary inverted pendulum system," *Journal of Control and Decision*, vol. 10, no. 2, pp. 270-279, 2023.

[136] F.N. ŞEN and U. Beldek, "Genetic Algorithm Based Stabilization of Rotary Inverted Pendulum by State Feedback," *Research Square*, pp. 1-26, 2022. [Online]. Available: https://assets-eu.researchsquare.com/files/rs-2373423/v1_covered.pdf?c=1671274778.

[137] S. Babushanmugham, S. Srinivasan and E. Sivaraman, "Assessment of optimisation techniques for sliding mode control of an inverted pendulum," *International Journal of Applied Engineering Research*, vol. 3, pp. 11518-1524, 2018.

[138] M.F. Hamza, H.J. Yap and I.A. Choudhury, "Genetic algorithm and particle swarm optimization based cascade interval type 2 fuzzy PD controller for rotary inverted pendulum system," *Mathematical Problems in Engineering*, *2015*(1), p.695965, 2015.

[139] M.J. Blondin and P.M. Pardalos, "A holistic optimization approach for inverted cart-pendulum control tuning," *Soft Computing*, vol. 24, no. 6, pp. 4343-4359, 2020.

[140] A. Dolgui, F. Sgarbossa and M. Simonetto, "Design and management of assembly systems 4.0: systematic literature review and research agenda," *International Journal of Production Research*, vol. 60, no. 1, pp. 184-210, 2022.

[141] D.A. Rossit, F. Tohmé and M. Frutos, "An Industry 4.0 approach to assembly line resequencing," *The International Journal of Advanced Manufacturing Technology*, vol. 105, pp. 3619-3630, 2019.

[142] F. Pilati, G. Lelli, A. Regattieri and E. Ferrari, "Assembly line balancing and activity scheduling for customised products manufacturing," *The International Journal of Advanced Manufacturing Technology*, vol. 120*, no. 5, pp. 3925-3946, 2022.

[143] N.A. Schmid, B. Montreuil and V. Limère, "A case study on the integration of assembly line balancing and feeding decisions," *IFAC-PapersOnLine*, vol. 55, no. 10, pp. 109-114, 2022.

[144] S. Ling, D. Guo, Y. Rong and G.Q. Huang, "Real-time data-driven synchronous reconfiguration of human-centric smart assembly cell line under graduation intelligent manufacturing system," *Journal of Manufacturing Systems*, vol. 65, pp. 378-390, 2022.

[145] H.H. Aung and T.T.E. Aung, "Simulation and Implementation of PLC based for Nonstop Filling Process using PLCSIM and HMI," *International Journal of All Research Writings*, vol. 2, no. 3, pp. 134-137, 2019.

[146] Z.K. Win and T.T. New, "PLC based automatic bottle filling and capping system," *International Journal of Trend in Scientific Research and Development*, vol. 3, no. 6, pp. 389-392, 2019.

[147] N. Nadgauda, S.A. Muthukumaraswamy and S.U. Prabha, "Smart automated processes for bottle-filling industry using PLC-SCADA system," In *Intelligent Manufacturing and Energy Sustainability: Proceedings of ICIMES 2019*, pp. 693-702, Springer Singapore, 2020.

[148] S.V. Viraktamath, A.S. Umarfarooq, V. Yallappagoudar and A.P. Hasankar, "Implementation of automated bottle filling system using PLC," In *Inventive Communication and Computational Technologies: Proceedings of ICICCT 2019*, pp. 33-41, Springer Singapore, 2020.

[149] A.N. Abubakar, S.L. Dhar, A.A. Tijjani and A.M. Abdullahi, "Automated liquid filling system with a robotic arm conveyor for small scale industries," *Materials Today: Proceedings*, vol. 49, pp. 3270-3273, 2022.

[150] K.S. Kiangala and Z. Wang, "An Industry 4.0 approach to develop auto parameter configuration of a bottling process in a small to medium scale industry using PLC and SCADA," *Procedia Manufacturing*, vol. 35, pp. 725-730, 2019.

[151] S. Kannan, "Smart process measurement and automation: challenges, solution and future direction," *CSI Transactions on ICT*, vol. 7, no. 2, pp. 93-98, 2019.

[152] S. Gil, G.D. Zapata-Madrigal, R. García-Sierra and L.A. Cruz Salazar, "Converging IoT protocols for the data integration of automation systems in the electrical industry," *Journal of Electrical Systems and Information Technology*, vol. 9, no. 1, p. 1, 2022.

[153] M. Azarmipour, H. Elfaham, C. Gries and U. Epple, "PLC 4.0: A control system for industry 4.0," In *IECON 2019-45th Annual Conference of the IEEE Industrial Electronics Society*, vol. 1, pp. 5513-5518, 2019.

[154] E.R. Alphonsus and M.O. Abdullah, "A review on the applications of programmable logic controllers (PLCs)," *Renewable and Sustainable Energy Reviews*, vol. 60, pp. 1185-1205, 2016.

[155] OMRON Corporation, "NJ/NX-series CPU Unit Built-in EtherCAT Port User's Manual (W505)", *Industrial Automation Company*, Kyoto, Japan, 2022.

[156] J. Fischer, B. Vogel-Heuser and D. Friedrich, "Configuration of PLC software for automated warehouses based on reusable components-an industrial case study," In *2015 IEEE 20th Conference on Emerging Technologies & Factory Automation (ETFA)*, pp. 1-7, 2015.

[157] K. Langlois, T. van der Hoeven, D.R. Cianca, T. Verstraten, T. Bacek, B. Convens, C. Rodriguez-Guerrero, V. Grosu, D. Lefeber and B. Vanderborght, "Ethercat tutorial: An introduction for real-time hardware communication on windows [tutorial]," *IEEE Robotics & Automation Magazine*, vol. 25, no. 1, pp. 22-122, 2018.

[158] F. Pilati, G. Lelli, A. Regattieri and E. Ferrari, "Assembly line balancing and activity scheduling for customised products manufacturing," *The International Journal of Advanced Manufacturing Technology*, vol. 12, no. 5, pp. 3925-3946, 2022.

[159] V. Feliu-Batlle and R. Rivas-Perez, "Control of the temperature in a petroleum refinery heating furnace based on a robust modified Smith predictor," *ISA Transactions*, vol. 112, pp. 251–270, 2021.

[160] M. Kumar, D. Prasad, B.S. Giri and R.S. Singh, "Temperature control of fermentation bioreactor for ethanol production using IMC-PID controller," *Biotechnology Reports*, vol. 22, p.e 00319, 2019.

[161] J. Taborek, G.F. Hewitt and N.H. Afgan, "Heat exchangers–theory and practice," *International Center for Heat and Mass Transfer*, Hemisphere, Washington, D.C., 1983

[162] T. Venegas, M. Qu, K. Nawaz and L. Wang, "Critical review and future prospects for desiccant coated heat exchangers: Materials, design, and manufacturing," *Renewable and Sustainable Energy Reviews*, vol. 151, p. 111531, 2021.

[163] F. Rößler, V. Krumova, S. Gewald, A. Bauernfeind, P. Freko, I. Thomas, H.J. Zander, S. Rehfeldt and H. Klein, "Hazard Analysis of Fixed-Tube-Sheet Shell-and-Tube Heat Exchangers," *Chemie Ingenieur Technik*, vol. 94, no. 5, pp. 727-737, 2022.

[164] H.Z. Jin, Y. Gu and G.F. Ou, "Corrosion risk analysis of tube-and-shell heat exchangers and design of outlet temperature control system," *Petroleum Science*, vol. 18, no. 4, pp. 1219-1229, 2021.

[165] S.M. Jafari, F. Saramnejad and D. Dehnad, "Designing and application of a shell and tube heat exchanger for nanofluid thermal processing of liquid food products," *Journal of food process engineering*, vol. *41*, no. 3, p.e 12658, 2018.

[166] P. Bichkar, O. Dandgaval, P. Dalvi, R. Godase and T. Dey, "Study of shell and tube heat exchanger with the effect of types of baffles," *Procedia Manufacturing*, vol. 20, pp. 195-200, 2018.

[167] G. Dong and M. Deng, "Operator & Fractional Order Based Nonlinear Robust Control for a Spiral Counter-flow Heat Exchanger with Uncertainties and Disturbances," *Machines*, vol. 10, no. 5, p. 335, 2022.

[168] Q. Jin, Y. Yu and Y. Xia, "Active control for system with multiple microchannel heat exchangers using disturbance observer," *Numerical Heat Transfer, Part A: Applications*, vol. 85, no. 6, pp. 958-973, 2024.

[169] C.B. Carvalho, E.P. Carvalho and M.A. Ravagnani, "Implementation of a neural network MPC for heat exchanger network temperature control," *Brazilian Journal of Chemical Engineering*, vol. 37, no. 4, pp. 729-744, 2020.

[170] M. Ouyang, Y. Wang, F. Wu and Y. Lin, "Continuous Reactor Temperature Control with Optimized PID Parameters Based on Improved Sparrow Algorithm," *Processes*, vol. 11, no. 5, p. 1302, 2023.

[171] T. Thepmanee, S. Pongswatd, F. Asadi and P. Ukakimaparn, "Implementation of control and SCADA system: Case study of Allen Bradley PLC by using WirelessHART to temperature control and device diagnostic," *Energy Reports*, vol. 8, pp. 934-941, 2022.

[172] A.A. Jamil, W.F. Tu, S.W. Ali, Y. Terriche and J.M. Guerrero, "Fractional-order PID controllers for temperature control: A review," *Energies*, vol. *15*, no. 10, p. 3800, 2022.

[173] Z. Li, J. Liu, X. Yang, X. Huang, L. Jia and M. Li "Novel effective room temperature-based predictive feedback control method for large-scale district heating substation," *Applied Thermal Engineering*, vol. 218, p. 119241, 2023.

[174] M.C. Maya-Rodriguez, I. Carvajal-Mariscal, R. López-Muñoz, M.A. Lopez-Pacheco and R. Tolentino-Eslava, "Temperature Control of a Chemical Reactor Based on Neuro-Fuzzy Tuned with a Metaheuristic Technique to Improve Biodiesel Production," *Energies*, vol. 16, no. 17, p. 6187, 2023.

[175] W. Miao and B. Xu, "Application of Feedforward Cascade Compound Control Based on Improved Predictive Functional Control in Heat Exchanger Outlet Temperature System," *Applied Sciences*, vol. 13, no. 12, p. 7132, 2023.

[176] G. Hou, L. Gong, M. Wang, X. Yu, Z. Yang and X. Mou, "A novel linear active disturbance rejection controller for main steam temperature control based on the simultaneous heat transfer search," *ISA transactions*, vol. 122, pp. 357-370, 2022.

[177] Z. Gao, T.A. Trautzsch and J.G. Dawson, "A stable self-tuning fuzzy logic control system for industrial temperature regulation," *IEEE Transactions on Industry Applications*, vol. 38, no. 2, pp. 414-424, 2002.

[178] L. Pekař, "Modeling and identification of a time-delay heat exchanger plant," In *Advanced Analytic and Control Techniques for Thermal Systems with Heat Exchangers*, pp. 23-48, Academic Press, 2020.

[179] T. Zhang, J.T. Wen, J. Catano and R. Zhou, "Stability analysis of heat exchanger dynamics," In *2009 American Control Conference*, pp. 3656-3661, 2009.

[180] M. Al-Dhaifallah, "Heat exchanger control using fuzzy fractional-order PID," In *2019 16th International Multi-Conference on Systems, Signals & Devices (SSD)*, pp. 73-77, 2019.

[181] R. Li, F. Wu, P. Hou and H. Zou, "Performance assessment of FO-PID temperature control system using a fractional order LQG benchmark," *IEEE Access*, vol. 8, pp. 116653-116662, 2020.

[182] S. Liu, L. Zhang, B. Niu, X. Zhao and A.M. Ahmad, "Adaptive neural finite-time hierarchical sliding mode control of uncertain under-actuated switched nonlinear systems with backlash-like hysteresis," *Information Sciences*, vol. 599, pp. 147-169, 2022.

[183] X. Chen, H. Zhao, H. Sun, S. Zhen and A. Al Mamun, "Optimal adaptive robust control based on cooperative game theory for a class of fuzzy underactuated mechanical systems," *IEEE Transactions on Cybernetics*, vol. 52, no. 5, pp. 3632-3644, 2020.

[184] T. Shuprajhaa, S.K. Sujit, and K. Srinivasan, "Reinforcement learning based adaptive PID controller design for control of linear/nonlinear unstable processes," *Applied Soft Computing*, vol. 128, p. 109450, 2022.

[185] M.L. Hammadih, K.A. Hosani and I. Boiko, "Interpolating sliding mode observer for a ball and beam system," *International Journal of Control*, vol. 89, no. 9, pp. 1879-1889, 2016.

[186] T. Yang, H. Chen, N. Sun and Y. Fang, "Adaptive neural network output feedback control of uncertain underactuated systems with actuated and unactuated state constraints," *IEEE Transactions on Systems, Man, and Cybernetics: Systems*, vol. 52, no. 11, pp. 7027-7043, 2021.

[187] H.G. Jang, C.H. Hyun, and B.S. Park, "Neural network control for trajectory tracking and balancing of a ball-balancing robot with uncertainty," *Applied Sciences*, vol. 11, no. 11, p. 4739, 2021.

[188] S. Kong, J. Sun, C. Qiu, Z. Wu and J. Yu, "Extended state observer-based controller with model predictive governor for 3-D trajectory tracking of underactuated underwater vehicles," *IEEE Transactions on Industrial Informatics*, vol. 17, no. 9, pp. 6114-6124, 2020.

[189] H. Liang, H. Li, and D. Xu, "Nonlinear model predictive trajectory tracking control of underactuated marine vehicles: Theory and experiment," *IEEE Transactions on Industrial Electronics*, vol. 68, no. 5, pp. 4238-4248, 2020.

[190] A. Das and P. Roy, "Improved performance of cascaded fractional-order SMC over cascaded SMC for position control of a ball and plate system," *IETE Journal of Research*, vol. 63, no. 2, pp. 238-247, 2017.

[191] D. Udekwe, O.O. Ajayi, O. Ubadike, K. Ter and E. Okafor, "Comparing actor-critic deep reinforcement learning controllers for enhanced performance on a ball-and-plate system," *Expert Systems with Applications*, vol. 245, p. 123055, 2024.

[192] M.R. Elshamy, E. Nabil, A. Sayed, and B. Abozalam, "Enhancement of the Ball Balancing on the Plate using hybrid PD/Machine learning techniques," *Journal of Physics: Conference Series*, vol. 2128, no. 1, p. 012028, IOP Publishing, 2021.

[193] M. Borah, P. Roy and B.K. Roy, "Enhanced performance in trajectory tracking of a ball and plate system using fractional order controller," *IETE Journal of Research*, vol. 64, no. 1, pp. 76-86, 2018.

[194] V. Srivastava and S. Srivastava, "Hybrid optimization based PID control of ball and beam system," *Journal of Intelligent & Fuzzy Systems*, vol. 42, no. 2, pp. 919-928, 2022.

[195] L. Zheng and R. Hu, "Robust and fast visual tracking for a ball and plate control system: design, implementation and experimental verification," *Multimedia tools and applications*, vol. 78, pp. 13279-13295, 2019.

[196] V.T. Do and S.G. Lee, "Neural integral backstepping hierarchical sliding mode control for a ridable ballbot under uncertainties and input saturation," *IEEE Transactions on Systems, Man, and Cybernetics: Systems*, vol. 51, no. 11, pp. 7214-7227, 2020.

[197] J. Ma, H. Tao and J. Huang, "Observer integrated backstepping control for a ball and plate system," *International journal of dynamics and control*, vol. 9, pp. 141-148, 2021.

[198] S. Zaare and M.R. Soltanpour, "The position control of the ball and beam system using state-disturbance observe-based adaptive fuzzy sliding mode control in presence of matched and mismatched uncertainties," *Mechanical Systems and Signal Processing*, vol. 150, p. 107243, 2021.

[199] M.R. Elshamy, B. Abozalam, A. Sayed and E. Nabil, "Real-time control design and implementation of ball balancer system based on machine learning and machine vision," *Concurrency and Computation: Practice and Experience*, vol. 34, no. 27, p.e 7317, 2022.

[200] H.G. Jang, C.H. Hyun and B.S. Park, "Virtual angle-based adaptive control for trajectory tracking and balancing of ball-balancing robots without velocity measurements," *International Journal of Adaptive Control and Signal Processing*, vol. 37, no. 8, pp. 2204-2215, 2023.

[201] F. Haddad and J. Tamimi, "A comparative simulation and experimental study for control of a ball and plate system using model-based controllers," *International Journal of Dynamical Systems and Differential Equations*, vol. 13, no. 2, pp. 91-107, 2023.

[202] E. Zakeri, S.A. Moezi and M. Eghtesad, "Optimal interval type-2 fuzzy fractional order super twisting algorithm: A second order sliding mode controller for fully-actuated and under-actuated nonlinear systems," *ISA transactions*, vol. 85, pp. 13-32, 2019.

[203] A. Kassem, H. Haddad and C. Albitar, "Comparison between different methods of control of ball and plate system with 6dof stewart platform," *IFAC-PapersOnLine*, vol. 48, no. 11, pp. 47-52, 2015.

[204] L. Morales, M. Gordón, O. Camacho, A. Rosales and D. Pozo, "A comparative analysis among different controllers applied to the experimental ball and plate system," In *2017 International Conference on Information Systems and Computer Science (INCISCOS)*, pp. 108-114, 2017.

[205] F. Doostdar and H. Mojallali, "An ADRC-based backstepping control design for a class of fractional-order systems," *ISA transactions*, vol. 121, pp. 140-146, 2022.

[206] J. Velasco, Ó. Barambones, I. Calvo, P. Venegas and C.M. Napole, "Validation of a Stewart platform inspection system with an artificial neural network controller," *Precision Engineering*, vol. 74, pp. 369-381, 2022.

[207] M.K. Saleem, M.L.U.R. Shahid, A. Nouman, H. Zaki and M.A.U.R. Tariq, "Design and implementation of adaptive neuro-fuzzy inference system for the control of an uncertain ball and

beam apparatus," *Mehran University Research Journal of Engineering & Technology*, vol. 41, no. 2, pp. 178-184, 2022.

[208] D. Kan, B. Xing, W. Xie and L. Zhu, "A minimum phase output based tracking control of ball and plate systems," *International Journal of Dynamics and Control*, vol. 10, no. 2, pp. 462-472, 2022.

[209] D.F. Hesser, S. Mostafavi, G.K. Kocur and B. Markert, "Identification of acoustic emission sources for structural health monitoring applications based on convolutional neural networks and deep transfer learning," *Neurocomputing*, vol. 453, pp. 1-12, 2021.

[210] D. Chavez, "Design and development of neuromorphic estimation and control algorithms for the ball on plate testbed," (Doctoral dissertation, New Mexico State University), 2023.

[211] P. Kravets and V. Shymkovych, "Hardware implementation neural network controller on FPGA for stability ball on the platform," In *Advances in Computer Science for Engineering and Education II*, pp. 247-256. Springer International Publishing, 2020.

[212] O. Hadoune and M. Benouaret, "ANFIS multi-tasking algorithm implementation scheme for ball-on-plate system stabilization," *Indonesian Journal of Electrical Engineering and Informatics (IJEEI)*, vol. 10, no. 4, pp. 983-995, 2022.

[213] J.F. Li and F.H. Xiang, "RBF network adaptive sliding mode control of ball and plate system based on reaching law," *Arabian Journal for Science and Engineering*, vol. 47, no. 8, pp. 9393-9404, 2022.

[214] A. Kovalev, Y. Tian and Y. Meng, "Prediction of ball-on-plate friction and wear by ANN with data-driven optimization," *Friction*, vol. 12, pp. 1235–1249, 2024.

[215] N. Khaled, B. Pattel and A. Siddiqui, "Digital twin development and deployment on the cloud: developing cloud-friendly dynamic models using Simulink®/SimscapeTM and Amazon AWS," *Academic Press*, 2020.

[216] C.C. Ker, C.E. Lin and R.T. Wang, "Tracking and balance control of ball and plate system," *Journal of the Chinese Institute of Engineers*, vol. 30, no. 3, pp. 459-470, 2007.

[217] Quanser Inc. "Peripherals to Accelerate Control System Design and Implementation," vol. 12, 2010.

[218] MicroMo Electronics Inc. "Faulhaber DC-Micromotors Series 2338," Clearwater-Florida, 2015.

[219] G. Rigatos, K. Busawon, J. Pomares and M. Abbaszadeh, "Nonlinear optimal control for the wheeled inverted pendulum system," *Robotica*, vol. 38, no. 1, pp. 29-47, 2020.

[220] G. Rigatos, M. Abbaszadeh and M.A. Hamida, "Nonlinear optimal control for the inertia wheel inverted pendulum," *Cyber-Physical Systems*, vol. 6, no. 2, pp. 55-75, 2020.

[221] M.A. Ebrahim, M.E. Mousa, E.M. Said, M.M. Zaky and S.A. Kotb, "Optimal design of hybrid optimization technique for balancing inverted pendulum system," *WSEAS Trans. Syst.*, vol. 19, pp. 138-148, 2020.

[222] D.T. Mai-Phuong, P. Van-Hung, N. Ngoc-Khoat and P. Van-Minh, "Balancing a practical inverted pendulum model employing novel meta-heuristic optimization-based fuzzy logic controllers," *International Journal of Adv. Computer Science and Appl*, vol. 13, no. 4, pp. 547-553, 2022.

[223] A. Unluturk and O. Aydogdu, "Machine learning based self-balancing and motion control of the underactuated mobile inverted pendulum with variable load," *IEEE Access*, vol. 10, pp. 104706-104718, 2022.

[224] Y.F. Chen and A.C. Huang, "Adaptive control of rotary inverted pendulum system with time-varying uncertainties," *Nonlinear Dynamics*, vol. 76, pp. 95-102, 2014.

[225] M.A. Sahnehsaraei and M.J. Mahmoodabadi, "Approximate feedback linearization based optimal robust control for an inverted pendulum system with time-varying uncertainties," *International Journal of Dynamics and Control*, vol. 9, pp. 160-172, 2021.

[226] C. Sotelo, A. Favela-Contreras, F. Beltrán-Carbajal, G. Dieck-Assad, P. Rodríguez-Cañedo and D. Sotelo, "A novel discrete-time nonlinear model predictive control based on state space model," *International Journal of Control, Automation and Systems*, vol. 16, pp. 2688-2696, 2018.

[227] L. Alvarez-Hidalgo and I.S. Howard, "Gain scheduling for state space control of a dual-mode inverted pendulum," In *2022 International Conference on System Science and Engineering (ICSSE)*, pp. 039-046, 2022.

[228] M.E. Girgis and R.I. Badr, "Optimal fractional-order adaptive fuzzy control on inverted pendulum model," *International Journal of Dynamics and Control*, vol. 9, pp. 288-298, 2021.

[229] M. Abdullah, A.A. Amin, S. Iqbal and K. Mahmood-ul-Hasan, "Swing up and stabilization control of rotary inverted pendulum based on energy balance, fuzzy logic, and LQR controllers," *Measurement and Control*, vol. 54, no. 9-10, pp. 1356-1370, 2021.

[230] M. Llama, A. Flores, R. Garcia-Hernandez and V. Santibañez, "Heuristic global optimization of an adaptive fuzzy controller for the inverted pendulum system: Experimental comparison," *Applied Sciences*, vol. 10, no. 18, p. 6158, 2020.

[231] E.Y. Bejarbaneh, A. Bagheri, B.Y. Bejarbaneh and S. Buyamin, "Optimization of model reference adaptive controller for the inverted pendulum system using CCPSO and DE algorithms," *Automatic Control and Computer Sciences*, vol. 52, pp. 256-267, 2018.

[232] J. Iqbal, M. Ullah, S.G. Khan, B. Khelifa and S. Ćuković, "Nonlinear control systems-A brief overview of historical and recent advances," *Nonlinear Engineering*, vol. 6, no. 4, pp. 301-312, 2017.

[233] M.F. Hamza, H.J. Yap, I.A. Choudhury, A.I. Isa, A.Y. Zimit and T. Kumbasar, "Current development on using Rotary Inverted Pendulum as a benchmark for testing linear and nonlinear control algorithms," *Mechanical Systems and Signal Processing*, vol. 116, pp. 347-369, 2019.

[234] J. Apkarian, P. Karam, P. and M. Levis, "Instructor workbook: Inverted pendulum experiment for MATLAB®/Simulink® users," *Quanser Inc,* Markham, ON, Canada*, 2011*.

[235] D.J. Limebeer and M. Massaro, "Dynamics and optimal control of road vehicles," Oxford University Press, 2018.

[236] P. Wang, Z. Man, Z. Cao, J. Zheng and Y. Zhao, "Dynamics modelling and linear control of quadcopter," In *2016 International Conference on Advanced Mechatronic Systems (ICAMechS)*, pp. 498-503, 2016.

[237] T. Gurriet, M. Mote, A. Singletary, P. Nilsson, E. Feron and A.D. Ames, "A scalable safety critical control framework for nonlinear systems," *IEEE Access*, vol. 8, pp. 187249-187275, 2020.

[238] N. Minorsky, "Control problems," *Journal of the Franklin Institute,* vol. 232, no. 6, pp. 519–551, 1941.

[239] O. Gonzalez and A. Rossiter, "Fast hybrid dual mode NMPC for a parallel double inverted pendulum with experimental validation," *IET Control Theory & Applications*, vol. 14, no. 16, pp. 2329-2338, 2020.

[240] M. Alamir and A. Murilo, "Swing-up and stabilization of a Twin-Pendulum under state and control constraints by a fast NMPC scheme," *Automatica*, vol. 44, no. 5, pp. 1319-1324, 2008.

[241] V.G. Pratheep, E.B. Priyanka, S. Thangavel and K. Gomathi, "Genetic algorithm–based robust controller for an inverted pendulum using model order reduction," *Journal of Testing and Evaluation*, vol. 49, no. 4, pp. 2441-2455, 2021.

[242] A. Jain, A. Sharma, V. Jately, B. Azzopardi and S. Choudhury, "Real-time swing-up control of non-linear inverted pendulum using Lyapunov based optimized fuzzy logic control," *IEEE Access*, vol. 9, pp. 50715-50726, 2021.

[243] I. Chawla and A. Singla, "Real-time control of a rotary inverted pendulum using robust LQR-based ANFIS controller," *International Journal of Nonlinear Sciences and Numerical Simulation*, vol. 19, no. 3-4, pp. 379-389, 2018.

[244] S. Pramanik and S. Anwar "Robust controller design for rotary inverted pendulum using H∞ H∞ and μ μ-synthesis techniques," *The Journal of Engineering*, vol. 3, pp. 249-260, 2022.

[245] E. Zakeri, S.A. Moezi and M. Eghtesad "Optimal interval type-2 fuzzy fractional order super twisting algorithm: A second order sliding mode controller for fully-actuated and under-actuated nonlinear systems," *ISA transactions*, vol. 85, pp. 13-32, 2019.

[246] D. Mukherjee, P. Kundu and A. Ghosh, "A Better Stability Control of Inverted Pendulum System Using FMINCON Based FOPID Controller Over Fractional Order Based MRAC Controller," *International Journal of Natural Computing Research (IJNCR)*, vol. 8, no. 1, pp. 18-30, 2019.

[247] M.R. Zangeneh-Madar and A.H. Mazinan, "Control of the inverted pendulum system: a Smith fractional-order predictive model representation," *Sādhanā*, vol. 45, pp. 1-5, 2020.

[248] J.J. Wang and G.Y. Liu, "Hierarchical sliding-mode control of spatial inverted pendulum with heterogeneous comprehensive learning particle swarm optimization," *Information Sciences*, vol. 495, pp. 14-36, 2019.

[249] A. Pandey and D.M. Adhyaru, "Robust control design for rotary inverted pendulum with unmatched uncertainty," *International Journal of Dynamics and Control*, vol. 11, no. 3, pp. 1166-1177, 2023.

[250] P. Dwivedi, S. Pandey and A.S. Junghare, "Stabilization of unstable equilibrium point of rotary inverted pendulum using fractional controller," *Journal of the Franklin Institute*, vol. 354, no. 17, pp. 7732-7766, 2017.

[251] M.F. Masrom, N.M. A Ghani and M.O. Tokhi, "Particle swarm optimization and spiral dynamic algorithm-based interval type-2 fuzzy logic control of triple-link inverted pendulum system: A comparative assessment," *Journal of Low Frequency Noise, Vibration and Active Control*, vol. 40, no. 1, pp. 367-382, 2021.

[252] A. Gutarra, S. Palomino, E.J. Alegria and J. Cisneros, "Fuzzy Controller Design for Rotary Inverted Pendulum System Using Genetic Algorithms," In *2022 IEEE ANDESCON*, pp. 1-6, 2022.

[253] S. Alimoradpour, M. Rafie and B. Ahmadzadeh, "Providing a genetic algorithm-based method to optimize the fuzzy logic controller for the inverted pendulum," *Soft Computing*, vol. 26, no. 11, pp. 5115-5130, 2022.

[254] D. Vishnu and F.M. Joseph, "A Non Linear PID Fuzzy Approach for Stabilization of Inverted Pendulum Using Particle Swarm Optimisation," *International Journal of Engineering Research & Technology (IJERT)*, vol. 2, no. 8, pp. 1364-1369, 2013.

[255] A. Nagarajan and A.A. Victoire, "Optimization reinforced PID-sliding mode controller for rotary inverted pendulum," *IEEE Access*, vol. 11, pp. 24420-24430, 2023.

LIST OF PUBLICATIONS

Journal Papers

1. **Basant Tomar,** Narendra Kumar, Mini Sreejeth, "Augmentation in Performance of Real-Time Balancing and Position Tracking Control for 2-DOF Ball Balancer System Using Intelligent Controllers," *Wireless Personal Communications*, vol. 138, pp. 2227–2257, 2024, **SCIE**, (**IF: 1.9**), DOI: 10.1007/s11277-024-11591-5. (**Published**)

2. **Basant Tomar,** Narendra Kumar, Mini Sreejeth, "PLC and SCADA based Temperature Control of Heat Exchanger System through Fractional Order PID Controller using Metaheuristic Optimization Techniques," *Heat and Mass Transfer*, vol. 60, pp. 1585–1602, 2024, **SCIE**, (**IF: 1.7**), DOI: 10.1007/s00231-024-03509-5. (**Published**)

3. **Basant Tomar,** Narendra Kumar, Mini Sreejeth, "Robust control of Rotary Inverted Pendulum using Metaheuristic Optimization Techniques Based PID and Fractional Order $PI^\lambda D^\mu$ Controller," *Journal of Vibration Engineering & Technologies*, 2024, **SCIE**, (**IF: 2.1**), DOI: 10.1007/s42417-024-01399-9. (**Published**)

4. **Basant Tomar,** Narendra Kumar, Mini Sreejeth, "Real-Time Balancing and Position Tracking Control of 2-DOF Ball Balancer using PID with Integral ANTI-WINDUP Controller," *Journal of Vibration Engineering & Technologies*, vol. 12, pp. 5055-5071, 2023, **SCIE**, (**IF: 2.1**), DOI: 10.1007/s42417-023-01179-x. (**Published**)

5. **Basant Tomar,** Narendra Kumar, Mini Sreejeth, "Real Time Automation and Ratio Control Using PLC & SCADA in Industry 4.0," *Computer Systems Science & Engineering,* vol. 45, no. 2, pp. 1495-1516, 2022, **SCIE**, (**IF: 4.397**), DOI: 10.32604/csse.2023.030635. (**Published**)

6. **Basant Tomar,** Narendra Kumar, Mini Sreejeth, "A Smart PLC and SCADA based Control Framework for Automated Assembly Line in Process Industry with Effluent Ratio Control Strategy," *IEEE Transactions on Automation Science and Engineering,* 2024, **SCIE**, (**IF: 5.4**), (**Under Review**).

Conference Papers

1. **Basant Tomar,** Narendra Kumar, Mini Sreejeth, "Optimal Control of Rotary Inverted Pendulum Using Continuous Linear Quadratic Gaussian (LQG) Controller," In Proceedings of *14th International Conference on Computing Communication and Networking Technologies (ICCCNT)*, pp. 1-6, 2023. **(SCOPUS),** DOI: 10.1109/ICCCNT56998.2023.10306449. (**Published**)

2. **Basant Tomar,** Narendra Kumar, "Fuzzy Logic Based Braking System for Metro Train," In Proceedings of *IEEE International Conference on Intelligent Technologies (CONIT)*, pp. 1-4, 2021. **(SCOPUS),** DOI: 10.1109/CONIT51480.2021.9498360. (**Published**)

3. **Basant Tomar,** Narendra Kumar, "Method and System for Developing an Automated Assembly Line in a Chemical Process Plant," *International Conference on Innovations and Ideas Towards Patents (ICIIP 2021)*, **Official Journal of the Indian Patent Office**, Journal No. 35/21, (**Published**), Application No. 202111035331 A.

4. **Basant Tomar,** Narendra Kumar, "PLC and SCADA based System for Automating Industrial Operations," *International Conference on Innovations and Ideas Towards Patents (ICIIP 2021)*, **Official Journal of the Indian Patent Office**, Journal No. 37/21, (**Published**), Application No. 202111040407 A.

Patents

1. **Basant Tomar,** Narendra Kumar, "Method and System for Developing an Automated Assembly Line in a Chemical Process Plant," **Official Journal of the Indian Patent Office**, Journal No. 35/21, (**Published & Reply to FER Filed**), Application No. 202111035331.

2. **Basant Tomar,** Narendra Kumar, "PLC and SCADA based System for Automating Industrial Operations," **Official Journal of the Indian Patent Office**, Journal No. 37/21, (**Published and Under examination for Grant**), Application No. 202111040407.

DELHI TECHNOLOGICAL UNIVERSITY

(Formerly Delhi College of Engineering)

Shahbad Daulatpur, Main Bawana Road, Delhi–110042

PLAGIARISM VERIFICATION

Title of the Thesis: **Investigations on Automated and Non-Linear Control Systems**

Total Pages: **183**

Name of the Scholar: **Basant Tomar**

Supervisor: **Prof. Narendra Kumar II**

Co-Supervisor: **Prof. Mini Sreejeth**

Department: **Electrical Engineering**

This is to report that the above thesis was scanned for similarity detection. Process and outcome are given below:

Software used: **Turnitin**

Submission ID: **2753566442**

Similarity Index: **53%**

Self-Publication(s) Similarity Index: **45%**

Final Total Similarity Index: **8%**

Total Word Count: **52,148**

Date: **September 8, 2024**

Candidate's Signature

Signature of Supervisor(s)

Plagiarism Report (Digital Receipt)

turnitin

Digital Receipt

This receipt acknowledges that Turnitin received your paper. Below you will find the receipt information regarding your submission.

The first page of your submissions is displayed below.

Submission author:	Basant Tomar
Assignment title:	PhD Thesis Report
Submission title:	Final thesis
File name:	BT_PHDthesis DTU.docx
File size:	16.15M
Page count:	183
Word count:	52,148
Character count:	298,253
Submission date:	08-Sep-2024 10:35PM (UTC+0530)
Submission ID:	2753566442

INVESTIGATIONS ON AUTOMATED AND NON-LINEAR CONTROL SYSTEMS

A Thesis Submitted
In Fulfilment of the Requirements
for the Degree of

DOCTOR OF PHILOSOPHY
by
BASANT TOMAR
(Enrollment No.: 2K20/PHDEE/04)

Under the Supervision of
Prof. NARENDRA KUMAR II
Professor in Dept. of Electrical Engineering, DTU
Prof. MINI SREEJETH
Professor in Dept. of Electrical Engineering, DTU

Department of Electrical Engineering

DELHI TECHNOLOGICAL UNIVERSITY
(Formerly Delhi College of Engineering)
Shahbad Daulatpur, Main Bawana Road, Delhi-110042, INDIA

SEPTEMBER 2024

Curriculum Vitae

BASANT TOMAR

2K20/PHDEE/04

Department of Electrical Engineering,

Delhi Technological University, Delhi, India

Email: basanttomar18@gmail.com

EDUCATION

Name of course	Year	College/ school	CGPA/ %
Ph.D. in Electrical Engineering (Control & Automation)	2020- 2024	Delhi Technological University	7.67/10
M. Tech. in Control and Instrumentation Engineering	2018-2020	Delhi Technological University	7.9/10
B. E. in Instrumentation and Control Engineering	2012-2016	Netaji Subhas Institute of Technology	67.30%
AISSCE (Class XII)	2011	Little Flowers Public Senior Secondary School, Delhi	88.6%
AISSE (Class X)	2009	Little Flowers Public Senior Secondary School, Delhi	87.6%

RESEARCH AREAS

- Instrumentation and control, PLC and SCADA automation, Fuzzy systems, Real-time Control Systems, Industrial Automation, Linear and Non-Linear Control Systems

PROFESSIONAL EXPERIENCE

Ph.D. Scholar	**Delhi Technological University, New Delhi**	August 2020 – June 2024

- Thesis entitled "Investigations on Automated and Non-Linear Control Systems" under the **supervision** of Prof. Narendra Kumar II and Prof. Mini Sreejeth
- **Teaching Assistant in Dept. of Electrical Engg.:** Conducting Labs and Coursework classes of B.Tech. and MTech students
- **Teaching Experience:** SCADA, Measurement, Linear Integrated Control Systems, Instrumentation, Basic Electrical Engineering, Advanced control system, Process control laboratory
- Quality Assurance of measuring instruments
- Electronic/Instrumentation system design, Data acquisition
- Maintaining efficiency in attaining good accuracy in getting results of my project work
- Tuning of desired sensors and actuators

Mentee-intern	**Addverb Technologies Pvt. Ltd., Noida, Uttar Pradesh**	Jan 2020 – June 2020

- Training, Testing and Commissioning of Robots; Quality improvement and assurance of finished robots.
- Design, test, and commission control systems, including systems with different PLC controllers in the same system.
- Interpret customer specifications and drawings, applying them to design platforms while considering industry regulations and requirements.
- PLC, HMI and SCADA software development, testing & commissioning on **Siemens** and **Rockwell** Platforms.
- Designing, implementing, and maintaining HMI and SCADA systems according to project requirements.
- Oversee the installation, configuration, and programming of PLC systems, ensuring alignment with project goals and regulatory requirements.
- Troubleshoot and resolve technical issues related to PLC and SCADA systems.
- Perform system integration, testing, and commissioning at client sites.

- Deploy PLC software & VFD parameters in a machine, validate all functions per the Test sheet and maintain documentation.
- Collaborate with project engineers and other team members to understand project requirements and deliver high-quality solutions.

Faculty of Applied Mathematics	**Tritiya Maritime Academy, New Delhi**	Oct 2016 – Dec 2017

- Delivering lectures, conducting seminars, and mentoring students in various aspects of Applied Mathematics for competitive exams.
- Material and course development such as handouts, practice problems, and quizzes for student sessions.
- Designing and organizing a course curriculum to follow throughout multiple sessions, ensuring that all relevant topics are covered and building up to a comprehensive understanding of the material.
- Assess students' strengths and weaknesses in mathematics and create personalized study plans to help students improve their scores on the mathematics section in various competitive exams.
- Providing clear, concise, and actionable feedback on practice problems and exercises to help students identify areas of improvement.

RESEARCH PAPERS

Augmentation in Performance of Real-Time Balancing and Position Tracking Control for 2-DOF Ball Balancer System Using Intelligent Controllers	• Wireless Personal Communications, 2024, **SCIE**, (I.F = 1.9) https://doi.org/10.1007/s11277-024-11591-5
PLC and SCADA based Temperature Control of Heat Exchanger System through Fractional Order PID Controller using Metaheuristic Optimization Techniques	• Heat and Mass Transfer, 2024, **SCIE**, (IF: 1.7) https://doi.org/10.1007/s00231-024-03509-5
Robust control of Rotary Inverted Pendulum using Metaheuristic Optimization Techniques Based PID and Fractional Order $PI^\lambda D^\mu$ Controller	• Journal of Vibration Engineering & Technologies, 2024, **SCIE**, (I.F = 2.1) https://doi.org/10.1007/s42417-024-01399-9
Real-Time Balancing and Position Tracking Control of 2-DOF Ball Balancer Using PID with Integral ANTI-WINDUP Controller	• Journal of Vibration Engineering & Technologies, 2023, **SCIE**, (I.F = 2.1) https://doi.org/10.1007/s42417-023-01179-x
Real Time Automation and Ratio Control Using PLC & SCADA in Industry 4.0	• Computer Systems Science & Engineering, 2022, **SCI**, (I.F = 4.397) https://tsp.techscience.com/csse/v45n2/50404
Optimal Control of Rotary Inverted Pendulum Using Continuous Linear Quadratic Gaussian (LQG) Controller	• 14th International Conference on Computing Communication and Networking Technologies (ICCCNT), 2023 https://ieeexplore.ieee.org/document/10306449
Fuzzy Logic Based Braking System for Metro Train	• 2021 IEEE International Conference on Intelligent Technologies (CONIT) https://ieeexplore.ieee.org/document/9498360
PLC and SCADA Based Industrial Automated System	• 2020 IEEE International Conference for Innovation in Technology (INOCON) https://ieeexplore.ieee.org/document/9298190

PATENTS

Title of Innovation/Patent	Application No.	Date of Filing	Date of Publication	Publisher
PLC and SCADA Based Automating System for Industrial Operations	202111040407	06/09/2021	10/09/2021 Under examination for Grant	Official Journal of the Indian Patent Office
Method and System for Developing an Automated Assembly Line in A Chemical Process Plant	202111035331	05/08/2021	27/08/2021 FER issued: Reply Filed for Grant	Official Journal of the Indian Patent Office

- IEEE Access, Wireless Personal Communications, Measurement, ISA Transactions

INTERNSHIPS AND TRAININGS

Intern	**APTRON, Noida, Uttar Pradesh**	March 2020 – April 2020

- Strong proficiency in Ladder Logic PLC programming, particularly with Siemens (e.g., SIMATIC S7, TIA Portal), Allen Bradly (RsLogix500, RsLogix5000) and OMRON (e.g., Sysmac Studio) platforms, including programming logic, motion control, and communication protocols.
- Develop and program PLC and SCADA systems for automation projects.
- Configuring and programming PLC, HMI and SCADA software to ensure smooth operation and efficient data acquisition.
- Develop PLC, SCADA and HMI programs using Ladder Logic PLC programming language; Test and validate for commissioning
- Integrating HMI and SCADA systems with other control systems and ensuring seamless data exchange
- Hands-on experience with commissioning field devices, controllers/field instrumentation.
- Hands-on experience of SCADA/HMI configurations/point programming.

Intern	**CETPA Infotech Pvt. Ltd., Noida, Uttar Pradesh**	2019

- Assist in database management, including data collection, organization, and analysis.
- Work on different Python libraries, leveraging them for data analysis, modelling, and simulation.
- Utilize data visualization tools such as Tableau/Power BI and Excel to create visually appealing charts, graphs, and maps

Intern	**DRDO (INMAS), Ministry of Defense, New Delhi**	June 2015 – Aug 2015

- Completed the projects on **Data Acquisition and Signature Estimation of a shock tube technique for blast wave simulation using LabView and construction of Halbach array.**

Trainee	**NTPC, New Delhi**	June 2014 – Aug 2014

- **Engagement activities**: Carefully examined processes at each level, studied various sensors, calibration of instruments and controlling devices at the plant site
- Worked on the project of **designing an actuator for controlling the water level in drum**.

Trainee	**Indian Institute of Technology (IIT), Delhi**	June 2013 – Aug 2013

- Training conducted by Kyrion Roboworx Pvt. Ltd. on embedded systems and robotics
- Completed the project on "**Line Follower Robot.**

TECHNICAL SKILLS

- **Programming Languages**: C, Python PLC Coding, MATLAB, Simulink
- **PLC Software**: TIA Portal, RSLOGIX-5000 and WPL-SOFT
- **Simulation**: Using MATLAB/Simulink & LABVIEW.
- **SCADA Software:** Siemens SCADA WinCC and InTouch WONDERWARE SCADA
- **Other software:** Quarc real-time control software
- Proficiency in Microsoft Office, Excel, PowerPoint, and **Power BI** for data analysis and visualization**.**
- Designing virtual circuits using ISIS PROTEUS.
- Electronic/Instrumentation system design, Data acquisition.
- Practical knowledge of calibration of the instruments.

ACADEMIC PROJECTS

- Simulation of the braking system of metro trains on various parameters using **FUZZY LOGIC TOOLBOX.**
- Simulation of segregation, filling and counting of bottle filling system using **PLC & SCADA.**
- Project on **Glucose control in ICU diabetic patients** with the help of **PID** and optimizing the plant model with the help of **Genetic Algorithm.**

ACADEMIC ACHIEVEMENTS

- Recipient of **DTU PhD** *Fellowship* from Aug. 2020 – June 2024
- Amongst the **top 1 percentile** of the nation in the **GATE exam**
- Recipient of **Post Graduate** *Scholarship* from **AICTE** during M.Tech (Aug. 2018 – July 2020)
- **Grade ('A')** in Process Instrumentation and Control, Microcontroller and Embedded Systems, CAD, A&D Communication
- **Other coursework undertaken**: Microprocessor, Industrial Electronics, Control systems, AI, SCADA and EMS

EXTRA-CURRICULAR ACTIVITIES

- **2nd position** holder in speech competition (Leprosy) at the **National level.**
- Selected for quiz competition, **"Bharat ko Jano"** two times at the national level.
- Active participation in debates at school, zonal, and district levels.
- Received merit certificates in essay writing and paintings by **Avantika.**

DECLARATION

I hereby declare that the details furnished above are true and correct to the best of my knowledge and belief.

~BASANT TOMAR